Functional degradable polymers *via* RAFT/MADIX mediated polymerization of cyclic ketene acetals and vinyl monomers

Guillaume G Hedir

Submitted for the degree of Doctor of Philosophy

Department of Chemistry

WARWICK
THE UNIVERSITY OF WARWICK

May 2016

Table of Contents

List of Figures, Schemes and Tables

Figures

Schemes

Tables

Acknowledgments

Firstly, I would like to thank my supervisors Rachel O'Reilly and Andrew Dove for the opportunity to work in their labs, but also for their guidance and support over the last three and half years, thank you both for your help. Whilst quite challenging sometimes, your high expectations kept pushing me for which I am grateful. I also wish to thank BP for funding this PhD, especially Emma Chapman for her support, and the University of Warwick for the great facilities.

Thanks to Cecilia, Helen, Craig, Anaïs and Chiara for your help and useful discussions on chemistry aspects of the different projects. A huge thanks to all previous and current members of the O'Doveilly group for making the life in the lab more sociable and for indeed proving that there is a life in the countryside… Special thanks to Dafni, Ruairí, Becky, Anthony, Alice, Anne, Laura, Ed and Marianne for your advice and support, you guys made this PhD more fun. Thank you to Marvin, an MSc student who helped out a lot with the work performed in Chapter 5. As promised, a special thanks to Annette "The Wife" for being a great friend (with or without wine), you surely had an impact on my life here.

Finally and most importantly… Thanks to my family… my parents "Maurice" and "Mauricette", my brother and Pascale, for their constant help and encouragement throughout this often difficult journey, I would not have coped without countless Skype/Facetime therapy sessions. Thanks to my long-time friends Laurène, Audrey, Sylvain and David for not giving up on me even when our life took different paths. And to you CB, thanks for your support and unconditional encouragements, I promise I won't put "the Lab" before everything anymore!

Declaration of Authorship

This thesis is submitted to the University of Warwick in support for the degree of Doctor of Philosophy. It has been composed by myself and has not been submitted in any previous applications for any degree. The work presented (including data generated and data analysis) was carried out by the author except in the case outlined below:

- The reactivity ratios in Chapters 2 and 3 were determined by Dr Yan Kang (University of Warwick) using Contour a program developed by Dr Van Herk (Eindhoven University of Technology).
- The MALDI-TOF mass spectrum in Chapter 3 was performed by Dr Dafni Moatsou (University of Warwick).
- The copolymerization presented in Chapter 4 were performed and analyzed by Dr Craig Bell (University of Warwick).
- The SLS experiments in Chapters 3, 5 and 6 were performed by either Dr Daniel Wright or Mr Lewis Blackman (University of Warwick).
- The TEM images in Chapter 6 were obtained by Dr Anaïs Pitto-Barry (University of Warwick).
- The starting reagent used for the synthesis of the alkyne-functional dithiomaleimide in Chapter 6 was prepared by Dr Mathew Robin (University of Warwick).

Publications

1. Functional Degradable Polymers by Xanthate-Mediated Polymerization, G. G. Hedir, C. A. Bell, N. S. Ieong, E. Chapman, I. Collins, R. K. O'Reilly, A. P. Dove, ***Macromolecules***, 2014, 47, 2847-2852. **(Chapter 2)**

2. Functional Degradable Polymers by Radical Ring-Opening Copolymerization of MDO and Vinyl Bromobutanoate: Synthesis, Degradability and Post-Polymerization Modification, G. G. Hedir, C. A. Bell, R. K. O'Reilly, A. P. Dove, ***Biomacromolecules***, 2015, 7, 2049–2058. **(Chapter 3)**

3. Controlling the synthesis of degradable vinyl polymers by xanthate-mediated polymerization, C. A. Bell, G. G. Hedir, R. K. O'Reilly and A. P. Dove, ***Polymer Chemistry,*** 2015, 6, 7447-7454. **(Chapter 4)**

4. Amphiphilic Block Copolymer Self-Assemblies of Poly(NVP)-***b***-poly(MDO-***co***-vinyl esters): Tunable Dimensions and Functionalities, G. G. Hedir, A. Pitto-Barry, A. P. Dove, R. K. O'Reilly, ***Journal of Polymer Science Part A: Polymer Chemistry,*** 2015, 53, 2699-2710. **(Chapter 6)**

5. Preparation of degradable copolymers containing tuneable thermoresponsive properties by copolymerization of MDO and novel oligo-vinyl acetate derivative monomers, G. G. Hedir, M. Langlais, M. C. Arno, A. P. Dove, R. K. O'Reilly, *In preparation*. **(Chapter 5)**

Summary of thesis

This thesis explores the synthesis of functional degradable polymers *via* the radical ring-opening polymerization (rROP) of cyclic ketene acetal (CKA) monomers and their copolymerization with vinyl ester monomers using the reversible addition-fragmentation chain transfer (RAFT/MADIX) polymerization.

Chapter 1 introduces the polymerization technique used in this thesis (namely RAFT polymerization) and gives a summary of the conventional and new approaches to synthesize poly(esters) for use as degradable materials, with a focus on the arising use of rROP of CKA monomers.

In Chapter 2 the copolymerization of the CKA 2-methylene-1,3-dioxepane (MDO) and vinyl acetate (VAc) is investigated using RAFT/MADIX polymerization with a view towards the formation of degradable copolymers with controlled molecular weights and narrow dispersities.

Chapter 3 discusses the use of the palladium vinyl exchange reaction to create a novel functional bromine derivative monomer of VAc, vinyl bromobutanoate (VBr). The homopolymerization of VBr and copolymerization with MDO using the RAFT/MADIX polymerization is further reported to produce homopolymers and degradable copolymers with functional pendent groups able to be further modified post-polymerization to introduce different properties to the polymer materials.

In Chapter 4 further investigation into the RAFT/MADIX copolymerization of VAc and MDO, as well as its homopolymerization, is explored using a different chain transfer agent (CTA) in order to understand the cause of the lower degree of control observed for some of the copolymerizations in Chapter 2.

Chapter 5 describes the formation of degradable hydrophilic copolymers showing tunable thermoresponsive properties *via* the copolymerization of MDO and novel oligo(ethylene glycol) methyl ether vinyl acetate monomers.

In Chapter 6 the copolymerization of MDO with vinyl ester monomers is presented using a macro-CTA of poly(*N*-vinylpyrrolidone) to create amphiphilic block copolymers of poly(NVP)-*b*-poly(MDO-*co*-vinyl esters) able to self-assemble in water to form degradable nanoparticles.

Chapter 7 provides a summary of the work reported in Chapters 2-6 and potential perspectives for the methodology designed in this thesis.

Abbreviations

ABCN	1,1'Azobis(cyclohexanecarbonitrile)
AIBN	2,2'-Azobis(isobutyronitrile)
AN	Acrylonitrile
Ar	Aromatic
ATRP	Atom transfer radical polymerization
BMDO	5,6-Benzo-2-methylene-1,3-dioxepane
CKA	Cyclic ketene acetal
CMRP	Cobalt mediated radical polymerization
CRP	Controlled radical polymerization
CTA	Chain transfer agent
CuAAc	Copper(I)-catalyzed alkyne-azide cycloaddition
d	Doublet
D_{av}	Average diameter
DBU	1,8-Diazabicyclo[5.4.0]undec-7-ene
D_h	Hydrodynamic diameter
DLS	Dynamic light scattering
$Đ_M$	Dispersity
DMDO	4,7-Dimethyl-2-methylene-1,3-ddioxepane
DMF	Dimethyl formamide
DP	Degree of Polymerization
DTM	Dithiomaleimide
eq.	Equivalents

FRP	Free radical polymerization
FTIR	Fourier transform infrared spectroscopy
GMA	Glycidyl methacrylate
HEMA	2-Hydroxyethyl methacrylate
IV	Intrinsic viscosity
J	Coupling constant
k_{eq}	Equilibrium constant
LA	Lactide
LAM	Less activated monomer
LCST	Lower critical solution temperature
m	Multiplet
m/z	Mass-to-charge ratio
MA	Methyl acrylate
MADIX	Macromolecular design by interchange of xanthates
MALDI-TOF MS	Matrix-assisted laser desorption/ionization – time of flight mass spectrometry
MAM	More activated monomer
MDHL	2-Methylene-4-hexyl-1,3-dioxalane
MDL	2-Methylene-1,3-dioxalane
MDO	2-Methylene-1,3-dioxepane
MEMA	2-Methoxyethoxy methacrylate
MEO_2MA	2-(2'-methoxyethoxy)ethyl methacrylate)
MeO_2VAc	Di(ethylene glycol) methyl ether vinyl acetate

MEO_3MA	Tri(ethylene glycol) methyl ether methacrylate
MeO_3VAc	Tri(ethylene glycol) methyl ether vinyl acetate
MeOVAc	Ethylene glycol methyl ether vinyl acetate
MMA	Methyl methacrylate
M_n	Number average molecular weight
MPDL	2-Methylene-4-phenyl-1,3-dioxolane
M_w	Weight average molecular weight
N_{agg}	Aggregation number
***n*BA**	*n*-Butyl acrylate
NIPAm	*N*-isopropylacrylamide
NLLS	Nonlinear least squares
NMP	Nitroxide mediated polymerization
NMR	Nuclear Magnetic Resonance
NVP	*N*-Vinylpyrrolidone
OEGMA	Oligo ethylene gycol methyl ether methacrylate
PA	Propargyle acrylate
PBS	Phosphate buffer solution
PCL	Poly(ε-caprolactone)
PEG	Poly(ethylene glycol)
PEGMA	Poly(ethylene glycol) methyl ether methacrylate
PMDETA	*N*,*N*,*N*',*N*',*N*''-Pentamethyldiethylene triamine
Poly(AA)	Poly(acrylic acid)
Poly(BMDO)	Poly(5,6-benzo-2-methylene-1,3-dioxepane)

Poly($_{D,L}$LA)	Poly($_{D,L}$-lactide)
Poly(DEAAm)	Poly(*N*,*N*-diethylacrylamide)
Poly(MDO)	Poly(2-methylene-1,3-dioxepane)
Poly(MMA)	Poly(methyl methacrylate)
Poly(MPC)	Poly(2-methacyloyloxyethyl phosphorylcholine)
Poly(MPDL)	Poly(2-methylene-4-phenyl-1,3-dioxalane)
Poly(VAc)	Poly(vinyl acetate)
Poly(VCap)	Poly(*N*-vinylcaprolactam)
Poly(VPip)	Poly(*N*-vinylpiperidone)
q	Scattering vector
RAFT	Reversible addition-fragmentation chain transfer
RDRP	Reversible deactivated radical polymerization
R_h	Hydrodynamic radius
RI	Refractive index
ROMP	Ring-opening methathesis polymerization
ROP	Ring-opening polymerization
rROP	Radical ring-opening polymerization
rt	Room temperature
s	Singlet
SEC	Size exclusion chromatography
SLS	Static light scattering
St	Styrene
t	Triplet

TEGME	Tetra(ethylene glycol) monomethyl ether
TEM	Transmission emission microscopy
TEMPO	2,2,6,6-Tetramethyl-1-piperidinylox
T_g	Glass transition
THF	Tetrahydrofuran
UCST	Upper critical solution temperature
UV	Ultraviolet
UV-vis	Ultraviolet/visible
VAc	Vinyl acetate
VBr	Vinyl bromobutanoate
VCap	*N*-vinylcaprolactam
VClAc	Vinyl chloroacetate
VCP	Vinyl cyclopropane
VL	Vinyl levulinate
VPip	*N*-Vinylpiperidone
δ	Chemical shift
δ-VL	δ-valerolactone
ε-CL	ε-caprolactone
λ	Wavelength

1 Introduction

1.1 Abstract

In this Chapter, two key aspects will be introduced: the first discusses concepts and recent developments in polymerization techniques used to produce well-defined polymers with controlled molecular weights and narrow molecular weight distributions, with a focus on the reversible addition-fragmentation chain transfer polymerization. The second introduces an overview of the approaches previously reported to produce degradable aliphatic poly(esters) with specific attention given to the use of the radical ring-opening polymerization of cyclic ketene acetal monomers.

1.2 Polymerization techniques

Conventional polymerization techniques (step-growth polymerization or chain-growth polymerization) are usually uncontrolled processes where the polymers obtained are ill-defined with broad dispersities, unpredictable molecular weights and are limited to simple architectures, owing to the lack of functional chain-ends available for further block copolymer synthesis. Contrary to this, "living" polymerization techniques are regularly producing well-defined polymers with narrow dispersities and predictable molecular weights as a consequence of the near complete elimination of chain termination and/or chain transfer reactions terminating the propagation processes. The main difference between a step-growth/chain-growth polymerization process and a living polymerization is the linearity of the molecular weight evolution with conversion, observed for the latter process, which allows for a better control over the polymer molecular weights (Figure 1.1).[1]

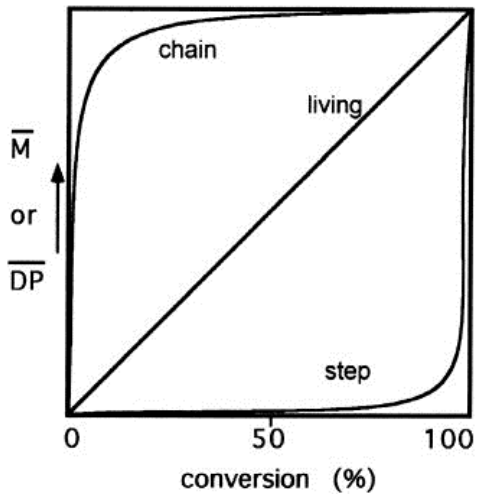

Figure 1.1. Schematic representation of the difference in molecular weight ($\overline{M}$) evolution as a function of conversion between chain-growth, step-growth and living polymerizations.[1]

1.2.1 Living polymerizations

A living polymerization process is defined as a polymerization reaction in which chain termination and chain transfer are absent. To identify whether or not a polymerization is living, Quirk *et al*. reported a series of criteria which have to be fulfilled including:[2]

- The polymerization process can be carried out until all the monomer contained in the mixture has been consumed, and further addition of monomer will result in the continuation of the reaction,
- The molecular weights of the polymers and the degree of polymerization (DP) are linear in correlation with the monomer conversion,
- The molecular weight of the polymers can be controlled by varying the ratio of initiator/monomer,
- The amount of active growing polymer chains in the reaction is constant and independent of the monomer conversion throughout the reaction,
- Polymers with narrow molecular weight distributions are produced,
- Block copolymers can be produced by sequential addition of other monomers,
- Polymers with chain-end functionalities can be prepared quantatively.

The first report of a living polymerization process was reported in 1956 by Swarc *et al*. for the anionic and cationic polymerization of styrene using sodium naphthalene as initiator.[3] Since this initial publication, anionic and cationic polymerizations have been successfully reported for a vast array of monomers and polymeric architectures.[4,5] Nevertheless, such ionic living polymerizations have since been reported to suffer from poor tolerance to functional groups, extremely stringent reaction conditions and the need for an extremely high level of monomer and solvent purity. As a consequence of these limiting criteria, the development of alternative polymerization technique requiring less stringent reaction conditions, increased tolerance to functional group and impurities trace has emerged. As such, "controlled" polymerization techniques exhibiting "pseudo-living" behaviour were later developed, including ring-opening polymerization (ROP),[6] ring-opening metathesis polymerization (ROMP)[7] and reversible-deactivation radical polymerization (RDRP).[8-10]

1.2.2 Conventional free radical polymerization

In conventional free radical polymerization (FRP), there are three main mechanistic steps occurring: initiation, propagation and termination.[11,12] In the initiation step, reactive radicals are formed from the homolytic cleavage of initiator compounds which will subsequently react with monomers to form the first growing polymer chains. During the propagation step, the additions of further monomer units on the polymer chains occurs and allows for growth of the polymer chains. Finally in the termination step, recombination of radical-radical coupling chains and/or disproportionation reactions results in the formation of dead polymer chains that cannot further propagate. In conventional FRP, the rate of termination is significantly greater than the rate of propagation resulting in an increase of terminated chains, hence explaining the short lifetime of propagating radicals. The rate of initiation is also slower than the rate of propagation which indicates that while some polymer chains will grow, some will still be in the initiating stage of the process.[12,13] Additionally, it should be

noted that chain transfer reactions are also present in most radical polymerization processes. Indeed, these chain transfer reactions occur between propagating radicals and other atoms from solvent, monomer or polymer species then resulting in the formation of irregular dead polymer chains.[13] As a consequence of these irregular dead polymer chains, the conventional free radical polymerization process produces ill-defined polymers, with unpredictable molecular weights and broad molecular weight distributions. To overcome the formation of such ill-defined polymers, the development of reversible-deactivation radical polymerizations (RDRP), also often referred to as controlled radical polymerizations (CRP) have become increasingly prevalent in the last decade.

1.2.3 Reversible deactivation radical polymerization (RDRP)

RDRPs are radical polymerization processes in which the conditions of living polymerization introduced in section 1.2.1 are fulfilled. Such techniques usually have a high tolerance to functional groups and require lower monomers purities hence rendering them simpler and synthetically easier polymerization processes. In the RDRP processes, the concentration of propagating radicals is controlled to minimize the occurrence of termination reactions therefore all polymer chains have an equal chance of propagating and can therefore grow at a constant rate.[9] The number of termination reactions is reduced and kept to a low percentage of the radical reactions, to produce well-defined polymers with controlled molecular weights and narrow molecular weight distributions. Among the most common RDRP techniques are Atom Transfer Radical Polymerization (ATRP),[14-17] Nitroxide-Mediated Polymerization (NMP)[18-20] and Reversible Addition-Fragmentation chain Transfer polymerization (RAFT).[21-25] In all of these polymerization processes, a simple compound is employed to mediate the polymerization through which initiation and termination reactions of growing polymer chains are controlled *via* the formation of an equilibrium between active and dormant polymer chains. In the NMP process, this equilibrium is obtained using an

alkoxyamine compound which reversibly captures the propagating species to form a dormant species. Under this condition the amount of active species is kept relatively low therefore limiting the occurrence of termination reactions (Scheme 1.1).[18]

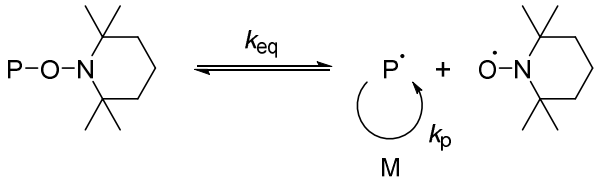

Scheme 1.1. Schematic representation of the equilibrium occurring during the NMP process using TEMPO.

Similarly, in the ATRP process, control of the process is obtained through the use of a transition metal catalyst (*e.g.* Cu, Ru and Fe).[14] Most common ATRP processes use a Cu(I)/ligand complex where a reversible equilibrium between the active and dormant species is obtained by end capping the propagating radical polymer chains with an halide leaving group (Scheme 1.2).[14,15]

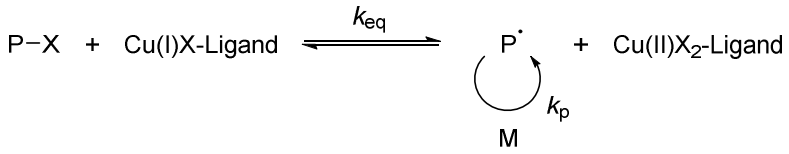

Scheme 1.2. Schematic representation of the equilibrium occurring during the ATRP process.

1.2.4 Reversible addition-fragmentation chain transfer (RAFT) polymerization

Amongst all "controlled" polymerization techniques, the RAFT polymerization has now become perhaps the most widely used and investigated RDRP process in the field of polymer synthesis as a consequence of its robust synthetic conditions as well as its remarkable versatility in polymerizing a wide variety of monomers.[26] Polymers and copolymers synthesized by the RAFT polymerization have a predictable and easily controlled molecular weights with narrow dispersities, typically $Đ_M \leq 1.4$, hence fulfilling characteristics of a "living" polymerization processes. Firstly developed by Moad *et al.* in the late 90s at the

Commonwealth Scientific and Industrial Research Organization (CSIRO) in Australia, the RAFT polymerization technique uses a thiocarbonyl compound as a chain transfer agent (CTA) to mediate the polymerization and create an equilibrium between active and dormant species which reduces the chance of termination reactions.[21,24] While the term RAFT is most commonly used to describe this technique, it should be noted that it is also often referred as Macromolecular Design *via* Interchange of Xanthates (MADIX), in which xanthate compounds are used as chain transfer agents. The MADIX process was concurrently developed in France by Zard *et al*. with the industrial collaboration of Rhodia, and is now considered as a specific type of RAFT polymerization.[27,28] The general mechanism of RAFT is similar to the one of a conventional FRP, with the addition of two significant steps: pre-equilibrium and main equilibrium (Scheme 1.3). Similar to the conventional FRP, the process begins with the decomposition of a thermal initiator to produce radical species ($I^{\bullet}$) which subsequently react with monomers (M) to form the first radical polymer chains ($P_n^{\bullet}$, Scheme 1.3a). These oligomeric chains then react with the thiocarbonyl group of the CTA to form a radical polymer intermediate in the pre-equilibrium (Scheme 1.3b). The intermediate can then undergo a reversible fragmentation to either produce a polymeric CTA and release a radical R-group ($R^{\bullet}$), or revert to the initial growing polymer chain ($P_n^{\bullet}$) and reform the CTA. The radical R-group can then reinitiate the polymerization of further monomers to produce other growing polymer chains, P_n and P_m, (Scheme 1.3c). When all the CTA has been reacted and all polymer chains are capped by the RAFT CTA end-group, the reaction enters the main equilibrium (Scheme 1.3d). During this equilibrium, rapid exchange between active and dormant species occurs allowing all polymer chains to grow at a similar rate and ensure that the concentration of active radicals is kept low, hence reducing the probability of termination reactions occurring. However, some termination can still occur during the polymerization process (Scheme 1.3e) but the occurrence is dramatically reduced compared to conventional

free radical polymerization. Under these conditions, well-defined polymers with controlled molecular weights and narrow dispersities are usually obtained.

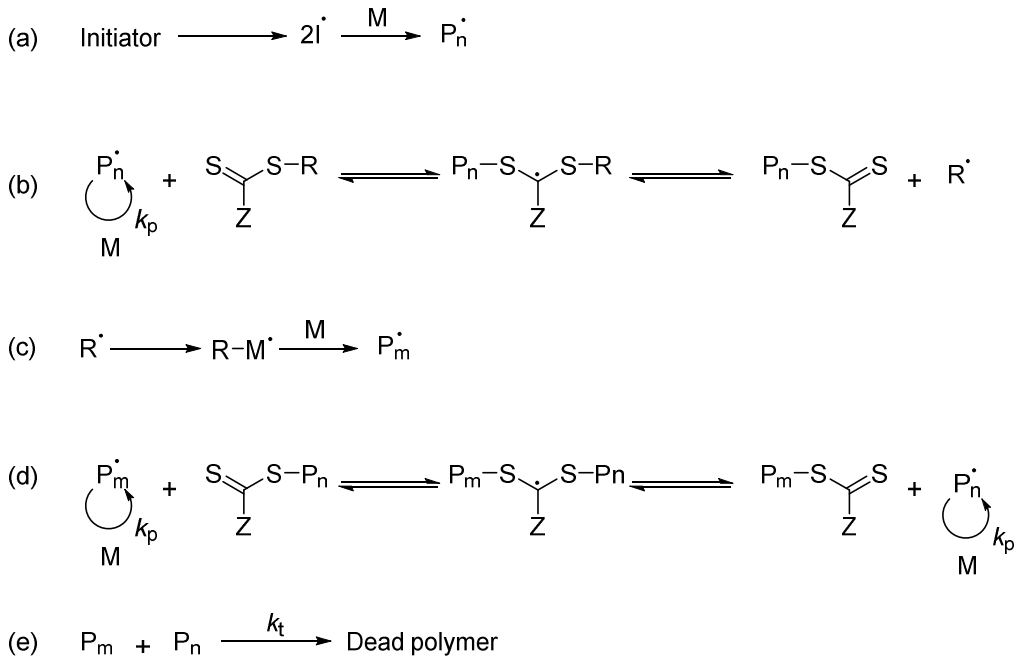

Scheme 1.3. Schematic representation of the general mechanism occurring in the RAFT polymerization with (a) initiation, (b) pre-equilibrium, (c) propagation and re-initiation, (d) main equilibrium and (e) termination.[24]

1.2.4.1 Importance of the RAFT chain transfer agent

The choice of the CTA is an important parameter of the RAFT process and its structure can significantly affect whether the polymerization will achieve living-like conditions and produce well-defined polymers with controlled molecular weights and narrow dispersities.[29,30] The type of Z and R groups of the thiocarbonyl compound strongly affect the efficiency of the CTA by influencing the addition and fragmentation rates of the polymerization process. The nature of the Z group influences the stability of the thiocarbonyl group and hence the stability of the radical intermediate formed during the main RAFT equilibrium. Electron withdrawing groups (Z = -Ph, -SR) will tend to increase the reactivity of the thiocarbonyl bond towards radicals.[22] Under such conditions, the formation of the

radical intermediate is favoured as it will be more stable than the propagating radicals. Conversely, electron donating groups (Z = -OPh, -$N(Et)_2$) will have the opposite effect and the radical intermediate will not be stabilized as the reactivity of the thiocarbonyl bond will be decrease towards the radicals. Based on the nature of the Z group, four different types of CTA have been reported: dithioesters, trithiocarbonates, dithiocarbamates and xanthates (Figure 1.2).[22,25,31,32]

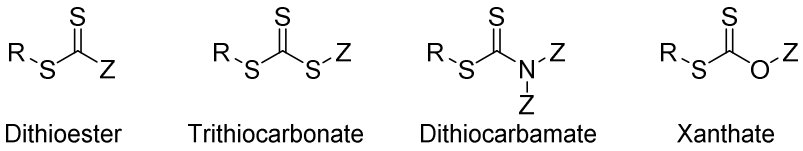

Figure 1.2. Schematic representation of the four types of chain transfer agents used during the RAFT polymerization process.

More activated monomers (MAMs), such as styrenes, acrylates, methacrylates or acrylamides form more stable propagating radicals and therefore require RAFT CTAs with higher chain transfer constants and a higher ability to fragment such as dithioesters or trithiocarbonates. In comparison, less activated monomers (LAMs) such as vinyl acetate (VAc), *N*-Vinylpyrolidone (NVP) and other vinyl ester monomers form unstable radicals requiring the use of RAFT CTAs with lower chain transfer constants, such as xanthates and dithiocarbamates. Using dithioester and trithiocarbonate chain transfer agents on less activated monomers such as VAc would lead to a polymerization with inhibited and retarded effects as a consequence of the poor leaving groups of the monomer which will lead to a low fragmentation rate and hence a poor control of the polymerization process. Similarly, using xanthates and dithiocarbamates on more activated monomers such as acrylates would lead to an inefficient control over the polymerization as a consequence of the decreased reactivity of the carbonyl bond. Encompassing the stability of the Z group and differing monomer reactivities, Moad *et al*. presented guidelines for the selection of the RAFT agents to use (Figure 1.3).[33]

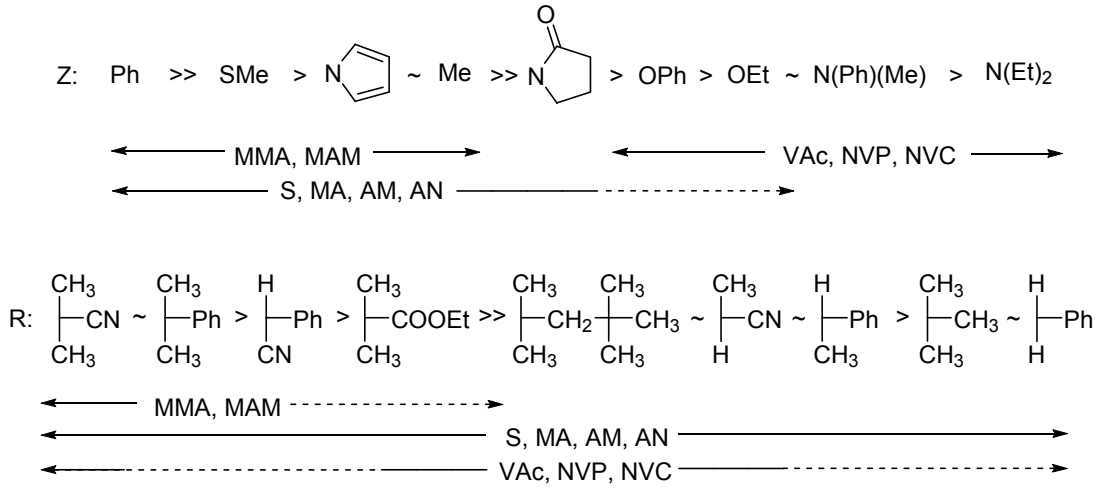

Figure 1.3. Schematic representation of the guidelines for the selection of the correct RAFT agent for various monomer systems. For the Z group, the fragmentation rate increases from left to right. For R group, the fragmentation rates decrease from left to right. Reproduced from [33]

The nature of the R group of the CTA is also an important parameter affecting the successful outcome of the polymerization. Indeed, the R group should be a good leaving group compared to the propagating polymer chains and also be able to effectively re-initiate the polymerization.[23] Hence, caution should be taken for the choice of both the Z and R groups to be use in the chain transfer agent. Correct selection of the Z and R groups enables successful control of the polymerization of a wide range of monomers, hence rendering the RAFT polymerization process a very versatile and applicable technique.

1.3 Degradable Polymers

Synthetic and natural polymers are now indispensable materials to our modern everyday life as a consequence of their range of properties which make them applicable in various diverse areas including: packaging, building materials, transport, support for electronic devices and agriculture.[34-36] Nevertheless, the increasing environmental legislation regarding the resistance of polymeric waste and its disposability have now made degradable polymers a major area of debate. Indeed, while polymers have been intensively used in various industries owing to their remarkable properties, their resistance to chemical, physical and

biological degradation has now become a source of issue.[37] Additionally, the recent increase in the application of polymer based materials in the biomedical field (*e.g.* tissue engineering scaffolds, drug delivery, regenerative medicine, gene therapy or bio-nanotechnology) has highlighted the apparent challenge to find polymeric materials incorporating biocompatibility, non-toxicity and biodegradability.[35,38] While the biocompatible and non-toxic properties of materials have been well-defined in the literature as materials able to interact with a biological system without damaging it, the definition of biodegradability for polymers can often vary upon the field of application to which is it employed.[34,36] Despite this, a common and general definition previously reported by Albertsson and co-workers defined the biodegradation of a polymer as the deterioration of its physical and chemical properties and a decrease of its molecular mass down to the formation of small molecular weight products under the influence of microorganisms.[39] A similar definition can also apply to the non-biological processes where degradation of polymers occurs when the deterioration of the properties results from photo-oxidation, thermo-oxidation or basic and acid hydrolysis instead of through the use of microorganisms. While many natural polymers are biodegradable (*e.g.* poly(saccharides)), synthetic polymers such as conventional vinyl polymers (poly(styrene), poly(ethylene) *etc.*) are generally resistant to degradation as a consequence of the carbon-carbon linkages preventing the hydrolysis of the polymer backbone. Nevertheless, it should be noted that some degradation for the latter polymers can sometimes occur but tends to be limited to the degradation of the functional pendent groups of the polymers, therefore leaving behind the remaining main polymer backbone.[40,41] Conversely, polymers containing heteroatom backbones are able to undergo degradation processes in which both functional pendent groups and the main backbone can be reduced to smaller segments of polymers (called oligomers).[42] Therefore, the formation of degradable polymers can often be engineered by prudent addition of chemical linkages such as anhydride, ester, carbonate, amide or disulfide bonds, amongst others (Figure 1.4).

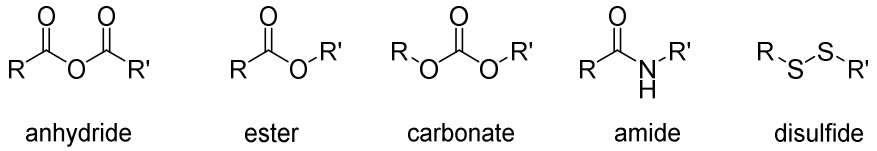

Figure 1.4. Schematic representation of heteroatom groups able to undergo degradation.

For those types of polymers, the degradation usually occurs *via* the hydrolysis or enzymatic cleavage of the labile heteroatom linkages that result in a scission of the polymer backbone into lower molecular mass fractions (Scheme 1.4). Degradable polymers with hydrolyzable chemical bonds are therefore nowadays intensively studied and investigated as they have become ideal candidate materials to be used in biomedical, pharmaceutical, agricultural and packaging applications.[38]

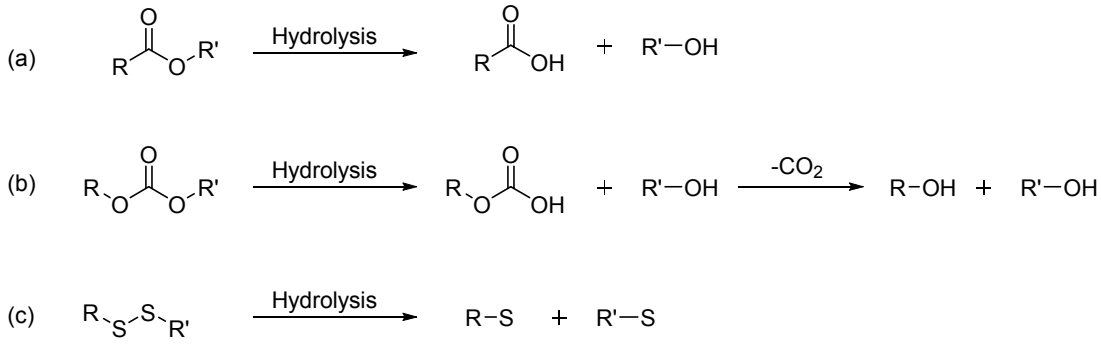

Scheme 1.4. Schematic representation of the hydrolysis of (a) ester, (b) carbonate and (c) disulfide linkages.

The chemical nature of the degradation products is also a significant aspect of the degradation, as their toxicity will determine whether the polymers are biocompatible or not.[43] In this demanding area, polyesters have become the most common degradable polymers studied and investigated as a consequence of their good mechanical and thermal properties and their easy degradation under various conditions.[34,39,44,45] Poly(lactide), poly(glycolide), poly(butylene succinate), poly(ethylene terephthalate) and poly(ε-caprolactone) and their

copolymers are amongst the most common polyesters which have all been intensively employed as degradable materials in the biomedical field.

1.3.1 Poly(esters) as degradable polymers

Although poly(esters) have been investigated for several decades, the concept of degradability for such polymers only emerged in late 60s where their hydrolytic sensitivity was discovered.[46] These polymers are mainly synthesized *via* two processes: the polycondensation of combinations of diols and dicarboxylic acids (Scheme 1.5a) or by the ring-opening polymerization (ROP) of cyclic ester monomers such as lactones and lactides (Scheme 1.5b).[34] Indeed, most commercially available degradable poly(esters) are produced by these two polymerization processes, with both having advantages and limitations. While polycondensation was firstly discovered by Carothers in the early 30s,[47,48] and later widely studied and used as a successful way of producing poly(esters) for many decades, it usually requires high temperatures and long polymerization times to obtain polymers with high molecular weights. This approach also reduces control over the polymer chain lengths and therefore forms polymers with broad molecular weights distributions.[34,39,46,49] Conversely, the ROP of cyclic ester monomers can be performed in milder conditions and also produce poly(esters) with high molecular weights while still maintain a better degree of control compared to the polycondensation processes. Additionally, recent developments of various catalysts and initiators has now enabled the synthesis of poly(esters) with "living" features, where control over the polymer chain length and retention of end-functionalities can be obtained.[6,49-52]

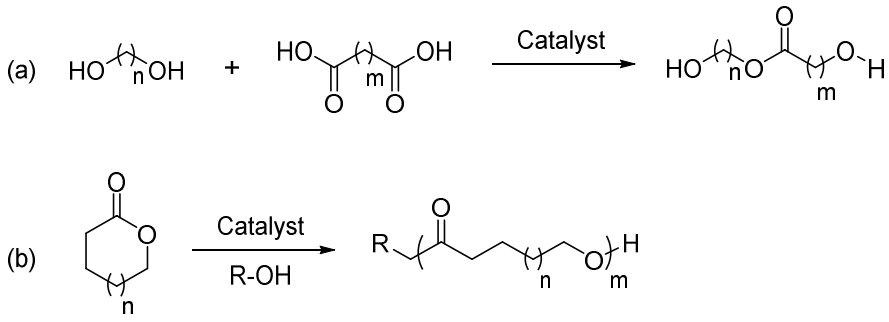

Scheme 1.5. Schematic representation of the formation of poly(esters) from (a) polycondensation of diols and dicarboxilic acids and (b) ring-opening polymerization of cyclic esters.

1.3.1.1 Polyesters by ring-opening polymerization (ROP)

Most common aliphatic poly(esters) used in the biomedical field are currently produced by the ROP technique, with poly(δ-valerolactone), poly(ε-caprolactone), poly(lactide) and poly(glycolide) being the most common, and which are obtained from their corresponding cyclic ester monomers: δ-valerolactone, ε-caprolactone, lactide and glycolide respectively. Various ROP processes have been investigated using a wide range of catalysts, including metal-based catalysts,[53,54] enzyme catalysts[55,56] and organic catalysts.[57-59] While the use of metal-based catalysts have been widely applied and successfully used for the production of well-defined poly(esters), they have shown to present some limitations. Indeed, the presence of metal impurities can often be observed in the final polymers, requiring further purification steps for their complete removal which can have an impact on both the quality and efficiency of the synthesis, especially when such polymers are used in the biomedical applications and therefore must not contain trace amounts of metals. To avoid such contamination of the final polymers, enzyme catalysts have for many years been seen as an alternative "greener chemistry" approach for the synthesis of poly(esters) using ROP.[55,60,61] Nevertheless, while the successful formation of poly(esters) using this route has been widely reported, it also suffers from a lower degree of control observed during the polymerization as a consequence of the enzymes requiring aqueous media in order to retain their activity during the reaction.

Indeed, the presence of water during the ROP of cyclic esters often leads to trans-esterification reactions and subsequent formation of cyclic ester polymers affecting the controlled aspect of the polymerization. On the other hand, in the last two decades developments in organic catalysts have resulted in significant improvements for the formation of well-defined and controlled poly(esters) using ROP (Scheme 1.6) in comparison with metal-based and enzyme catalysts.[57-59,62] In fact, the use of organic catalysts for ROP presents many advantages including: ability to form catalysts *via* simple synthetic reactions (suitably simple to easily scale therefore many are commercially available), their air and moisture stability rendering them easy to handle and store, as well as the ability to easily remove the residual catalyst from the final polymers *via* simple washing procedures.

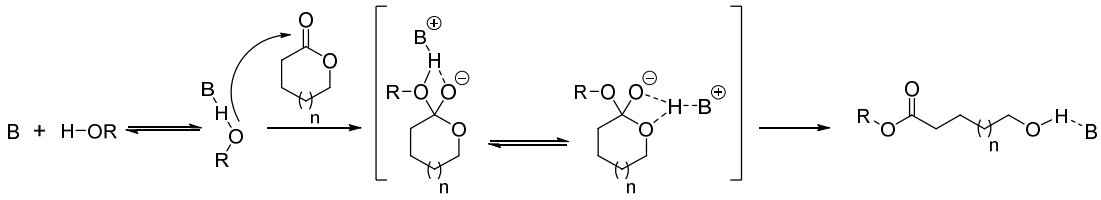

Scheme 1.6. Schematic representation of the formation of poly(esters) by ROP using organic catalyst.

Amongst the most common organic catalysts used for ROP 1,8-diazobicyclo[5.4.0]undec-7-ene (DBU), 7-methyl-1,5,7-triazabicyclo[4.4.0]dec-5-ene (MTBD) and 1,5,7-triazabicyclo[4.4.0]dec-5-ene (TBD), also commonly known as "superbases", are frequently used. Such catalysts have been found to exhibit significantly high catalytic activity and robust properties enabling them to be used under various reactions conditions, including cyclic esters with differing ring sizes, a diverse range of solvents and functional groups, whilst still maintaining control over the molecular weights and dispersities of the final polymers.[63-66]

1.3.1.2 Functional poly(esters) by ROP

A large amount of research has been focused on the incorporation of further functional groups onto polymers in an attempt to target and diversify the physical and chemical properties of the final materials and target specific applications (*e.g.* biological, therapeutic or fluorescent properties).[67-69] To this aim, various approaches have been developed and reported to produce functional poly(esters). Amongst these approaches the synthesis of new functional cyclic ester monomers (Cl-ε-CL, functional lactide *etc.*),[67-71] the chain-end modifications of the poly(esters) by using a functional initiator and catalyst,[69,70] and the copolymerization of different cyclic esters with other monomers can be found.[71,72] While all these approaches have been successful in the incorporation of functional groups onto the poly(esters), and hence able to diversify the properties of the final polymers, some limitations were nevertheless observed. Indeed, the synthesis of new functional cyclic ester monomers is often limited to functional groups that are compatible with the catalyst and ROP process but are also synthetically challenging as a consequence of the arduous experimental conditions required which tend to have yield-lowering protection and deprotection steps.[49,73] The chain-end modification approach suffers from the low functional group density along the polymer, especially when polymers with high molecular weights are targeted.[69,70] Similarly, the copolymerization of cyclic ester monomers with other monomers containing functional groups is also restricted by the poor match in reactivity ratios between the monomers which therefore lead to an inefficient incorporation of functionality density onto the polymer backbone as well as forming copolymers with broad molecular weight distributions if the monomers do not present similar reactivity.[49,52,74-76] As a result of these limitations, other alternative methods to produce poly(esters) where different functional groups can be incorporated have been developed.

1.3.1.3 Polyesters by radical ring-opening polymerization (rROP)

While the use of ROP to produce poly(esters) has mainly been seen as the dominant technique to produce polymers with degradable properties, an alternative approach has regained significant interest in the polymer materials field over the last decade: the radical Ring-Opening Polymerization (rROP).[77-79] Indeed the rROP of cyclic monomers (mainly cyclic ketene acetals, CKAs) has been seen as an unconventional but successful approach for the production of polymers containing degradable ester repeat units in their backbone.[78,79] Firstly introduced in the early 80s in various studies by Bailey *et al*., this approach uses the presence of an exo-methylene double bond functionality on the cyclic ketene acetal monomer which can undergo polymerization *via* radical addition and force the cyclic monomer to ring-open itself, hence producing a growing ester chain able to subsequently form a poly(ester) after further monomer addition.[80-85] CKA monomers can be synthesized in a two-step processes consisting of an acetal exchange reaction followed by a dehydrohalogenation.[80] For example, 2-methylene-1,3-dioxepane (MDO, a 7 membered cyclic ester monomer, **CKA 1**) is obtained from the reaction between chloroacetaldehyde-dimethylacetal with 1,4-butanediol to form the 2-chloromethyl-1,3-dioxepane which is then treated with potassium *t*-butoxide to produce, after purification using washes and distillation, the final CKA MDO (Scheme 1.7a).[80] Similarly, the benzyl functional version, 5,6-benzo-2-methylene-1,3-dioxepane (BMDO, **CKA 2**) can be synthesized from the acetal exchange reaction of 1,2-benzene dimethanol followed by dehydrohalogenation (Scheme 1.7b).[86]

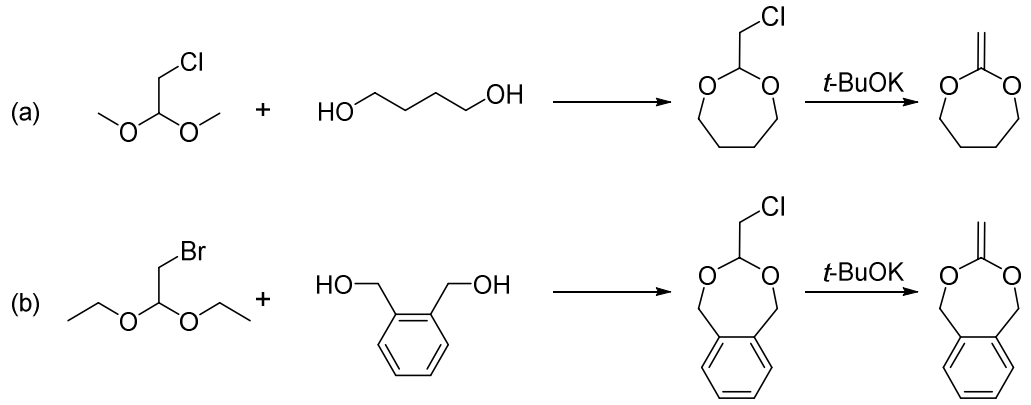

Scheme 1.7. Schematic representation of the synthetic formation of cyclic ketene acetals (a) 2-methylene-1,3-dioxepane (MDO, **CKA 1**) and (b) 5,6-Benzo-2-methylene-1,3-dioxepane (BMDO, **CKA 2**).

Using this synthetic approach various CKA monomers have been produced where the ring sizes (*e.g.* 5, 6, 7 membered ring) and functional groups (*e.g.* phenyl, alkyl *etc.*) can be modified to produce a wide array of CKA structures, which can be polymerized by rROP to form polyesters with different properties (Figure 1.5).[78,79] The synthesis of MDO (**CKA 1**) was of particular interest as it was found to produce, after polymerization, a polymer with a similar structure to conventional poly(ε-caprolactone) (PCL) (Scheme 1.8), hence providing an alternative radical production for this widely used poly(ester).[80]

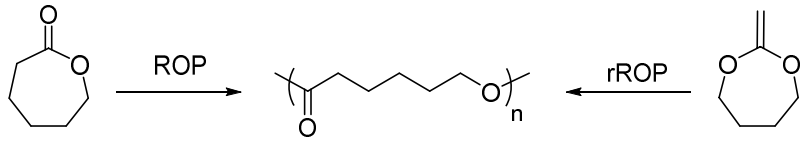

Scheme 1.8. Schematic representation for the parallel synthesis of poly(esters) from the ROP of ε-CL and the rROP of 2-methylene-1,3-dioxepane.

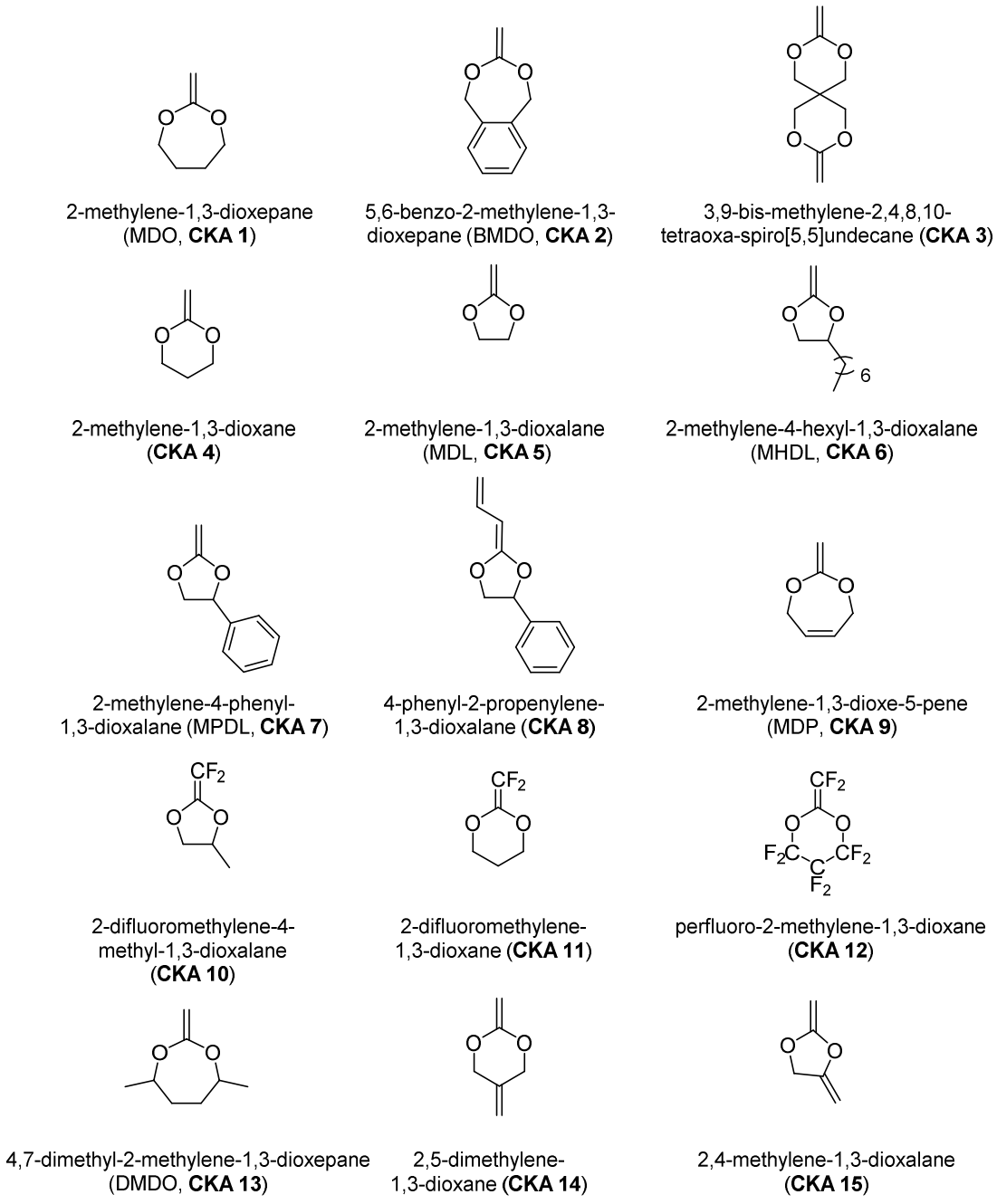

Figure 1.5. Schematic representation of different cyclic ketene acetals (CKAs).

The first radical ring-opening polymerizations of CKAs were reported by Bailey *et al*. with the rROP of 3,9-dimethylene-1,5,7,11-tetraoxaspiro-[5,5] undecane (**CKA 3**) and 2-methylene-1,3-dioxepane (**CKA 1**), using conventional radical thermal initiators such as benzoyl peroxide, di-*t*-butylperoxide or 2,2'-azobis(isobutyronitrile) (AIBN) under various

conditions, where polymerizations were carried out in bulk, in solution and at different temperatures (60 to 150 °C).[80-85] During the rROP of CKAs, Bailey *et al*. reported that the mechanism was similar to the conventional free radical polymerization technique where the process starts with (Scheme 1.9a) the decompositions of an initiator to produce radical species that will react with the double bond of the CKA.[80] The cyclic radical intermediate then isomerizes by radical ring-opening polymerization to create the initial primary radical containing the ester repeat units (Scheme 1.9b). The reaction then repeats itself and the primary radical containing the ester repeat unit grows to produce poly(ester) chains (Scheme 1.9c).

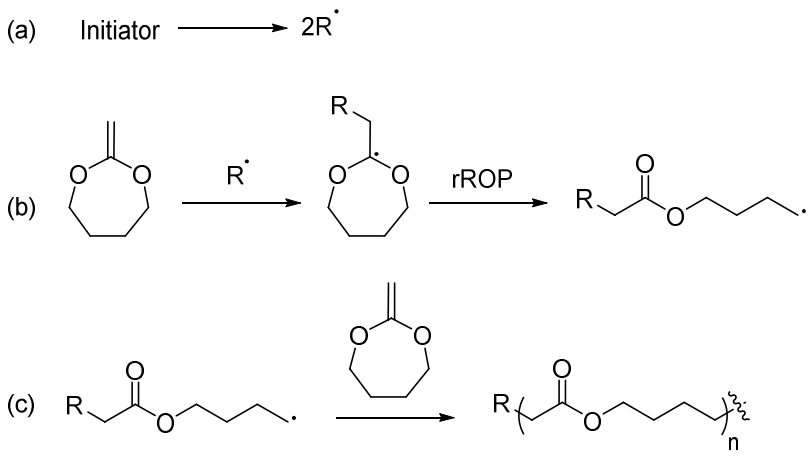

Scheme 1.9. Schematic representation of the mechanism for the radical ring-opening polymerization (rROP) of MDO (**CKA 1**).

While Bailey and co-workers investigated the successful synthesis of poly(esters) from the rROP of CKA monomers such as MDO, they also reported the occurrence of a side reaction in which ring-retention of the CKA could be observed during the polymerization.[80] Indeed, the formation of the cyclic intermediate produces a tertiary radical (Scheme 1.9b) which can also react and produce a poly(acetal) structure within the poly(ester) backbone (Scheme 1.10). The occurrence of such ring-retention reactions during the rROP have been shown to be dependent on various parameters including: the polymerization temperature, CKA

monomer structure (ring sizes, substituents), and the monomer and initiator concentrations.[81,87-89]

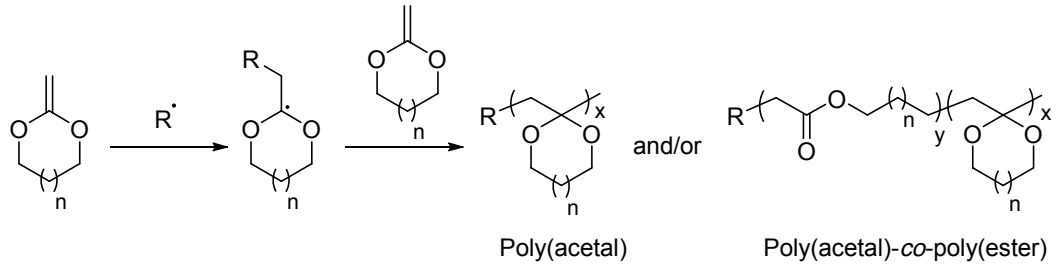

Scheme 1.10. Schematic representation of the ring-retention reaction occurring during the rROP of CKA monomers and formation of either poly(acetal) and poly(acetal)-*co*-poly(ester) structures.

For example, the rROP of the 7-membered non-functional CKA, MDO (**CKA 1**) and phenyl-functionalized BMDO (**CKA 2**) was found to occur *via* quantitative ring-opening of the monomers for polymerizations carried out at various temperatures from 50 to 120 °C.[80,81,90,91] Conversely, the 5-membered ring CKA, 2-methylene-1,3-dioxalane (MDL, **CKA 5**) was found to produce poly(esters) containing ring-retained units throughout the polymer backbone as a consequence of the poor stability of the primary radical obtained during the rROP.[87] The ratio of ring-opened and ring-retained units within the polymers was found to vary when the temperature of the polymerization was changed. Indeed, for a polymerization carried out at 60 °C, only 50% of the polymer chains were composed of ring-opened units *vs*. 83% reached when the same polymerization was carried out at 125 °C. A similar effect was observed when the concentration of the monomer in the polymerization mixture was decreased leading to more ring-retained polymer structures.[87] For these CKAs, the introduction of a phenyl or hexyl functional groups on the ring, to create 2-methylene-4-phenyl-1,3-dioxolane (MPDL, **CKA 7**) and 2-methylene-4-hexyl-1,3-dioxalane (MHDL, **CKA 6**), was able to increase the stability of the primary radical and produced polymers with full ring-opening of the monomer across a wide range of temperatures from 60 to 150 °C.[87,88,92]

Although Bailey and co-workers reported the radical ring-opening polymerization of MDO (**CKA 1**) as an interesting approach to produce a poly(ester) with the same structure as the poly(ester) obtained from the conventional ROP of poly(ε-caprolactone) (PCL), their report was lacking in the characterization of the poly(MDO) structure.[80] Hence, Gonsalves *et al*. later further investigated the polymerization of MDO for 72 h using AIBN as the initiator at 50 °C and highlighted the presence of side reactions arising from the instability of the growing primary radical polymer chains.[91] Indeed, they observed that some side branches were formed along the polymer backbone and were resulting from the 1,4- and 1,7-hydrogen transfer reaction occurring during the polymerization (Scheme 1.11). Under their conditions, the amount of hydrogen transfer reactions and hence the amount of branches in the poly(MDO) backbone was found to reach 20% revealing that the structure of the final polymers was in fact a branched analogue to the structure obtained from the ROP of poly(ε-caprolactone). Further recent studies, mainly by Agarwal and co-workers, also investigated the effect of the 1,4- and 1,7-hydrogen transfer reactions and showed that the extent of branches in the radical ring-opening polymerization of MDO was dependent on the temperature at which the reactions were carried out [87,90] Indeed, for polymerizations carried out at temperatures above 100 °C, the amount of branches was found to be significantly lower.

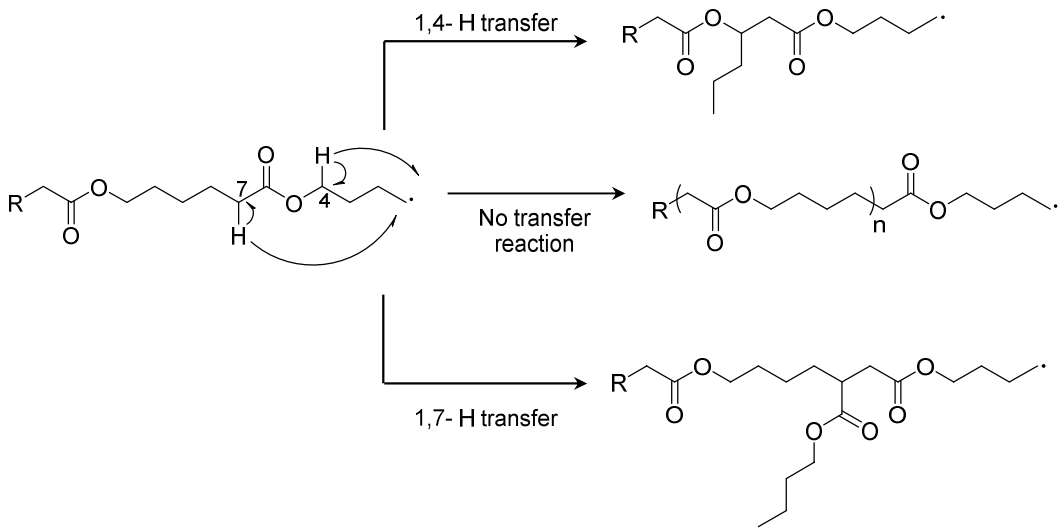

Scheme 1.11. Schematic representation of the possible branching occurring during the rROP of MDO *via* 1,4- and 1,7-hydrogen transfer.

1.3.1.4 Functional poly(esters) by radical ring-opening polymerization

As in the case of conventional poly(esters) made by ring-opening polymerization, a significant number of studies have attempted to incorporate further functional groups in the poly(esters) in order to target and diversify the properties of the final materials.[78,79] So far two approaches are predominant in the field of rROP: the incorporation of functional group on the CKA monomer and the copolymerization of a CKA with more conventional vinyl monomers. While the incorporation of further functionalities on CKAs still remains a challenge as a consequence of the often arduous steps to produce such monomers, a few examples have still been reported. Cho *et al*. reported the synthesis of 4-phenyl-2-propenylene-1,3-dioxolane (**CKA 8**), a vinyl ketene cyclic acetal substituted with a phenyl group, by a cyclization reaction of 2-bromo-1-phenylethyl-2-butenoate with potassium hydride.[93] While the successful formation of the functional CKA monomer was confirmed, a low yield of 16% was obtained for their synthetic approach hence highlighting the challenge in forming such functional monomers. The radical ring-opening polymerization of **CKA 8** using AIBN and benzoyl peroxide at either 55 or 78 °C lead to the successful formation of

poly(esters) containing double bonds in the main polymer backbone and a phenyl functional groups as a side chain (Scheme 1.12). The presence of double bonds within the backbone enables the incorporation of different functional groups *via* post-polymerization modifications (*e.g.* thiol-ene "click" chemistry). In contrast, the formation of poly(esters) with such functionalities still remain a challenge when using conventional ROP synthetic approach.[49,94,95]

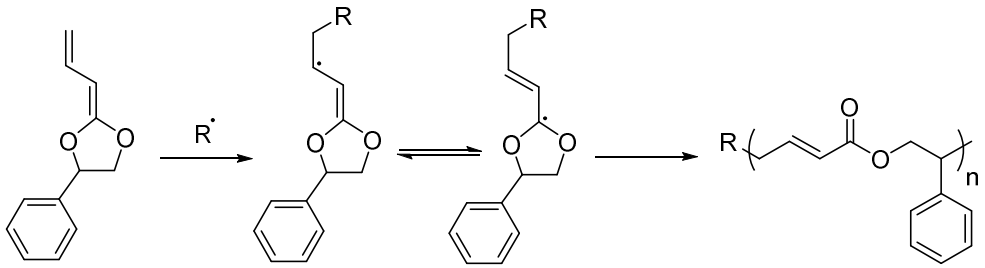

Scheme 1.12. Schematic representation of the radical ring-opening polymerization of 4-phenyl-2-propenylene-1,3-dioxolane, **CKA 8**.[93]

Similarly, Plikk *et al.* also investigated the incorporation of double bonds within the poly(ester) backbone *via* the synthesis of a more simple cyclic ketene acetal, 2-methylene-1,3-dioxe-5-pene (MDP, **CKA 9**), a CKA analogue of MDO.[96] While the radical ring-opening polymerization of MDP was confirmed, it was also observed that the structural nature of the poly(ester) formed was strongly dependent on the temperature at which the polymerization was carried out. Indeed, when low temperature was employed (50 °C) the polymerization was found to form polymers containing a mixture of ring-opened and ring-retained groups within the polymer backbone, with an estimation of 85% of ring-opened ester units. Conversely, when the polymerization of MDP was performed at 150 °C, the radical ring-opening of the monomer was interestingly found to lead to a new cyclization reaction where more stable 5-membered cyclic ester species, 3-vinyl-1,4-butyrolactones, were forming as the main reaction product (Scheme 1.13). Therefore, these results highlighted that while the incorporation of functionalities into CKA monomers can be

achieved, the nature of the functional groups can also affect the structure of the final poly(esters) through the occurrence of competitive side reactions.

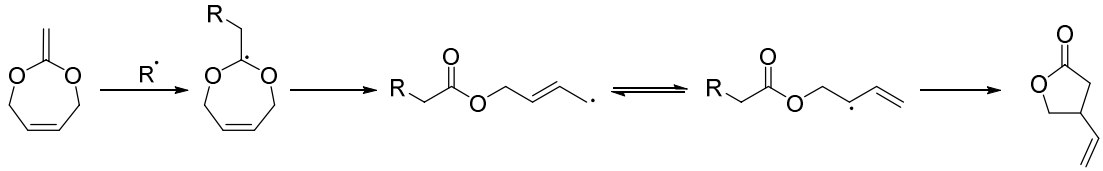

Scheme 1.13. Schematic representation of the radical ring-opening polymerization of MDP performed at 150 °C leading to the more stable 3-vinyl-1,4-butyrolactones.[96]

Other studies also investigated functional CKA monomers with varying results obtained when their radical ring-opening polymerization were carried out depending on their structure and functional groups.[97] Another example of functional CKA synthesis is the use of fluorinated or partially fluorinated CKAs to produce poly(esters) with fluorine functional groups presenting increased thermal, chemical and optical properties and with the potential to be used in the biomedical field as degradable materials for imaging. To this aim, Okamato and co-workers studied the formation of various fluorinated CKAs including 2-difluoromethylene-4-methyl-1,3-dioxolane (**CKA 10**), 2-difluoromethylene-1,3-dioxane (**CKA 11**) and perfluoro-2-methylene-1,3-dioxane (**CKA 12**).[98] The radical ring-opening polymerization of these fluorinated CKAs using initiators such as AIBN, tri(*n*-butyl)borane and benzoyl peroxide was found to successfully produce poly(esters) with fluorinated groups. However, the process was found to have a lower tendency to ring-open, in comparison to the hydrocarbon analogues, with ring-retention values between 96 and 15% obtained for reactions performed at 60, 80 or 130 °C.[98] This difference in ring-opened/ring-retained species was assumed to be observed as a consequence of the change in propagation rates occurring during these polymerizations.

The second approach to incorporate functionalities into poly(esters) is *via* the copolymerization of CKAs with more conventional vinyl monomers which have been widely studied as a consequence of the less challenging synthetic conditions.[78,79] Indeed, while the copolymerization with vinyl monomers leads to the incorporation of further functionalities in the polymers, it also provides an opportunity to incorporate degradable ester repeat units within the conventionally non-degradable backbone of vinyl polymers. Hence, this approach has been seen as a very advantageous route to produce degradable polymers *via* a radical, and therefore a more industrial applicable polymerization process (Figure 1.6).[77] The first examples of copolymerization of CKAs with vinyl monomers was reported by Bailey *et al.* in the early 80s with the copolymerization of the CKAs 4,7-dimethyl-2-methylene-1,3-dioxepane (DMDO, **CKA 13**) and 5,6-benzo-2-methylene-1,3-dioxepane (BMDO, **CKA 2**), with styrene (St) and methyl methacrylate (MMA) using AIBN and di-*tert*-butyl peroxide at 110 - 120 °C, to successfully produced degradable copolymers of poly(St-*co*-CKA) and poly(MMA-*co*-CKA) (Scheme 1.14).[87] In all cases, the quantitative ring-opening polymerization of the CKAs was confirmed with the absence of acetal units within the copolymer backbone.

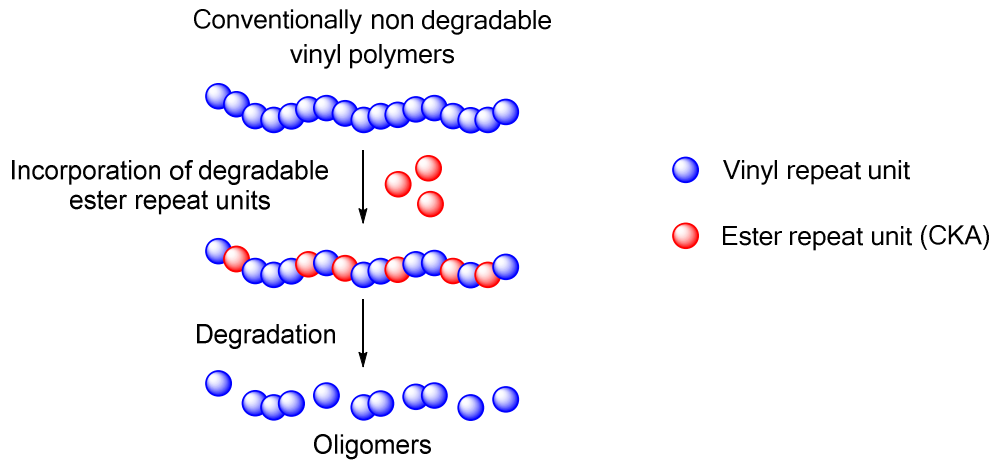

Figure 1.6. Schematic representation of the formation of degradable vinyl polymers *via* the copolymerization of CKA and vinyl monomers.

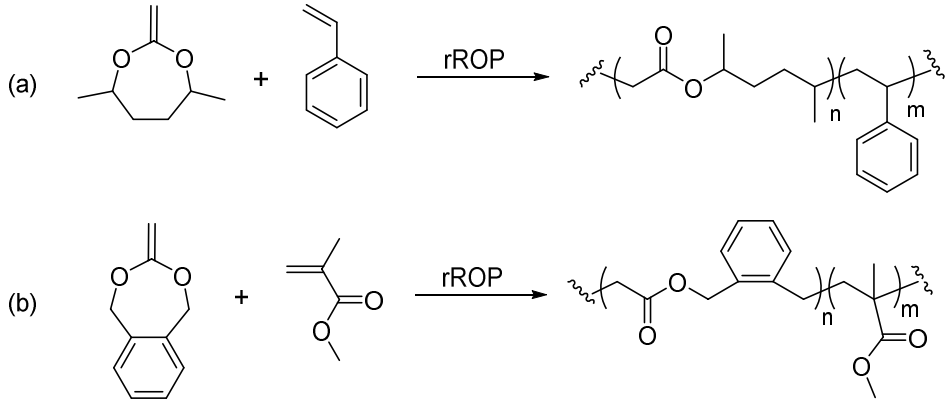

Scheme 1.14. Schematic representation of the formation of functional poly(esters) from the copolymerization of (a) DMDO, **CKA 13**, with styrene and (b) BMDO, **CKA 2**, with MMA.

Following on from the pioneering work of Bailey and co-workers,[80-85] many groups later investigated the copolymerization of CKAs with vinyl monomers including vinyl acetate (VAc),[99,100] glycidyl methacrylate (GMA), pentafluorostyrene (PFSt),[101] propargyle acrylate (PA),[102] methyl-methylene-butyrolactone,[103] 2-hydroxyethyl methacrylate (HEMA),[100] ethylene glycol methyl ether methacrylate (EGMA),[104] and 4-vinylanisole,[81] amongst others. Such copolymerizations have led to a wide range of degradable polymers with different physical, thermal, and chemical properties. Whilst in all cases the successful formation of copolymers of poly(CKA-*co*-Vinyl) with degradable properties was confirmed, the final microstructures of the copolymers were found to be strongly dependent on the reactivity ratios of the CKAs and vinyl monomers as it is often observed for any type of copolymerization. In their original study, Bailey *et al*. investigated the copolymerization of MDO (**CKA 1**) with St or methyl acrylate (MA) by conventional free radical polymerization and calculated the reactivity ratios of both monomers as $r_{MDO} = 0.023$ and $r_{MA} = 25.53$.[105] These results indicated that a predominantly blocky microstructure was obtained for the copolymer, poly(MDO-*co*-MA), in which a low incorporation of ester repeat units had been introduced into the final polymer, which therefore was mainly composed of MA repeat units. Similarly, other studies reported comparable results for the copolymerizations of MDO with

the vinyl monomers St, MMA and GMA where reactivity ratio values of $r_{MDO} = 0.021$ and $r_{St} = 22.6$,[106] $r_{MDO} = 0.057$ and $r_{MMA} = 34.12$,[107] and $r_{MDO} = 6.6$ and $r_{GMA} = 26.8$[108] were obtained for each system respectively, hence suggesting that the CKA monomers have lower reactivities compared to acrylate monomers. Additionally, the presence of functional groups on the CKA ring was found to have little effect on the expected microstructure of copolymers of CKA and acrylate monomers. Agarwal *et al*. reported the copolymerization of BMDO (**CKA 2**) and MMA obtaining reactivity ratios of $r_{BMDO} = 0.53$ and $r_{MMA} = 1.96$ suggesting an initial block microstructure with a tendency to form random copolymers for increasing polymerization times.[86] Interestingly, in most studies involving vinyl acrylate monomers, the reactivity of the CKAs was always found to be lower in comparison with the reactivity of acrylates and hence lead to the formation of a predominantly blocky microstructure copolymer. Conversely, the copolymerization of CKAs with less activated monomers such as VAc was found to produce copolymers with random or statistical microstructure as seen by the reactivity ratios calculated in similar studies by Agarwal *et al*. and also by Undin *et al*. for the system MDO/VAc ($r_{MDO} = 0.47$ and $r_{VAc} = 1.53$,[100] and $r_{MDO} = 0.93$ and $r_{VAc} = 1.71$,[99] for each study respectively). These results prompted the formation of copolymers with a better incorporation of ester repeat units across the polymer backbone in comparison with the copolymers formed between acrylates and CKAs.

While the copolymerization of CKAs with conventional vinyl monomers has enabled the successful synthesis of degradable vinyl polymers, some report also use vinyl monomers containing functional groups able to be further modified *via* post-polymerization modifications to incorporate a wider range of properties (Figure 1.7, Scheme 1.15).

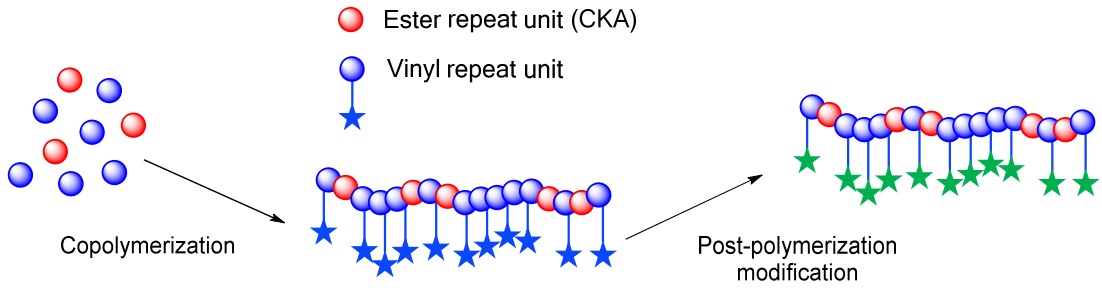

Figure 1.7. Schematic representation of the copolymerization of CKA and functional vinyl monomers to produce functional degradable polymers able to undergo post-polymerization modifications.

Indeed, Maji *et al*. investigated the copolymerization of MDO with propargyl acrylate (PA) as a route to produce degradable copolymers of poly(MDO-*co*-PA) containing alkyne functionalities able to be further modified *via* "click" chemistry. An azide functionalized poly(ethylene glycol) section was grafted onto the copolymer using $CuSO_4$ and DBU as the catalyst, to produce polymers with hydrophilic and biocompatible properties.[102] Furthermore, Unjin *et al*. later investigated the copolymerization of MDO with glycidyl methacrylate (GMA) to form a degradable copolymer with epoxy functionalities. These were modified by covalent immobilization of heparin to enhance the differentiation of osteogenic stem cells, whist varying the composition of the copolymer was found to increase the mechanical properties of the final material.[108,109] Zhang and co-workers also investigated such an approach with the copolymerization of protected 2-hydroxyethyl methacrylate (HEMA-TMS) monomer with the cyclic ketene acetal BMDO to produce a degradable copolymer containing hydroxyl pendent groups (after deprotection) able to be used to enhanced the properties of the materials and target applications such as drug delivery, soft contact lenses or artificial skin.[100]

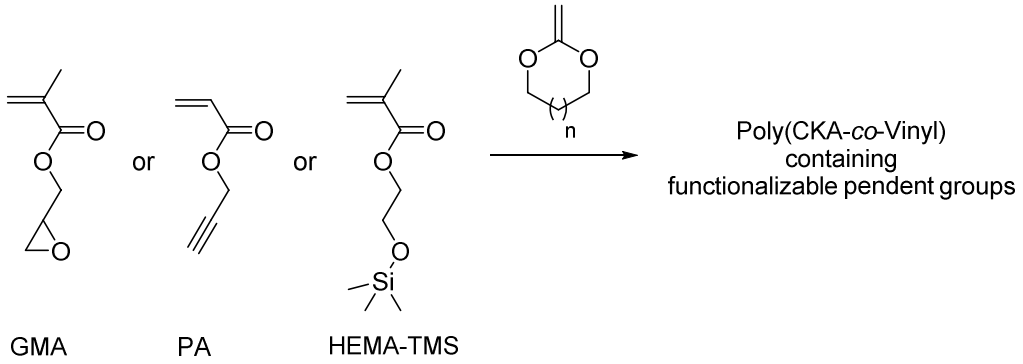

Scheme 1.15. Schematic representation of the copolymerization of GMA, PA and HEMA-TMS with CKA monomers to produce degradable copolymers able to undergo post-polymerization modifications.

1.3.2 Applications of RDRP techniques for the synthesis of degradable polymers from rROP

Although a large number of studies focusing on the homopolymerization and copolymerization of CKAs with vinyl monomers have been mainly performed by using conventional free radical polymerization, the increasing development in the area of controlled and "living" polymerization techniques (*e.g* NMP, ATRP, RAFT) has opened up a new area of research where such controlled techniques can be applied to CKA polymerization. Indeed, the use of such techniques to produce polymers with specific molecular weights, narrow molecular weight distributions and for the synthesis of block copolymers has, in the last decade, been seen as an emergent research area for the radical ring-opening polymerization of CKA monomers (Figure 1.8).

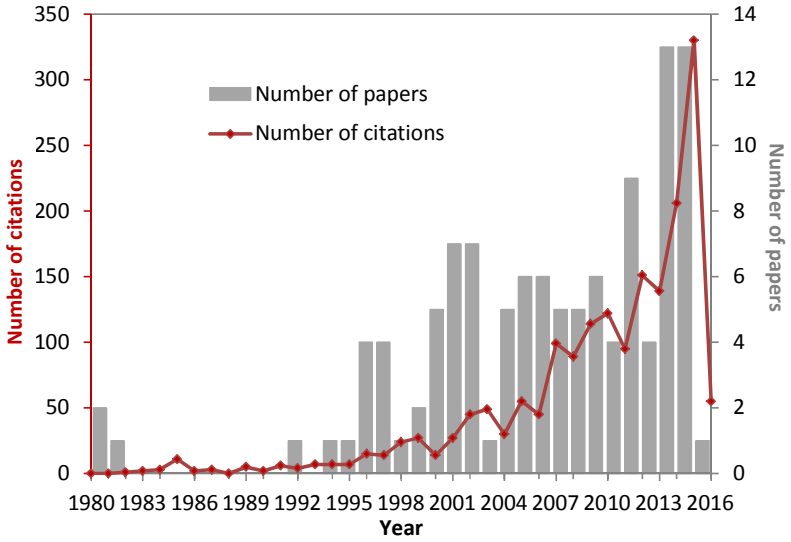

Figure 1.8. Number of papers and citations per year obtained by Web of Knowledge searching "2-methylene-1,3-dioxepane", April 2016.

The first example of a controlled polymerization process applied to the polymerization of a CKA was reported in the late 90s by Wei *et al*. for the rROP of MDO (**CKA 1**) using NMP and TEMPO (2,2,6,6-tetramethyl-1-piperidinyloxy) as the controlling agent (Scheme 1.16).[110,111] Under these conditions the complete ring-opening polymerization was observed with the formation of poly(esters) with "living" characteristics, as seen by the low dispersities ($Đ_M$ = 1.2 – 1.5) and the linear relationship between the number-average molecular weight, M_n, and the monomer conversion.

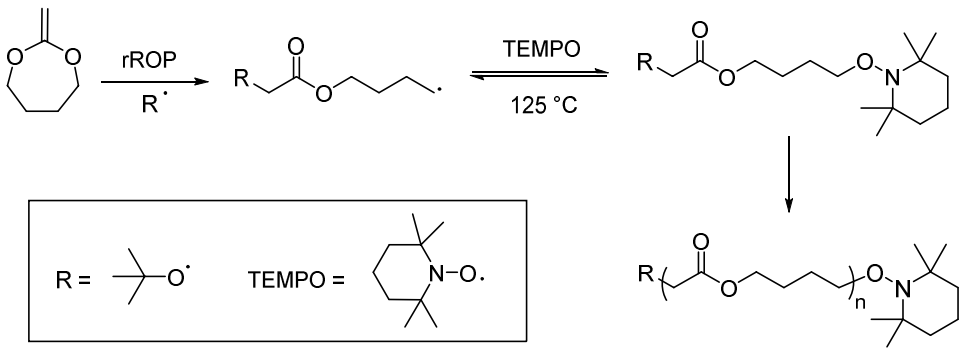

Scheme 1.16. Schematic representation of the controlled polymerization of MDO using NMP and TEMPO as reported by Wei *et al*.[110,111]

Other groups later studied the use of a controlled polymerization process in an attempt to mediate the polymerization of CKA monomers. Both Pan *et al*. and Yuan *et al*. investigated the polymerization of BMDO (**CKA 2**), DMDO (**CKA 13**) and MPDL (**CKA 7**) by ATRP using ethyl-α-bromobutyrate/CuBr/2,2-bipyridine at 120 °C for different polymerization times.[112,113] While the polymerization of BMDO was found to produce poly(esters) with narrow dispersities ($Đ_M$ < 1.40), controlled molecular weights and full ring-opened structure, the results obtained for MPDL and DMDO were less conclusive.[112] Indeed, although "living" features were observed in both cases, the final microstructure of poly(MPDL) and poly(DMDO) were found to consist of a mixture of ring-opened and ring-retained repeat units which was in contradiction with what had been previously reported for their polymerization using conventional free radical polymerization.[81,87,92] Additionally, for the study of MPDL, the ratio of ring-opened/ring-retained within the polymers as well as the controlled nature of the polymerization were found to vary depending on the temperature at which the reaction was carried out. When the polymerization was carried out at a higher temperature, 140 °C, the dispersity of the polymers was low, $Đ_M$ = 1.18, and the amount of ring-opened units within the backbone was high. Conversely, polymers with a broader dispersity of 1.42 were obtained for a polymerization performed at 80 °C while the amount of ring-opened units in the backbone was reduced.[112] Furthermore, other groups investigated the use of different RDRP techniques for control over the CKA polymerization. Indeed, initial studies were carried out by He *et al*. and reported the use of RAFT polymerization to mediate the homopolymerization of BMDO at 120 °C for 48 h using 1-(ethoxycarbonyl)prop-1-yl-dithiobenzoate as the chain transfer agent and dicumyl peroxide as the radical initiator.[114] Using such polymerization conditions, full radical ring-opening polymerization occurred and produced poly(esters) with controlled molecular weights, narrow dispersities ($Đ_M$ = 1.29 – 1.76), whist retaining the RAFT chain-end functionalities further confirming the controlled nature of the process.

The use of other "controlled" polymerization techniques for the copolymerization of CKAs with conventional monomers has also previously been attempted and aimed at producing degradable vinyl polymers with defined molecular weights. In an early report, Yuan *et al.* continued the use of ATRP with ethyl-α-bromobutyrate/CuBr/2,2-bipyridine but this time for the copolymerization of DMDO (**CKA 13**) and various vinyl monomers: styrene (St), acrylonitrile (AN) and methyl acrylate (MA).[115] The copolymerization of DMDO and St was found to lead to polymers with narrow dispersities ($Đ_M$ = 1.32 – 1.47) and a microstructure composed of 67 mol% ring-opened repeat units in the final copolymer. Nevertheless, the final content of BMDO within the polymer backbones was found to be relatively low with values between 3.3 and 7.3 mol%, suggesting a poor incorporation of degradable ester repeat units throughout the backbones. This observation was explained by the higher reactivity of styrene compared to the CKA monomers, as previously reported by Bailey *et al.* for a system of MDO and MMA (r_{St} = 22.6 and r_{MDO} = 0.057).[106] Furthermore, for the copolymerization of DMDO with AN and MA, a higher content of CKA within the polymer backbones (≈ 53%) could be achieved during the ATRP copolymerization but with lower conversions (20 – 29%) and boarder dispersities ($Đ_M$ = 1.53 – 1.90), especially for the polymerization with AN as a co-monomer. Similarly, Matyjaszewski and co-workers explored the copolymerization of BMDO and *n*-butyl acrylate (*n*BA) by also using ATRP with ethyl-2-bromoisobutyrate, with *N*,*N*,*N*',*N*''-pentamethyldiethylenetriamine/CuBr as the initiator and catalyst respectively.[116] For their studies different monomer feeds were investigated with BMDO feeds ranging from 20 to 80 mol% and yielding poly(BMDO-*co*-*n*BA) containing varying degradable content of 11 to 48 mol% and with dispersities between 1.54 and 1.84. The conversions of the monomers and yield were found to decrease as the content of BMDO in the copolymerization mixture was increased suggesting a lower reactivity of BMDO compared with *n*BA. This observation was confirmed by the determination of the reactivity ratios, obtained as r_{BMDO} = 0.08 and r_{nBA} = 3.7, implying a slightly better incorporation of the

CKA in the copolymer backbone when compared with other CKA/acrylate monomer systems.[105,107,109]

In the last three years, other groups have started to investigate the use of RDRP techniques for the copolymerization of CKAs with vinyl monomers, including Kobben *et al*. who reported the copolymerization of BMDO with MMA mediated by RAFT polymerization. The polymerization was carried out in anisole and at 110 °C using dicumyl peroxide and methyl-2-[([octylthio]carbonothioyl)thio]propanoate as initiator and chain transfer agent respectively.[117] While the controlled nature of the process was proposed, inferred from the low dispersities ($Đ_M$ < 1.50) obtained from the poly(BMDO-*co*-MMA) samples, a small low molecular weight tailing effect was often observed and hypothesized to result from the degradation product of the BMDO segments within the polymer. Furthermore, to extend the process of RAFT polymerization of this co-monomer system, they also used pentaerythritol-tetrakis-(3-(S-methyl-2-propanoatotrithiocarbonyl) propanoate), a four-armed chain transfer agent, to produce star polymers able to degrade under basic conditions (Figure 1.9).

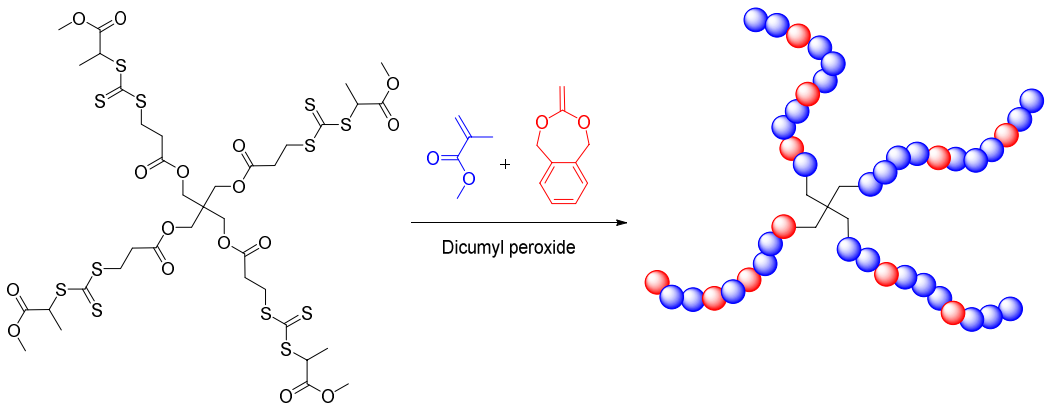

Figure 1.9. Schematic representation of the copolymerization of BMDO and MMA using a four-arm functional RAFT CTA as reported by Kobben *et al*.[117]

Similarly, d'Ayala *et al*. explored the RAFT mediated copolymerization of BMDO (**CKA 13**) with VAc for 24 h in toluene at 80 °C using AIBN and methyl (ethoxycarbonothioyl)sulfanyl acetate as xanthate chain transfer agent.[118] In their studies, the

content of BMDO in the co-monomer feed was varied from 5 to 30 mol% and was found to yield copolymers, poly(BMDO-*co*-VAc), containing up to 24 mol% of ester repeat units within the backbone. The full ring opening of BMDO was in all cases confirmed leading to successful linear degradable vinyl polymers. The controlled nature of the copolymerization process was evidenced by the obtained narrow molecular weight distributions ($Đ_M$ = 1.20 – 1.25) as well as the successful retention of the RAFT chain-ends on the polymer chains. These polymers were able to be further chain extended with VAc to create block copolymers of poly(BMDO-*co*-VAc)-*b*-poly(VAc) as confirmed from the increase in molecular weights from 2590 to 6000 g/mol after chain extension observed by size exclusion chromatography (SEC).

Additionally, Delplace *et al*. recently explored the copolymerization of various CKAs (BMDO, MDO and MPDL) with oligo (ethylene glycol) methyl ether methacrylate (OEGMA) and AN or St at 90 °C in anhydrous toluene using the NMP technique to produce degradable and comb-like PEG-based copolymers.[119,120] While three different CKAs were investigated, the use of BMDO and MDO was found to be limited to a low monomer feed (20 and 40 mol%) as a consequence of the poor control obtained for these copolymerizations when OEGMA conversions were ranging from 23% to 64%. Additionally, the final content of CKA units within the polymer backbone could not be quantified as a result of overlapping signals by ^{1}H Nuclear Magnetic Resonance (NMR) analysis, and while for some samples the amount could be identified it was notably low with a value of 6.4 mol%. Conversely, the use of MPDL was found to produce well-defined PEG-based copolymers with variable amounts of ester repeat units while maintaining a good control of the polymerization process as seen by the low dispersities (1.26 – 1.48) . The final copolymer toxicity was also assessed on different cell lines and revealed the cell-viability of the materials and its potential use in the biomedical field (Figure 1.10).

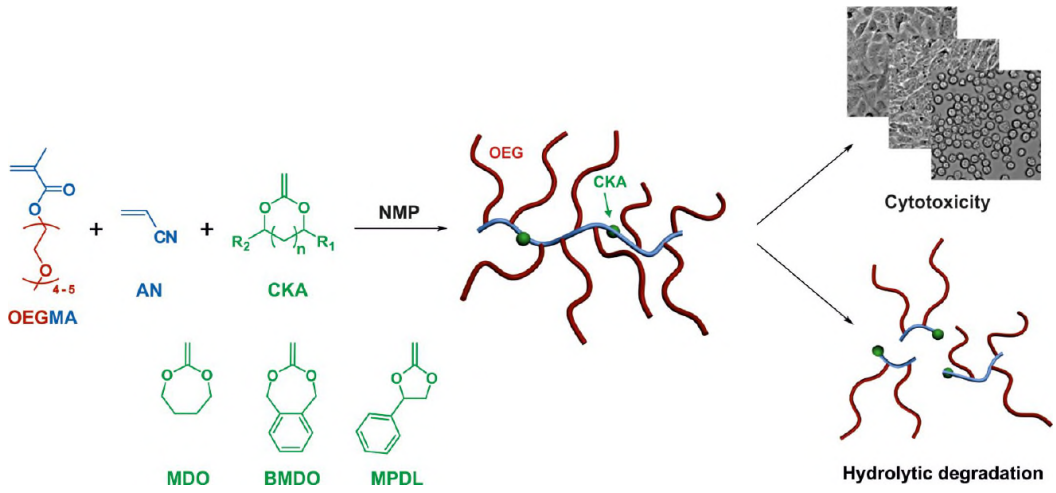

Figure 1.10. Schematic representation of the synthesis, cytotoxicity and degradability of PEG-based copolymers from nitroxide-mediated rROP of oligo(ethylene glycol) methyl ether (OEGMA), acrylonitrile (AN) and CKAs as reported by Delplace *et al*.[119]

While all these examples clearly highlight the ability to use controlled polymerization techniques on the homopolymerization and copolymerization of CKAs, there is still significant progress which can be made to develop a methodology which could be apply to CKAs with different ring sizes and functionalities to produce poly(esters) with controlled molecular weights, narrow dispersities, with a good incorporation of ester units to impart efficient degradability.

1.4 Self-assembly of polymers

Since the initial research into the formation of self-assemblies in nature, for example the formation of cell membranes from the self-assembly of phospholipids, such an understanding has become an essential part of our everyday life. Indeed, self-assemblies of small molecules consisting of one or more hydrophobic tail and a hydrophilic head group are nowadays found in a variety of applications such as cleaning products, cosmetic solutions and surfactants.[121] While the stability of self-assemblies of small molecules is often low, self-assemblies of polymeric materials tend to exhibit greater stability as a consequence of the higher mechanical and physical properties of the polymers. Furthermore, as a consequence

of the wide range of applications for these polymeric self-assemblies such as drug delivery vehicles,[122-126] nanoparticle imaging agents[127,128] and catalytic nanoreactors,[129-132] as well as the emergent development of controlled polymerization techniques (*e.g.* ROP, ATRP, NMP, RAFT), the desire to understand and synthesize self-assembled structures using polymers has significantly increased in recent decades.[125,133] The main polymers investigated for self-assembly are linear amphiphilic block copolymers, consisting of a hydrophilic block and a hydrophobic block (Figure 1.11).

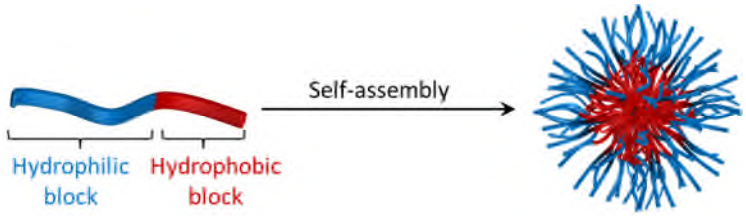

Figure 1.11. Schematic representation of the self-assembly of linear amphiphilic block copolymers.

These block copolymers will self-assemble in a specific medium to minimize the unfavourable hydrophilic/hydrophobic interactions between the polymer chains and surrounding medium.[125,133] Various morphologies can be obtained from the self-assembly of block copolymers, including spherical micelles,[133] cylindrical micelles,[125] lamellae[134] and vesicles,[135] among others (Figure 1.12). The morphology of self-assemblies is determined by the packing parameter, p, (equation 1):

$$p = \frac{v}{a_0 l_c} \qquad \text{(equation 1)}$$

where v is the volume of the hydrophilic tail, a_0 is the contact area of the hydrophilic head group and l_c is the length of the hydrophobic tail. Different morphologies can be formed depending on the value of the packing parameter: if $p < 1/3$, spherical micelles are obtained, if $1/3 < p < ½$, cylindrical micelles are observed and is $½ < p < 1$, vesicle structures are observed.[125]

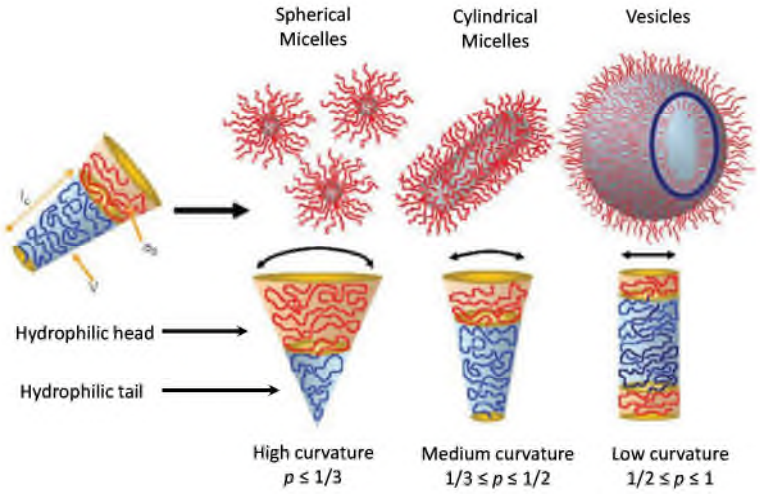

Figure 1.12. Schematic representation of the effect of the amphiphilic balance on the inherent curvature of the polymer and therefore on the adopted morphology of the polymer in solution.[125]

While the formation of self-assemblies has been thoroughly investigated with various polymers, the use of poly(esters) for the formation of nanoparticles remains an emergent topic.[94,136] Indeed, the potential to form self-assemblies with biocompatible, non-toxic and degradable properties could allow them to be applicable in the biomedical field. The first example of the self-assembly of poly(esters) was reported by Wooley and co-workers who investigated the synthesis of block copolymers of poly(ε-caprolactone)-*b*-poly(*tert*-butyl acrylate) (PCL-*b*-PtBA).[137] While the initial block copolymer PCL-*b*-PtBA was synthesized by a combination of ROP of ε-caprolactone and ATRP of *tert*-butyl acrylate, the polymer was later selectively hydrolyzed in order to obtain, after modifications, poly(ε-caprolactone)-*b* –poly(acrylic acid) (PCL-*b*-PAA) which was then self-assembled in aqueous medium to form well-defined spherical nanoparticles with hydrodynamic diameter, D_h, of 100 nm. Further modifications of the nanoparticles were also performed to cross-link the particles' shell in order to reinforce the structure to form, after degradation of the PCL core, polymeric nanocages. Following on from this pioneering work, many other groups later investigated the formation of self-assemblies using poly(esters), such as nanoparticles from PLLA-*b*-PNIPAm,[138] PCL-*b*-PHEMA[139,140] or PCL-*b*-poly(dimethylaminoethyl methacrylate)

(PDAEMA).[141] While the self-assemblies of poly(ester) based block copolymers has been widely investigated with polymers such as PCL or PLLA, the use of poly(esters) obtained from radical ring-opening polymerization of CKAs for the formation is self-assemblies is however significantly limited. Indeed, Jin *et al*. recently studied the copolymerization of MDO (**CKA 1**), EGMA and 7-(2-methacryloyloxyethoxy)-4-methylcoumarin methacrylate (CMA) using the conventional free radical polymerization at 90 °C using AIBN as the initiator (Figure 1.13).[142] The triblock copolymer synthesized, poly(MDO-*co*-EGMA-*co*-CMA) was found to self-assemble in aqueous medium and form nanoparticles with D_h ranging from 38 to 74 nm depending on the ratio of MDO/EGMA incorporated in the copolymers. The self-assemblies could then be cross-linked upon exposure to long wavelength of UV light at λ = 635 nm in order to encapsulate anticancer drug doxorubicin (DOX). Furthermore, the nanoparticles were found to show no signs of cytotoxicity while being able to undergo efficient degradation under enzymatic environments.

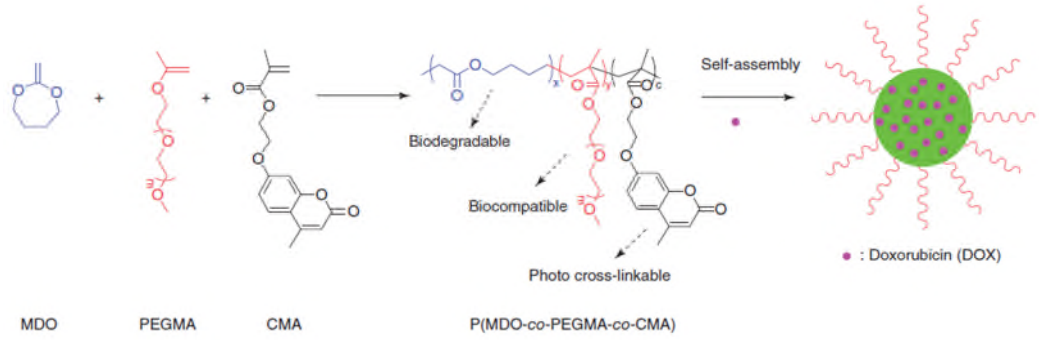

Figure 1.13. Schematic representation of the formation of degradable, cross-linkable self-assemblies of poly(MDO-*co*-EGMA-*co*-CMA) as reported by Jin *et al*.[142]

Although this example highlights the possibility of forming self-assemblies using degradable polymers from CKA monomers, there is still a broad range of monomers and polymer systems which could be investigated as a consequence of the various functional CKAs available and conventional vinyl monomers able to be copolymerized.

1.5 Responsive Polymers

Responsive polymers, often called "smart" polymers, are an interesting class of materials that have the ability to respond to external stimuli. The incorporation of such polymeric properties into linear block copolymers, branched polymers *etc*. can affect the amphiphilic balance of the polymers and change their properties and behaviour of the materials. Indeed, when the change in properties is significant enough, the polymer can adopt a different morphology. These types of changes for responsive polymers have been widely investigated in the biomedical and pharmaceutical fields for drug delivery[143,144] and nanoreactors.[145,146] Various common stimuli parameters have previously been investigated including: temperature,[147,148] pH,[149,150] and carbon dioxide.[151,152]

1.5.1 Thermoresponsive polymers

Within the "smart" polymer category, polymers that undergo a change in aqueous solubility upon temperature are classified as thermoresponsive polymers. Two types of thermoresponsive polymers can be found: those which display a lower critical solution temperature (LCST) and those that display an upper critical solution temperature (UCST). Polymers presenting an LCST phase transition are usually soluble below their LCST temperature and become insoluble above. Conversely, UCST polymers are insoluble below their UCST temperature and become soluble above. The phase separation of thermoresponsive polymers can be illustrated by plotting the temperature against the concentration to form a phase diagram (Figure 1.14).

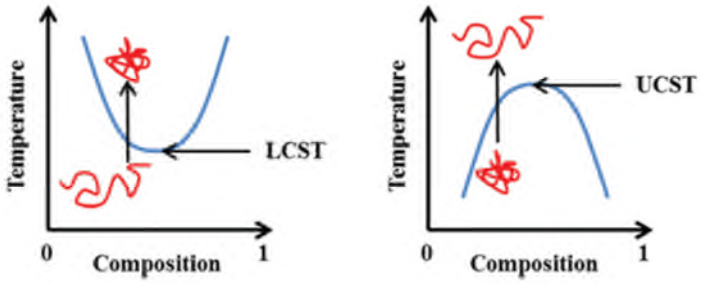

Figure 1.14. Schematic representation of the phase diagrams associated with the LCST and UCST observed for thermoresponsive polymers.[153]

The actual LCST and UCST are defined as the highest (or lowest for the UCST) point of the phase diagram. However in practice the phase diagram of thermoresponsive polymers is rarely determined and the LCST or UCST reported are in fact "cloud" points. The cloud point can be defined as the temperature at which a phase separation between the polymer and the aqueous medium will be observed at a specific concentration. The phase separation can be understood from the Flory-Huggins theory and the Gibbs free energy of mixing (ΔG_{mix}). For a system of two species, 1 and 2, the Gibbs free energy of mixing is dependent on both enthalpy and entropy (equation 2):

$$\Delta G_{mix} = kT\left[\frac{\varphi_1}{N_1} ln\varphi_1 + \frac{\varphi_2}{N_2} ln\varphi_2 + \chi\varphi_1\varphi_2\right] \qquad \text{(equation 2)}$$

Where, k is the Boltzmann constant, T is the temperature in Kelvin, φ_1 and φ_2 are the volume fractions of 1 and 2 respectively, N_1 and N_2 are the number of lattice sites occupied by species 1 and 2 and χ is the Flory-Huggins interaction parameter. In the case of a polymer in solution, the entropy of mixing will always be favoured, whereas the enthalpy of mixing will mostly depends on the interaction parameter, χ, which is also dependent on an entropic term, A, and enthalpic term, B (equation 3). Usually, when B is negative $\chi < 0$ and the mixing will be favoured, whereas when B is positive, $\chi > 0$ the mixing will be disfavoured.

$$\chi \cong \mathrm{A} + \frac{B}{T} \qquad \text{(equation 3)}$$

In the case of the LCST behaviour, χ depends strongly on the hydrogen bonding interactions between the polymer chains and the surrounding aqueous medium. Below the LCST the polymer is soluble and the polymer chains are flexible and in the form of an extended coil, whereas as the temperature is increased and the LCST is reached, the hydrogen bonding interactions are disrupted allowing the formation of intra- and inter-molecular interactions between polymer chains. Hence the polymers become insoluble in the aqueous medium and collapse and aggregate into a globular conformation (Figure 1.15).

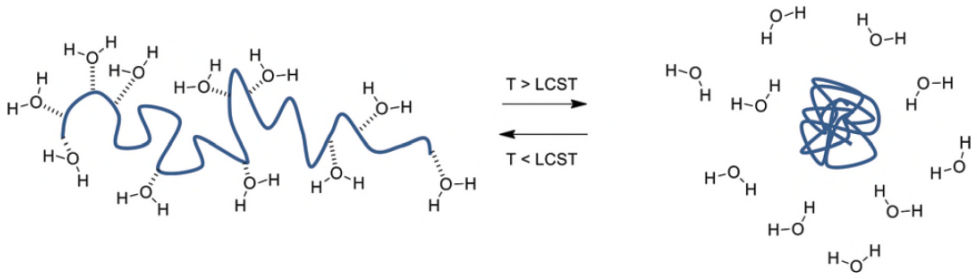

Figure 1.15. Schematic representation of the changes occurring for a polymer in solution below (left) and above (right) its LCST.[153]

Many polymers have been found to show thermoresponsive properties including: poly(*N*-vinylcaprolactam) (poly(VCL)),[154] poly(*N*-vinylpiperidone) (poly(VPip)),[155] poly(*N*,*N*-diethylacrylamide) (poly(DEAAm),[156] poly(*N*-isopropylacrylamide) (poly(NIPAm)),[157,158] and poly(ethylene glycol) (PEG).[159] Amongst them, poly(NIPAm) is probably the most studied and investigated thermoresponsive polymer as a consequence of its sharp phase transition close to body temperature (32 °C) which makes it an ideal candidate for biomedical applications. Furthermore, the copolymerization of NIPAm with other monomers (*e.g.* acrylic acid) has enabled variation of its transition temperature. Nevertheless, while presenting interesting thermoresponsive properties, its inability to degrade has often been a limitating parameter in biomedical or pharmaceutical areas. To overcome this issue, various research groups have attempted to incorporate degradability within poly(NIPAm)-based materials. Amongst them, Armes and co-workers reported the synthesis of disulfide-based

poly(NIPAm) triblock copolymers of poly(*N*-isopropylacrylamide)-*b*-poly(2-methacryloyloxyethyl phosphorylcholine)-*b*-poly(*N*-isopropylacrylamide) (PNIPAm-*b*-PMPC-*b*-PNIPAm) using ATRP.[160] In their study, the material was found to form a free-standing gel as a consequence of the disulfide linkages between the self-assemblies of the triblock copolymers which were able to undergo quantitative degradation under a physiological environment using the tripeptide, glutathione, while conserving a phase separation around 37 °C. More recently, Gibson and co-workers also investigated the incorporation of disulfide linkages into the homopolymer of poly(NIPAm) *via* the polycondensation of a RAFT-derived telechelic macromonomer of poly(NIPAm), to produce a degradable polymer having an LCST of 46.4 °C before degradation and 62.3 °C after reduction of the disulfide linkages.[161] The incorporation of degradability into thermoresponsive polymers has also been investigated using copolymerization of thermo-responsive monomers with CKAs. Indeed, Matyjaszewski and co-workers investigated the copolymerization of NIPAm and BMDO (**CKA 2**) using both the ATRP and RAFT polymerization techniques.[162] While the successful synthesis of copolymers with controlled molecular weights and narrow dispersities ($Đ_M$ < 1.2) was demonstrated, the addition of degradable BMDO repeat units within the polymer backbone was also found to influence the temperature of the phase transition, with values between 32 and 19 °C for an increasing amount of BMDO. A similar approach was later performed by Lutz *et al*. for the copolymerization of BMDO with oligo (ethylene glycol) methyl ether methacrylates (OEGMA, another thermoresponsive monomer) and 2-(2-methoxyethoxy)ethyl methacrylate (MEO_2MA) using conventional free radical polymerization to produce copolymers with tunable thermoresponsive and degradable properties.[163] Indeed, while the successful formation of poly(BMDO-*co*-OEGMA-*co*-MEO_2MA) was confirmed by both ^{1}H Nuclear Magnetic Resonance (NMR) and SEC analysis, the copolymers in solution were found to show LCST values ranging from 31 to 67 °C depending on the content of OEGMA and

MEO_2MA incorporated with the polymer backbone (Figure 1.16). The degradation of these copolymers was also successfully observed by the decrease in molecular weight from 12.2 kg/mol to 2.7 kg/mol before and after hydrolysis under basic conditions and confirmed by SEC analysis.

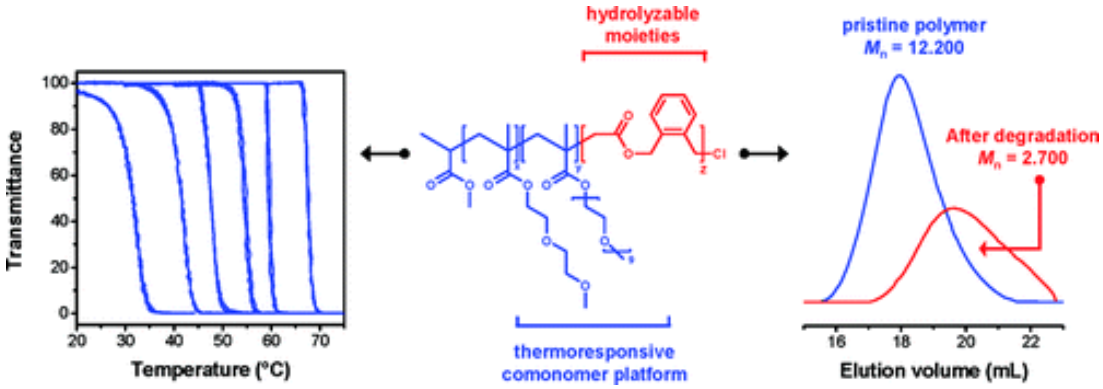

Figure 1.16. Schematic representation of the formation of degradable, thermoresponsive copolymers of BMDO with OEGMA and MEO2MA as reported by Lutz *et al*.[163]

These two last examples highlight the possibility of using CKA monomers to produce degradable copolymers that possess thermoresponsive properties which can be tuned easily by varying the copolymer compositions. While these two studies investigated the use of BMDO, other CKAs having different ring sizes and functionalities could also be used for the synthesis of such materials.

1.6 Conclusion

In this Chapter, the concept of "living" and controlled polymerization techniques has been introduced, with particular attention given to the RAFT polymerization technique which has been used in this thesis. The concept and synthetic approaches to produce degradable polymers, mainly aliphatic poly(esters), has also been discussed. The discovery and early developments of poly(esters) *via* the radical ring-opening polymerization of CKA monomers has been seen as attractive and alternative approach to produce degradable materials. This

approach has recently re-attracted a great amount of attention, with numerous studies using the improved controlled polymerization techniques to obtain well-defined polymers with controlled molecular weights and narrow dispersities. A summary of the pioneering studies regarding the CKA monomers and their copolymerizations has been introduced, as well as the recent trends regarding their use for the formation of degradable materials bearing functionalities able to increase the range of properties targeted for such materials.

1.7 References

(1) Darling, T. R.; Davis, T. P.; Fryd, M.; Gridnev, A. A.; Haddleton, D. M.; Ittel, S. D.; Matheson, R. R.; Moad, G.; Rizzardo, E. *J. Polym. Sci., Part A: Polym. Chem.* **2000**, *38*, 1706.

(2) Quirk, R. P.; Lee, B. *Polym. Int.* **1992**, *27*, 359.

(3) Szwarc, M. *Nature* **1956**, *178*, 1168.

(4) Hadjichristidis, N.; Pitsikalis, M.; Pispas, S.; Iatrou, H. *Chem. Rev.* **2001**, *101*, 3747.

(5) Aoshima, S.; Kanaoka, S. *Chem. Rev.* **2009**, *109*, 5245.

(6) Penczek, S.; Cypryk, M.; Duda, A.; Kubisa, P.; Słomkowski, S. *Prog. Polym. Sci.* **2007**, *32*, 247.

(7) Bielawski, C. W.; Grubbs, R. H. *Prog. Polym. Sci.* **2007**, *32*, 1.

(8) Braunecker, W. A.; Matyjaszewski, K. *Prog. Polym. Sci.* **2008**, *33*, 165.

(9) Goto, A.; Fukuda, T. *Prog. Polym. Sci.* **2004**, *29*, 329.

(10) Matyjaszewski, K. *Prog. Polym. Sci.* **2005**, *30*, 858.

(11) Colombani, D. *Prog. Polym. Sci.* **1997**, *22*, 1649.

(12) Odian, G. In *Principles of Polymerization*; John Wiley & Sons, Inc.: 2004, p 1.

(13) Young, R. J.; Lovell, P. A. In *Introduction to polymers*; CRC Press: 2011, p 61.

(14) Kato, M.; Kamigaito, M.; Sawamoto, M.; Higashimura, T. *Macromolecules* **1995**, *28*, 1721.

(15) Wang, J.-S.; Matyjaszewski, K. *J. Am. Chem. Soc.* **1995**, *117*, 5614.

(16) Matyjaszewski, K.; Patten, T. E.; Xia, J. *J. Am. Chem. Soc.* **1997**, *119*, 674.

(17) Matyjaszewski, K.; Gaynor, S.; Wang, J.-S. *Macromolecules* **1995**, *28*, 2093.

(18) Hawker, C. J.; Bosman, A. W.; Harth, E. *Chem. Rev.* **2001**, *101*, 3661.

(19) Hawker, C. J. *J. Am. Chem. Soc.* **1994**, *116*, 11185.

(20) Georges, M. K.; Veregin, R. P. N.; Kazmaier, P. M.; Hamer, G. K. *Macromolecules* **1993**, *26*, 2987.

(21) Chiefari, J.; Chong, Y. K.; Ercole, F.; Krstina, J.; Jeffery, J.; Le, T. P. T.; Mayadunne, R. T. A.; Meijs, G. F.; Moad, C. L.; Moad, G.; Rizzardo, E.; Thang, S. H. *Macromolecules* **1998**, *31*, 5559.

(22) Chiefari, J.; Mayadunne, R. T. A.; Moad, C. L.; Moad, G.; Rizzardo, E.; Postma, A.; Thang, S. H. *Macromolecules* **2003**, *36*, 2273.

(23) Moad, G.; Rizzardo, E.; Thang, S. H. *Aust. J. Chem.* **2005**, *58*, 379.

(24) Moad, G.; Rizzardo, E.; Thang, S. H. *Aust. J. Chem.* **2006**, *59*, 669.

(25) Moad, G.; Rizzardo, E.; Thang, S. H. *Aust. J. Chem.* **2009**, *62*, 1402.

(26) Moad, G.; Rizzardo, E.; Thang, S. H. *Polymer* **2008**, *49*, 1079.

(27) Zard, S. Z. *Angew. Chem. Int. Ed.* **1997**, *36*, 672.

(28) Destarac, M.; Brochon, C.; Catala, J.-M.; Wilczewska, A.; Zard, S. Z. *Macromol. Chem. Phys.* **2002**, *203*, 2281.

(29) Keddie, D. J.; Moad, G.; Rizzardo, E.; Thang, S. H. *Macromolecules* **2012**, *45*, 5321.

(30) Moad, G.; Chong, Y. K.; Postma, A.; Rizzardo, E.; Thang, S. H. *Polymer* **2005**, *46*, 8458.

(31) Skey, J.; O'Reilly, R. K. *Chem. Commun.* **2008**, 4183.

(32) Wood, M. R.; Duncalf, D. J.; Rannard, S. P.; Perrier, S. *Org. Lett.* **2006**, *8*, 553.

(33) Moad, G.; Rizzardo, E.; Thang, S. H. *Acc. Chem. Res.* **2008**, *41*, 1133.

(34) Okada, M. *Prog. Polym. Sci.* **2002**, *27*, 87.

(35) Nair, L. S.; Laurencin, C. T. *Prog. Polym. Sci.* **2007**, *32*, 762.

(36) Luckachan, G. E.; Pillai, C. K. S. *J. Polym. Environ.* **2011**, *19*, 637.

(37) Vert, M.; Santos, I. D.; Ponsart, S.; Alauzet, N.; Morgat, J.-L.; Coudane, J.; Garreau, H. *Polym. Int.* **2002**, *51*, 840.

(38) Mitrus, M.; Wojtowicz, A.; Moscicki, L. In *Thermoplastic Starch*; Wiley-VCH Verlag GmbH & Co. KGaA: 2010, p 1.

(39) Albertsson, A.-C.; Karlsson, S. In *Chemistry and Technology of Biodegradable Polymers*; Blackie: Glasgow, 1994, p 7.

(40) Funhoff, A. M.; van Nostrum, C. F.; Janssen, A. P. C. A.; Fens, M. H. A. M.; Crommelin, D. J. A.; Hennink, W. E. *Pharm. Res.* **2004**, *21*, 170.

(41) Wall, L. A.; Straus, S.; Flynn, J. H.; McIntyre, D.; Simha, R. *J. Phys. Chem.* **1966**, *70*, 53.

(42) Swift, G. In *Degradable Polymers Principles and Applications 2nd Edition*; Kluwer Academic Publishers: 2002, p 379.

(43) Marin, E.; Briceño, M. I.; Caballero-George, C. *Int. J. Nanomedicine* **2013**, *8*, 3071.

(44) Vroman, I.; Tighzert, L. *Materials* **2009**, *2*, 307.

(45) Rydz, J.; Sikorska, W.; Kyulavska, M.; Christova, D. *Int. J. Mol. Sci.* **2015**, *16*, 564.

(46) Zhang, C. In *Biodegradable Polyesters*; Wiley-VCH Verlag GmbH & Co. KGaA: 2015, p 1.

(47) Carothers, W. H.; Arvin, J. A. *J. Am. Chem. Soc.* **1929**, *51*, 2560.

(48) Carothers, W. H.; Arvin, J. A.; Dorough, G. L. *J. Am. Chem. Soc.* **1930**, *52*, 3292.

(49) Williams, C. K. *Chem. Soc. Rev.* **2007**, *36*, 1573.

(50) Stanford, M. J.; Dove, A. P. *Chem. Soc. Rev.* **2010**, *39*, 486.

(51) Lecomte, P.; Jérôme, C. *Adv. Polym. Sci.* **2012**, *245*, 173.

(52) Jérôme, C.; Lecomte, P. *Adv. Drug Deliv. Rev.* **2008**, *60*, 1056.

(53) Carpentier, J.-F. *Macromol. Rapid Commun.* **2010**, *31*, 1696.

(54) Mecerreyes, D.; Jérôme, R. *Macromol. Chem. Phys.* **1999**, *200*, 2581.

(55) Kobayashi, S. *Macromol. Symp.* **2006**, *240*, 178.

(56) Castano, M.; Zheng, J.; Puskas, J. E.; Becker, M. L. *Polym. Chem.* **2014**, *5*, 1891.

(57) Kamber, N. E.; Jeong, W.; Waymouth, R. M.; Pratt, R. C.; Lohmeijer, B. G. G.; Hedrick, J. L. *Chem. Rev.* **2007**, *107*, 5813.

(58) Dove, A. P. *ACS Macro Lett.* **2012**, *1*, 1409.

(59) Thomas, C.; Bibal, B. *Green Chem.* **2014**, *16*, 1687.

(60) Albertsson, A.-C.; Srivastava, R. K. *Adv. Drug Deliv. Rev.* **2008**, *60*, 1077.

(61) Kobayashi, S. *Macromol. Rapid Commun.* **2009**, *30*, 237.

(62) Kiesewetter, M. K.; Shin, E. J.; Hedrick, J. L.; Waymouth, R. M. *Macromolecules* **2010**, *43*, 2093.

(63) Lohmeijer, B. G. G.; Pratt, R. C.; Leibfarth, F.; Logan, J. W.; Long, D. A.; Dove, A. P.; Nederberg, F.; Choi, J.; Wade, C.; Waymouth, R. M.; Hedrick, J. L. *Macromolecules* **2006**, *39*, 8574.

(64) Onbulak, S.; Tempelaar, S.; Pounder, R. J.; Gok, O.; Sanyal, R.; Dove, A. P.; Sanyal, A. *Macromolecules* **2012**, *45*, 1715.

(65) Pratt, R. C.; Lohmeijer, B. G. G.; Long, D. A.; Waymouth, R. M.; Hedrick, J. L. *J. Am. Chem. Soc.* **2006**, *128*, 4556.

(66) Martello, M. T.; Burns, A.; Hillmyer, M. *ACS Macro Lett.* **2012**, *1*, 131.

(67) Cajot, S.; Lecomte, P.; Jerome, C.; Riva, R. *Polym. Chem.* **2013**, *4*, 1025.

(68) Riva, R.; Schmeits, S.; Stoffelbach, F.; Jerome, C.; Jerome, R.; Lecomte, P. *Chem. Commun.* **2005**, 5334.

(69) Carrot, G.; Hilborn, J. G.; Trollsås, M.; Hedrick, J. L. *Macromolecules* **1999**, *32*, 5264.

(70) Korich, A. L.; Walker, A. R.; Hincke, C.; Stevens, C.; Iovine, P. M. *J. Polym. Sci., Part A: Polym. Chem.* **2010**, *48*, 5767.

(71) Jacquier, V.; Miola, C.; Llauro, M.-F.; Monnet, C.; Hamaide, T. *Macromol. Chem. Phys.* **1996**, *197*, 1311.

(72) de Freitas, A. G. O.; Trindade, S. G.; Muraro, P. I. R.; Schmidt, V.; Satti, A. J.; Villar, M. A.; Ciolino, A. E.; Giacomelli, C. *Macromol. Chem. Phys.* **2013**, *214*, 2336.

(73) Liu, M.; Vladimirov, N.; Fréchet, J. M. J. *Macromolecules* **1999**, *32*, 6881.

(74) Wilson, J. A.; Hopkins, S. A.; Wright, P. M.; Dove, A. P. *Macromolecules* **2015**, *48*, 950.

(75) Li, G.; Lamberti, M.; Pappalardo, D.; Pellecchia, C. *Macromolecules* **2012**, *45*, 8614.

(76) Wurth, J. J.; Shastri, V. P. *J. Polym. Sci., Part A: Polym. Chem.* **2013**, *51*, 3375.

(77) Delplace, V.; Nicolas, J. *Nat Chem* **2015**, *7*, 771.

(78) Agarwal, S. *Polym. Chem.* **2010**, *1*, 953.

(79) Agarwal, S. In *Biodegradable Polyesters*; Wiley-VCH Verlag GmbH & Co. KGaA: 2015, p 25.

(80) Bailey, W. J.; Ni, Z.; Wu, S.-R. *J. Polym. Sci., Part A: Polym. Chem.* **1982**, *20*, 3021.

(81) Bailey, W. J.; Ni, Z.; Wu, S. R. *Macromolecules* **1982**, *15*, 711.

(82) Endo, T.; Bailey, W. J. *J. Polym. Sci., Polym. Lett. Ed.* **1975**, *13*, 193.

(83) Endo, T.; Bailey, W. J. *J. Polym. Sci., Part A: Polym. Chem.* **1975**, *13*, 2525.

(84) Bailey, W. J.; Endo, T. *J. Polym. Sci., Polym. Symp.* **1978**, *64*, 17.

(85) Bailey, W. J.; Endo, T. *J. Polym. Sci., Part A: Polym. Chem.* **1976**, *14*, 1735.

(86) Wickel, H.; Agarwal, S.; Greiner, A. *Macromolecules* **2003**, *36*, 2397.

(87) Bailey, W. J.; Wu, S.-R.; Ni, Z. *Macromol. Chem. Phys.* **1982**, *183*, 1913.

(88) Bailey, W. J.; Wu, S.-R.; Ni, Z. *J. Macromol. Sci. A.* **1982**, *18*, 973.

(89) Yokozawa, T.; Hayashi, R.; Endo, T. *J. Polym. Sci., Part A: Polym. Chem.* **1990**, *28*, 3739.

(90) Agarwal, S. *Polym. J.* **2007**, *39*, 163.

(91) Jin, S.; Gonsalves, K. E. *Macromolecules* **1997**, *30*, 3104.

(92) Endo, T.; Okawara, M.; Bailey, W. J.; Azuma, K.; Nate, K.; Yokono, H. *J. Polym. Sci., Polym. Lett. Ed.* **1983**, *21*, 373.

(93) Cho, I.; Kim, S.-K. *J. Polym. Sci., Part C: Polym. Lett.* **1990**, *28*, 417.

(94) Pounder, R. J.; Dove, A. P. *Polym. Chem.* **2010**, *1*, 260.

(95) Ates, Z.; Thornton, P. D.; Heise, A. *Polym. Chem.* **2011**, *2*, 309.

(96) Plikk, P.; Tyson, T.; Finne-Wistrand, A.; Albertsson, A.-C. *J. Polym. Sci., Part A: Polym. Chem.* **2009**, *47*, 4587.

(97) Sanda, F.; Takata, T.; Endo, T. *Macromolecules* **1994**, *27*, 1099.

(98) Liu, W.; Mikeš, F.; Guo, Y.; Koike, Y.; Okamoto, Y. *J. Polym. Sci., Part A: Polym. Chem.* **2004**, *42*, 5180.

(99) Undin, J.; Illanes, T.; Finne-Wistrand, A.; Albertsson, A.-C. *Polym. Chem.* **2012**, *3*, 1260.

(100) Agarwal, S.; Kumar, R.; Kissel, T.; Reul, R. *Polym. J.* **2009**, *41*, 650.

(101) Agarwal, S. *J. Polym. Res.* **2006**, *13*, 403.

(102) Maji, S.; Zheng, M.; Agarwal, S. *Macromol. Chem. Phys.* **2011**, *212*, 2573.

(103) Agarwal, S.; Kumar, R. *Macromol. Chem. Phys.* **2011**, *212*, 603.

(104) Grabe, N.; Zhang, Y.; Agarwal, S. *Macromol. Chem. Phys.* **2011**, *212*, 1327.

(105) Sun, L. F.; Zhuo, R. X.; Liu, Z. L. *J. Polym. Sci., Part A: Polym. Chem.* **2003**, *41*, 2898.

(106) Bailey, W. J.; Endo, T.; Gapud, B.; Lin, Y.-N.; Ni, Z.; Pan, C.-Y.; Shaffer, S. E.; Wu, S.-R.; Yamazaki, N.; Yonezawa, K. *J. Macromol. Sci. A.* **1984**, *21*, 979.

(107) Roberts, G. E.; Coote, M. L.; Heuts, J. P. A.; Morris, L. M.; Davis, T. P. *Macromolecules* **1999**, *32*, 1332.

(108) Undin, J.; Finne-Wistrand, A.; Albertsson, A.-C. *Biomacromolecules* **2014**, *15*, 2800.

(109) Undin, J.; Finne-Wistrand, A.; Albertsson, A.-C. *Biomacromolecules* **2013**, *14*, 2095.

(110) Wei, Y.; Connors, E. J.; Jia, X.; Wang, B. *Chem. Mater.* **1996**, *8*, 604.

(111) Wei, Y.; Connors, E. J.; Jia, X.; Wang, C. *J. Polym. Sci., Part A: Polym. Chem.* **1998**, *36*, 761.

(112) Yuan, J.-Y. P., Cai-yuan *Chin. J. Polym. Sci.* **2001**, *20*, 9.

(113) Pan, C.-Y.; Lou, X.-D. *Macromol. Chem. Phys.* **2000**, *201*, 1115.

(114) He, T.; Zou, Y.-F.; Pan, C.-Y. *Polym. J.* **2002**, *34*, 138.

(115) Yuan, J.-Y.; Pan, C.-Y. *Eur. Polym. J.* **2002**, *38*, 2069.

(116) Huang, J.; Gil, R.; Matyjaszewski, K. *Polymer* **2005**, *46*, 11698.

(117) Kobben, S.; Ethirajan, A.; Junkers, T. *J. Polym. Sci., Part A: Polym. Chem.* **2014**, *52*, 1633.

(118) d'Ayala, G. G.; Malinconico, M.; Laurienzo, P.; Tardy, A.; Guillaneuf, Y.; Lansalot, M.; D'Agosto, F.; Charleux, B. *J. Polym. Sci., Part A: Polym. Chem.* **2014**, *52*, 104.

(119) Delplace, V.; Tardy, A.; Harrisson, S.; Mura, S.; Gigmes, D.; Guillaneuf, Y.; Nicolas, J. *Biomacromolecules* **2013**, *14*, 3769.

(120) Delplace, V.; Harrisson, S.; Tardy, A.; Gigmes, D.; Guillaneuf, Y.; Nicolas, J. *Macromol. Rapid Commun.* **2014**, *35*, 484.

(121) Mai, Y.; Eisenberg, A. *Chem. Soc. Rev.* **2012**, *41*, 5969.

(122) Meng, F.; Zhong, Z.; Feijen, J. *Biomacromolecules* **2009**, *10*, 197.

(123) Rodríguez-Hernández, J.; Chécot, F.; Gnanou, Y.; Lecommandoux, S. *Prog. Polym. Sci.* **2005**, *30*, 691.

(124) Elsabahy, M.; Wooley, K. L. *Chem. Soc. Rev.* **2012**, *41*, 2545.

(125) Blanazs, A.; Armes, S. P.; Ryan, A. J. *Macromol. Rapid Commun.* **2009**, *30*, 267.

(126) Pawar, P. V.; Gohil, S. V.; Jain, J. P.; Kumar, N. *Polym. Chem.* **2013**, *4*, 3160.

(127) Ge, Z.; Liu, S. *Chem. Soc. Rev.* **2013**, *42*, 7289.

(128) Trubetskoy, V. S. *Adv. Drug Deliv. Rev.* **1999**, *37*, 81.

(129) Gaitzsch, J.; Huang, X.; Voit, B. *Chem. Rev.* **2016**, *116*, 1053.

(130) Cotanda, P.; O'Reilly, R. K. *Chem. Commun.* **2012**, *48*, 10280.

(131) Cotanda, P.; Petzetakis, N.; O'Reilly, R. K. *MRS Communications* **2012**, *2*, 119.

(132) Vriezema, D. M.; Comellas Aragonès, M.; Elemans, J. A. A. W.; Cornelissen, J. J. L. M.; Rowan, A. E.; Nolte, R. J. M. *Chem. Rev.* **2005**, *105*, 1445.

(133) Riess, G. *Prog. Polym. Sci.* **2003**, *28*, 1107.

(134) Limouzin-Morel, C.; Dutertre, F.; Moussa, W.; Gaillard, C.; Iliopoulos, I.; Bendejacq, D.; Nicolai, T.; Chassenieux, C. *Soft Matter* **2013**, *9*, 8931.

(135) Discher, D. E.; Eisenberg, A. *Science* **2002**, *297*, 967.

(136) Dove, A. P. *Chem. Commun.* **2008**, 6446.

(137) Zhang, Q.; Remsen, E. E.; Wooley, K. L. *J. Am. Chem. Soc.* **2000**, *122*, 3642.

(138) Hales, M.; Barner-Kowollik, C.; Davis, T. P.; Stenzel, M. H. *Langmuir* **2004**, *20*, 10809.

(139) Wiltshire, J. T.; Qiao, G. G. *Macromolecules* **2006**, *39*, 9018.

(140) Le Hellaye, M.; Lefay, C.; Davis, T. P.; Stenzel, M. H.; Barner-Kowollik, C. *J. Polym. Sci., Part A: Polym. Chem.* **2008**, *46*, 3058.

(141) Liu, H.; Xu, J.; Jiang, J.; Yin, J.; Narain, R.; Cai, Y.; Liu, S. *J. Polym. Sci., Part A: Polym. Chem.* **2007**, *45*, 1446.

(142) Jin, Q.; Maji, S.; Agarwal, S. *Polym. Chem.* **2012**, *3*, 2785.

(143) Zhang, Q.; Re Ko, N.; Kwon Oh, J. *Chem. Commun.* **2012**, *48*, 7542.

(144) Mura, S.; Nicolas, J.; Couvreur, P. *Nat. Mater.* **2013**, *12*, 991.

(145) Zayas, H. A.; Lu, A.; Valade, D.; Amir, F.; Jia, Z.; O'Reilly, R. K.; Monteiro, M. J. *ACS Macro Lett.* **2013**, *2*, 327.

(146) Jiang, X.; Xiong, D. A.; An, Y.; Zheng, P.; Zhang, W.; Shi, L. *J. Polym. Sci., Part A: Polym. Chem.* **2007**, *45*, 2812.

(147) Gibson, M. I.; O'Reilly, R. K. *Chem. Soc. Rev.* **2013**, *42*, 7204.

(148) Roy, D.; Brooks, W. L. A.; Sumerlin, B. S. *Chem. Soc. Rev.* **2013**, *42*, 7214.

(149) Dai, S.; Ravi, P.; Tam, K. C. *Soft Matter* **2008**, *4*, 435.

(150) Doncom, K. E. B.; Willcock, H.; O'Reilly, R. K. *J. Polym. Sci., Part A: Polym. Chem.* **2014**, *52*, 3026.

(151) Lin, S.; Theato, P. *Macromol. Rapid Commun.* **2013**, *34*, 1118.

(152) Guo, Z.; Feng, Y.; Wang, Y.; Wang, J.; Wu, Y.; Zhang, Y. *Chem. Commun.* **2011**, *47*, 9348.

(153) Phillips, D. J.; Gibson, M. I. *Polym. Chem.* **2015**, *6*, 1033.

(154) Cortez-Lemus, N. A.; Licea-Claverie, A. *Prog. Polym. Sci.* **2016**, *53*, 1.

(155) Ieong, N. S.; Redhead, M.; Bosquillon, C.; Alexander, C.; Kelland, M.; O'Reilly, R. K. *Macromolecules* **2011**, *44*, 886.

(156) Idziak, I.; Avoce, D.; Lessard, D.; Gravel, D.; Zhu, X. X. *Macromolecules* **1999**, *32*, 1260.

(157) Blackman, L. D.; Wright, D. B.; Robin, M. P.; Gibson, M. I.; O'Reilly, R. K. *ACS Macro Lett.* **2015**, *4*, 1210.

(158) Schild, H. G. *Prog. Polym. Sci.* **1992**, *17*, 163.

(159) Lutz, J.-F.; Hoth, A. *Macromolecules* **2006**, *39*, 893.

(160) Li, C.; Madsen, J.; Armes, S. P.; Lewis, A. L. *Angew. Chem. Int. Ed.* **2006**, *45*, 3510.

(161) Phillips, D. J.; Gibson, M. I. *Chem. Commun.* **2012**, *48*, 1054.

(162) Siegwart, D. J.; Bencherif, S. A.; Srinivasan, A.; Hollinger, J. O.; Matyjaszewski, K. *J. Biomed. Mater. Res. A.* **2008**, *87A*, 345.

(163) Lutz, J.-F.; Andrieu, J.; Üzgün, S.; Rudolph, C.; Agarwal, S. *Macromolecules* **2007**, *40*, 8540.

2 Functional Degradable Polymers by Xanthate-Mediated Polymerization

2.1 Abstract

In this Chapter the copolymerization of vinyl acetate (VAc) and 2-methylene-1,3-dioxepane (MDO) is presented using the Reversible Addition-Fragmentation Chain Transfer (RAFT) polymerization (also known as MADIX (Macromolecular Design *via* Interchange of Xanthates) when xanthates are used as chain transfer agent) to deliver a range of functional degradable polymers *via* a controlled radical ring-opening polymerization process. The copolymerization could be tuned to vary the incorporation of degradable segments in the polymer backbone to create degradable materials with predictable molecular weight and low dispersity values while also featuring side-chain functionality. Additionally, the methodology was also applied to other less activated monomers including *N*-vinylpyrrolidone (NVP), *N*-vinylpiperidone (VPip) and vinyl chloroacetate (VClAc) resulting in the formation of other degradable copolymers containing different functionalities.

2.2 Introduction

Aliphatic polyesters are an interesting class of polymers that are widely applied in the biomedical field as a consequence of their ability to undergo degradation in physiological conditions.[1-3] The most commonly used aliphatic polyesters are synthesized *via* ring-opening polymerization (ROP) of cyclic lactones *(e.g.* ε-caprolactone (CL), lactide (LA)) in the presence of a catalyst and/or an initiator.[4-9] Poly(ε-caprolactone) (PCL), possibly the most studied polyester, has been widely studied and applied in the biomedical field owing to its excellent mechanical strength, thermal properties, bio-compatibility, and non-toxicity, all of which make it an ideal polymer candidate as an implantable carrier or in tissue engineering applications.[10,11]

A large amount of research has been focused on the incorporation of functionalities into the PCL backbone in an attempt to increase the range of properties that could be targeted.[12-16] However, the incorporation of functional groups into PCL remains synthetically challenging and is currently limited to only a few approaches: functionalization of ε-caprolactone (CL),[12,13,17,18] chain end modification,[14,15] and/or copolymerization of CL with functional monomers.[16,19] While all these approaches have been successful towards the aim of introducing additional functionalities into PCL, they present some limitations including arduous syntheses and yield-lowering protection/deprotection steps during the functional monomers synthesis reactions, poor functional group compatibility with the catalyst and polymerizations conditions, and/or a poor match of reactivity ratios of the monomers for copolymerization approaches.[7,14,15,17,20-25]

In recent years, studies have presented an alternative route for the synthesis of a PCL-like polymer by the radical ring-opening polymerization (rROP) of the seven membered cyclic ketene acetal (CKA) 2-methylene-1,3-dioxepane (MDO) (Scheme 2.1).[26-29] This approach leads to a polymer containing the same repeat units as for conventional PCL synthesized by the ROP of CL and opens a new way of synthesizing functional degradable PCL-like polymers by copolymerization of MDO with functional vinyl monomers by radical polymerization.

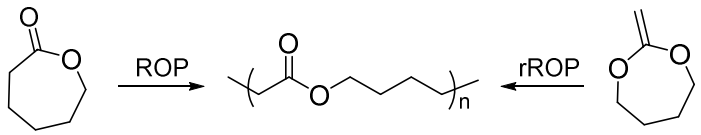

Scheme 2.1. Schematic representation of the analogy between the formation of PCL from ROP of CL and PCL-substitute from rROP of MDO.

Indeed, the copolymerization of MDO with vinyl monomers such as methyl methacrylate (MMA),[30,31] methyl acrylate (MA),[32] styrene (St),[33-38] propargyl

acrylate (PA),[39] and vinyl acetate (VAc)[26,40] has been reported to successfully form degradable polymers. The copolymerization of VAc and MDO monomers is of particular interest as a consequence of its ability to form copolymers with a random monomer distribution as a result of their similar reactivity ratios.[26,40] These copolymerizations were initially performed by conventional free radical polymerization leading to the formation of polymers with broad molecular weight distributions and poor control of their molecular weight. These drawbacks can be overcome by the use of controlled polymerization techniques, such as reversible deactivation radical polymerizations (RDRP), which have recently attracted a wide interest in an attempt to synthesize controlled and well-defined polymers from the rROP of CKAs.[36,41-46] The use of RDRP techniques to produce degradable polymers from the rROP of cyclic ketene acetals has mainly been applied to two substituted CKAs: 5,6-benzo-2-methylene-1,3-dioxepane (BMDO)[36,42-44,46-49] and 2-methylene-4-phenyl-1,3-dioxolane (MPDL) (Scheme 2.2).[36,46]

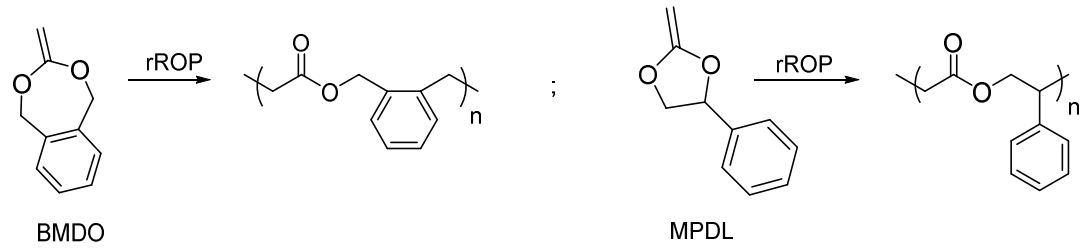

Scheme 2.2. Schematic representation of the radical ring-opening polymerization of BMDO (left) and MPDL (right) towards the formation of their corresponding polymers.

In these examples, controlled aspects of the polymerization were shown, as well as the incorporation of degradable units in the vinyl polymeric backbone. However, incorporation of aromatic groups (*e.g.* BMDO) into the polymer backbone drastically alters the physical properties of the final polymer (*e.g.* crystallinity, glass transition temperature, T_g) and does not provide a viable alternative route for the synthesis of PCL. A limited number of defined methodologies to produce controlled and well-

defined PCL-substitute polymers from the non-functional CKA, MDO, have been reported and only a few attempts were conducted using RDRP techniques.[36,49,50] Wei and co-workers investigated the use of 2,2,6,6-tetramethyl-1-piperidinyloxy (TEMPO), a nitroxide-mediated polymerization (NMP) technique, to partially control the polymerization of MDO and showed good increase of the molecular weights while maintaining a decrease of the dispersities.[41,50] However, the process was limited to low monomer conversions and high reaction temperatures, often leading to multimodal peaks. More recently, Delplace and co-workers also investigated the use of NMP to mediate the copolymerization of poly(ethylene glycol) methyl ether methacrylate (PEGMA) and MMA with MDO and demonstrated control with dipersities, $Đ_M$, < 1.40. Nevertheless, initial monomer feeds used were only 20 and 40 mol% in MDO limiting the final incorporation of ester repeat units in the final copolymers as a consequence of the differences in reactivity ratios between CKAs and acrylate monomers.[36,46]

In this chapter the RAFT/MADIX (Macromolecular Design by Interchange of Xanthates) copolymerization of the CKA MDO with VAc and other vinyl monomers in an attempt to produce well-defined, side-chain functional biodegradable polymers *via* a facile radical polymerization method is presented.

2.3 Results and Discussion

2.3.1 Initial investigations of the copolymerization of MDO and VAc using RAFT/MADIX polymerization

To demonstrate the potential use of a controlled polymerization technique on the co-monomer system of VAc and MDO, the RAFT/MADIX technique was chosen as a consequence of its simple approach and its high tolerance to a wide range of conditions.[51-53] The use of xanthates as chain transfer agents (CTAs) has been

previously reported for the successful controlled polymerization of VAc.[54-57] Hence, initial experiments were performed where three different xanthate CTAs (Figure 2.1), analogues of a xanthate previously reported for the polymerization of "less activated" vinyl monomers,[57,58] were herein used to mediate the copolymerization of MDO and VAc. The copolymerizations were performed in bulk at 60 °C, with 2,2'-azobis(isobutyronitrile) (AIBN) as the radical initiator, and a CTA, either *O*-hexyl-*S*-methyl 2-propionylxanthate (CTA 1), *O*-isopropyl-*S*-methyl 2-propionylxanthate (CTA 2), or *O*-ethyl-*S*-methyl 2-propionylxanthate (CTA 3) (Figure 2.1), such that $[MDO]_0/[VAc]_0/[AIBN]_0/[CTA]_0$ = 30:70:0.1:1. After five hours of polymerization, the copolymers, poly(MDO-*co*-VAc), from each set of conditions were characterized using ^{1}H NMR spectroscopy and size exclusion chromatography (SEC) and compared with each other.

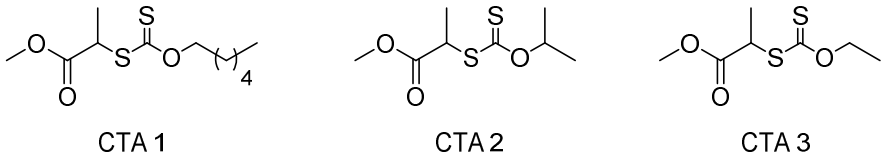

Figure 2.1. Schematic representation of the chemical structures of the three different xanthates used as chain transfer agents in the bulk polymerization of VAc and MDO.

The initial copolymerization using CTA 1 was found to lead to a copolymer with a low dispersity ($Đ_M$ = 1.40) indicating that good control was maintained during the reaction (Table 2.1) while good monomer conversions could be achieved. In comparison, the copolymerization using CTA 2, was found to produce a copolymer of poly(MDO-*co*-VAc) with a higher dispersity, $Đ_M$, of 1.69, suggesting that a less control polymerization was occurring, potentially as a consequence of a side reaction where the Z-group of the CTA could be eliminated during the polymerization and produce a copolymer with dead chain ends (this aspect is investigated in Chapter 4). Similarly, the reaction using CTA 3 was initially found to show good control of the

copolymerization at an early stage (MDO monomer conversions < 20%) but an increase in dispersities was also observed when the monomer conversions increased leading to a poor control of the polymerization, compared to CTA 1. Therefore, following these initial results and to maintain a good degree of control throughout the process, the copolymerizations of MDO and VAc presented in this chapter were all performed using the CTA with the longer alkyl chain as the Z group (CTA 1) as it was the most suited chain transfer agent to achieve the desired synthesis of well-defined and controlled copolymers of poly(MDO-*co*-VAc).

Table 2.1. Characterization data for the copolymerization of MDO and VAc (30/70 mol%) using CTAs 1, 2 and 3 as the chain transfer agents.

CTA	VAc conv. [a] (%)	MDO conv. [a] (%)	M_n [theo b] (kg/mol)	M_n [SEC c] (kg/mol)	$Đ_M$ [c]
1	40	30	3.7	4.6	1.40
2	42	28	3.7	7.0	1.69
3	35	17	2.9	4.0	1.46

[a] conversion determined by ^{1}H NMR spectroscopy, [b] theoretical molecular weight based on monomer conversion (^{1}H NMR spectroscopy),[c] obtained by SEC analyses in $CHCl_3$

Following the previous results for the choice of the CTA for the copolymerization of MDO and VAc, further experiments were conducted where the reaction was performed using similar conditions, 60 °C, in bulk, AIBN, and CTA 1 (Scheme 2.3). The copolymerization was conducted such that $[MDO]_0/[VAc]_0/[AIBN]_0/[CTA\ 1]_0$ = 50:50:0.1:1. After five hours of reaction, the resultant polymer displayed a dispersity, $Đ_M$, < 1.60 when analyzed by size exclusion chromatography (SEC). ^{1}H NMR spectroscopic analysis revealed monomer conversions of 62% and 44% for VAc and MDO respectively and a molecular weight close to that expected on the basis of the monomer:CTA ratio which indicates high retention of the chain-end. These observations suggest that CTA 1 was again well-suited to copolymerize the MDO/VAc system even for different ratios of monomers. Additionally, the

controlled aspect of the polymerization was also confirmed by the good correlation between the UV trace of the SEC at λ = 280 nm (absorbing wavelength of xanthates) and the RI trace showing that the xanthate group has been retained throughout the polymerization (Figure 2.2).

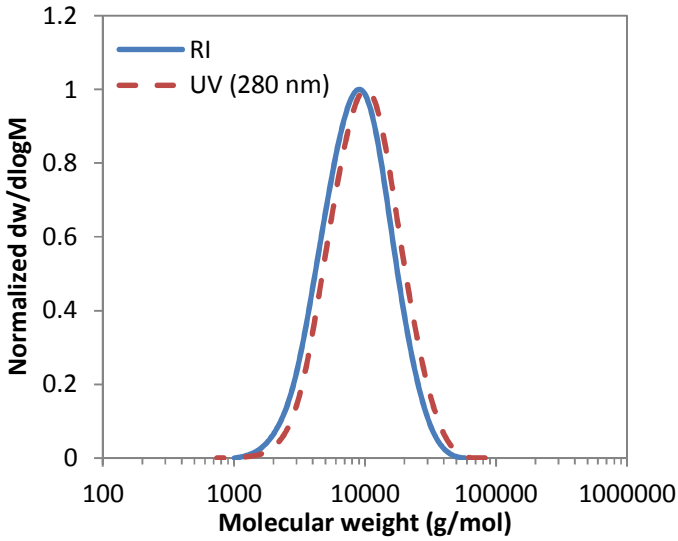

Figure 2.2. Size exclusion chromatograms of poly(MDO-*co*-VAc) (50:50) obtained by RAFT/MADIX polymerization after 5 h, blue trace using RI detection and red dash trace using UV detection at λ = 280 nm (SEC, $CHCl_3$).

In an attempt to reduce the apparent viscosity of the polymerization mixture which tends to increase as the monomer conversions increase in the case of VAc polymerization, the copolymerizations were also performed in solution using chloroform, acetone, dichloromethane, toluene, or benzene as solvent (Table 2.2). While using a solvent resulted in the reduction of the apparent viscosity of the polymerization mixture and give the possibility to reach higher monomer conversions, the control of the process was found not to be drastically affected by the presence of the solvent as seen by the similar dispersities of 1.43 - 1.52 obtained under these conditions. However, benzene was chosen as the polymerization solvent for further studies as a consequence of its low chain transfer constant toward vinyl

acetate (K_c = 3.6 × 10^4 s^{-1}) which was assumed would prevent the potential formation of small dead chains resulting from termination side reactions which could affect the degree of control of the process.[59]

Table 2.2. Characterization data for the copolymerization of MDO and VAc (30/70 mol%) using CTA 1 as the chain transfer agent in the presence of different solvents (15 wt%).

Solvent	VAc conv. [a] (%)	MDO conv.[a] (%)	M_n [theo b] (kg/mol)	M_n [SEC c] (kg/mol)	$Đ_M$ [c]
Chloroform	36	29	3.4	3.9	1.45
Acetone	26	20	2.5	1.7	1.43
Dichloromethane	36	30	3.5	3.0	1.50
Toluene	22	16	2.1	1.5	1.45
Benzene	25	19	2.3	2.5	1.40

[a] conversion determined by ^{1}H NMR spectroscopy, [b] theoretical molecular weight based on monomer conversion (^{1}H NMR spectroscopy),[c] obtained by SEC analyses in $CHCl_3$.

2.3.2 Detailed study of the copolymerization of MDO and VAc

In an attempt to further investigate the polymerization, a detailed RAFT/MADIX copolymerization study of MDO and VAc was conducted at 60 °C in benzene (15 wt%) in order to increase the monomer conversions, such that $[MDO]_0/[VAc]_0/[AIBN]_0/[CTA\ 1]_0$ = 30:70:0.1:1, where aliquots of the polymerization reaction were analyzed at different points (1 h to 16 h). Poly(MDO-*co*-VAc) with controlled number average molecular weight (M_n) and low dispersities ($Đ_M$ = 1.21-1.60) were synthesized (Table 2.3).

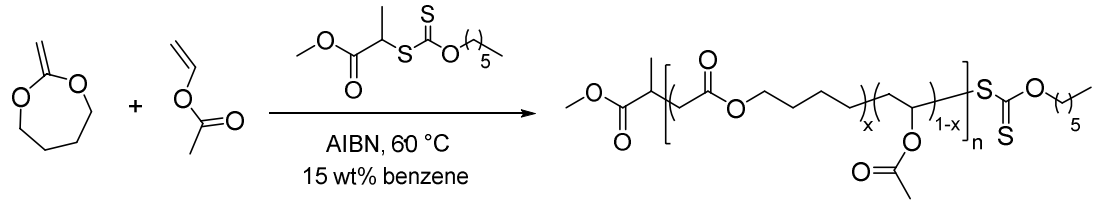

Scheme 2.3. Schematic representation of the synthesis of poly(MDO-*co*-VAc) copolymers mediated by RAFT/MADIX polymerization.

Table 2.3. Characterization data for the copolymerization of MDO and VAc (30/70 mol%) using CTA 1 for different time points.

Time (h)	VAc conv.[a] (%)	MDO conv.[a] (%)	M_n [theo b] (kg/mol)	M_n [obs c] (kg/mol)	$Đ_M$ [d]
1	3	7	0.4	0.9	1.25
2	13	10	1.1	1.6	1.30
3	16	13	1.4	1.9	1.37
4	19	15	1.6	2.0	1.39
5	21	17	1.8	2.3	1.40
7	32	20	2.7	3.0	1.42
9	45	27	3.6	3.8	1.49
16	62	44	5.3	7.8	1.55

[a] conversion determined by ^{1}H NMR spectroscopy, [b] theoretical molecular weight based on monomer conversion (^{1}H NMR spectroscopy),[c] observed molecular weight obtained by ^{1}H NMR spectroscopy end-group analysis, [d] dispersities obtained by SEC analyses in $CHCl_3$.

The conversion of MDO was found to be lower than VAc over the course of the polymerization, with the exception of the first time point at 1 h which is potentially due to the incertitude of the integrations obtained by ^{1}H NMR spectroscopy at too low monomer conversions. The higher reactivity of VAc observed in this experiment was in agreement with its higher reactivity ratio as reported by previous studies carried out using conventional free radical polymerization techniques.[26,40] Nevertheless, in order to confirm that the presence of CTA 1 in the copolymerization mixture was not affecting the reactivity of the monomers, the reactivity ratios, r_{MDO} and r_{VAc}, were also investigated under the RAFT/MADIX polymerization conditions. The reactivity ratios of MDO and VAc were determined by carrying out a series of copolymerizations with different MDO:VAc ratios, namely 10:90; 20:80; 30:70; 40:60; 50:50; 60:40; 70:30; 80:20, and 90:10. These copolymerization reactions were carried out under the same conditions as previously discussed (in the presence of AIBN, benzene and at 60 °C). The molar fraction of the two monomers in the copolymer was obtained by ^{1}H NMR spectroscopy at low conversions (< 15%) in order to avoid the compositional drift effect which could affect the reactivity of the monomers. A representative ^{1}H NMR spectrum of a mixture of VAc and MDO is shown

in Figure 2.3. The mole fraction of the two monomers in the initial feed, f_1 and f_2 for MDO and VAc respectively, was obtained by comparing the integrals of the signal that corresponds to the terminal vinyl protons (c) and signal that corresponds to the double bonds of the cyclic ketene acetal (e). After polymerization the copolymer is formed and signals became broader, the conversions of each monomer were calculated by comparing the signals (c) and (e) with the corresponding signals of the copolymer for the CH vinyl repeat unit (c') and the CH_2 signals for the ester repeat unit (e'). The data obtained for the different copolymerization points are summarized in Table 2.4.

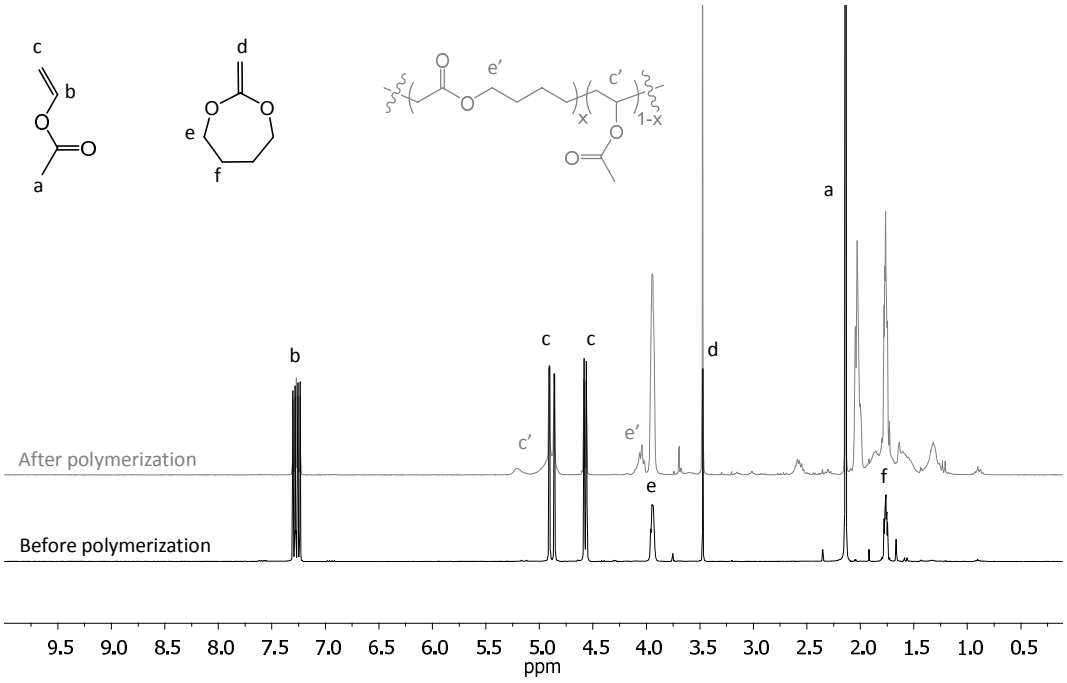

Figure 2.3. ^{1}H NMR spectra of a mixture of MDO and VAc (23/77) before polymerization (bottom) and 15 min after polymerization and no precipitation (top) using the RAFT/MADIX polymerization process, at an overall monomer conversion of 8%.

Table 2.4. Mole ratio of monomers in the initial feed and copolymers used for the determination of the reactivity ratios of MDO and VAc in the presence of CTA 1 and benzene.

Mole ratio in initial feed (MDO/VAc) [a]	MDO conversion (%) [a]	VAc conversion (%) [a]	Mole fraction in copolymer (MDO/VAc) [a]
14:86	8	5	22:78
23:77	8	8	25:75
35:65	9	12	29:71
42:58	9	12	36:64
53:47	9	10	51:49
65:35	8	10	60:40
77:23	8	10	75:25
80:20	5	2	91:9
90:10	5	1	98:2

[a] determined by ^{1}H NMR spectroscopy.

By plotting F_1 (ratio of MDO in copolymer) *versus* f_1 (ratio of MDO in initial feed), the reactivity ratios of MDO and VAc were calculated using Contour, a software developed by van Herk and co-workers,[60] which applies a non-linear least squares (NLLS) method. This calculates the best fitting curve which determines the reactivity ratios of the two monomers. The result obtained from the software is presented in Figure 2.4 and shows that the reactivity ratios of the monomers, in the presence of the CTA, are equal to $r_{MDO} = 1.03 \pm 0.06$ and $r_{VAc} = 1.22 \pm 0.07$. These values confirm the higher reactivity of VAc observed during the copolymerization, and are in agreement with previous reports.[26,40] It can be noted that there is a small difference from the values reported by Agarwal and co-workers ($r_{MDO} = 0.47$ and $r_{VAc} = 1.53$)[40] and Albertsson and co-workers ($r_{MDO} = 0.93$ and $r_{VAc} = 1.71$).[26] These differences are attributed to the different calculation methods employed, namely Kelen Tudos and Fineman-Ross respectively, which both involve a linear fit approach. This linear fitting is deemed inaccurate as it is based on the assumption of a linearity in the Mayo Lewis model.[61]

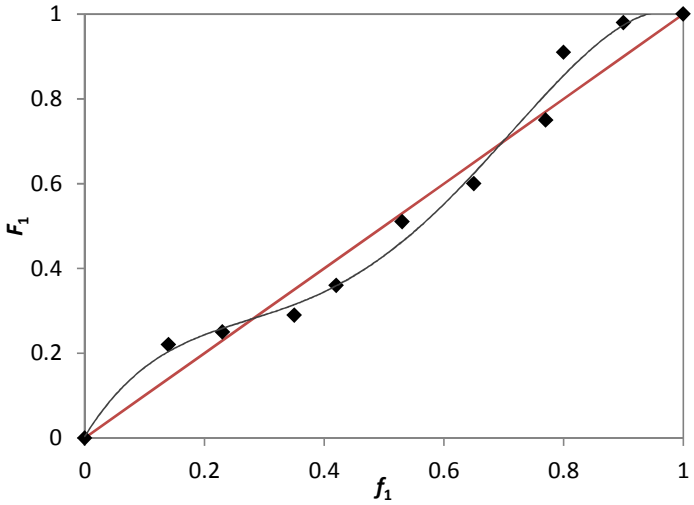

Figure 2.4. Plot of F_1 *vs* f_1 for the copolymerization of MDO [1] and VAc [2] using CTA 1 in benzene leading to calculated reactivity ratios results of $r_1 = 1.03 \pm 0.06$ and $r_2 = 1.22 \pm 0.07$. (Nonlinear least squares (NLLS) method). The red line is the plot of F_1 *vs* f_1 for an ideal polymerization, where $r_1 = r_2 = 1$).

The observed polymer molecular weights (M_n ^{obs}) were obtained by integration of the protons from the VAc and MDO polymer backbone at δ = 4.8 - 5.2 and 4.2 ppm respectively, and referenced to the characteristic resonance of the CH_2 protons adjacent to the xanthate group at δ = 4.5 ppm (Figure 2.5). The theoretical molecular weights (M_n ^{theo}) were based on monomer conversions as determined by ^{1}H NMR spectroscopy. The M_n ^{obs} values showed good correlation to the M_n ^{theo} values over the first 9 h of the polymerization, which indicates retention of the active xanthate group at the polymer chain end. Beyond 9 h of polymerization, however, there was a deviation in the values of M_n ^{obs} and M_n ^{theo}, which indicated that termination reactions were occurring, in turn leading to a loss of the CTA end group and a resultant loss of polymerization control supported by the broadening of the distribution of the resultant copolymer (Figure 2.6). This loss of the CTA end-group was hypothesized to be attributed to the fragmentation of the Z-group occurring during the copolymerization reaction (detailed in Chapter 4). However, by stopping the copolymerization before the 9 h point, narrow distribution polymers with

controlled molecular weights and good monomer conversions were reached for both vinyl and CKA monomers (> 20%).

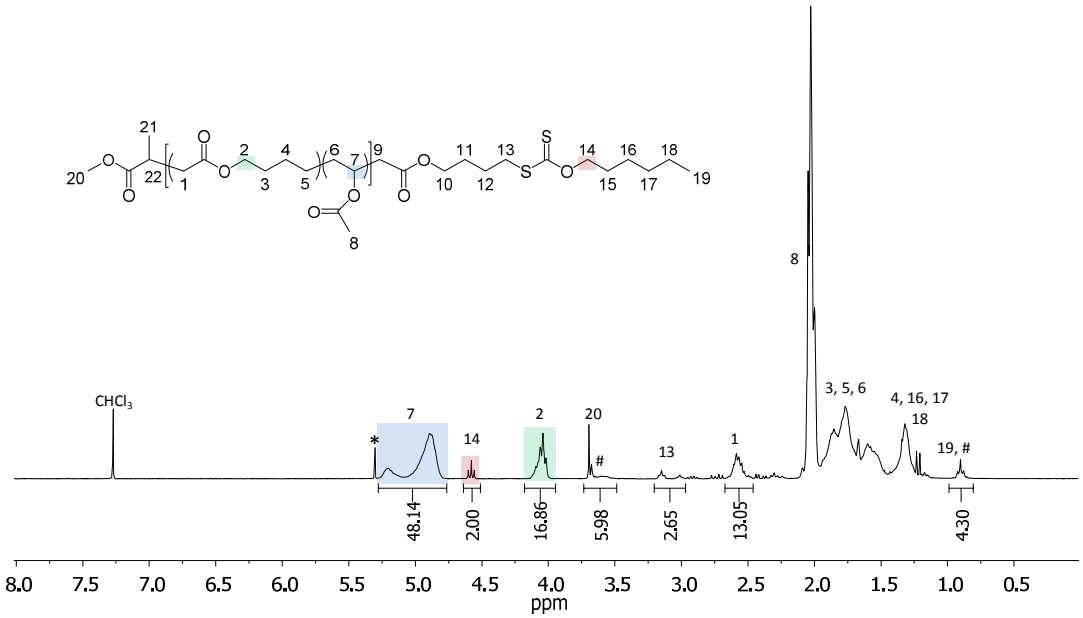

Figure 2.5. ^{1}H NMR spectrum of poly(MDO-*co*-VAc) synthesized using RAFT/MADIX polymerization, (400 MHz, $CDCl_3$), * residual signal of dichloromethane, # signals of the side reactions of 1,4- and 1,7-hydrogen transfer.

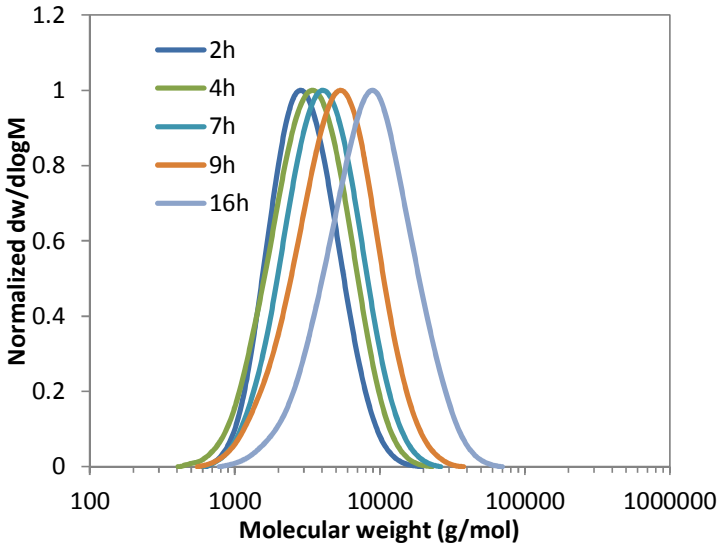

Figure 2.6. SEC traces of poly(MDO-*co*-VAc) (30/70 mol%) for different polymerization times obtained during the detailed study.

To increase the degradability of the synthesized copolymers, the incorporation of ester repeat units was altered by increasing the ratio of MDO in the monomer feed to 70 mol%. Following the polymerization, as previously described, the final composition of the copolymer revealed an incorporation of 61% of MDO and 39% of VAc in the polymer, as determined by ^{1}H NMR spectroscopy after 7 h of reaction. Further analyses of the copolymers using ^{1}H NMR spectroscopy and SEC analysis revealed that the copolymerizations were well-defined with dispersities between 1.20 and 1.52 with a controlled process maintained up to 16 h. Similarly to the copolymerization with a lower amount of MDO in the initial feed, a broadening of the distribution and an increase in dispersity was observed, suggesting a loss of the end group after 16 h of polymerization (Table 2.5 and Figure 2.7). By terminating the polymerization before this time, a controlled and defined copolymer with increased content of degradable linkages was obtained.

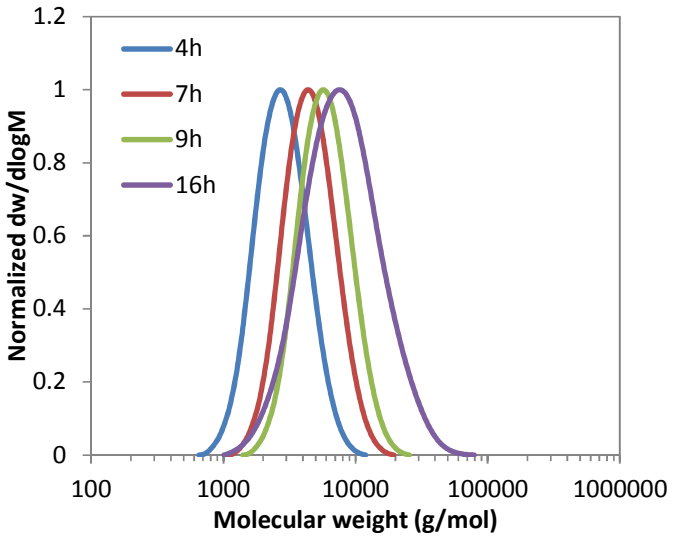

Figure 2.7. SEC traces of poly(MDO-*co*-VAc) (70/30 mol%) for different polymerization times.

Table 2.5. Characterization data for the copolymerization of MDO and VAc (70/30 mol%) using CTA 1 for different time points.

Time (h)	VAc conv.[a] (%)	MDO conv.[a] (%)	M_n theo [b] (kg/mol)	M_n obs [c] (kg/mol)	$Đ_M$ [d]
2	5	4	0.5	0.8	1.20
4	10	9	1.0	1.7	1.21
7	22	15	1.8	2.4	1.24
9	24	18	2.1	2.9	1.27
16	52	27	3.5	5.0	1.52

[a] conversion determined by ^{1}H NMR spectroscopy, [b] theoretical molecular weight based on monomer conversion (^{1}H NMR spectroscopy), [c] observed molecular weight obtained by ^{1}H NMR spectroscopy end-group analysis, [d] dispersities obtained by SEC analyses in $CHCl_3$.

2.3.3 Possible ring-retention and branching investigations

Initial investigations in the field of cyclic ketene acetals by Gonsalves and co-workers[29] have highlighted the potential side reactions that can occur during the radical ring-opening polymerization (rROP) of MDO. The growing alkyl primary radical produced during the reaction is highly reactive and can undergo intramolecular hydrogen transfer (also called backbiting) to produce a more stable form of radical. As such, two types of re-arrangements can be observed, the 1,7- and 1,4-hydrogen transfer abstraction, both of which lead to the formation of small side branching on the main polymer backbone of poly(MDO) (Scheme 1.11). The extent of hydrogen abstraction, and hence the amount of branching contained in the homopolymer and copolymers of MDO, is dependent on the polymerization temperature and the nature of the initiator.[62] The presence of small branching on the homopolymer, poly(MDO), can affect the density, crystallinity and thermal properties of the resultant materials and therefore differ from the properties of the conventional PCL polymer which does not contain branched side chains.[63]

In an attempt to investigate these types of side reactions, ^{1}H NMR spectroscopy analyses were performed on the samples of poly(MDO-*co*-VAc), which revealed the presence of resonances at δ = 0.90 ppm and 3.68 ppm, characteristic of side-chain reactions that result from the 1,4- and 1,7-hydrogen transfer, or backbiting, during the rROP of MDO. These

resonances are very similar to those observed by Agarwal and co-workers and Albertsson and co-workers in different copolymerizations of vinyl monomers with MDO.[26,28] Further ^{1}H NMR spectroscopic analysis led to an estimation of the side-chains that occurred from these processes to be 10-15% of the MDO repeat units within the copolymer. The estimation was obtained after comparison of the side-chain branch integrals (δ = 0.90 ppm and 3.68 ppm) with the CH_2 close to the MDO carbonyl group signal (δ = 4.00 ppm) (Figure 2.8).

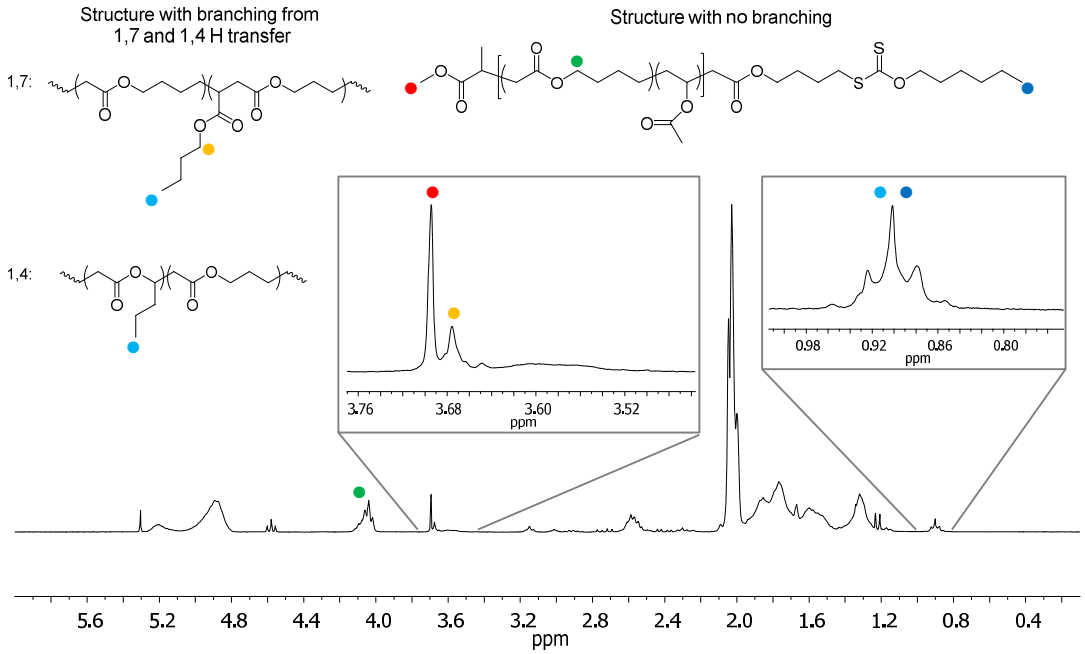

Figure 2.8. ^{1}H NMR spectrum of poly(MDO-*co*-VAc) (30/70 mol%) highlighting the potential side branching occurring from the 1,4- and 1,7-hydrogen transfer reaction (400 MHz, $CDCl_3$).

Another often observed side reaction during the radical ring-opening polymerization of MDO is the formation of polyacetal in which the cyclic ketene acetal ring is retained (Scheme 2.4). In their initial work,[64] Bailey and co-workers performed ^{1}H and ^{13}C NMR spectroscopy analyses on the homopolymer, poly(MDO), and observed a ring-retention of the acetal where the ratio compared to the ring-opened form, the polyester version, was dependent on the polymerization temperature at which the reaction was carried out. Agarwal

and co-workers also investigated this side reaction on different vinyl monomers/MDO copolymerizations and also found that a ring-retention of the acetal often occurred.[62] In order to determine the degree of ring-opening of MDO in the copolymers synthesized using the RAFT/MADIX polymerization technique used in this chapter, ^{13}C NMR spectroscopic analysis was undertaken similarly to the previously reported free radical copolymerizations of MDO monomers.[65,66] In all cases, total ring-opening of the cyclic MDO monomer was observed as indicated by the absence of characteristic signals for the acetal quaternary carbon peak at δ = 100-110 ppm (Figure 2.9).[65,66]

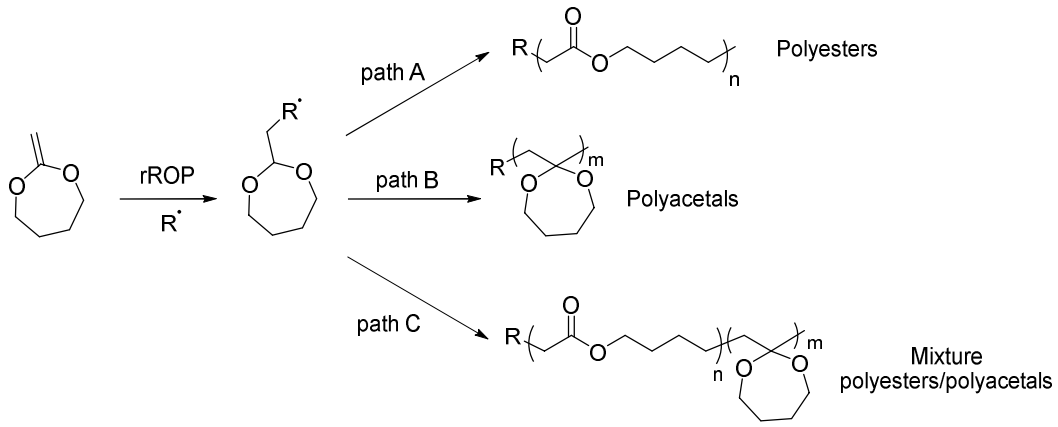

Scheme 2.4. Schematic representation of the possible pathways for the radical ring-opening polymerization of MDO and the resulting polymers.

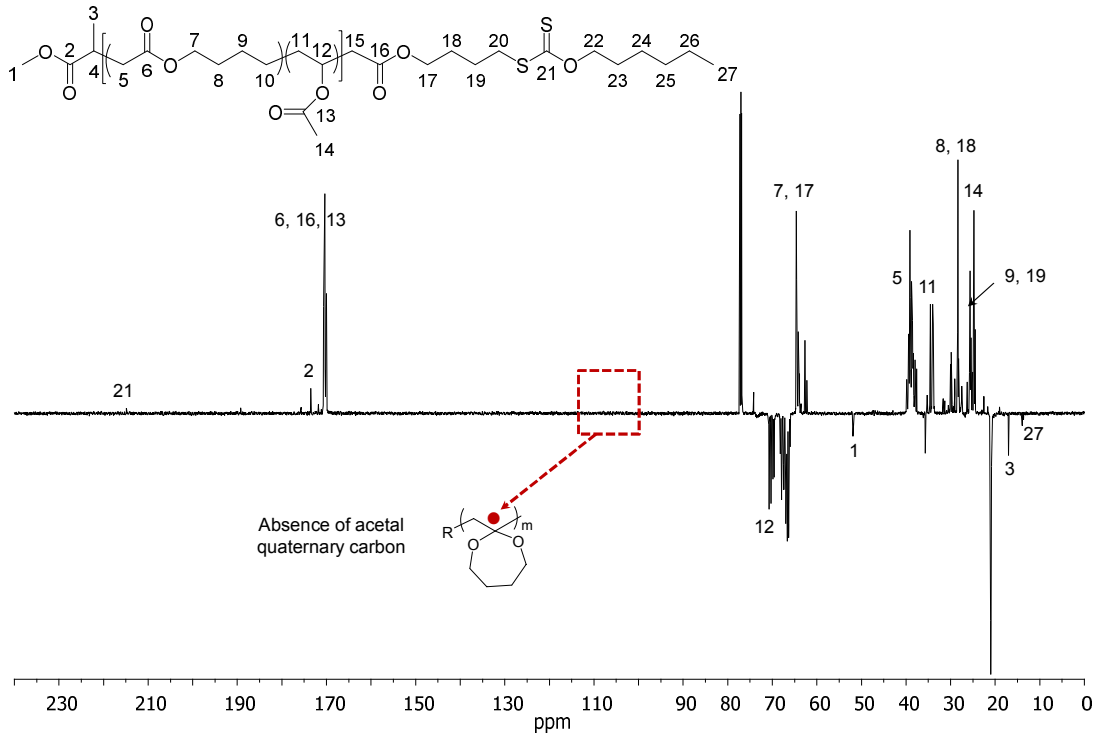

Figure 2.9. ^{13}C NMR spectrum of poly(MDO-*co*-VAc) formed using CTA 1 revealing the absence of acetal quaternary carbon expected from the ring-retention of MDO during the copolymerization (125 MHz, $CDCl_3$).

2.3.4 Chain extension experiments of poly(MDO-*co*-VAc)

In order to assess the controlled nature of the polymerization, chain extension experiments were carried out in an attempt to synthesize a block copolymer with poly(MDO-*co*-VAc) where the reaction would only be successful if the xanthate chain end had remained on the polymer chains. Extension of poly(MDO-*co*-VAc) (30:70 mol%) with VAc was performed to create a block copolymer of poly(MDO-*co*-VAc)-*b*-poly(VAc). ^{1}H NMR spectroscopy and SEC analyses confirmed the controlled character of this polymerization process, with a complete shift of the distribution and the absence of a shoulder in the SEC analysis, indicating successful chain extension (Figure 2.10) upon addition of the second block of poly(VAc).

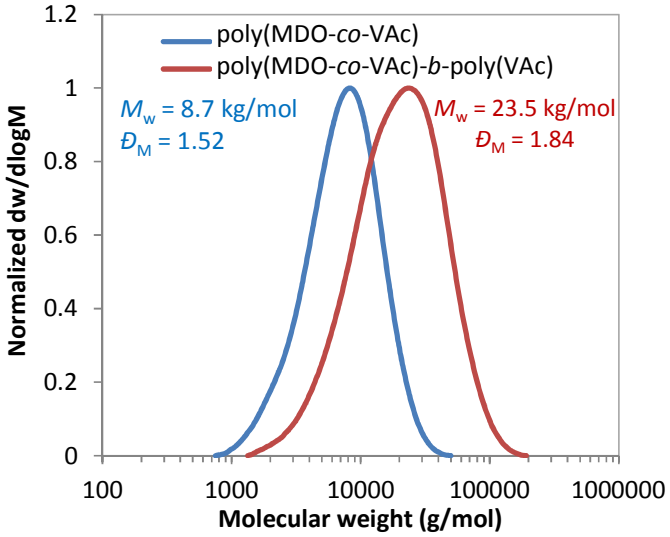

Figure 2.10. SEC traces (RI detector, with $CHCl_3$ as the eluent) of the chain extension of poly(MDO-*co*-VAc) (30/70 mol%) with VAc.

However, the dispersity of the final block copolymer after chain extension was found to be significantly higher with a value of 1.84. This increase in dispersity after chain extension with VAc can be explained by the hypothesis that despite having a certain amount of copolymer chains still retaining their CTA end group, small portions do not contain that CTA end group and are therefore "dead chain ends", limiting the chain extension processes. From this experiment it can be concluded that despite some termination reactions taking place during the copolymerization of VAc and MDO, the majority of the polymer chains retain their xanthate chain end, as evidenced by the reasonable chain extension shown here. This further complements the previously shown data that suggest the controlled RAFT/MADIX polymerization of MDO and VAc under the employed conditions.

2.3.5 Targeting higher molecular weight copolymers

Further investigation towards the development of higher molecular weight copolymers of poly(MDO-*co*-VAc) was performed by targeting increased degrees of

polymerization (DPs). Similarly to the previous results shown whereby targeting a DP of 100 resulted in copolymers with narrow molecular weights distribution, the synthesis of higher molecular weight copolymer was performed by varying the amount of CTA initially introduced in the copolymerization mixture such that DPs of 200, 400 and 600 were targeted. SEC and ^{1}H NMR spectroscopic analyses of the copolymers suggested that the polymerizations were controlled with characteristic signals of the CTA end group observed in the ^{1}H NMR spectra and the monomodal traces obtained by SEC analyses (Figure 2.11). The number-average molecular weights obtained were found to be between 6.8 and 17.4 kg/mol (Table 2.6), the dispersities were however found to increase as the targeted molecular weights increased. While this is indicative of a possible loss of control in the polymerization, a broadening of the dispersities could also be attributed to a consequence of increased target DP, which is commonly observed for controlled radical polymerization techniques. In such cases, the increase in dispersities can be explained by the accumulation of irreversible termination reactions occurring in the polymerization mixture. These reactions tend to be more prominent when a higher ratio of $[Initiator]_0/[CTA]_0$ is employed while longer polymerization times are also required.[56,67,68]

Table 2.6. Characterization data of poly(MDO-*co*-VAc) for targeted DPs of 200, 400, and 600, (30/70 mol% VAc/MDO).

Target DP	Actual DP [e]	VAc conv.[a] (%)	MDO conv.[a] (%)	M_n [theo b] (kg/mol)	M_n [obs c] (kg/mol)	$Đ_M$ [d]
200	74	41	27	6.8	6.1	1.49
400	135	40	19	11.4	8.1	1.63
600	190	36	21	17.4	11.3	1.73

[a] conversion determined by ^{1}H NMR spectroscopy, [b] theoretical molecular weight based on monomer conversion (^{1}H NMR spectroscopy), [c] observed molecular weight obtained by ^{1}H NMR spectroscopy end-group analysis, [d] dispersities obtained by SEC analyses in $CHCl_3$, [e] determined by ^{1}H NMR spectroscopy.

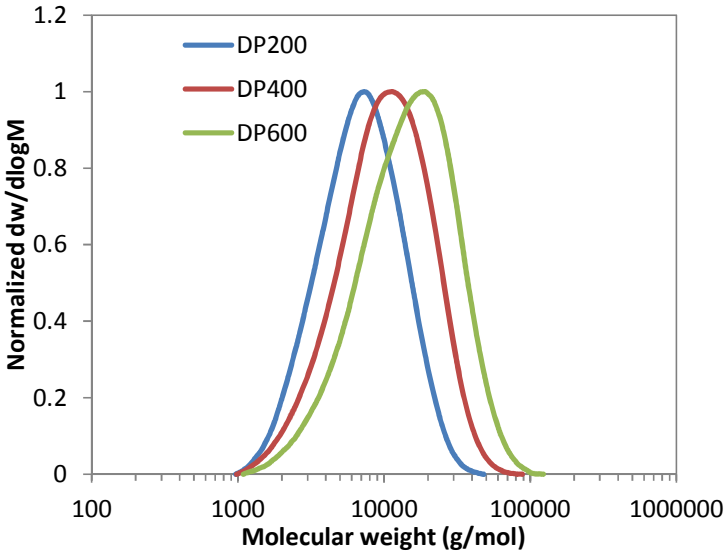

Figure 2.11. SEC traces of poly(MDO-*co*-VAc) (30/70 mol%) for targeted DPs of 200, 400, and 600 (SEC $CHCl_3$).

2.3.6 Degradation experiments

With a recent increase in the area of biocompatible and biodegradable materials, the copolymerization of CKA monomers with vinyl monomers has been seen as the simplest route to incorporate easily cleavable ester linkages into the vinyl polymer backbone and hence introduce degradability in such polymers.[69] Most studies in this field have reported the successful degradation of these copolymers under different conditions. Indeed, various groups reported using basic conditions where potassium hydroxide in methanol was used at different temperatures to successfully degrade copolymers of CKAs and vinyl monomers.[70] While these conditions have been used for degradation studies of CKA copolymers, they have also been shown to provide simulated accelerated *in vivo* conditions for the degradation of PCL.[71] Other studies also investigated the use of enzymes such as *Lipase Candida*,[45,72] *Lipase Pseudomonas Cepacia*,[73] or *Proteinase K*,[32] as a way to degrade the ester linkages of the copolymer backbone.

In an attempt to confirm the degradability of the poly(MDO-*co*-VAc) samples discussed in this chapter, hydrolysis experiments were performed in a solution of potassium hydroxide in methanol (KOH, 1.5 M) at 40 °C for 5 h as a simple accelerated method of degradation for polyesters. After the hydrolysis period, the degraded polymer was investigated using SEC analysis and in all cases, a decrease in the molecular weight of the samples was observed (Figure 2.12). This result indicates the successful insertion of degradable ester units within the polymer backbone from the MDO rROP copolymerization.

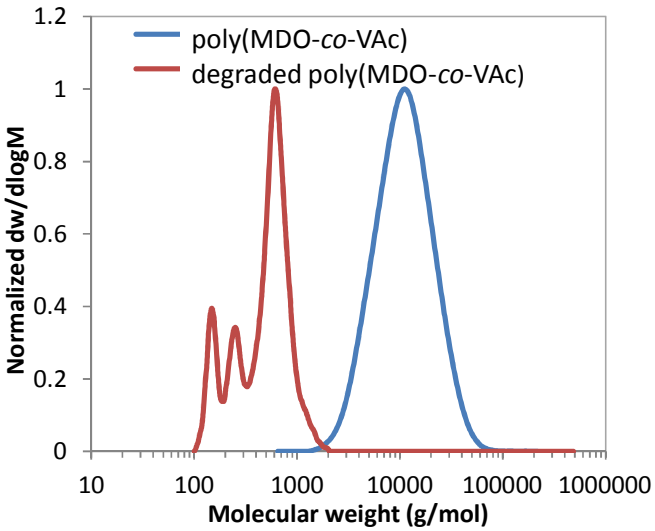

Figure 2.12. SEC traces of the poly(MDO-*co*-VAc) (30/70 mol%) before and after degradation in potassium hydroxide in methanol for 5 h at 40 °C, (SEC $CHCl_3$, RI detector, PS used as standard.

The incorporation of different amounts of ester repeat units, *via* the use of a larger amount of MDO in the initial monomer feed, was expected to lead to a copolymer with a higher degradability and potentially a faster degradation process. This aspect will be further investigated using similar copolymers in Chapter 3.

2.3.7 Synthesis of other functional copolymers

In order to further expand the applicability of the copolymerization of MDO using RAFT/MADIX, it was suggested that vinyl monomers with different functional groups could also be employed to produce other degradable copolymers with narrow molecular weight distributions. To this end, the controlled copolymerization of MDO was also applied to other vinyl monomers to enable the incorporation of different functional groups into the degradable polymer backbone. Such a task remains challenging through conventional ROP techniques on account of the difficult functional monomer syntheses and purification processes. Here, the copolymerizations of MDO with other "less" activated monomers, *N*-vinylpyrrolidone (NVP), *N*-vinylpiperidone (VPip) and commercially available vinyl chloroacetate (VClAc), were investigated (Scheme 2.5) as initial examples of the versatility of the controlled MDO RAFT/MADIX copolymerization approach.

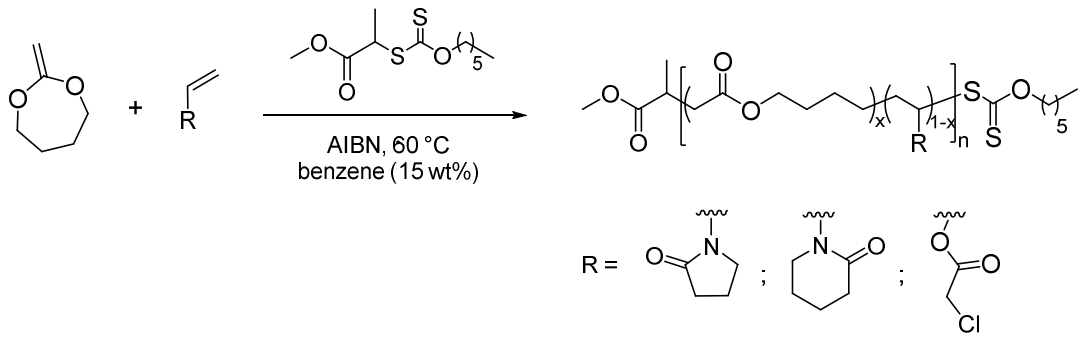

Scheme 2.5. Schematic representation of the synthesis of poly(MDO-*co*-NVP), poly(MDO-*co*-VPip) and poly(MDO-*co*-VClAc) copolymers mediated by RAFT/MADIX polymerization.

The copolymerizations with each monomer were performed using similar conditions as before (*i.e.* AIBN, benzene, CTA 1, 60 °C) where the initial feed ratio was fixed to $[MDO]_0/[NVP/VPip/VClAc]_0/[AIBN]_0/[CTA\ 1]_0$ = 30:70:0.1:1. The copolymerizations were carried out for 5 h and the final copolymers were investigated using ^{1}H NMR spectroscopy and SEC analysis. In all cases, the

controlled aspect of the polymerization process was observed as seen by the low dispersity values of 1.30, 1.26 and 1.48 for poly(MDO-*co*-NVP), poly(MDO-*co*-VPip), and poly(MDO-*co*-VClAc) respectively being observed by SEC analyses. The monomodal traces of each copolymer also suggested that the polymerizations were performed in a controlled manner (Figure 2.13). These initial results demonstrated the broader utility of the RAFT/MADIX polymerization approach for the synthesis of well-defined degradable polymers (Table 2.7).

Table 2.7. Characteristic data of poly(MDO-*co*-NVP), poly(MDO-*co*-VPip) and poly(MDO-*co*-VClAc) synthesized by RAFT/MADIX polymerization.

Copolymer	Monomer conv.[a] (%)	MDO conv.[a] (%)	M_n theo [b] (kg/mol)	M_n SEC [c] (kg/mol)	$Đ_M$ [c]
Poly(MDO-*co*-NVP)	60 (NVP)	32	6.0	5.3	1.30
Poly(MDO-*co*-VPip)	31 (VPip)	15	3.4	2.1	1.26
Poly(MDO-*co*-VClAc)	19 (VClAc)	11	2.2	5.0	1.48

[a] conversion determined by ^{1}H NMR spectroscopy, [b] theoretical molecular weight based on monomer conversion (^{1}H NMR spectroscopy), [c] Average molecular weights and dispersities obtained by SEC analyses in either DMF or $CHCl_3$.

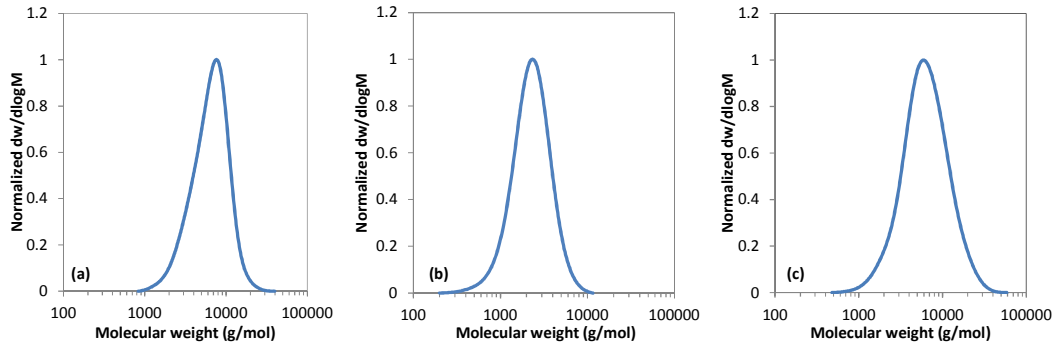

Figure 2.13. Size exclusion chromatograms of poly(MDO-*co*-NVP) (a), poly(MDO-*co*-VPip) (b) and poly(MDO-*co*-VClAc) (c) synthesized by RAFT/MADIX polymerization, (SEC, DMF or $CHCl_3$).

Furthermore, the use of VClAc as a co-monomer was also pursued as it could enable access to a much broader range of materials through the use of post-polymerization modification reactions. Post-polymerization modification approaches have been

widely applied in the field of polymer science for many years as an interesting tool to incorporate further functional groups which could increase the range of properties available for the final polymers.[74,75]

In an attempt to further functionalize the degradable copolymers introduced in this section, the post-polymerization modification of poly(MDO-*co*-VClAc) was conducted using an azidation modification approach. The reaction was conducted using sodium azide, NaN_3, in dimethyl formamide (DMF) at room temperature for 48 h (Scheme 2.7). After reaction, the solvent was removed *in vacuo* and the modified copolymer was dissolved in a small amount of toluene and re-precipitated in hexane several times before being characterized by ^{1}H NMR spectroscopy, SEC analysis and FTIR spectroscopy.

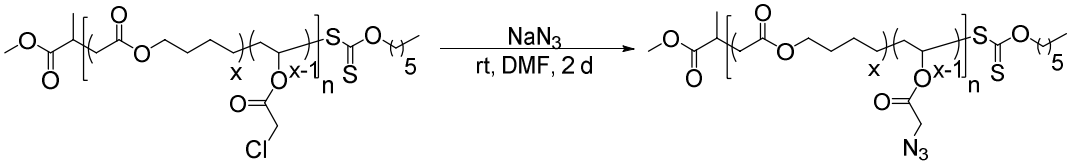

Scheme 2.6. Schematic representation of the post-polymerization modification of poly(MDO-*co*-VClAc) *via* azidation.

The successful modification of poly(MDO-*co*-VClAc) into poly(MDO-*co*-VN_3) was confirmed by ^{1}H NMR spectroscopy analysis where a clear shift in the CH_2-Cl characteristic peak at δ = 4.0 ppm was observed with the CH_2-N_3 at δ = 3.90 ppm appearing after the azidation modification (Figure 2.14). The full conversion of the chlorine functional groups to azide groups was however not determined as the CH_2-Cl characteristic peak at δ = 4.0 ppm overlapped with the CH_2-O-CO of the MDO repeat units. Nevertheless, it could be assumed that some chlorine groups were remaining as seen by the appearance of a third peak in the vinyl region, around

δ = 5.40-20 ppm, which is tentatively assigned to the formation of three diads in the modified copolymers, MDO/VClAc, MDO/VN_3Ac and VClAc/VN_3Ac.

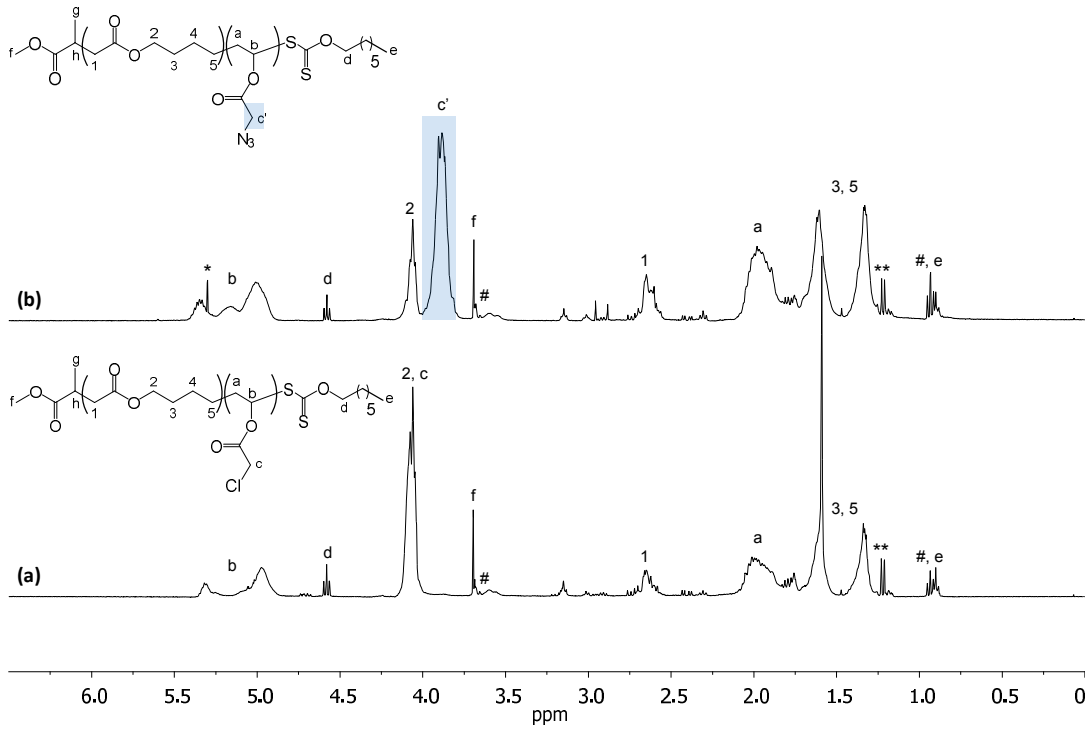

Figure 2.14. ^{1}H NMR spectra of poly(MDO-*co*-VClAc) before (a) and after (b) post-polymerization modification using azidation, (400 MHz, $CDCl_3$), * residual dichloromethane, ** residual diethyl ether, and # signals of the side branching from the 1,4- and 1,7-hydrogen transfer.

The azidation modification was also confirmed by the appearance of a signal at ν = 2105 cm^{-1} on the FTIR spectrum which corresponds to the stretching vibration of N=N=N (Figure 2.15). Finally, further investigations using SEC analysis suggested that the azidation modification had no deleterious effect on the copolymer as the molecular weights and dispersities before and after azidation were found to not significantly change (Figure 2.16). The small tailing effect that could be observed at higher molecular weights after azidation of the copolymer could be explained by different interactions of the modified copolymer with the column used during the SEC analysis.

The further post-polymerization modification of the azide functional copolymer, poly(MDO-*co*-VN_3Ac) with "click chemistry" to further increase the functionality of the final copolymer was not performed in this chapter. Nevertheless, the azidation reaction highlights the potential concept of using monomers with functional groups able to be modified to easily attach different groups and target desired applications.[76,77] These types of modifications will be further investigated in Chapters 3 and 6 on similar copolymers.

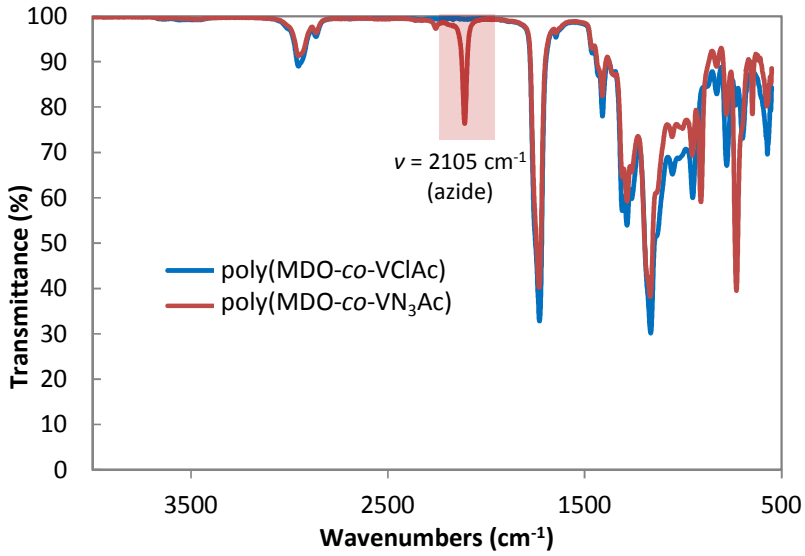

Figure 2.15. FTIR spectrum of poly(MDO-*co*-VClAc) before and after post-polymerization modification using azidation and highlighted signal corresponding to the N_3 vibrations.

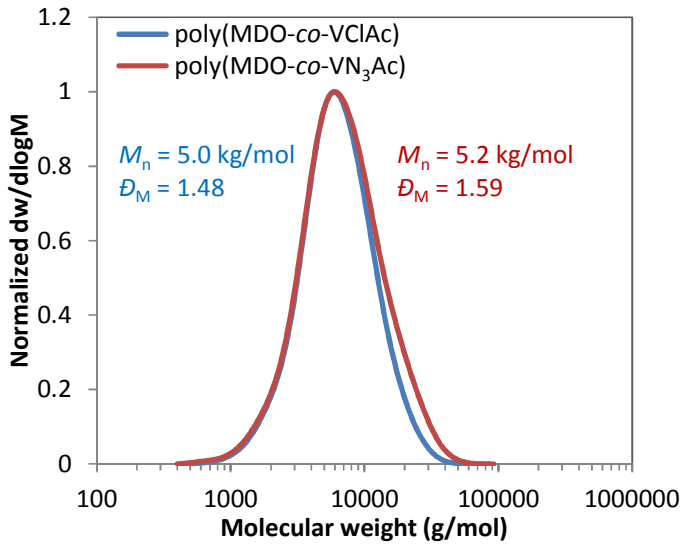

Figure 2.16. Size exclusion chromatograms of poly(MDO-*co*-VClAc) before and after post-polymerization modification using azidation, (SEC, $CHCl_3$).

2.3.8 Synthesis of block copolymers of poly(MDO-*co*-VAc) using a poly(NVP) macro-CTA

Following the promising results obtained for the synthesis of well-defined copolymers of MDO, further experiments were performed using a macro-CTA for the copolymerization of MDO and VAc towards to formation of different block copolymers. In recent years, the development of block copolymers presenting degradable properties has significantly increased as a consequence of the arising development of controlled polymerization techniques which have made their synthesis easily accessible. With the aim of forming block copolymers containing hydrophilic properties, the synthesis of the first portion of the block polymer was obtained by the RAFT/MADIX polymerization of NVP to form a poly(NVP) macro-CTA, 1 (DP = 20, M_n = 2.2 kg/mol, $Đ_M$ = 1.19) using a similar synthetic approach previously reported by Ieong *et al*. for the synthesis of hydrophilic polylactams.[58] In initial experiments, the synthesis of the block copolymers, having different amount of MDO, were investigated such that $[VAc]_0/[MDO]_0/[\text{macro-NVP CTA1}]_0/[AIBN]_0$

= 10:90:0.1:1 or 30:70:0.1:1. Characterization analysis of these block copolymers was found to form well-defined poly(NVP)-*b*-poly(MDO-*co*-VAc), with a net increase in molecular weights being observed by SEC analysis alongside dispersity values of 1.28 and 1.49 after chain growth (Figure 2.17).

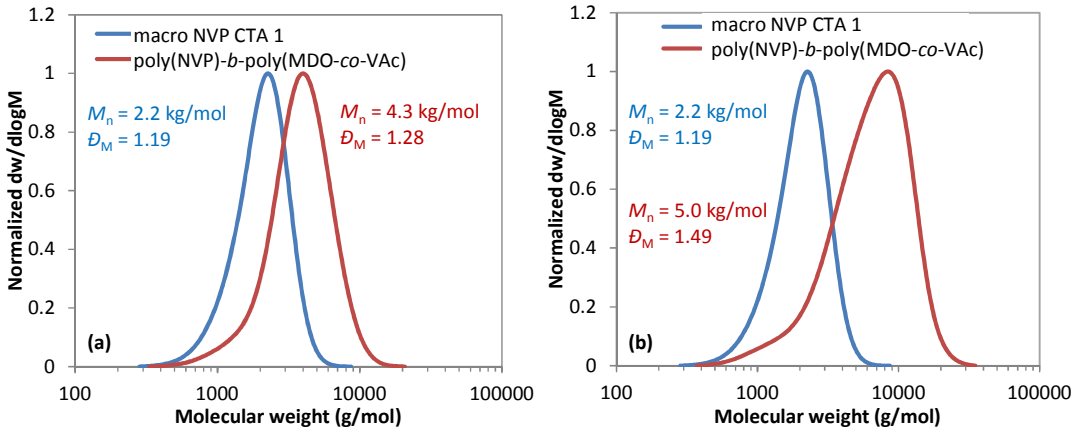

Figure 2.17. Size exclusion chromatograms of the chain extension of the macro-NVP CTA 1 with MDO and VAc (a, 30/70) and (b, 10/90) to form the corresponding block copolymers poly(NVP)-*b*-poly(MDO-*co*-VAc), (SEC, DMF).

While these results confirmed the applicability of using a macro-CTA for the copolymerization of MDO and VAc for the formation of block copolymers, it also revealed the potential in using such methodology to prepare amphiphilic block copolymers. This aspect will be further investigated and presented in Chapter 6.

2.4 Conclusions

In this chapter, the synthesis of copolymers of MDO mediated by a controlled polymerization technique is reported and resulted in functional degradable copolymers based on the broadly applicable polyester PCL. Well-defined copolymers with different degrees of degradability were successfully synthesized, as seen by ^{1}H NMR spectroscopy and SEC analysis, where good control over molecular

weight and end group fidelity was observed. Additionally, the incorporation of side chain functional groups was also shown to be possible by the copolymerization of MDO with other vinyl functional monomers, which extends the utility of the process reported. Further chain growth of the MDO/VAc copolymers using a macro-NVP CTA was also performed towards the formation of block copolymers. These results illustrate the great potential of using the RAFT/MADIX polymerization technique to control the copolymerization of CKAs and vinyl monomers to yield well-defined degradable copolymers with narrow molecular weight distributions while targeting a wider range of properties and applications.

2.5 Experimental

2.5.1 Materials

The following chemicals were used as received; alumina, activated basic (Al_2O_3: Sigma-Aldrich, Brockmann I, standard grade, ~ 150 mesh, 58 Å), carbon disulfide (CS_2: Fisher Scientific, AR grade), cesium carbonate (Cs_2CO_3: Alfa Aesar, 99%), magnesium sulfate ($MgSO_4$: anhydrous, Fisher Scientific, LR grade), methyl 2-bromopropionate (MBP: Sigma-Aldrich, 98 %), silica gel (SiO_2: Apollo Scientific, 40-63 micron), sodium chloride (NaCl: Fisher Scientific, > 99%), sodium hydride (NaH: Sigma-Aldrich, 60 wt% dispersion in mineral oil), sodium hydrogen carbonate ($NaHCO_3$: Fisher Scientific, > 99), sodium azide (NaN_3, Sigma-Aldrich, 99%). 2,2'Azobis(2-methyl propionitrile) (AIBN, Sigma-Aldrich, > 98%) was re-crystallized from methanol prior use.

The following solvents were used as received; acetone (VWR International, AR grade), chloroform ($CHCl_3$: VWR International, AR grade), dichloromethane (CH_2Cl_2: VWR International, AR grade), diethyl ether (Fisher Scientific, LR grade), ethyl acetate (VWR International, AR grade), *N*,*N*-dimethylformamide (DMF: Sigma-Aldrich, HPLC grade), 1-

hexanol (Acros Organics, 98%), petroleum spirit (BR 40 - 60 °C, VWR International, AR grade), and tetrahydrofuran (THF: VWR International, AR grade).

The following monomers were deinhibited before use by distillation over CaH_2, distillation pressure: 0.015 atm, 90-92 °C): vinyl acetate (VAc: Sigma-Aldrich, > 99%) vinyl chloroacetate (VClAc: Alfa Aesar, 99%) and *N*-vinylpyrrolidone (NVP: Sigma-Aldrich, > 99 %). *N*-vinylpiperidone (VPip) was donated by BASF, stored in a desiccator and sublimed prior use. 2-Methylene-1,3-dioxepane (MDO) was synthesized using the previously described method of Bailey *et al*.[27] *O*-ethyl-*S*-methyl 2-propionylxanthate (CTA 3) was synthesized using the previously described method of Skey *et al*.[57]

2.5.2 Characterization methods

Nuclear magnetic resonance (^{1}H and ^{13}C NMR) spectra were recorded at either 400 MHz or 100 MHz in $CDCl_3$ on a Bruker DPX-400 spectrometer at 293 K. Chemical shifts are reported as δ in parts per million (ppm) and referenced to the chemical shift of the residual solvent resonances ($CDCl_3$ ^{1}H: δ = 7.26 ppm; ^{13}C δ = 77.16 ppm). The resonance multiplicities are described as s (singlet), d (doublet), t (triplet), q (quartet) or m (multiplet).

Size exclusion chromatography (SEC) analyses were performed on a system composed of a Varian 390-LC-Multi detector using a Varian Polymer Laboratories guard column (PLGel 5 μM, 50 × 7.5 mm), two mixed-D Varian Polymer Laboratories columns (PLGel 5μM, 300 × 7.5 mm) and a PLAST RT autosampler. Detection was conducted using a differential refractive index (DRI) and an ultraviolet (UV) detector set to λ = 280 nm as the xanthate absorbing wavelength. The eluting solvent was either $CHCl_3$ or DMF (HPLC grade), containing 2% triethylamine (TEA) for $CHCl_3$ as solvent and 0.1% LiBr for DMF, at 303 K (or 323 K for the DMF system) at a flow rate of 1.0 mL/min. Polystyrene (PS) (162 - 2.4 ×

10^5 g.mol) or poly(methyl methacrylate) (PMMA) (200 – 1.0 × 10^6 g/mol) standards were used for calibration. Molecular weights and dispersities were determined using Cirrus v3.3 SEC software.

Infrared (IR) spectroscopy was carried out using a Perkin Elmer Spectrometer 100 FT-IR. 16 scans from 600 to 4000 cm^{-1} were collected, and the spectra were corrected for background absorbance.

2.5.3 Synthesis of *O*-hexyl *S*-methyl 2-propionylxanthate (CTA 1)

To a three-neck 100 mL round bottom flask under N_2 was added 60 wt% sodium hydride (1.75 g, 0.044 mol). The vessel was then cooled to 0 °C using an ice bath and dry THF (50 mL) was added *via* cannula transfer. After complete addition of THF, 1-hexanol (4.07 g, 0.040 mol) was added slowly, and then stirred at 0 °C for 10 min until no further outgassing was observed. Carbon disulfide (3.33 g, 0.044 mol) was then added and the solution was stirred at 0 °C for 10 min and at room temperature for 1 h. Methyl 2-bromopropionate (7.30 g, 0.044 mol) was then added directly and stirred for a further 2 h while a white precipitate was observed upon stirring. The reaction was then filtered to remove any formed salts, and the solvent was evaporated to dryness. The residue was then dissolved in ethyl acetate (100 mL) and washed with deionized water (2 × 100 mL) and brine (2 × 100 mL). The organic phase was dried over anhydrous magnesium sulfate, filtered and the solvent was evaporated to dryness. Column chromatography (silica gel, 9:1 petroleum spirit/EtOAc) afforded the target compound as a pale yellow oil (5.1 g, 48%). R_f (9:1 petroleum spirit/EtOAc) 0.38; HRMS *m/z* Theory: 287.0746 ($M\text{-}Na^+$); Found: 287.0749; Elemental analysis: Calculated for $C_{11}H_{20}O_3S_2$: C, 49.97%; H, 7.62%; Found: C, 50.43%; H, 7.66%. ^{1}H NMR (400 MHz, $CDCl_3$, ppm): 4.56 (t, $CH_2CH_2\mathit{CH_2}O$, 2H, $^3J_{H\text{-}H}$ = 5.2 Hz), 4.41 (q, $S\mathit{CH}CH_3$, 1H, $^3J_{H\text{-}H}$ = 6.7 Hz), 3.75 (s, $(C{=}O)O\mathit{CH_3}$, *3H*), 1.78 (m, $CH_2\mathit{CH_2}CH_2O$, 2H, $^3J_{H\text{-}H}$ = 6.6 Hz), 1.56 (d, $SCH\mathit{CH_3}$, 3H, $^3J_{H\text{-}H}$ = 7.2 Hz), 1.25-1.48 (m, $CH_3\mathit{(CH_2)_3}CH_2$, 6H), δ 0.90 (t, $\mathit{CH_3}CH_2$, 3H,

$^{3}J_{H\text{-}H}$ = 6.8 Hz); ^{13}C NMR (100 MHz, $CDCl_3$, ppm): δ 212.3 (CH_2OCSS), 172.0 ($COOCH_3$), 74.7 (CH_2OCS), 52.9 ($COOCH_3$), 47.1 ($SCHCH_3$), 31.5 ($CH_3CH_2CH_2$), 28.2 (CH_2CH_2OCS), 25.7 ($CH_3CH_2CH_2CH_2$), 22.6 ($CH_3CH_2CH_2$), 17.1 ($SCHCH_3CO$), 14.1 ($CH_3CH_2CH_2$). FTIR (ν_{max}, cm^{-1}): 2954-2860 (C-H alkyl stretch), 1739 (C=O stretch), 1452 (C-O stretch), 1046 (C-S stretch).

2.5.4 Synthesis of *O*-isopropyl *S*-methyl-propionylxanthate (CTA 2)

To a three-neck 100 mL round bottom flask under N_2 was added 60 wt% sodium hydride (2.38 g, 0.099 mol). The vessel was then cooled to 0 °C using an ice bath and dry CH_2Cl_2 (50 mL) was added *via* cannula transfer. After complete addition of CH_2Cl_2, isopropanol (65 mL) was added slowly, and then stirred at 0 °C for 2 h until no further outgassing was observed. Carbon disulfide (7.56 g, 0.099 mol) was then slowly added, the solution turned yellow. The solution was stirred at room temperature for 2 h. 1-Ethyl-2-bromo propionate (6 g, 0.033 mol) was then added directly and stirred for 15 h. A white precipitate was observed to form upon stirring. The reaction was then filtered to remove any formed salts then reduced in volume to dryness. The residue was then dissolved in CH_2Cl_2 (100 mL) and washed with Na_2CO_3 1 M (2 × 50 mL), KOH 1M (2 × 50 mL) and brine (2 × 100 mL). The solvent was removed from the organic phase under reduced pressure and the residue was dried over anhydrous magnesium sulfate before purification. Column chromatography (silica gel, 9:1 Hexane/EtOAc) afforded the target compound as a light yellow oil (6.56 g, 84.2%). R_f (9:1 Hexane/EtOAc) 0.34; HRMS *m/z* Theory: 245.0277 ($M\text{-}Na^+$); Found: 245.0284; Elemental analysis: Calculated for $C_8H_{14}O_3S_2$: C, 43.22%; H, 6.35%, Found: C, 43.12%; H, 6.26%. ^{1}H NMR (400 MHz, $CDCl_3$, ppm): 5.73 (m, $OCHCH_3$, 1H, $^{3}J_{H\text{-}H}$ = 6.2 Hz), 4.38 (q, $SCHCH_3$, 1H, $^{3}J_{H\text{-}H}$ = 7.4 Hz), 3.74 (s, OCH_3, 2H), 1.52 (d, $SCHCH_3$, 3H, $^{3}J_{H\text{-}H}$ = 7.4 Hz), 1.39 (dd, $CH(CH_3)_2$, 6H, $^{2}J_{H\text{-}H}$ = 3.2 Hz, $^{3}J_{H\text{-}H}$ = 7.4 Hz); ^{13}C NMR (100 MHz, $CDCl_3$, ppm): δ 212.3 ($O(C{=}S)S$), 172.1 ($CH(C{=}O)O$), 78.5 ($CH(CH_3)_2$), 52.8 ($C{=}O(OCH_3)$), 46.7

(S(*C*H)CH_3), 21.3 (CH(*C*H_3)$_2$), 16.9 (CH_3(CH)C=O). FTIR (ν_{max}, cm^{-1}): 2982 (C-H alkyl stretch), 1733 (C=O stretch), 1450 (C-O stretch), 1045 (C-S stretch).

2.5.5 Synthesis of *O*-ethyl *S*-methyl-propionylxanthate (CTA 3)

O-ethyl *S*-methyl-propionylxanthate (CTA 3) was synthesized using the previous reported procedure by Skey *et al*.[57] To a 100 mL round bottom flask, Cs_2CO_3 (5.40 g, 16.57 mmol) was dissolved in ethanol (50 mL) and stirred for 2 h at room temperature. CS_2 (1.26 g, 16.57 mmol) was added and the solution slowly turned yellow. 1-Methyl-2-bromo propionate (1.00 g, 5.53 mmol) was added and the mixture was stirred for 13 h before being filtered and the salt washed with acetone (20 mL) and CH_2Cl_2 (20 mL). The solvent was then removed from the filtrate under reduced pressure resulting in a yellow/green oil. The oil was dissolved in CH_2Cl_2 (100 mL) and extracted with a brine solution (2 x 200 mL). The solvent was removed from the organic layer under reduced pressure and the light yellow oil was purified by column chromatography (silica gel, 9:1 petroleum spirit/EtOAc) to afford the pure compound as a pale yellow oil (4.5 g, 60%). Elemental analysis: Calculated for $C_7H_{12}O_3S_2$: C, 40.37%: H, 5.81%; Found: C, 40.42%; H, 5.81%. ^{1}H NMR (400 MHz, $CDCl_3$, ppm) δ : 4.40 (q, CO(C*H*CH_3)S, 1H, $^3J_{H\text{-}H}$ = 6.9 Hz), 3.70 (s, C*H*$_3$O(C=O), 3H), 3.65 (q, (C=S)OC*H*$_2$$CH_3$, 2H, $^3J_{H\text{-}H}$ = 7.4 Hz), 1.53 (d, SCHC*H*$_3$, 3H, $^3J_{H\text{-}H}$ = 7.3 Hz), 1.37 (t, OCH_2C*H*$_3$, 3H, $^3J_{H\text{-}H}$ = 7.4 Hz). ^{13}C NMR (100 MHz, CDCl3, ppm) δ: 213.2 (CH_2O*C*SS), 172.1 (*C*OOCH_3), 73.5 (O*C*$H_2$$CH_3$), 52.9 (*C*$H_3$OCO), 47.6 (S*C*H$CH_3$), 18.1 (SCH*C*$H_3$CO), 14.1 (*O*$CH_2$*C*$H_3$). FTIR ($\nu_{max}$, cm^{-1}): 2954-2860 (C-H alkyl stretch), 1739 (C=O stretch), 1452 (C-O stretch), 1046 (C-S stretch).

2.5.6 Typical procedure for the copolymerization of MDO and VAc using the RAFT/MADIX polymerization

In an inert environment, MDO (0.113 g, 9.9×10^{-4} mol), VAc (0.200 g, 2.3×10^{-3} mol), CTA 1 (9.2 mg, 3.9×10^{-5} mol), AIBN (0.55 mg, 3.8×10^{-6} mol) and benzene (15 wt%) were placed into an ampoule and sealed. The resulting solution was stirred and heated to 60 °C for 5 h before the polymerization was quenched by plunging the ampoule into an ice bath. An aliquot was taken prior its precipitation in order to determine the monomer conversions using ^{1}H NMR spectroscopy. The polymer was dissolved in a small amount of $CHCl_3$ or CH_2Cl_2 and precipitated several times in hexane until no further monomer residue was observed. Finally, the colorless solid was dried under vacuum. ^{1}H NMR (400 MHz, $CDCl_3$, ppm) δ: 5.30-4.75 (m, CH_2CHOCO backbone, 1H), 4.58 (t, $SCOCH_2CH_2$ end-group, 2H, $^3J_{H\text{-}H} = 5.9$ Hz), 4.16-3.91 (m, $COOCH_2CH_2CH_2$ backbone, 2H), 3.68 (s, CH_3CCOCH end-group, 3H), 2.95-3.20 (m, $COOCH_2CH_2CH_2CH_2SC$, 2H), 2.60 (m, $CH_2COOCH_2CH_2$ backbone, 2H), 2.05 (m, $CHOOCCH_3$ backbone), 1.95-1.45 (m, $CHCH_2OCO$ backbone, 1H, $CH_2CHOCOCH_2$ backbone, 2H, $CH_3OCOCHCH_3$ end-group, 1H, $CH_3OCOCHCH_3$ end-group, 3H), 1.45-1.10 (m, $CH_2CH_2CH_2CH_3$ end-group, 2H, $CH_2CH_2CH_2CH_3$ end-group, 2H, $CH_2COOCH_2CH_2CH_2$, 2H), 0.90 (t, $CH_2CH_2CH_2CH_3$ end-group, 3H). Conversion by ^{1}H NMR spectroscopy: VAc conv. = 23%, MDO conv. = 16%, M_n (SEC, $CHCl_3$) = 2.9 kg/mol, $Đ_M = 1.41$, M_n (^{1}H NMR) = 2.5 kg/mol.

2.5.7 Typical procedure for chain growth experiments

Poly(MDO-*co*-VAc) was synthesized according to the procedure described above, (M_n (^{1}H NMR) = 3.5 kg/mol, M_n (SEC, $CHCl_3$) = 5.7 kg/mol, $Đ_M$ = 1.52). The copolymer, poly(MDO-*co*-VAc) (0.40 g, 0.11 mmol), VAc (0.20 g, 2.32 mmol), (AIBN, 0.37 mg, 2.25×10^{-6} mmol) were dissolved in benzene (40 wt%) and placed into a sealed ampoule before being degassed by three freeze-pump-thaw cycles. The polymer mixture was then heated at

60 °C for 5 h to afford the diblock poly(MDO-*co*-VAc)-*b*-poly(VAc). The polymer was purified by three precipitations into cold hexane and dried *in vacuo*. ^{1}H NMR ($CDCl_3$, ppm) δ: 5.30-4.75 (m, CH_2CHOCO backbone, 1H), 4.58 (t, $SCOCH_2CH_2$ end-group, 2H, $^3J_{H\text{-}H}$ = 6.0 Hz), 4.16-3.91 (m, $COOCH_2CH_2CH_2$ backbone, 2H), 3.68 (s, CH_3CCOCH end-group, 3H), 2.95-3.20 (t, $COOCH_2CH_2CH_2CH_2SC$, 2H), 2.60 (m, $CH_2COOCH_2CH_2$ backbone, 2H), 2.05 (m, $CHOOCCH_3$ backbone), 1.95-1.45 (m, $CHCH_2OCO$ backbone, 1H, $CH_2CHOCOCH_2$ backbone, 2H, $CH_3OCOCHCH_3$ end-group, 1H, $CH_3OCOCHCH_3$ end-group, 3H), 1.45-1.10 (m, $CH_2CH_2CH_2CH_3$ end-group, 2H, $CH_2CH_2CH_2CH_3$ end-group, 2H, 2H, $CH_2COOCH_2CH_2CH_2$ backbone, 2H), 0.90 (m, $CH_2CH_2CH_2CH_3$ end-group, 3H). Conversion by ^{1}H NMR spectroscopy: VAc conv. = 51%, M_n (^{1}H NMR, $CDCl_3$) = 9.1 kg/mol, M_n (SEC, $CHCl_3$) = 13.8 kg/mol, $Đ_M$ = 1.84.

2.5.8 Typical procedure for the degradation experiments

In a typical experiment, 500 mg of the copolymer were placed in a 10 mL vial and dissolved in a small amount (0.5 mL) of CH_2Cl_2. A solution of KOH in methanol (0.1 M, 6 mL) was then added to the vial and stirred at 40 °C. After stirring for 5 h, the solvents were removed under vacuum. The polymer residues were re-dissolved in $CHCl_3$ and filtered in order to remove the residual salt and the solution was analyzed by SEC analysis ($CHCl_3$).

2.5.9 Typical procedure for the copolymerization of MDO and NVP using the RAFT/MADIX polymerization

In a typical experiment, NVP (0.25 g, 2.2×10^{-3} mol), MDO (0.11 g, 9.6×10^{-4} mol), CTA 1 (7.1 mg, 2.7×10^{-5} mol), AIBN (0.52 mg, 3.21×10^{-6} mol), and benzene (30 wt%) were placed into a sealed ampoule before being degassed by three freeze-pump-thaw cycles. The resulting solution was stirred at 60 °C for 16 h before the polymerization was quenched by plunging the ampoule into an ice bath. An aliquot was taken prior to precipitation in order to

determine the monomer conversions using ^{1}H NMR spectroscopy. The copolymer was dissolved in a small amount of CH_2Cl_2 and precipitated several times in cold diethyl ether until no further monomer residue was observed by ^{1}H NMR spectroscopy analysis. Finally the white powder was dried under vacuum. ^{1}H NMR (400 MHz, $CDCl_3$, ppm) δ: 4.58 (t, SCOCH_2CH$_2$ end-group, 2H, $^3J_{H\text{-}H}$ = 6.0 Hz), 4.16-3.95 (m, COOCH_2CH$_2$CH$_2$ backbone, 2H), 3.95-3.45 (m, CH$_2$CHNCOCH$_2$ backbone, 1H, CH_3OCOCHCH$_3$ end-group, 3H), 3.45-2.85 (m, CHNCH_2CH$_2$CH$_2$ NVP$_{ring}$, 2H), 2.65-2.10 (m, CH_2COOCH$_2$CH$_2$CH$_2$ backbone, 2H, NCH$_2$CH$_2$CH_2 NVP$_{ring}$, 2H, COOCH$_2$CH$_2$CH_2CH$_2$ backbone, 2H), 2.85-1.80 (m, NCH$_2$CH_2CH$_2$ NVP$_{ring}$, 2H), 1.70-1.10 (m, COOCH$_2$CH_2CH$_2$ backbone, 2H, CH$_2$CH_2CH$_2$CH$_3$ end-group, 2H, CH$_2$CH$_2$CH_2CH$_3$ end-group, 2H, CH$_2$CH$_2$CH$_2$CH$_3$ end-group, 2H), 0.90 (t, CH$_2$CH$_2$CH$_2$CH_3 end-group, 3H). Conversion by ^{1}H NMR spectroscopy: NVP conv. = 60%, MDO conv. = 32%, M_n (SEC, $CHCl_3$) = 5.3 kg/mol, $Đ_M$ = 1.30, M_n (^{1}H NMR) = 7.4 kg/mol.

2.5.10 Typical procedure for the copolymerization of MDO and VPip using the RAFT/MADIX polymerization

In a typical procedure, VPip (0.30 g, 2.49×10^{-3} mol), MDO (0.12 g, 1.1×10^{-3} mol), CTA 1 (9.4 mg, 3.55×10^{-5} mol), AIBN (0.58 mg, 3.53×10^{-6} mol) and benzene (15 wt%) were placed into a sealed ampoule before being degassed by three freeze-pump-thaw cycles. The resulting solution was stirred at 60 °C for 5 h before the polymerization was quenched by plunging the ampoule into an ice bath. An aliquot was taken prior its precipitation in order to determine the monomer conversions using ^{1}H NMR spectroscopy. The copolymer was dissolved in a small amount of CH_2Cl_2 and precipitated several times in cold hexane until no further monomer residue was observed. Finally the white powder was dried under vacuum. ^{1}H NMR (400 MHz, $CDCl_3$, ppm) δ: 4.95-4.30 (m, CH$_2$CHNCOCH$_2$ backbone, 1H, SCOCH_2CH$_2$ end-group, 2H), 4.25-3.90 (m, COOCH_2CH$_2$CH$_2$ backbone, 2H), 3.80-3.60 (m,

$CH_3OCOCHCH_3$ end-group, 3H), 3.50-2.25 (m, $NCH_2CH_2CH_2CH_2$ $VPip_{ring}$, 2H, $COOCH_2CH_2CH_2CH_2CH_2$ backbone, 2H), 2.25-2.10 (m, $NCH_2CH_2CH_2CH_2$ $VPip_{ring}$, 2H), 2.0-1.10 (m, $NCH_2CH_2CH_2CH_2$ $VPip_{ring}$, 2H, $NCH_2CH_2CH_2CH_2$ $VPip_{ring}$, 2H, $COOCH_2CH_2CH_2CH_2$ backbone, 2H, $COOCH_2CH_2CH_2$ backbone, 2H, $CH_2CH_2CH_2CH_3$ end-group, 2H, $CH_2CH_2CH_2CH_3$ end-group, 2H), 0.90 (m, $CH_2CH_2CH_2CH_3$ end-group, 3H). Conversion by ^{1}H NMR spectroscopy: VPip conv. = 31%, MDO conv. = 15%, M_n (SEC, $CHCl_3$) = 2.1 kg/mol, $Đ_M$ = 1.30.

2.5.11 Typical procedure for the copolymerization of MDO and VClAc using the RAFT/MADIX polymerization

In an inert environment, MDO (0.113 g, 9.9×10^{-4} mol), VClAc (0.20 g, 2.3×10^{-3} mol), CTA 1 (9.2 mg, 3.9×10^{-5} mol), AIBN (0.54 mg, 3.8×10^{-6} mol) and benzene (15 wt%) were placed into an ampoule and sealed. The resulting solution was stirred and heated to 60 °C for 5 h before the polymerization was quenched by plunging the ampoule into an ice bath. An aliquot was taken prior to precipitation in order to determine the monomer conversions using ^{1}H NMR spectroscopy. The polymer was dissolved in a small amount of $CHCl_3$ or CH_2Cl_2 and precipitated several times in hexane until no further monomer residue was observed. Finally the colorless solid was dried under vacuum. ^{1}H NMR (400 MHz, $CDCl_3$, ppm) δ: 5.35-4.75 (m, CH_2CHOCO backbone, 1H), 4.58 (t, $SCOCH_2CH_2$ end-group, 2H, $^3J_{H\text{-}H}$ = 5.8 Hz), 4.16-3.91 (m, $COOCH_2CH_2CH_2$ backbone, 2H, $CHOCOCH_2Cl$, 2H), 3.70 (s, CH_3CCOCH end-group, 3H), 3.20-2.90 (m, $COOCH_2CH_2CH_2CH_2SC$, 2H), 2.60 (m, $CH_2COOCH_2CH_2$ backbone, 2H), 2.05 (m, $CHOOCCH_3$ backbone, 3H), 1.95-1.45 (m, $CHCH_2OCO$ backbone, 1H, $CH_2CHOCOCH_2$ backbone, 2H, $CH_3OCOCHCH_3$ end-group, 1H, $CH_3OCOCHCH_3$ end-group, 3H), 1.45-1.10 (m, $CH_2CH_2CH_2CH_3$ end-group, 2H, $CH_2CH_2CH_2CH_3$ end-group, 2H, $CH_2COOCH_2CH_2CH_2$, 2H), 0.90 (m, $CH_2CH_2CH_2CH_3$

end-group, 3H). Conversion by ^{1}H NMR spectroscopy: VClAc conv. = 19%, MDO conv. = 11%, M_n (SEC, $CHCl_3$) = 5.0 kg/mol, $Đ_M$ = 1.48, M_n (^{1}H NMR) = 3.4 kg/mol.

2.5.12 Typical procedure for the post-polymerization modification of poly(MDO-*co*-VClAc)

Poly(MDO-*co*-VClAc) was synthesized according to the procedure described above, (M_n (^{1}H NMR) = 3.4 kg/mol, M_n (SEC, $CHCl_3$) = 5.0 kg/mol, $Đ_M$ = 1.48). The copolymer poly(MDO-*co*-VClAc) (0.65 g, 0.19 mmol) was dissolved in DMF (10 mL) and NaN_3 (0.15 g, 2.31 mmol) was added to the mixture before stirring at room temperature for 2 days. The solvent was removed under vacuum and the polymer was re-dissolved in a small amount of toluene before being precipitated into cold hexane. The polymer was dried *in vacuo* to afford a colorless solid. ^{1}H NMR (400 MHz, $CDCl_3$, ppm) δ: 5.35-4.75 (m, CH_2CHOCO backbone, 1H), 4.58 (t, $SCOCH_2CH_2$ end-group, 2H, $^3J_{H\text{-}H}$ = 5.9 Hz), 4.16-4.00 (m, $COOCH_2CH_2CH_2$ backbone, 2H), 4.00-3.90 (m, $CHOCOCH_2N_3$, 2H), 3.70 (s, CH_3CCOCH end-group, 3H), 3.20-2.90 (t, $COOCH_2CH_2CH_2CH_2SC$, 2H), 2.60 (m, $CH_2COOCH_2CH_2$ backbone, 2H), 2.05 (m, $CHOOCCH_3$ backbone), 1.95-1.45 (m, $CHCH_2OCO$ backbone, 1H, $CH_2CHOCOCH_2$ backbone, 2H, $CH_3OCOCHCH_3$ end-group, 1H, $CH_3OCOCHCH_3$ end-group, 3H), 1.45-1.10 (m, $CH_2CH_2CH_2CH_3$ end-group, 2H, $CH_2CH_2CH_2CH_3$ end-group, 2H, $CH_2COOCH_2CH_2CH_2$, 2H), 0.90 (m, $CH_2CH_2CH_2CH_3$ end-group, 3H). M_n (^{1}H NMR) = 3.9 kg/mol, M_n (SEC, $CHCl_3$) = 5.2 kg/mol, $Đ_M$ = 1.59.

2.5.13 Typical procedure for the synthesis of the macro-CTA, poly(NVP)

In an typical polymerization, NVP (30.0 g, 0.27 mol), CTA 1 (1.43 g, 5.4×10^{-3} mol), AIBN (88.5 mg, 5.40×10^{-4} mol), and benzene (15 wt%) were placed into a sealed ampoule before being degassed by three freeze-pump-thaw cycles. The resulting solution was stirred and heated to 60 °C for 5 h before the polymerization was quenched by plunging the ampoule

into an ice bath. An aliquot was taken prior to precipitation in order to determine the monomer conversions using ^{1}H NMR spectroscopy. The polymer was dissolved in $CHCl_3$ and precipitated several times in diethyl ether, then collected and dried in a vacuum oven at room temperature overnight. ^{1}H NMR (400 MHz, $CDCl_3$, ppm) δ: 4.58 (t, SCOCH_2CH$_2$ end-group, 2H, $^3J_{H\text{-}H}$ = 6.0 Hz), 4.16-3.50 (m, CH$_2$CHNCOCH$_2$ backbone, 1H, CH_3OCOCHCH$_3$ end-group, 3H), 3.45-2.65 (m, CHNCH_2CH$_2$CH$_2$ NVP$_{ring}$, 2H), 2.65-1.10 (m, NCH$_2$CH$_2$CH_2 NVP$_{ring}$, 2H, NCH$_2$CH_2CH$_2$ NVP$_{ring}$, 2H, CH$_2$CHNCH$_2$ backbone, 2H, CH$_2$CH_2CH$_2$CH$_3$ end-group, 2H, CH$_2$CH$_2$CH_2CH$_3$ end-group, 2H, CH$_2$CH$_2$CH$_2$CH$_3$ end-group, 2H), 0.90 (t, CH$_2$CH$_2$CH$_2$CH_3 end-group, 3H). Conversion by ^{1}H NMR spectroscopy: NVP conv. = 30%, M_n (SEC, $CHCl_3$) = 2.2 kg/mol, $Đ_M$ = 1.19, M_n (^{1}H NMR) = 2.5 kg/mol.

2.5.14 Typical procedure for the synthesis of the block copolymer poly(NVP)-*b*-poly(MDO-*co*-VAc)

In a typical experiment, poly(NVP) macro-CTA (0.25 g, 0.074 mmol) was dissolved in benzene (30 wt%). MDO (0.25 g, 2.19 mmol), VAc (0.45 g, 5.22 mmol) and AIBN (1.2 mg, 0.0073 mmol) were added and stirred at room temperature until total dissolution. The mixture was introduced into an ampoule and degassed by four freeze-pump thaw cycles and sealed under nitrogen. The polymerization was carried out for 5 h at 60 °C and then quenched in an ice bath. An aliquot was taken prior to precipitation in order to determine the monomer conversions using ^{1}H NMR spectroscopy. The block copolymer, poly(NVP)-*b*-poly(MDO-*co*-VAc), was dissolved in a small amount of CH_2Cl_2 (1 mL) and purified by several precipitations in diethyl ether. The sample was dried under vacuum overnight to yield a white solid. ^{1}H NMR (400 MHz, $CDCl_3$, ppm) δ: 5.30-4.75 (m, CH$_2$CHOCO backbone VAc, 1H), 4.58 (m, SCOCH_2CH$_2$ end-group, 2H), 4.16-3.90 (m, COOCH_2CH$_2$CH$_2$ backbone MDO, 2H), 3.90-3.45 (m, CH$_2$CHNCOCH$_2$ backbone NVP, 1H, CH_3OCOCHCH$_3$ end-group, 3H), 3.45-2.75 (m, CHNCH_2CH$_2$CH$_2$ NVP$_{ring}$, 2H), 2.65-2.45 (m, CH_2COOCH$_2$CH$_2$

backbone MDO), 2.45-2.10 (m, CHNC*H*$_2$CH$_2$CH$_2$ NVP$_{ring}$, 2H, COOCH$_2$CH$_2$C*H*$_2$ backbone MDO, 2H), 2.10-1.80 (m, OCOC*H*$_3$ backbone VAc, 3H, CHNCH$_2$C*H*$_2$CH$_2$ NVP$_{ring}$, 2H, CH$_3$OCOC*H*CH$_3$ end-group, 1H, CH$_3$OCOCHC*H*$_3$ end-group, 3H), 1.45-1.10 (m, CH$_2$C*H*$_2$CH$_2$CH$_3$ end-group, 2H, CH$_2$CH$_2$C*H*$_2$CH$_3$ end-group, 2H, C*H*$_2$CH$_2$CH$_2$CH$_3$ end-group, 2H), 0.90 (m, CH$_2$CH$_2$CH$_2$C*H*$_3$ end-group, 3H). Conversions by ^{1}H NMR spectroscopy: VAc conversion = 38%, MDO conversion = 23%, M_n (SEC, DMF) = 4.3 kg/mol, $Đ_M$ = 1.28.

2.6 References

(1) Albertsson, A.-C.; Varma, I. K. *Biomacromolecules* **2003**, *4*, 1466.

(2) Uhrich, K. E.; Cannizzaro, S. M.; Langer, R. S.; Shakesheff, K. M. *Chem. Rev. (Washington, DC, U. S.)* **1999**, *99*, 3181.

(3) Tsuji, H. *Macromol. Biosci.* **2005**, *5*, 569.

(4) Dove, A. P. *Chem. Commun.* **2008**, 6446.

(5) Pounder, R. J.; Dove, A. P. *Polym. Chem.* **2010**, *1*, 260.

(6) Thomas, C. M. *Chem. Soc. Rev.* **2010**, *39*, 165.

(7) Williams, C. K. *Chem. Soc. Rev.* **2007**, *36*, 1573.

(8) Kan, S.; Jin, Y.; He, X.; Chen, J.; Wu, H.; Ouyang, P.; Guo, K.; Li, Z. *Polym. Chem.* **2013**, *4*, 5432.

(9) Cooper, B. M.; Chan-Seng, D.; Samanta, D.; Zhang, X.; Parelkar, S.; Emrick, T. *Chem. Commun.* **2009**, 815.

(10) Bassi, A. K.; Gough, J. E.; Downes, S. *J. Tissue. Eng. Regen. Med.* **2012**, *6*, 833.

(11) Bassi, A. K.; Gough, J. E.; Zakikhani, M.; Downes, S. *J. Tissue. Eng.* **2011**, *2*.

(12) Cajot, S.; Lecomte, P.; Jerome, C.; Riva, R. *Polym. Chem.* **2013**, *4*, 1025.

(13) Riva, R.; Schmeits, S.; Stoffelbach, F.; Jerome, C.; Jerome, R.; Lecomte, P. *Chem. Commun.* **2005**, 5334.

(14) Carrot, G.; Hilborn, J. G.; Trollsås, M.; Hedrick, J. L. *Macromolecules* **1999**, *32*, 5264.

(15) Korich, A. L.; Walker, A. R.; Hincke, C.; Stevens, C.; Iovine, P. M. *J. Polym. Sci., Part A: Polym. Chem.* **2010**, *48*, 5767.

(16) Jacquier, V.; Miola, C.; Llauro, M.-F.; Monnet, C.; Hamaide, T. *Macromol. Chem. Phys.* **1996**, *197*, 1311.

(17) Liu, M.; Vladimirov, N.; Fréchet, J. M. J. *Macromolecules* **1999**, *32*, 6881.

(18) Vaida, C.; Takwa, M.; Martinelle, M.; Hult, K.; Keul, H.; Möller, M. *Macromol. Symp.* **2008**, *272*, 28.

(19) de Freitas, A. G. O.; Trindade, S. G.; Muraro, P. I. R.; Schmidt, V.; Satti, A. J.; Villar, M. A.; Ciolino, A. E.; Giacomelli, C. *Macromol. Chem. Phys.* **2013**, *214*, 2336.

(20) Jérôme, C.; Lecomte, P. *Adv. Drug Deliv. Rev.* **2008**, *60*, 1056.

(21) Hvilsted, S. *Polym. Int.* **2012**, *61*, 485.

(22) Campos, J. M.; Ribeiro, M. R.; Ribeiro, M. F.; Deffieux, A.; Peruch, F. *Eur. Polym. J.* **2013**, *49*, 4025.

(23) Li, G.; Lamberti, M.; Pappalardo, D.; Pellecchia, C. *Macromolecules* **2012**, *45*, 8614.

(24) Wilson, J. A.; Hopkins, S. A.; Wright, P. M.; Dove, A. P. *Macromolecules* **2015**, *48*, 950.

(25) Wurth, J. J.; Shastri, V. P. *J. Polym. Sci., Part A: Polym. Chem.* **2013**, *51*, 3375.

(26) Undin, J.; Illanes, T.; Finne-Wistrand, A.; Albertsson, A.-C. *Polym. Chem.* **2012**, *3*, 1260.

(27) Bailey, W. J.; Ni, Z.; Wu, S.-R. *J. Polym. Sci., Part A: Polym. Chem.* **1982**, *20*, 3021.

(28) Agarwal, S. *Polym. J* **2006**, *39*, 163.

(29) Jin, S.; Gonsalves, K. E. *Macromolecules* **1997**, *30*, 3104.

(30) Roberts, G. E.; Coote, M. L.; Heuts, J. P. A.; Morris, L. M.; Davis, T. P. *Macromolecules* **1999**, *32*, 1332.

(31) Agarwal, S. *Polym. J.* **2007**, *39*, 163.

(32) Sun, L. F.; Zhuo, R. X.; Liu, Z. L. *J. Polym. Sci., Part A: Polym. Chem.* **2003**, *41*, 2898.

(33) Wu, B.; Lenz, R. W. *J. Environ. Polym. Degrad.*, *6*, 23.

(34) Bailey, W. J.; Endo, T.; Gapud, B.; Lin, Y.-N.; Ni, Z.; Pan, C.-Y.; Shaffer, S. E.; Wu, S.-R.; Yamazaki, N.; Yonezawa, K. *Journal of Macromolecular Science: Part A - Chemistry* **1984**, *21*, 979.

(35) William, J. B.; Vijaya, K. K.; Jay, S. A. In *Agricultural and Synthetic Polymers*; American Chemical Society: 1990; Vol. 433, p 149.

(36) Delplace, V.; Tardy, A.; Harrisson, S.; Mura, S.; Gigmes, D.; Guillaneuf, Y.; Nicolas, J. *Biomacromolecules* **2013**, *14*, 3769.

(37) Morris, L. M.; Davis, T. P.; Chaplin, R. P. *Polymer* **2001**, *42*, 495.

(38) Xu, J.; Liu, Z.-L.; Zhuo, R.-X. *J. Appl. Polym. Sci.* **2007**, *103*, 1146.

(39) Maji, S.; Mitschang, F.; Chen, L.; Jin, Q.; Wang, Y.; Agarwal, S. *Macromol. Chem. Phys.* **2012**, *213*, 1643.

(40) Agarwal, S.; Kumar, R.; Kissel, T.; Reul, R. *Polym. J* **2009**, *41*, 650.

(41) Wei, Y.; Connors, E. J.; Jia, X.; Wang, C. *J. Polym. Sci., Part A: Polym. Chem.* **1998**, *36*, 761.

(42) Chung, I. S.; Matyjaszewski, K. *Macromolecules* **2003**, *36*, 2995.

(43) Huang, J.; Gil, R.; Matyjaszewski, K. *Polymer* **2005**, *46*, 11698.

(44) d'Ayala, G. G.; Malinconico, M.; Laurienzo, P.; Tardy, A.; Guillaneuf, Y.; Lansalot, M.; D'Agosto, F.; Charleux, B. *J. Polym. Sci., Part A: Polym. Chem.* **2014**, *52*, 104.

(45) Undin, J.; Finne-Wistrand, A.; Albertsson, A.-C. *Biomacromolecules* **2013**, *14*, 2095.

(46) Delplace, V.; Harrisson, S.; Tardy, A.; Gigmes, D.; Guillaneuf, Y.; Nicolas, J. *Macromol. Rapid Commun.* **2014**, *35*, 484.

(47) Yuan, J.-Y.; Pan, C.-Y.; Tang, B. Z. *Macromolecules* **2001**, *34*, 211.

(48) He, T. Z., Y.-F. and Pan, C.-Y. *Polym. J.* **2002**, *34*, 138.

(49) Tardy, A.; Delplace, V.; Siri, D.; Lefay, C.; Harrisson, S.; de Fatima Albergaria Pereira, B.; Charles, L.; Gigmes, D.; Nicolas, J.; Guillaneuf, Y. *Polym. Chem.* **2013**, *4*, 4776.

(50) Wei, Y.; Connors, E. J.; Jia, X.; Wang, B. *Chem. Mater.* **1996**, *8*, 604.

(51) McCormick, C. L.; Lowe, A. B. *Acc. Chem. Res.* **2004**, *37*, 312.

(52) Moad, G.; Rizzardo, E.; Thang, S. H. *Acc. Chem. Res.* **2008**, *41*, 1133.

(53) Chiefari, J.; Chong, Y. K.; Ercole, F.; Krstina, J.; Jeffery, J.; Le, T. P. T.; Mayadunne, R. T. A.; Meijs, G. F.; Moad, C. L.; Moad, G.; Rizzardo, E.; Thang, S. H. *Macromolecules* **1998**, *31*, 5559.

(54) Schmitt, J.; Blanchard, N.; Poly, J. *Polym. Chem.* **2011**, *2*, 2231.

(55) Stenzel, M. H.; Cummins, L.; Roberts, G. E.; Davis, T. P.; Vana, P.; Barner-Kowollik, C. *Macromol. Chem. Phys.* **2003**, *204*, 1160.

(56) Patel, V. K.; Vishwakarma, N. K.; Mishra, A. K.; Biswas, C. S.; Ray, B. *J. Appl. Polym. Sci.* **2012**, *125*, 2946.

(57) Skey, J.; O'Reilly, R. K. *Chem. Commun.* **2008**, 4183.

(58) Ieong, N. S.; Redhead, M.; Bosquillon, C.; Alexander, C.; Kelland, M.; O'Reilly, R. K. *Macromolecules* **2011**, *44*, 886.

(59) Kapur, S. L.; Joshi, R. M. *J. Polym. Sci.* **1954**, *14*, 489.

(60) Manders, B. G.; Smulders, W.; Aerdts, A. M.; van Herk, A. M. *Macromolecules* **1997**, *30*, 322.

(61) Saldivar-Guerra, E., Vivaldo-Lima, E. *Handbook of Polymer, Synthesis, Characterization and Processing* **2013**, *Wiley*, Hoboken.

(62) Agarwal, S. *Polym. Chem.* **2010**, *1*, 953.

(63) Agarwal, S. In *Biodegradable Polyesters*; Wiley-VCH Verlag GmbH & Co. KGaA: 2015, p 25.

(64) Bailey, W. J.; Wu, S.-R.; Ni, Z. *Macromol. Chem. Phys.* **1982**, *183*, 1913.

(65) Maji, S.; Zheng, M.; Agarwal, S. *Macromol. Chem. Phys.* **2011**, *212*, 2573.

(66) Agarwal, S.; Kumar, R. *Macromol. Chem. Phys.* **2011**, *212*, 603.

(67) Yang, L.; Luo, Y.; Li, B. *J. Polym. Sci., Part A: Polym. Chem.* **2005**, *43*, 4972.

(68) Jakubowski, W.; Min, K.; Matyjaszewski, K. *Macromolecules* **2006**, *39*, 39.

(69) Delplace, V.; Nicolas, J. *Nat Chem* **2015**, *7*, 771.

(70) Kobben, S.; Ethirajan, A.; Junkers, T. *J. Polym. Sci., Part A: Polym. Chem.* **2014**, *52*, 1633.

(71) Lam, C. X. F.; Savalani, M. M.; Teoh, S.-H.; Hutmacher, D. W. *Biomedical Materials* **2008**, *3*, 034108.

(72) Undin, J.; Finne-Wistrand, A.; Albertsson, A.-C. *Biomacromolecules* **2014**, *15*, 2800.

(73) Shi, Y.; Zhou, P.; Jérôme, V.; Freitag, R.; Agarwal, S. *ACS Biomater. Sci. Eng.* **2015**, *1*, 971.

(74) Gauthier, M. A.; Gibson, M. I.; Klok, H.-A. *Angew. Chem. Int. Ed.* **2009**, *48*, 48.

(75) Günay, K. A.; Theato, P.; Klok, H.-A. In *Functional Polymers by Post-Polymerization Modification*; Wiley-VCH Verlag GmbH & Co. KGaA: 2012, p 1.

(76) Dervaux, B.; Du Prez, F. E. *Chem. Sci.* **2012**, *3*, 959.

(77) Basko, M.; Bednarek, M.; Billiet, L.; Kubisa, P.; Goethals, E.; Du Prez, F. *J. Polym. Sci., Part A: Polym. Chem.* **2011**, *49*, 1597.

3 Radical Ring-Opening Copolymerization of MDO and Vinyl Bromobutanoate: Synthesis, Degradability and Post-Polymerization Modification

3.1 Abstract

In this Chapter, the concept of controlled copolymerization of MDO with vinyl monomers is extended to a vinyl acetate derivative monomer in order to target further functional degradable copolymers with different properties. To this end, the synthesis of vinyl bromobutanoate (VBr), a new vinyl acetate monomer obtained by the palladium-catalyzed vinyl exchange reaction between vinyl acetate (VAc) and bromobutyric acid is presented. The homopolymerization of this new monomer using the RAFT/MADIX polymerization technique is reported to form novel, well-defined and controlled polymers, with narrow molecular weight distributions, which contain pendent bromine functional groups able to be modified *via* post-polymerization modification reactions. Furthermore, the copolymerization of vinyl bromobutanoate with 2-methylene-1,3-dioxepane (MDO) is also presented to deliver a range of novel functional degradable copolymers, poly(MDO-*co*-VBr). The copolymer composition could be tuned to vary the amount of ester repeat units in the polymer backbone, and hence change the degradability, whilst still maintaining control over the final copolymers' molecular weights. Additionally, the incorporation of further functionalities *via* simple post-polymerization modifications such as azidation and the 1,3-dipolar cycloaddition of a PEG alkyne to an azide is also reported with modifications confirmed by ^{1}H NMR spectroscopy, Fourier Transform Infrared (FTIR) spectroscopy and SEC analyses.

3.2 Introduction

Since the discovery of modern polymer science by pioneers such as Staudinger more than seven decades ago,[1] the use of post-polymerization modifications reactions (also called *polymer analogous modifications*) has increasingly become an emergent technique in the polymer field as an appealing route to create functional materials.[2,3]

Amongst the most common post-polymerization modification reactions, thiol-ene additions,[4,5] Diels-Alder reactions,[6-8] and azide/alkyne cycloadditions[9-11] have all increased in use since the development of "living"/controlled radical polymerization techniques (*e.g.* NMP, RAFT, ATRP), the methods of which are far more tolerant to functional groups.[12-14] In more recent years, post-polymerization modifications have also been widely used on aliphatic polyesters, which have become an emergent class of polymer materials owing to their degradable properties within a physiological environment.[15,16] Such properties have allowed them to be used in a vast range of applications from implantable and injectable drug delivery devices to tissue engineering scaffolds for bone replacement.[17-20] In attempts to diversify the range of properties targeted for biomedical applications, much effort has recently been focused on the development of degradable aliphatic polyesters bearing functional groups which can be further modified by post-polymerization approaches.[17,21-24] Amongst these approaches, the synthesis of new cyclic ester monomers with modifiable functional groups, chain-end modifications of the ring-opening polymerization (ROP) initiator/catalyst or the copolymerization of cyclic ester monomer with other monomers have predominantly be investigated. In their work, Riva and co-workers investigated the copolymerization of ε-caprolactone (CL) with 6-chloro-ε-caprolactone, a functionalized derivative of CL, and successfully synthesized a novel polyester material with chloro functionalized pendent groups which could be subsequently post-polymerization modified into azide groups using sodium azide (Scheme 3.1).[25] The azido-functional polyester could then be further modified using the copper catalysed azide/alkyne cycloaddition to incorporate further properties in the degradable materials without degradation of the final polymer.

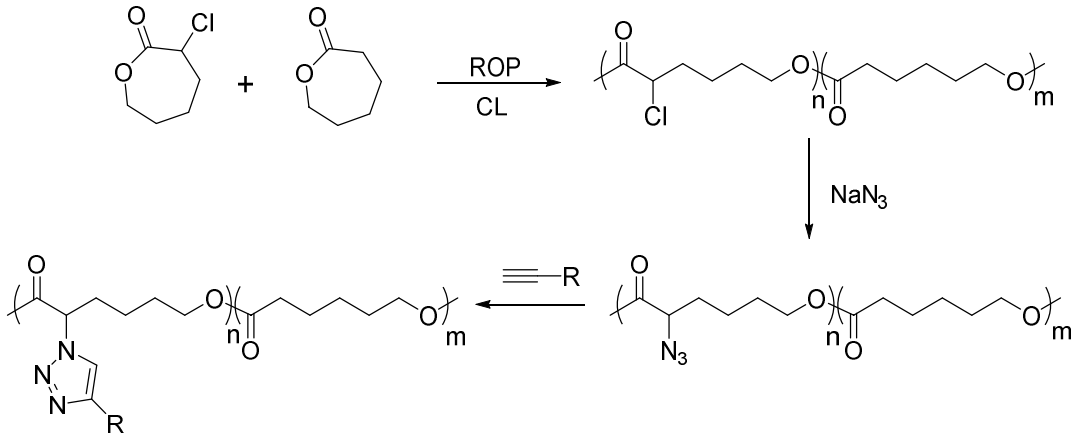

Scheme 3.1. Schematic representation of the synthesis of functionalized poly(ε-caprolactone) using azidation and azide/alkyne cycloaddition post-polymerization modifications performed by Riva and co-workers.[25]

While such approaches have been successful introduced additional functional groups into polyester materials, and making post-polymerization modifications possible, the challenging synthetic steps and compatibility of some functional groups with the ROP catalyst/initiator have afforded some limitations to this approach.[23,24,26-31]

As introduced in Chapter 2, the radical ring-opening polymerization (rROP) of 2-methylene-1,3-dioxepane (MDO, **CKA 1**) has been seen in recent years as an alternative route for the synthesis of functional polyesters,[32-35] where its copolymerization with other vinyl monomers enabled the synthesis of a new type of degradable and functional polymer.[36-41] In their work, Agarwal and co-workers investigated the copolymerization of MDO and propargyl acrylate (PA) in order to produce an alkyne-functionalized degradable copolymer, which could undergo a post-polymerization modification using "click" chemistry to attach a biocompatible and hydrophilic grafted poly(ethylene glycol) (PEG) segment into the copolymer backbone (Scheme 3.2).[41,42] While the successful copolymerization of these two monomers was realized and the incorporation of "clickable" functional pendent groups in the polymer backbone accomplished, the process was performed using conventional free radical polymerization and no control over the molecular weights or the dispersities of the

copolymer could be achieved. Furthermore, the copolymerization of cyclic ketene acetal, especially MDO, with acrylate monomers has also been reported to form copolymer with a blocky microstructure as a consequence of their different reactivity ratios and hence leading to a material with a poor degradability density.[43,44]

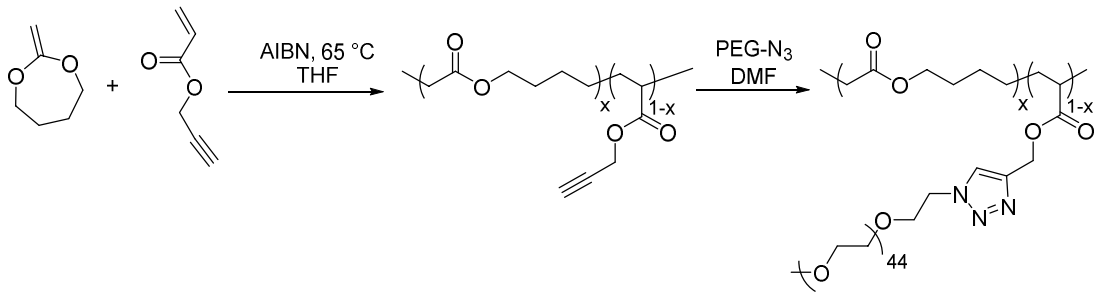

Scheme 3.2. Schematic representation of the copolymerization of MDO and PA followed by post-polymerization azidation with PEG azide as performed by Agarwal and co-workers.[42]

In Chapter 2, the copolymerization of MDO and VAc using the RAFT/MADIX polymerization technique was presented as a successful way to obtain well-defined and controlled functional copolymers of poly(MDO-*co*-VAc).[45] Inspired by this result, the controlled copolymerization of MDO with other vinyl monomers can therefore be seen as a promising new way to form functional degradable copolymers bearing a wider range of functionalities. For this task, vinyl acetate-derived monomers containing functional groups which can be modified after polymerization are likely to be ideal candidates as the reactivity ratios of MDO and VAc have been proven to lead to random incorporations of ester repeat units in the polymer backbone.[36,45,46] Such vinyl acetate derivative monomers (also called *vinyl esters*) can be easily synthesized *via* vinyl exchange reactions between vinyl acetate and carboxylic acid compounds, typically in the presence of a catalyst.[47-51] The vinyl exchange reactions used for the synthesis of vinyl acetate derived monomers have been reported to suffer from low yields which mainly depend on the amount of catalyst and the temperature at which they are performed.[49] Recently, Drockenmuller and co-workers

reported the synthesis of vinyl levulinate (VL) *via* the palladium-catalyzed vinyl exchange between levulinic acid and vinyl acetate in a high yield (typically above 70%) by reducing the concentration of catalyst and VAc.[47] The copolymerization of VL and VAc could then be performed, using cobalt-mediated radical polymerization (CMRP), to produce well-defined and controlled copolymers of poly(VL-*co*-VAc), where the functional ketone pendent groups could be modified using ketoxime "click" chemistry as a post-polymerization approach (Scheme 3.3).

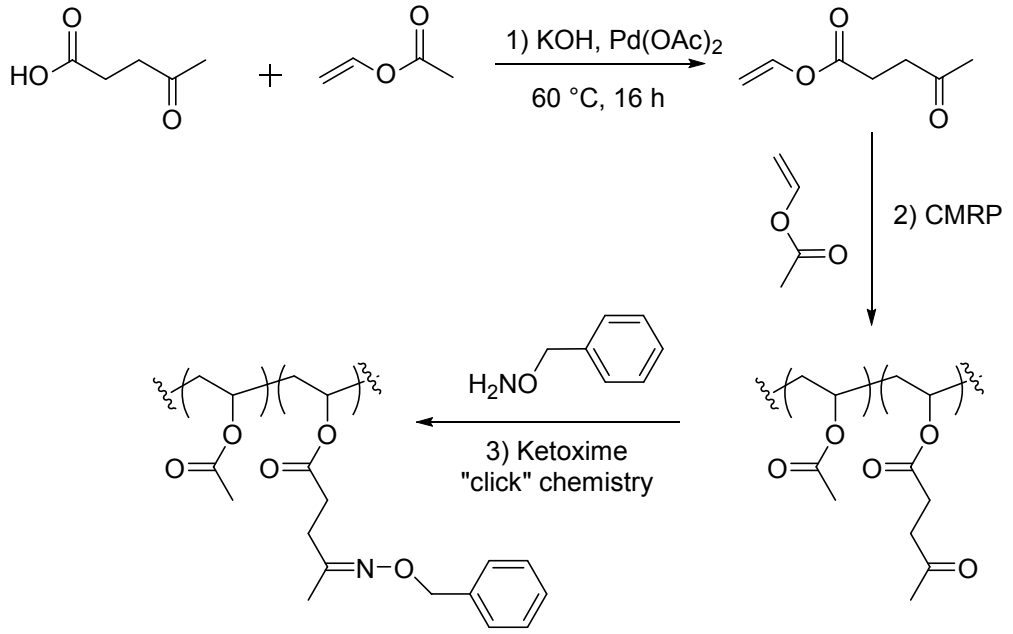

Scheme 3.3. Schematic representation of the synthesis of vinyl levulinate (VL) using the palladium vinyl exchange reaction (1), its copolymerization with VAc using cobalt-mediated radical polymerization (2) and functionalization using ketoxime "click" chemistry (3), as described by Drockenmuller and co-workers.[47]

Inspired by the improved method reported by Drockenmuller and co-workers, the hypothesis was made that the use of the optimized palladium-catalyzed vinyl exchange reaction could represent and important impact on the field of polymers, as it could provide a potentially limitless route to the production of a novel class of vinyl acetate derived monomers with different functionalities. These used in conjunction with the rROP of cyclic ketene acetal monomers, such as MDO, could create a new range of functional and degradable polymers.

3.3 Results and Discussion

3.3.1 Initial results

Following the demonstration of the potential to use the RAFT/MADIX polymerization technique to obtain well-defined and controlled functional degradable poly(MDO-*co*-VAc) copolymers in Chapter 2, the next focus of the project was to extend the range of functionalities contained in such polymers by using different vinyl acetate derived monomers. As briefly introduced in Chapter 2, the use of the commercially available chloride derivative monomer of VAc, vinyl chloroacetate (VClAc) presented an attractive way to increase the functionality range of poly(VAc) as the presence of the additional chloride group on the monomer could allow for post-polymerization modification using azidation and potential "click" chemistry reactions. However, after further investigation of the suitability of VClAc for the synthesis of degradable functional copolymers with MDO it was found that the copolymerization was limited to low monomer conversion. The hypothesis that the poor stability of the propagating MDO radical and the subsequent chain transfer to VClAc monomer detrimentally affected the polymerization was made. This would lead to the formation of long-chain branching in the resulting copolymer which could be observed by SEC analysis as a lower molecular shoulder was forming for VClAc conversions > 20% (Figure 3.1).

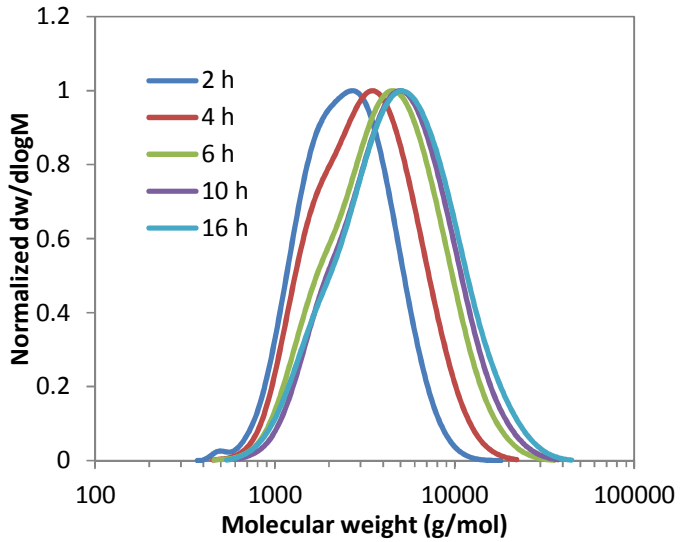

Figure 3.1. Size exclusion chromatograms of poly(MDO-*co*-VClAc) obtained by the RAFT/MADIX copolymerization at different reactions times, (SEC, $CHCl_3$).

In a further attempt to confirm the hypothesis of branching formation experimentally, the analysis of the copolymer poly(MDO-*co*-VClAc), obtained after 16 h of polymerization, was investigated by triple detection SEC analysis fitted with a viscometry detector. The determination of branches in polymers by SEC is based on the investigation of changes in the intrinsic viscosity (IV) as a function of molecular weight (M). For a constant molecular weight, the hydrodynamic size and IV will decrease as there is an increase in branching. As such, in the case of branched polymers, IV values will always be lower than the values for an analogous linear polymer as a consequence of the presence of branch points in the microstructure. This relationship between viscosity and molecular weight is described by the Mark-Houwink-Sakurada equation, which includes the Mark-Houwink constant, *a*, related to the polymer structure when in solution. For a polymer in a theta solvent $a = 0.5$, and for a linear polymer and flexible polymer in solution $0.5 < a < 0.8$.[52] Based in this concept, calculation of branching can be determined by the gradient (α) of the Mark-Houwink plot (log IV *versus* log M). The analysis of poly(MDO-*co*-VClAc) was performed by SEC (in

DMF) and the Mark-Houwink plot for the copolymer was obtained using the Agilent GPC/SEC software V1 (Figure 3.2a).

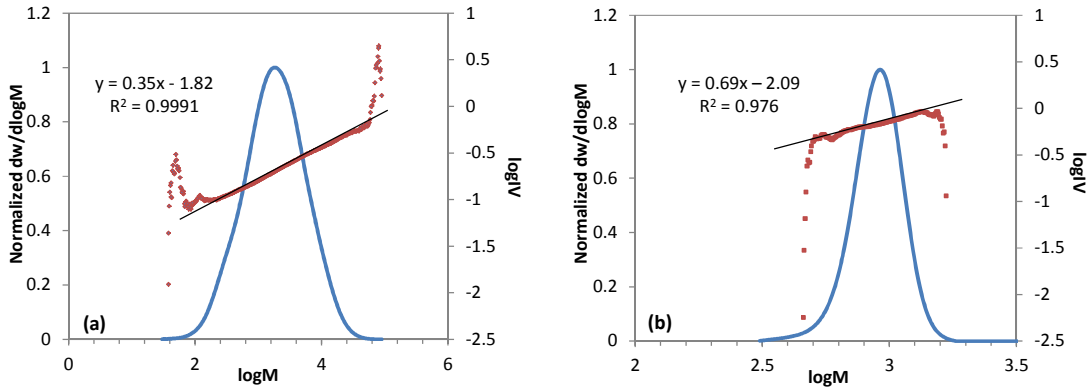

Figure 3.2. SEC chromatograms of the copolymer of poly(MDO-*co*-VClAc) (a) and homopolymer of poly(VClAc) (b) and Mark-Houwink plots obtained after analysis using the viscometry detector (SEC, DMF).

Based on the result obtained from the software, the gradient of the plot was measured and obtained as $a = 0.35$, which indicates that the polymer was adopting a more compact structure in the solvent than a linear and flexible polymer consistent with a branched structure being obtained. Further analysis of the analogous poly(VClAc) homopolymer was also performed where the gradient of the plot was obtained as $a = 0.69$ (Figure 3.2b) confirming a more linear structure in agreement with values previously reported for in the case of poly(VAc).[53,54] Following from this result, the hypothesis that branches could form during the copolymerization of MDO and VClAc was confirmed, with the branching potentially observed as a consequence of the combination of the poor stability of the MDO radical and the chain transfer occurring for VClAc.

In order to avoid this side reaction, a monomer in which the halide was less activated towards radical abstraction would present an analogous functional monomer that could be polymerized using CRP methodologies and eliminate the side reactions observed with VClAc. Hence the synthesis of a new monomer, vinyl

bromobutanoate, was proposed, using the palladium vinyl exchange reaction previously introduced.

3.3.2 Synthesis of vinyl bromobutanoate

Following on from the vinyl exchange reaction procedure previously reported by Drockenmuller and co-workers[47], the synthesis of a bromide functional monomer by the reaction of 4-bromo butyric acid and vinyl acetate using a palladium catalyzed vinyl exchange reaction was targeted (Scheme 3.4). This approach would create a novel vinyl monomer containing a longer bromine pendent group which will likely impart different properties in comparison to the commercially available VClAc monomer.

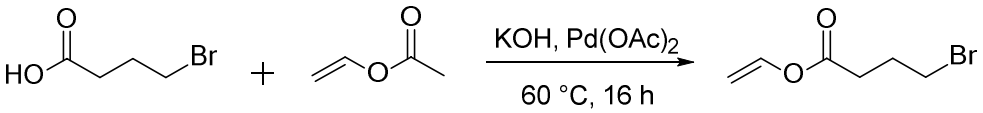

Scheme 3.4. Schematic representation of the palladium catalyzed reaction between 4-bromobutyric acid and vinyl acetate to prepare the monomer vinyl bromobutanoate, VBr.

The vinyl exchange reaction was initially performed for 16 h using 0.05 eq. of $Pd(OAc)_2$ as catalyst and 10 eq. of VAc (relative to 4-bromobutyric acid), and purification of the monomer by column chromatography and distillation. The successful formation of vinyl bromobutanoate (VBr) was confirmed by ^{1}H NMR spectroscopy (Figure 3.3), ^{13}C NMR spectroscopy (Figure 3.4) and elemental analysis. In an attempt to find the optimum conditions for the synthesis of this monomer, the reaction temperature was also varied between 25 °C and 60 °C, with the highest yield of 68% achieved when the reaction was carried out at 60 °C (Table 3.1), in good agreement with the report of Drockenmuller and co-workers.[47] Using these conditions, the synthesis of vinyl bromobutanoate could be scaled to yield 15 g of monomer after purification.

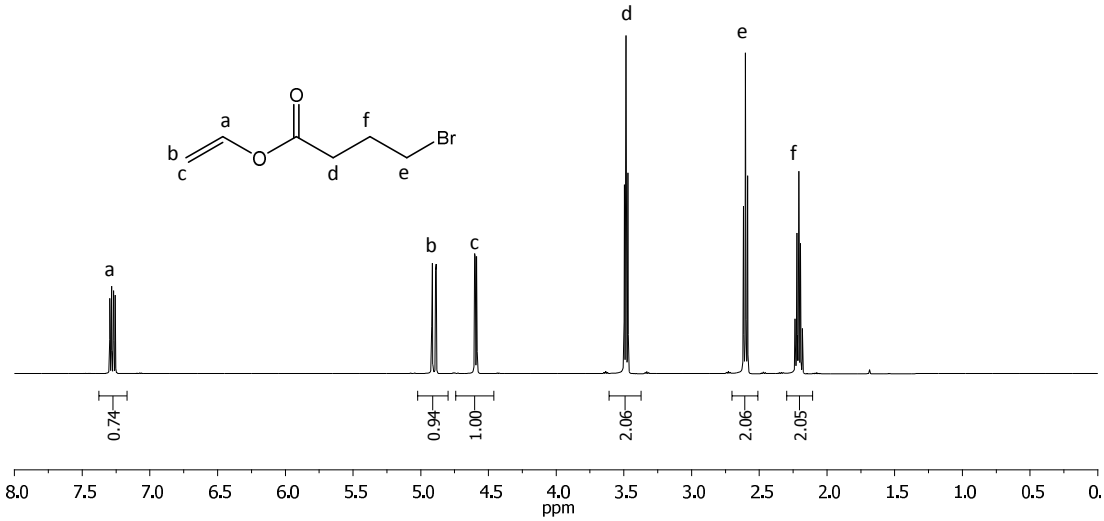

Figure 3.3. ^{1}H NMR spectrum of vinyl bromobutanoate synthesized by palladium catalyzed vinyl exchange reaction between 4-bromobutyric acid and vinyl acetate (300 MHz, $CDCl_3$).

Figure 3.4. ^{13}C NMR spectrum of vinyl bromobutanoate synthesized by palladium catalyzed vinyl exchange reaction between 4-bromobutyric acid and vinyl acetate (125 MHz, 293 K, $CDCl_3$).

Table 3.1. Results of the synthesis of vinyl bromobutanoate at different temperatures, VAc = 10 eq., $Pd(OAc)_2$ = 0.05 eq., 4-bromobutyric acid = 1 eq. and KOH = 0.1 eq., reaction time = 16 h.

Entry	Temperature (°C)	Yield (%)[a]
1	25	22
2	40	50
3	60	68

[a] Determined for the pure compound after purification by column chromatography and distillation.

3.3.3 Homopolymerization of VBr using the RAFT/MADIX polymerization

Following on from the successful synthesis of the new functional vinyl monomer and aiming to confirm that the monomer could be polymerized using the RAFT/MADIX polymerization technique, the homopolymerization of vinyl bromobutanoate (VBr) was initially performed in bulk at 60 °C, using 2,2'-azobis(isobutyronitrile) (AIBN) as the radical initiator and *O*-hexyl-*S*-methyl-2-propionylxanthate, CTA 1, as the chain transfer agent (CTA), such that $[VBr]_0/[AIBN]_0/[CTA\ 1]_0$ = 100:0.1:1. The choice of using CTA 1 as the chain transfer agent was made as a consequence of the successful results previously obtained in Chapter 2 where this CTA was used in mediating the copolymerization of MDO with VAc.

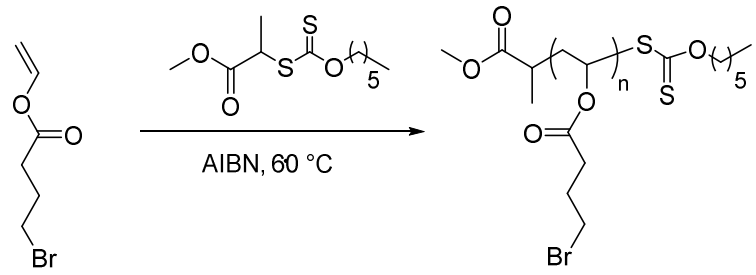

Scheme 3.5. Schematic representation of the homopolymerization of vinyl bromobutanoate using the RAFT/MADIX polymerization technique.

In an initial experiment, the polymerization was performed for 12 h resulting in the polymer poly(VBr) which displayed a dispersity, $Đ_M$, of 1.19 when analyzed by size exclusion chromatography (SEC). Further analysis using ^{1}H NMR spectroscopy

revealed a monomer conversion of 25%. In order to increase monomer conversion, polymerizations were also carried out for 16 h, 21 h and 26 h where conversions reached 35%, 49% and 69% with dispersity values of 1.20, 1.23 and 1.37 for each polymerization time respectively (Table 3.2 and Figure 3.5).

Table 3.2. Characterization data for the homopolymerization of VBr for different polymerization time points.

Time (h)	VBr conv.[a] (%)	M_n (SEC)[b] (kg/mol)	$M_n^{theo\ c}$ (kg/mol)	$M_n^{obs\ d}$ (kg/mol)	$Đ_M$ [b]
12	25	4.2	5.1	5.0	1.19
16	35	5.2	6.7	5.9	1.20
21	49	6.3	9.4	8.3	1.23
26	69	8.1	13.3	10.7	1.37

[a] conversions determined by ^{1}H NMR spectroscopy, [b] obtained by SEC analysis in $CHCl_3$, [c] theoretical molecular weight based on monomer conversion (^{1}H NMR spectroscopy), [d] observed molecular weight obtained by ^{1}H NMR spectroscopy end-group analysis.

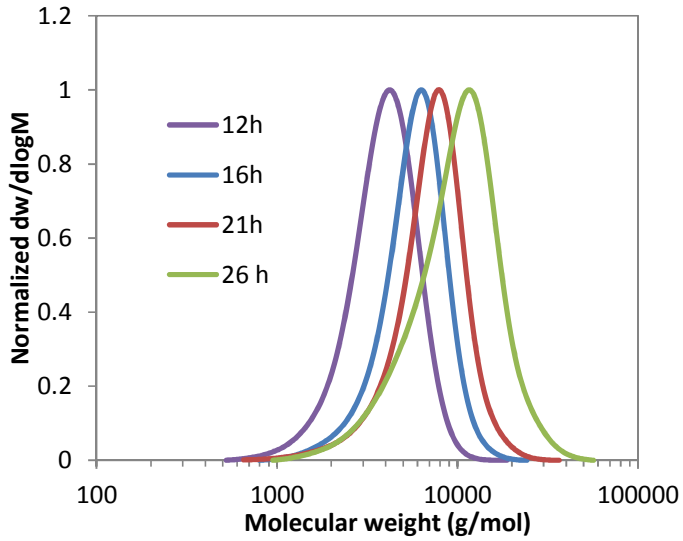

Figure 3.5. Size exclusion chromatograms of poly(VBr) obtained by the RAFT/MADIX polymerization for different reaction times, $[VBr]_0/[AIBN]_0/[CTA\ 1]_0$ = 100:0.1:1, 60 °C, (SEC, $CHCl_3$).

The low dispersity values obtained for the polymerization of VBr suggested that the polymerizations were performed in a controlled manner and that polymers with narrow molecular weight distributions and defined molecular weights were achieved.

The controlled aspect of the polymerization was also confirmed by the good agreement between the UV trace of the SEC at λ = 280 nm, attributed to the xanthate group, and the RI trace showing that the xanthate group has been retained throughout the polymerization (Figure 3.6).

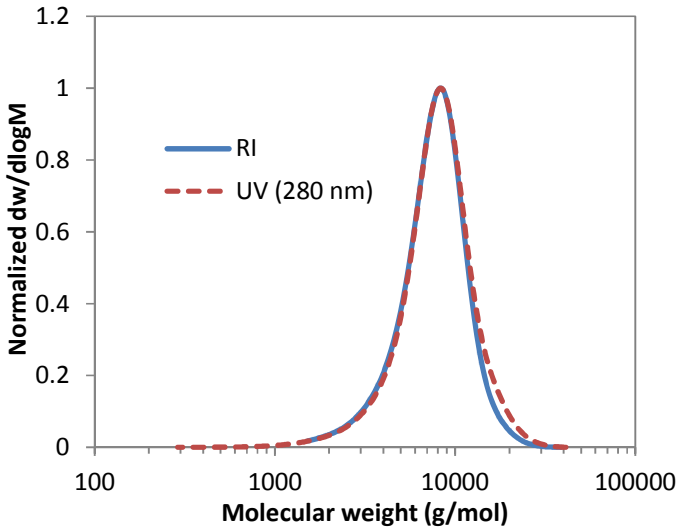

Figure 3.6. Size exclusion chromatograms of poly(VBr) obtained after 21 h of polymerization, blue trace using RI detection and red dashed trace using UV detection at λ = 280 nm, (SEC, $CHCl_3$).

The observed number-average molecular weights of the polymers by ^{1}H NMR spectroscopy, $M_n^{obs.}$, were obtained by integration of the resonances from the VBr polymer backbone at δ = 4.70-5.20 ppm (Figure 3.7, proton 2) and referenced with the characteristic resonance from the CH_2 protons from the xanthate group at δ = 4.50 ppm (Figure 3.7, proton 6). The theoretical molecular weight, $M_n^{theo.}$, were based on the monomer conversions obtained by ^{1}H NMR spectroscopic analysis. Both molecular weights, $M_n^{obs.}$ and $M_n^{theo.}$, were found to show a good correlation throughout the polymerization, which indicates a good retention of the active xanthate group was maintained on the polymer chain-ends. These observations suggested that the compatibility between the CTA 1 and the monomer was appropriate for the controlled synthesis of well-defined polymers of VBr.

Nevertheless, in order to prevent the potential increase in apparent viscosity of the polymerization mixture, the use of benzene was chosen for the copolymerization with MDO aiming at reaching higher monomer conversions as it was the case in Chapter 2.

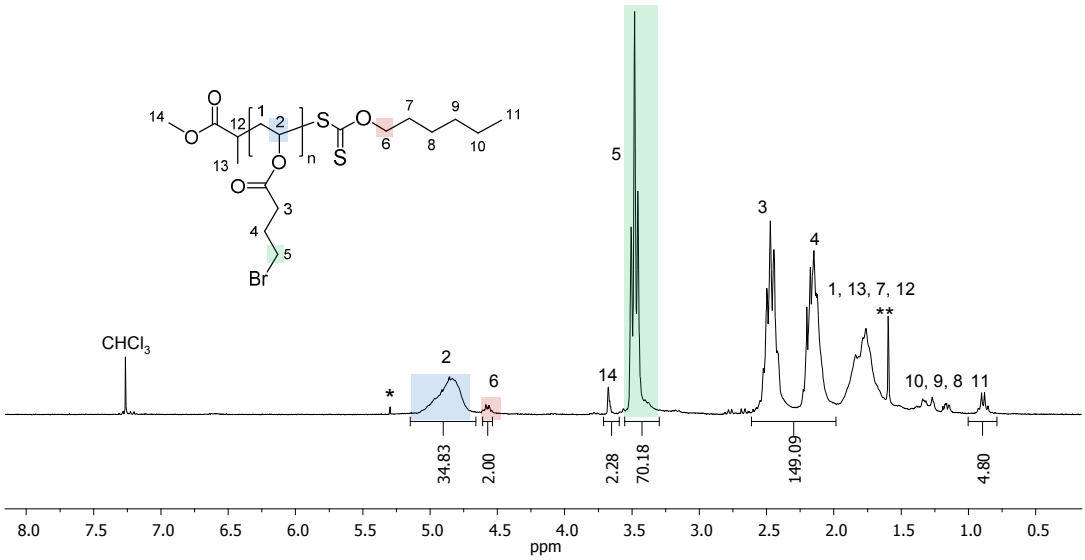

Figure 3.7. ^{1}H NMR spectrum of poly(VBr) synthesized using the RAFT/MADIX polymerization (400 MHz, $CDCl_3$), * indicates residual traces of dichloromethane and ** residual water traces.

Further polymerizations were carried out using benzene as a solvent in an attempt to investigate its effect on the polymerization. Many studies regarding the polymerization of VAc or vinyl monomers reported an increasing apparent viscosity of the polymerization mixture, which can often limit the reactions to low monomer conversions. The homopolymerization of VBr in the presence of benzene (15 wt%) was performed and the final polymer was investigated using ^{1}H NMR spectroscopy. The molecular weights, $M_n^{obs.}$ and $M_n^{theo.}$, were found to be very similar to a same polymerization performed without solvent. Additionally, the dispersities of the polymers were found to be very similar with values of 1.19 in the presence of benzene and 1.18 without for similar VBr monomer conversions (35% and 30%

respectively). These observations therefore indicated that the polymerization could be performed either in bulk or in solution without affecting either the controlled aspect of the polymerization or the quality of the final polymer.

3.3.4 Determination of the reactivity ratios of MDO and VBr

In order to synthesize functional and degradable polymers, the potential for efficient copolymerization of VBr with MDO was investigated by the determination of their reactivity ratios. As introduced in Chapter 2, the reactivity ratios of MDO and VAc in the presence of CTA 1 were determined to be close to unity (r_{MDO} = 1.03 ± 0.06 and r_{VAc} = 1.22 ± 0.07) which result in a copolymer structure close to ideal nature (*i.e.* almost random) leading to an efficient incorporation of degradable units throughout the polymer backbone.[45] To explore the behavior of the MDO/VBr copolymerization and prove the same ideal structure of the copolymers, the reactivity ratios of these two monomers were also studied using the Non-Linear Least Square (NLLS) method developed by Van Herk as previously used in Chapter 2.[55-57] Copolymerizations with different monomer feeds were targeted such that MDO varied from 10 mol% to 90 mol% (Table 3.3). The molar fractions of the two monomers in the initial feed and in the final copolymers were obtained by ^{1}H NMR spectroscopic analyses. The copolymerizations were quenched at low overall monomer conversions (typically < 15%) in order to avoid the effects of compositional drift, in which a change in f_A results in variation in F_A with an increasing conversion, which could occur during the copolymerization. Using the program Contour, as in Chapter 2, the plot of F_A, the mole fraction of M_A in the final copolymer (M_A being MDO), versus f_A, the initial mole fraction of monomer A was plotted and the reactivity ratios were calculated to be r_{MDO} = 0.96 ± 0.08 and r_{VBr} = 1.03 ± 0.09 (Figure 3.8). As in the case of MDO and VAc,[45] the reactivity ratios of MDO and VBr are close to unity, which indicates that the copolymers synthesized have a random structure. These values are also consistent with the observations that the conversion

of MDO is slightly lower than VBr over the course of the polymerization which indicates that MDO has a lower reactivity. The proximity of r_{MDO} and r_{VBr} to unity also demonstrates that the use of vinyl acetate derived monomers with MDO is a suitable technique to obtain polymers with a close to random incorporation of functional groups as well as an efficient incorporation of ester repeat units in the polymer backbone. Therefore the copolymerization is highly suited for the synthesis of functional degradable polymers.

Table 3.3. Mole fractions of monomer in the initial feed and copolymers using the RAFT/MADIX polymerization process in benzene (15 wt%), for the determination of reactivity ratios.

Target composition		Conversions (%) [a]		Actual initial comp.[a]		Polymer comp.[a]	
MDO	*VBr*	*MDO*	*VBr*	*MDO*	*VBr*	*MDO*	*VBr*
0.10	0.90	5	4	0.08	0.92	0.10	0.90
0.20	0.80	6	5	0.19	0.81	0.22	0.78
0.30	0.70	4.5	5	0.32	0.67	0.33	0.67
0.40	0.60	8	9	0.38	0.62	0.36	0.64
0.50	0.50	9	11	0.50	0.50	0.45	0.55
0.60	0.40	9	12	0.59	0.41	0.52	0.48
0.70	0.30	10	8	0.65	0.35	0.69	0.31
0.80	0.20	6	5	0.77	0.23	0.80	0.20
0.90	0.10	11	8	0.91	0.09	0.93	0.07

[a] determined by ^{1}H NMR spectroscopy.

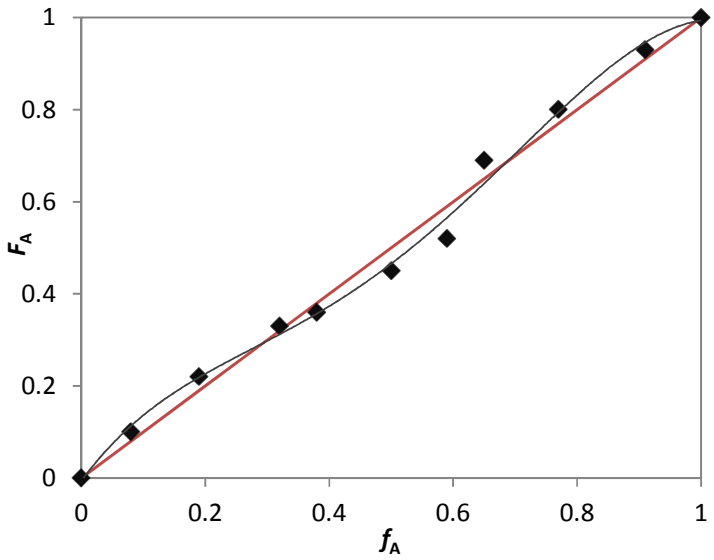

Figure 3.8. Plot of F_A *vs.* f_A for the copolymerization of MDO [A] and VBr [B] leading to reactivity ratios of $r_A = 0.96 \pm 0.08$ and $r_B = 1.03 \pm 0.09$. (Non-linear least squares (NLLS) method). The red line is the plot of F_A *vs* f_A for an ideal polymerization, where $r_1 = r_2 = 1$).

3.3.5 Copolymerization of VBr and MDO using the RAFT/MADIX polymerization

Following on from the results of the reactivity ratios for MDO and VBr, the ability to form well-defined and degradable copolymers of poly(MDO-*co*-VBr) was further investigated by the initial copolymerization with a low concentration of MDO such that $[VBr]_0/[MDO]_0/[AIBN]_0/[CTA\ 1]_0$ = 90:10:0.1:1. The copolymerization was carried out at 60 ºC for 16 h in the presence of benzene (15 wt%) (Scheme 3.6), and analyzed by ^{1}H NMR spectroscopy and SEC analysis.

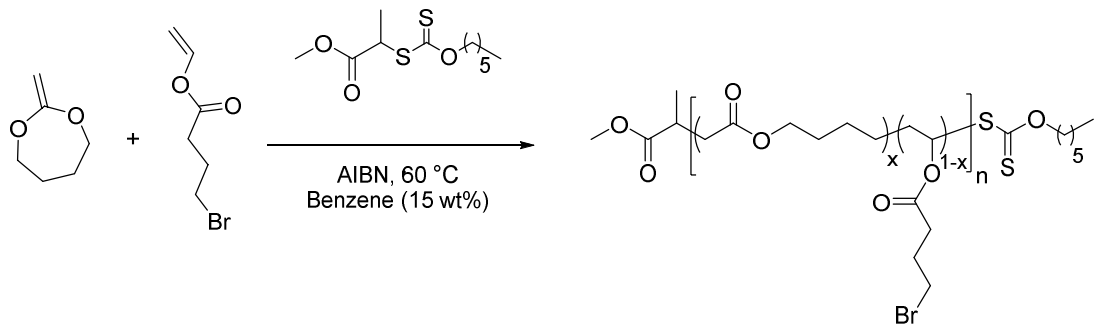

Scheme 3.6. Schematic representation of the synthesis of poly(MDO-*co*-VBr) copolymers mediated by RAFT/MADIX polymerization.

From this initial experiment, well-defined poly(MDO-*co*-VBr) was synthesized with good control over the molecular weight distribution as seen by the low dispersity value ($Đ_M$ = 1.54) and the good correlation between $M_n^{theo.}$ and $M_n^{obs.}$. The theoretical molecular weight was based on conversions of both monomers as determined by ^{1}H NMR spectroscopy, and the observed molecular weight was obtained by integration of the protons from the VBr and MDO polymer backbone at δ = 4.80-5.20 ppm (Figure 3.9, protons 2 and 4) and δ = 4.10 ppm (Figure 3.9, protons 6 and 11) respectively, and referenced to the characteristic resonance of the CH_2 protons from the xanthate end-group at δ = 4.50 ppm (Figure 3.9, proton 15). The monomer conversions after 16 h of both VBr and MDO were found to be 45% and 38% respectively. The successful copolymerization of MDO and VBr using the RAFT/MADIX polymerization technique was also confirmed by SEC analyses where good agreement between the traces of both UV detection (λ = 280 nm) and RI detection suggested a good retention of the xanthate on the copolymer of poly(MDO-*co*-VBr) (Figure 3.10).

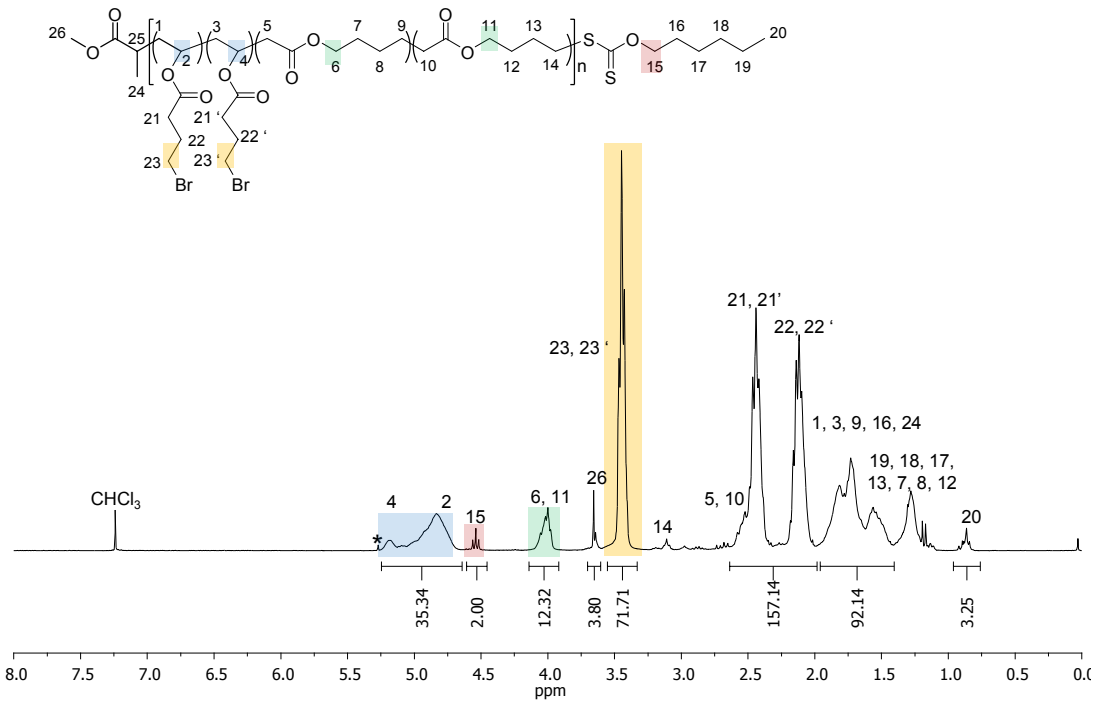

Figure 3.9. ^{1}H NMR spectrum of poly(MDO-*co*-VBr) synthesized by the RAFT/MADIX polymerization process, * indicates the residual trace of dichloromethane, (400 MHz, $CDCl_3$).

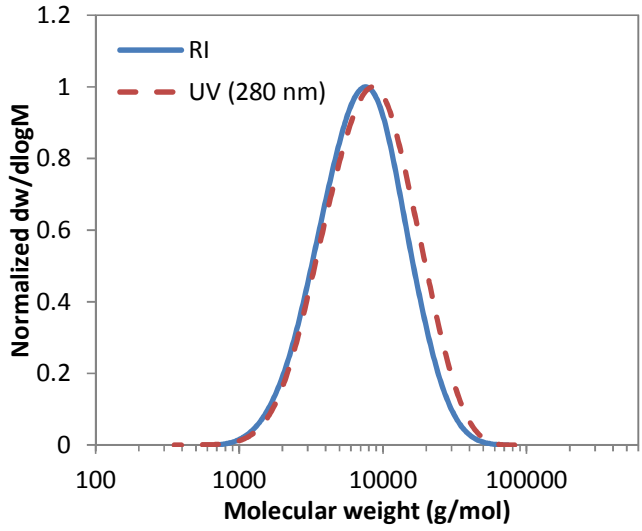

Figure 3.10. Size exclusion chromatograms of poly(MDO-*co*-VBr) (10/90 mol%) obtained by the RAFT/MADIX polymerization after 16 h, blue trace using RI detection and red dashed trace using UV detection at λ = 280 nm, (SEC, $CHCl_3$).

3.3.6 Detailed study of the copolymerization of MDO and VBr using RAFT/MADIX polymerization

In order to study the kinetics of the MDO/VBr system, a detailed study of the copolymerization was conducted where samples were taken after 3 h, 6 h, 9 h, 16 h, and 24 h and analyzed by ^{1}H NMR spectroscopy and SEC analysis. The conditions used were similar as in the initial investigation, however the concentration of MDO was increased such that $[VBr]_0/[MDO]_0/[AIBN]_0/[CTA\ 1]_0$ = 70:30:0.1:1 to obtain copolymers with higher incorporations of MDO in the backbone (similarly to Chapter 2). Under these conditions, poly(MDO-*co*-VBr) samples with controlled molecular weights (M_n) and low dispersities ($Đ_M$ = 1.15-1.59) were synthesized (Table 3.4). For the first 16 h of the polymerization, good control was maintained as a good correlation between observed molecular weight and theoretical molecular weight was observed; however, beyond this polymerization time a broadening of the dispersity value was observed as well as a deviation in the values of $M_n^{obs.}$ and $M_n^{theo.}$. These observations indicate a loss of the CTA end-group leading to termination reactions and broadening of the molecular weight distribution (Figure 3.11) as similarly observed in the case of the copolymerization of MDO and VAc in the presence of CTA 1 (previously presented in Chapter 2).

During this study, the monomer conversions were found to reach 41% and 25% for VBr and MDO respectively after 16 h where good control was maintained. However, after 24 h, the conversion reached a plateau of 73% and 41% for each monomer respectively, and no further increase in the conversion was observed even for extended polymerization times. This observation can be explained as a consequence of the depletion of radicals generated by the initiator, AIBN, at extended polymerization times.

Table 3.4. Characterization data for the copolymerization of MDO and VBr for different polymerization time points.

Time (h)	VBr conv.[a] (%)	MDO conv.[a] (%)	Polymer comp.[a] [VBr:MDO]	M_n (SEC) [b] (kg/mol)	M_n theo [c] (kg/mol)	M_n obs [d] (kg/mol)	$Đ_M$ [b]
3	2	5	49:51	1.6	0.7	1.6	1.15
6	4	16	37:63	2.0	1.1	2.0	1.23
9	24	19	75:25	3.7	4.0	4.8	1.44
16	41	25	79:21	5.6	6.2	8.8	1.59
24	73	41	80:20	7.3	11.3	16.2	1.85

[a] determined by ^{1}H NMR spectroscopy, [b] obtained by SEC analysis in $CHCl_3$, [c] theoretical molecular weight based on monomer conversion (^{1}H NMR spectroscopy), [d] observed molecular weight obtained by ^{1}H NMR spectroscopy end-group analysis.

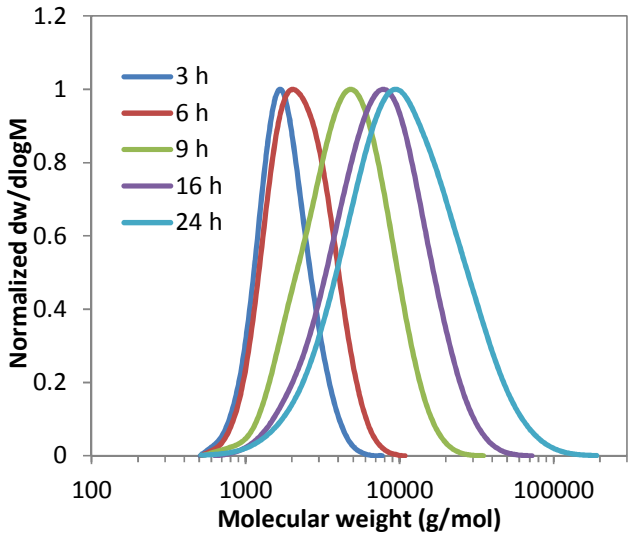

Figure 3.11. Size exclusion chromatograms of poly(MDO-*co*-VBr) obtained by the RAFT/MADIX polymerization for different polymerization times, $[VBr]_0/[MDO]_0/[AIBN]_0/[CTA\ 1]_0$ = 70:30:0.1:1, at 60 °C, (SEC, $CHCl_3$).

3.3.7 Copolymerization with different initial amounts of MDO

Aimed at increasing the degree of degradability of the targeted copolymers, the incorporation of ester repeat units in the copolymer backbone was altered by increasing the ratio of MDO in the monomer feed to 20, 30, 40 and 50 mol%. The copolymerizations were carried out at 60 ºC for 16 h or 20 h depending on the amount of MDO initially incorporated in the polymerization mixture. The samples

were then investigated using ^{1}H NMR spectroscopy and SEC analysis. In all cases, control of the polymerizations was maintained as confirmed by the low dispersity values observed by SEC analysis (Figure 3.12). Polymerization control was also proven by the correlation between the observed and theoretical molecular weights (Table 3.5).

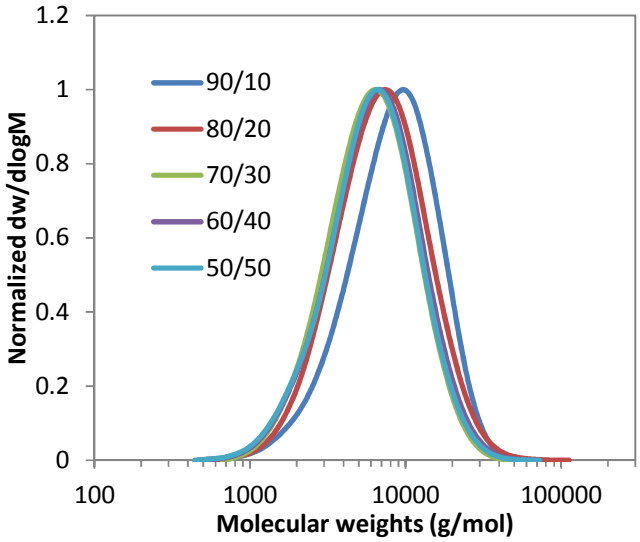

Figure 3.12. Size exclusion chromatograms of poly(MDO-*co*-VBr) obtained by the RAFT/MADIX polymerization for different monomer feeds, MDO/VBr, (SEC, $CHCl_3$).

For the samples with a targeted feed of 10 to 30 mol% in MDO, the polymerizations were performed for 16 h, reaching 38% to 47% in conversion for each monomer. For the polymerization containing a higher amount of MDO, the polymerizations were undertaken for 20 h in order to reach reasonable conversions for both monomers. Nevertheless, it can be noted that while the content of MDO was increased (40 and 50 mol%) in the monomer feed, the targeted conversions needed to be kept below 25% as higher values would have a detrimental effect on the dispersities of the final copolymers. This observation could be explained by the difficulty in controlling the homopolymerization of MDO using the RAFT/MADIX technique as a consequence of the fragmentation of the RAFT end-group from the polymer chains leading to a

broadening of the dispersities for such polymers (phenomenon investigated in Chapter 4). Nevertheless, these results suggested that copolymers containing higher amounts of degradable ester units in the polymer backbone could be achieved by simply varying the initial monomer feed used during the copolymerization.

Table 3.5. Characterization data for the copolymerization of VBr and MDO for different initial monomer feeds.

Time (h)	Initial monomer feed [VBr:MDO]	Polymer comp.[a] [VBr:MDO]	VBr [a] conv. (%)	MDO [a] conv. (%)	M_n SEC [b] (kg/mol)	M_n theo [c] (kg/mol)	M_n obs [d] (kg/mol)	$Đ_M$ [b]
16	90:10	91:09	45	38	6.5	8.2	7.5	1.54
16	80:20	84:16	47	35	5.5	8.0	8.5	1.57
16	70:30	74:26	38	30	4.9	6.9	7.4	1.50
20	60:40	73:27	44	24	4.9	6.2	6.5	1.56
20	50:50	66:34	37	19	4.8	4.7	5.3	1.55

[a] determined by ^{1}H NMR spectroscopy, [b] obtained by SEC analysis in $CHCl_3$, [c] theoretical molecular weight based on monomer conversion (^{1}H NMR spectroscopy), [d] observed molecular weight obtained by ^{1}H NMR spectroscopy end-group analysis.

3.3.8 Possible ring-retention and branching investigations

As previously investigated in Chapter 2 for the copolymer of MDO and VAc, the ring-retention and branching formation are two side reactions that can occur during the rROP of MDO, as initially investigated by Gonsalves and co-workers and Agarwal and co-workers.[34,39] Aiming to identify whether or not these side reactions do occur in the case of the copolymerization of MDO and VBr, ^{1}H NMR and ^{13}C NMR spectroscopic analyses were performed on the copolymers. ^{1}H NMR spectroscopy revealed the presence of resonances at δ = 0.90 ppm and δ = 3.65 ppm which are characteristic of the side-chain reactions that results from the 1,4- and 1,7-hydrogen transfer, or backbiting, during the rROP of MDO leading to the formation of small branches along the polymer backbone.[33,34] Using the same approach previously used in Chapter 2, comparison of the integrals of the side-chain branches at δ = 3.65 ppm and δ = 0.90 with the CH_2 obtained from the rROP of MDO at

δ = 4.00 ppm (Figure 3.13), the degree of branching was estimated to be around 10%, which is very similar to the value previously reported for poly(MDO-*co*-VAc) reported in Chapter 2. Similarly, ^{13}C NMR spectroscopic analysis was used to identify whether any ring-closed MDO units were present in the copolymers, poly(MDO-*co*-VBr), caused by the potential ring-retention of the MDO leading to a small amount of polyacetal structure in the copolymer as previously reported.[42,58] Analysis using ^{13}C NMR spectroscopy revealed the presence of a small peak at δ = 100.0 ppm which is characteristic of the acetal quaternary carbon commonly observed at δ = 100-110 ppm for ring-closed species observed during the rROP of MDO (Figure 3.14).

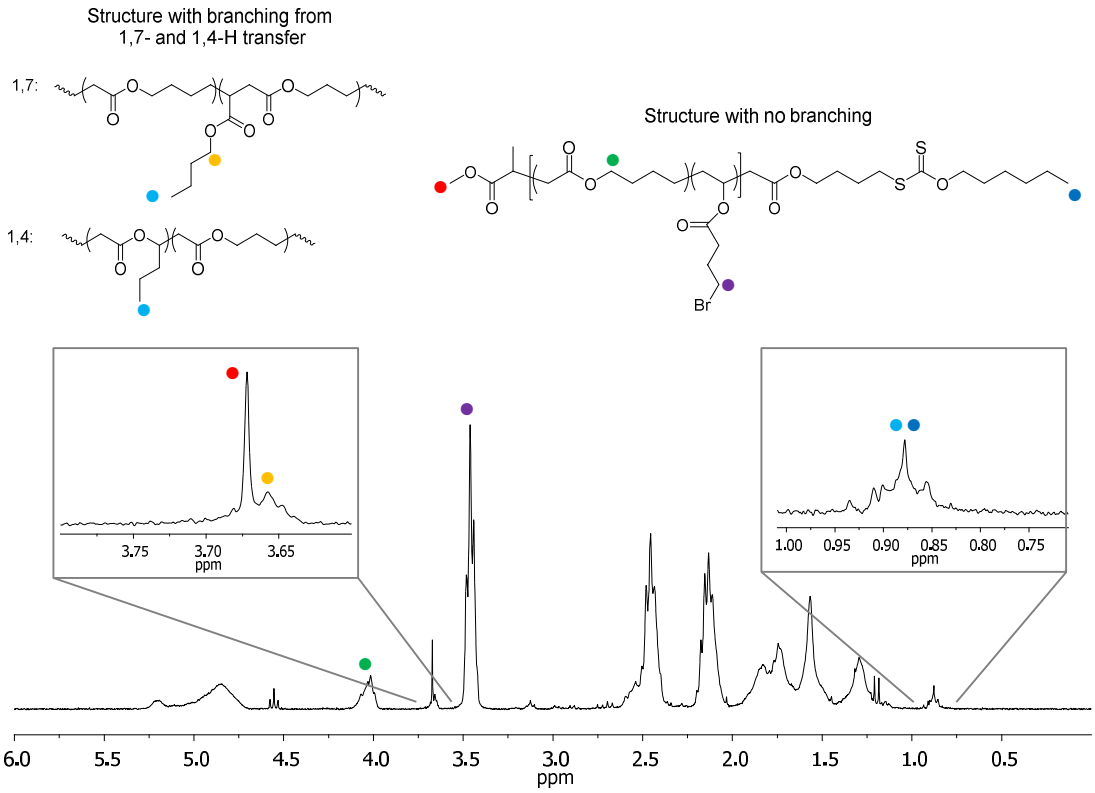

Figure 3.13. ^{1}H NMR spectrum of poly(MDO-*co*-VBr) (30/70 mol%) highlighting the potential side branching occurring from the 1,4- and 1,7-hydrogen transfer reaction (400 MHz, $CDCl_3$).

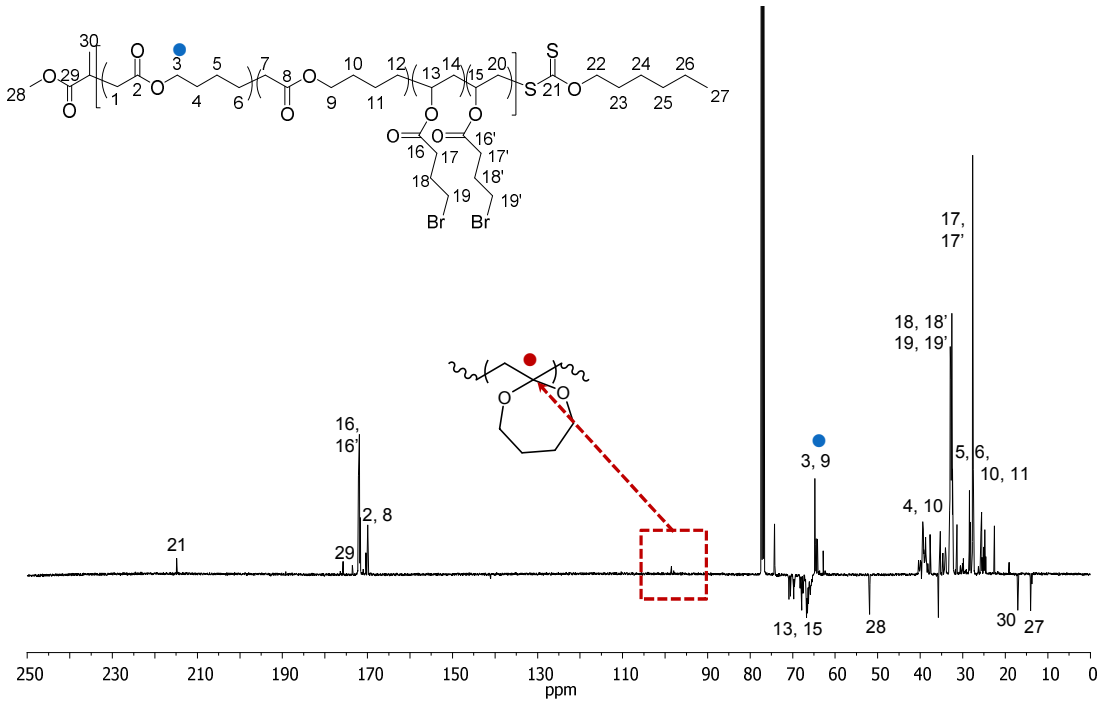

Figure 3.14. ^{13}C NMR spectrum of poly(MDO-*co*-VBr) using the RAFT/MADIX polymerization process, red point indicates a small portion of MDO ring-retained in the copolymer, (125 MHz, $CDCl_3$).

3.3.9 Chain extension experiments

As previously attempted for the copolymer of poly(MDO-*co*-VAc) in Chapter 2, chain growth experiments of the homopolymer, poly(VBr), and copolymer, poly(MDO-*co*-VBr), were conducted in order to assess the controlled nature of the polymerization process and confirm the retention of the CTA end-group on the polymer chains. The controlled nature of the polymerization would be confirmed only if the chain extensions were successful. Experiments where the chain growth of poly(VBr) and poly(MDO-*co*-VBr) with vinyl acetate (VAc) were performed to create two new block copolymers, poly(VBr)-*b*-poly(VAc) and poly(MDO-*co*-VBr)-*b*-poly(VAc). In both cases, after polymerization ^{1}H NMR spectroscopy and SEC analysis indicated the successful chain extension of the first polymer with a complete shift of the molecular weight distribution as well as the absence of low molecular

weight shoulders (observed by SEC analysis for both chain extensions, Figure 3.15a-b). In the case of the first polymer, poly(VBr)-*b*-poly(VAc), it can be observed that the dispersity before and after chain extension remains similar (1.20 *vs*.1.25) leading to the controlled formation of a well-defined block copolymer with a narrow molecular weight distribution. In comparison, for the block copolymer of poly(MDO-*co*-VBr)-*b*-poly(VAc) an increase in the dispersity of the final copolymer can be observed with a value of 1.87 after chain extension.

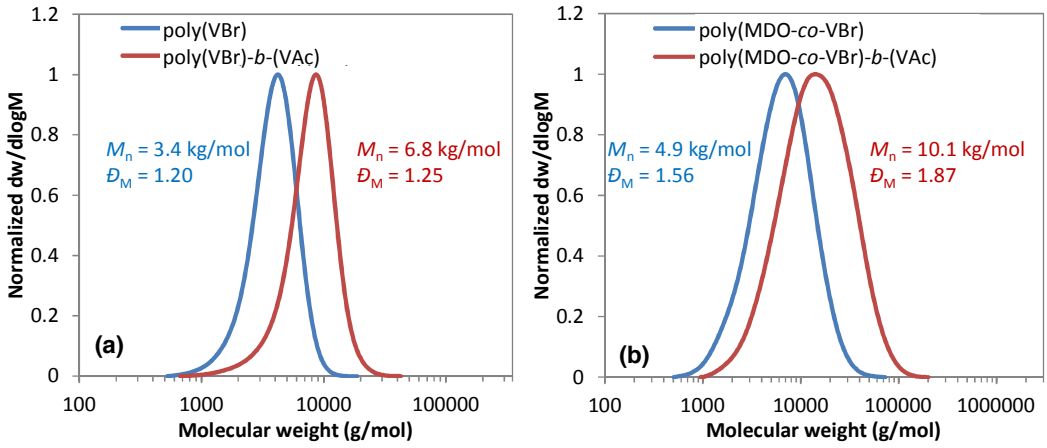

Figure 3.15. Size exclusion chromatograms of poly(VBr) and poly(MDO-*co*-VBr) before and after extension with vinyl acetate to create the two block polymers: (a) poly(VBr)-*b*-poly(VAc) and (b) poly(MDO-*co*-VBr)-*b*-poly(VAc), (SEC, $CHCl_3$).

This higher value is similar to the result observed for the chain extension of poly(MDO-*co*-VAc) in Chapter 2 where some loss of control during the polymerization occurred as a consequence of the presence of dead chain ends arising from the hypothetical fragmentation of the CTA end-group during the synthesis of the first block copolymer with MDO leading to a broadening of the molecular weight distributions (further investigated in Chapter 4). The successful chain extensions of poly(VBr) and poly(MDO-*co*-VBr) with VAc confirm the controlled nature of the polymerization process.

3.3.10 Degradation study of poly(MDO-co-VBr)

The degradation of polyesters remains an important subject of investigation as a consequence of their importance in biomedical applications.[15,16] Various studies have been reported, including Kobben and co-workers who successfully investigated the degradation of CKA copolymers under basic hydrolytic conditions using a methanol solution of potassium hydroxide.[44] Aiming at investigating the degradable behavior of the copolymer, poly(MDO-*co*-VBr), hydrolysis experiments were conducted using the similar method previously reported in Chapter 2 where the successful degradation of poly(MDO-*co*-VAc) was confirmed under KOH/methanol basic conditions. The degradability of the poly(MDO-*co*-VBr) samples was investigated by the hydrolysis of the copolymer in a solution of KOH (0.1 M) in methanol at 40 °C. The degradation of the copolymers was assessed by SEC analysis and monitored over different times of hydrolysis exposure. In all cases, net decreases in the molecular weights of the samples were observed by SEC analyses, as well as the increasing evolution of low molecular weight peaks (20 – 800 g/mol, Figure 3.16), proving that degradation occurred as a consequence of the even incorporation of ester units in the polymer backbone. It should also be noted that the molecular weights were found to decrease gradually as the exposure time of degradation was increased.

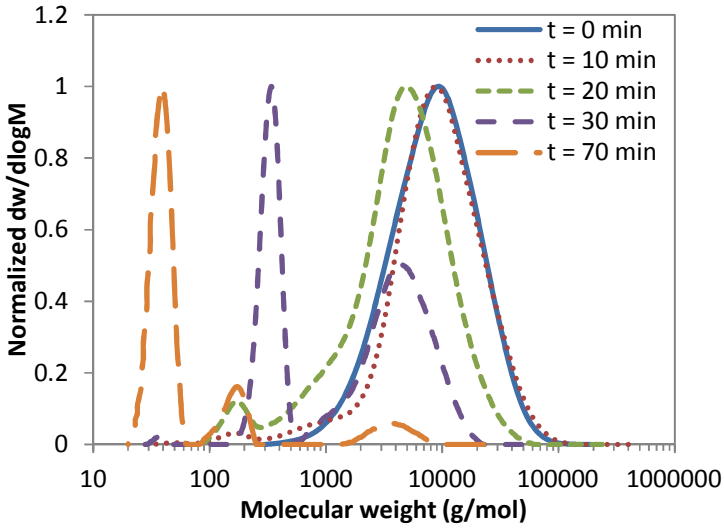

Figure 3.16. Size exclusion chromatograms of the degradation of poly(MDO-*co*-VBr) in a solution of KOH in methanol (0.1 M) at 40 °C for different time points, (SEC, $CHCl_3$).

Furthermore, in order to investigate the extent of degradability, two copolymers with different compositions, poly($MDO_{0.10}$-*co*-$VBr_{0.90}$)$_{55}$ and poly($MDO_{0.26}$-*co*-$VBr_{0.74}$)$_{54}$, were subjected to the same hydrolysis conditions and SEC analyses were recorded a different time points (Figure 3.17). During the experiment, it was observed that the degradation was faster in the case of the copolymer containing the larger amount of MDO in the polymer backbone: poly($MDO_{0.26}$-*co*-$VBr_{0.74}$)$_{54}$. For this sample, after only 30 min of hydrolysis the weight molecular weight, M_w (SEC), of the copolymer was significantly smaller and no polymer could be detected after 70 min. In comparison, the copolymer with the smaller incorporation of MDO, poly($MDO_{0.10}$-*co*-$VBr_{0.90}$)$_{55}$, was found to have a longer degradation process, as more than 170 min were required to fully degrade the sample. These observations prove that the degradability of the copolymer could be easily tuned by changing the copolymer composition and the amount of hydrolyzable ester repeat units in the polymer backbone.

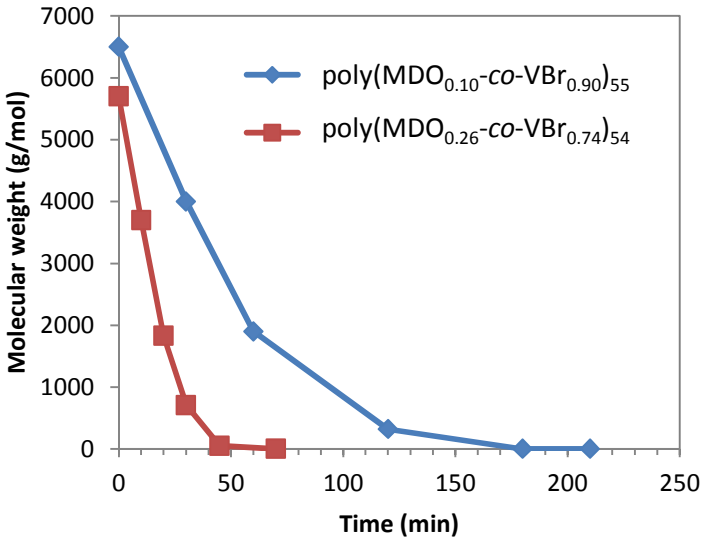

Figure 3.17. Molecular weight changes occurring during the hydrolysis of poly($MDO_{0.10}$-*co*-$VBr_{0.90}$)$_{55}$ and poly($MDO_{0.26}$-*co*-$VBr_{0.74}$)$_{54}$ at different time points, in a solution of KOH in methanol (0.1 M) at 40 °C.

3.3.11 Post-polymerization modifications using azidation and 1,3 cycloaddition

Following the successful controlled preparation of defined poly(VBr) and poly(MDO-*co*-VBr), and also inspired by the work of Riva and co-workers and Agarwal and co-workers for their post-polymerization works on functional polyesters,[25,42] the post-polymerization modification of the polymer studied in this chapter was firstly investigated using azidation in order to obtain a polymer containing azide pendent groups which could be used for further modifications using "click" chemistry. In the first step, the bromide pendent groups of the polymers were converted into azide groups using NaN_3 in DMF for 48 h (Scheme 3.7) after which the modified copolymer was recovered by precipitation in hexane and analyzed by ^{1}H NMR spectroscopy and SEC analysis.

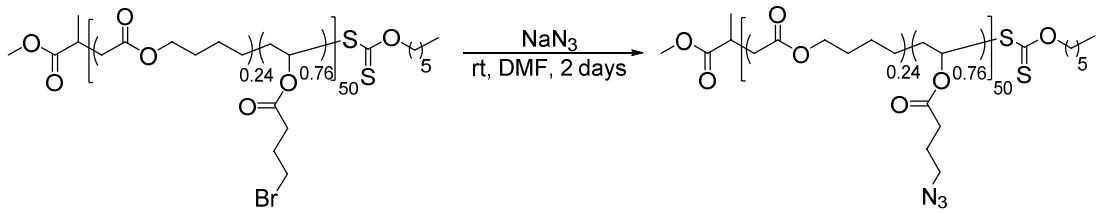

Scheme 3.7. Schematic representation of the post-polymerization modification of poly(MDO-*co*-VBr) using azidation.

Analyses of the modified poly(MDO-*co*-VBr) copolymers confirmed the successful conversion of the bromide groups to azide groups as seen by ^{1}H NMR spectroscopic analysis where a clear shift of the CH_2Br characteristic peak (δ = 3.50 ppm, Figure 3.18a, proton e) to the CH_2N$_3$ characteristic peak (δ = 3.40 ppm, Figure 3.18b, proton e') was observed, as well as the appearance of the signal at ν = 2094 cm^{-1} in the FTIR spectrum, characteristic of the stretching vibrations of N=N=N (Figure 3.19).

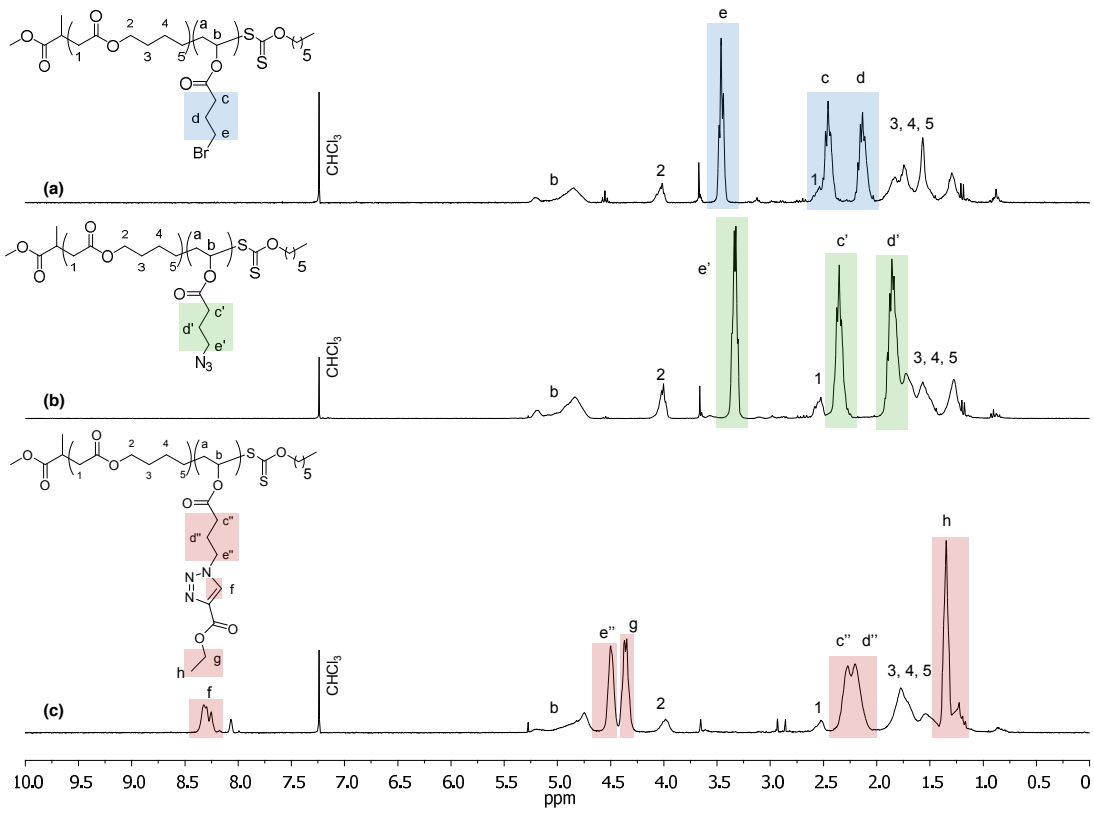

Figure 3.18. ^{1}H NMR spectra of the post-polymerization modification of poly(MDO-*co*-VBr) (a), after azidation with NaN_3 (b) and after 1,3-dipolar cycloaddition with ethyl propiolate (c). (400 MHz, $CDCl_3$).

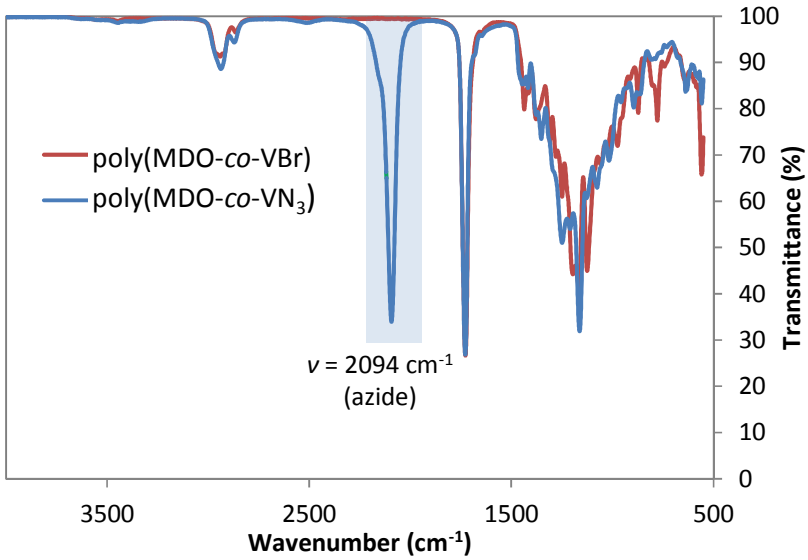

Figure 3.19. FTIR spectrum of poly(MDO-*co*-VBr) (30/70 mol%) before and after azidation using NaN_3.

Additionally, further SEC analyses on the modified copolymer before and after the azidation reaction revealed no changes in the molecular weight or the final dispersity, suggesting that the post-polymerization modification had no deleterious effect on the quality of the polymer sample (Figure 3.20).

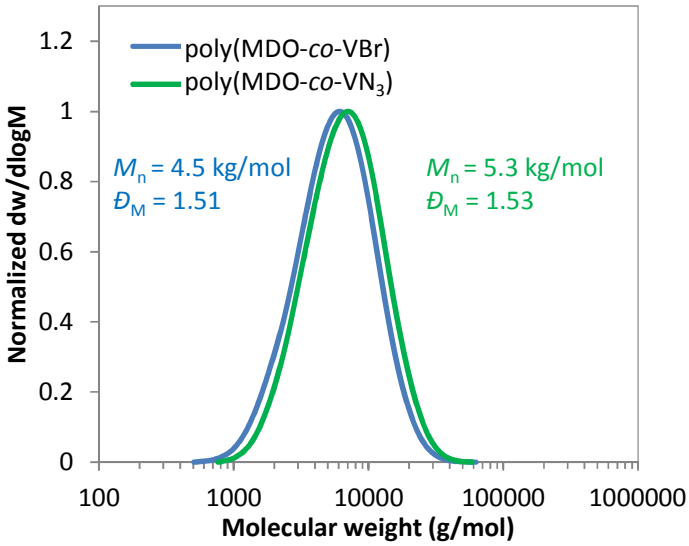

Figure 3.20. Size exclusion chromatograms of poly(MDO-*co*-VBr) (30/70 mol%) before and after the reaction with NaN_3 proving that the modification had no deleterious effect on the polymer sample, (SEC, $CHCl_3$).

In a second step, the post-polymerization modification of the copolymers was further investigated using the 1,3-dipolar cycloaddition reaction of azides with electron deficient alkynes.[59,60] When using an electron withdrawing group adjacent to the alkyne, this addition can be mediated at relatively low temperatures without the need of a copper catalyst.[10,59,61] The choice of not using the classical copper(I)-catalyzed alkyne-azide cycloaddition (CuAAC) reaction was made in order to avoid the presence of Cu(I) ions and their removal issues which could lead to potential toxicity problems in the final polymer. As an initial attempt, the equimolar reaction between ethyl propiolate and the copolymer, poly($MDO_{(0.24)}$-*co*-$VN_{3(0.76)})_{50}$, containing pendent azide groups was performed at 80 °C in DMF for 2 days (Scheme 3.8).

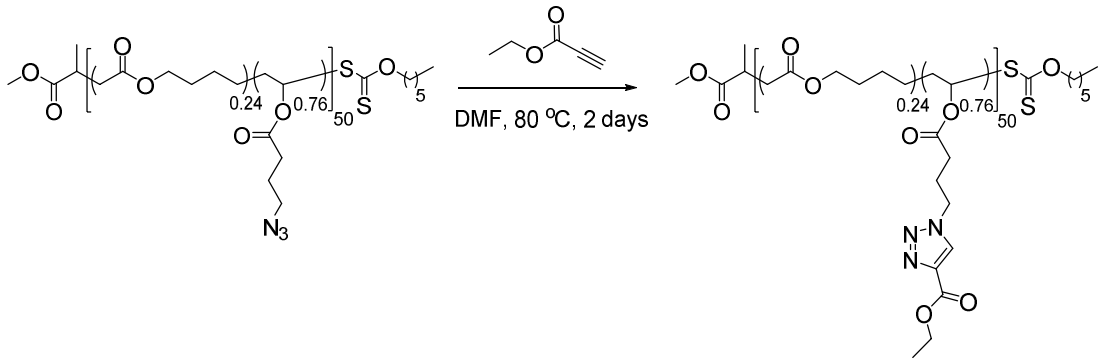

Scheme 3.8. Schematic representation of the post-polymerization modification of poly(MDO-*co*-VN_3) with the 1,3-dipolar cycloaddition with ethyl propiolate.

After recovering the polymer by precipitation in hexane, the successful reaction of ethyl propiolate with the copolymer was proven by ^{1}H NMR spectroscopy where the appearance of the characteristic resonance at δ = 8.25 ppm (Figure 3.18c, proton f) that corresponds to the triazole proton was observed as well as the formation of two new resonances at δ = 1.20 ppm and δ = 4.35 ppm (Figure 3.18c, protons h and g) from the CH_2 and CH_3 of the additional ethyl propiolate group respectively. After reaction, the change of chemical shift from δ = 3.40 ppm (Figure 3.18b, proton e') to δ = 4.50 ppm (Figure 3.18c, proton e'') of the CH_2 adjacent to the azide was also observed confirming the successful functionalization. The full conversion of the reaction was proven by the total disappearance of the characteristic CH_2N_3 resonance at δ = 3.40 ppm (Figure 3.18b, proton e'). Furthermore SEC analysis revealed an increase in molecular weight with no increase in dispersity, and retention of the monomodality of the distribution (Figure 3.21).

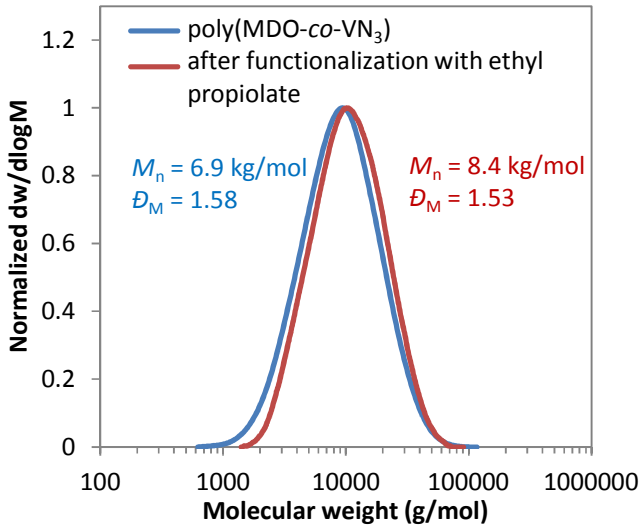

Figure 3.21. Size exclusion chromatograms of poly(MDO-*co*-VN_3) before and after the 1,3-dipolar cycloaddition reaction with ethyl propiolate, (SEC, $CHCl_3$).

While no degradation of the copolymer was observed after modification, a similar approach could potentially be performed to directly modify the monomer, as recently highlighted by Drockenmuller and co-workers in which the use of azidation and cycloaddition prior to polymerization was performed in combination with the palladium catalyzed vinyl exchange reaction to efficiently form functional vinyl ester 1,2,3-triazolium monomers.[62] This possibility was also investigated by the direct modification of the monomer, VBr, using the similar azidation reaction to produce the analogous azido monomer, vinyl azidobutanoate (VN_3), as confirmed by ^{1}H NMR spectroscopy analysis (Figure 3.22), which highlights the fact that the modifications could also potentially be performed before polymerization.

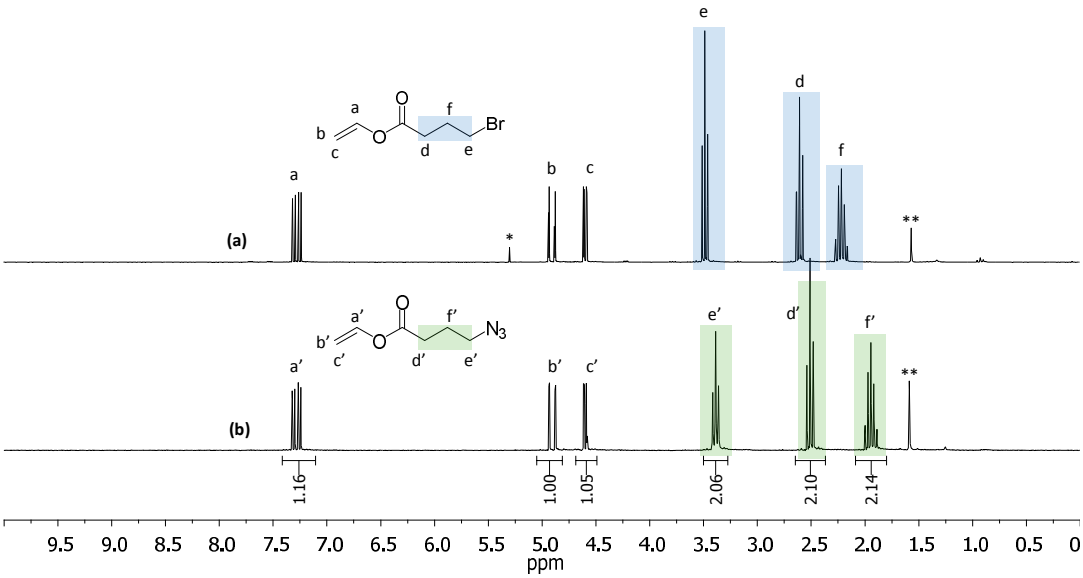

Figure 3.22. ^{1}H NMR spectra of the modification of vinyl bromobutanoate (a) using the azidation reaction to create the analogous azido monomer, (b) vinyl azidobutanoate, (300 MHz, $CDCl_3$), * indicates residual dichloromethane and ** residual water peaks.

Following on from the promising results of the post-polymerization of poly(MDO-*co*-VBr) using azidation and inspired by the work performed by Agarwal and co-workers on functional clickable polyesters by the rROP of CKA,[41,42] the post-polymerization modification was further extended by the reaction with a short chain poly(ethylene glycol) bearing an alkyne functional end-group which would lead to the incorporation of biocompatible and water-soluble properties to the final copolymer. The alkyne functional PEG, PEG(alkyne), was prepared in a single step reaction between the commercially available poly(ethylene glycol) methyl ether (PEG, average M_n = 550 Da, DP = 12) and propiolic acid (Scheme 3.9), and confirmed by ^{1}H NMR spectroscopy (Figure 3.23) as previously reported by Truong *et al*.[63]

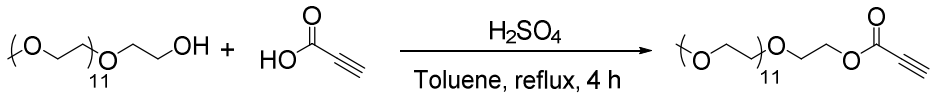

Scheme 3.9. Schematic representation of the synthetic approach for the synthesis of the PEG(alkyne).

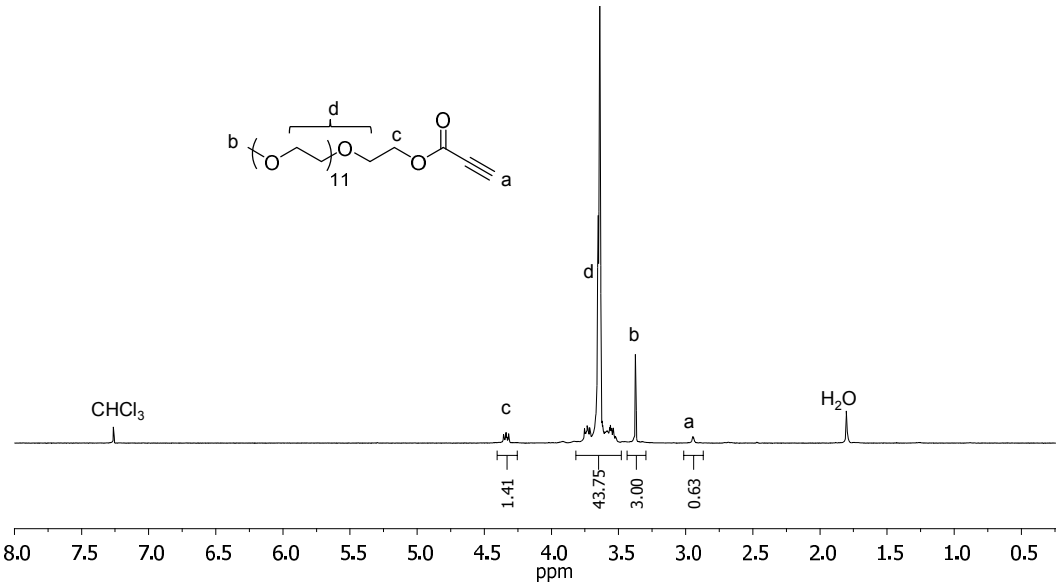

Figure 3.23. ^{1}H NMR spectrum of the functional PEG(alkyne) used for the post-polymerization, (300 MHz, $CDCl_3$).

The addition of the hydrophilic PEG into the copolymer was investigated by the equimolar reaction between PEG(alkyne) and poly($MDO_{(0.24)}$-*co*-$VN_{3(0.76)})_{36}$ using similar conditions as before: DMF at 80 °C for 24 h (Scheme 3.10). After recovering the functional copolymer by precipitation in hexane and dialysis (for 3 days) in order to remove any residual short PEG polymer, the functionalized polymer was analyzed by ^{1}H NMR spectroscopy, SEC analysis and FTIR spectroscopy.

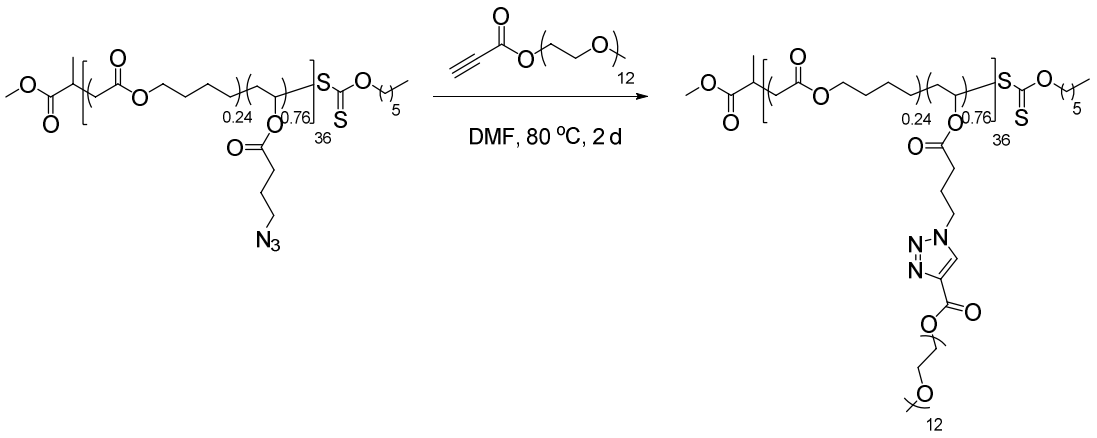

Scheme 3.10. Schematic representation of the post-polymerization modification of poly(MDO-*co*-VN_3) using a cycloaddition reaction with PEG alkyne.

Analysis using ^{1}H NMR spectroscopy revealed the successful addition of the PEG alkyne to the copolymer, poly(MDO-*co*-VN_3), as evidenced by the appearance of the triazole proton resonance at δ = 8.25 ppm (Figure 3.24, proton f) formed after the 1,3-dipolar cycloaddition with the PEG alkyne, as well as the appearance of characteristic signals of the additional PEG repeat units at δ = 3.50 ppm and 3.25 ppm (Figure 3.24, protons i and j). Further analysis using ^{1}H NMR spectroscopy revealed that 90% of the azide pendent groups of the copolymer were successfully functionalized while some residual azide groups were still observed at δ = 3.40 ppm using ^{1}H NMR spectroscopy (Figure 3.24, denoted with *). Moreover, FTIR spectroscopy reveled the continued presence of the stretching vibration of N=N=N, ν = 2095 cm^{-1} (Figure 3.25). Additionally, the 1,3-dipolar cycloaddition reaction was confirmed by SEC analysis where a clear shift of the molecular weight distribution was observed after the addition of the functional PEG on the polymer backbone (Figure 3.26). The number-average molecular weight, M_n, was found to increase from 4.8 kg/mol before addition to 12.7 kg/mol after addition confirming the successful reaction, while no deleterious effect on the polymer quality were observed as seen by the remaining low dispersity value after reaction. The successful addition of a small molecule and longer polymer chain *via* the 1,3-dipolar cycloaddition reaction on the azide pendent groups proves the great potential in using the new monomer, vinyl bromobutanoate, to synthesize novel poly(vinyl acetate) derivatives able to be further functionalized *via* post-polymerization modifications.

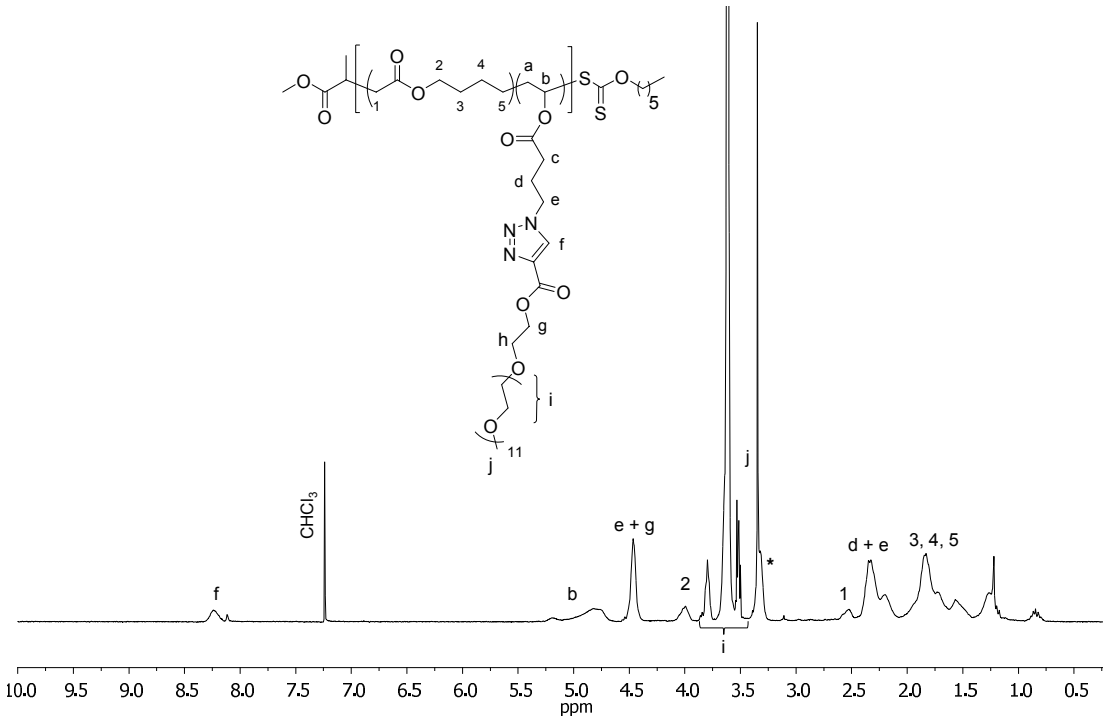

Figure 3.24. ^{1}H NMR spectrum of the copolymer after post-polymerization modification *via* 1,3-dipolar cycloaddition with PEG alkyne, M_n = 550 Da, DP = 12, (400 MHz, $CDCl_3$), * indicates the residual azide pendent groups unreacted during the reaction.

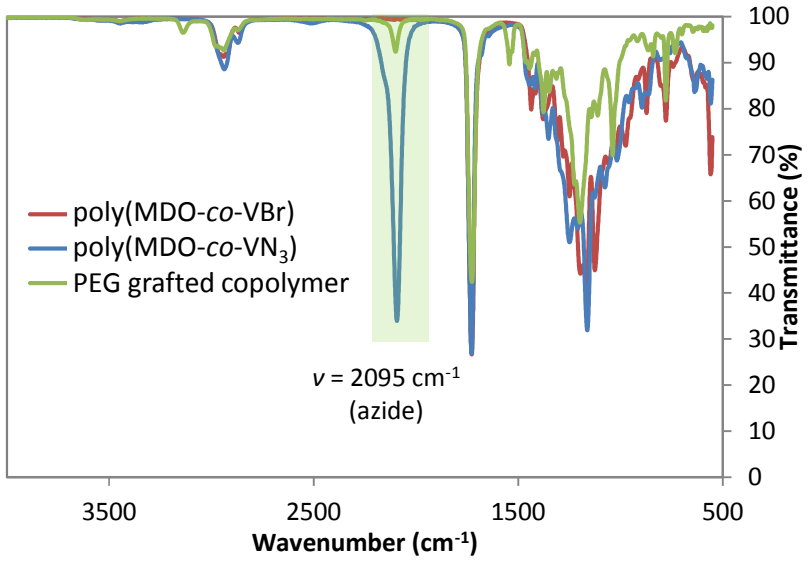

Figure 3.25. FTIR spectrum of poly(MDO-*co*-VBr), poly(MDO-*co*-VN_3) and the PEG grafted copolymer obtained after post-polymerization modifications.

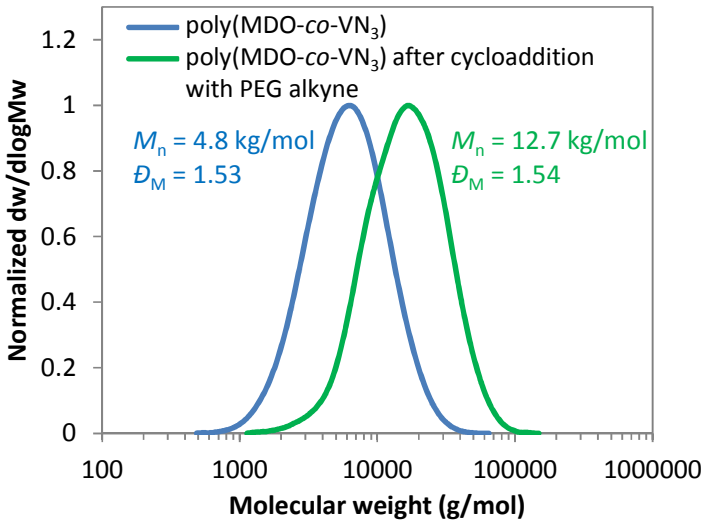

Figure 3.26. Size exclusion chromatogram of poly(MDO-*co*-VN_3) before and after the cycloaddition reaction with PEG alkyne, (SEC, $CHCl_3$).

3.3.12 Graft-copolymerization behaviour and degradation studies

Poly(ethylene glycol) based polymers and copolymers are amongst the most common materials used in the emerging field of drug delivery as a consequence of their biocompatibility, non-toxicity and high solubility in aqueous media.[64] Incorporation of PEG functional chains into other conventional polymers allows for the addition of hydrophilic properties into the final material and therefore changes dramatically their solubility behaviors. Aiming at investigating the behavior of the PEG-grafted copolymer experiments were carried out in order to identify the aqueous solubility and the degradability of the previously synthesized functional material. In an initial experiment, the graft-copolymer was found to be directly soluble in water which inferred that the solubility of the material was completely modified as a result of the incorporation of the hydrophilic block coming from the additional PEG pendent groups. Further investigation using Dynamic Light Scattering (DLS), revealed that after dissolution in water (18 $M\Omega.cm^{-1}$) at a concentration of 1 mg/mL, the graft-system was found to form small self-assembled particles with a hydrodynamic diameter, D_h, of 8 nm. It should however be noted that despite confirming the presence of

particles in the solution, the presence of larger aggregates could also been observed as seen by the larger peak on the DLS trace (Figure 3.27) which are assumed to be obtained as a result of the aggregation of smaller particles together. Further analysis using Static Light Scattering (SLS) confirmed the presence of particles in the solution with sizes in agreement with the results of DLS, and with a calculated aggregation number, N_{agg}, of 5 and a hydrodynamic radius, R_h, of 3.7 nm.

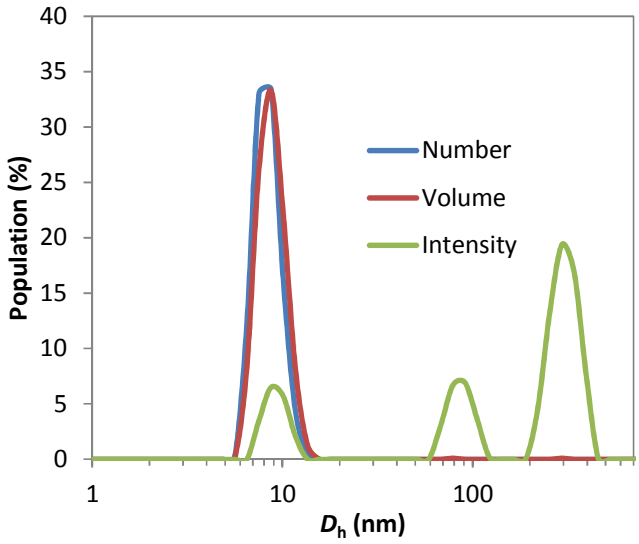

Figure 3.27. DLS traces of the particles obtained from the direct dissolution of the PEG-grafted copolymer in water.

Having successfully incorporated the hydrophilic PEG into the copolymer backbone and confirmed that the solubility was modified, the degradability of the graft-copolymer was investigated using the same accelerated hydrolytic conditions used in section 3.3.10, aiming to explore the effect of the PEG addition on the rate of degradation of the sample. The degradation experiments were performed in basic methanolic solution (KOH, 0.1 M) at 40 °C and it was observed that the graft-copolymers degraded rapidly, such that after 3 min under these hydrolytic conditions, disappearance of the main polymer peak on the SEC analyses was observed, alongside the appearance of lower molecular weight peaks at 200

and 1000 g/mol corresponding to degraded oligomers and remaining small PEG polymer chains (Figure 3.28).

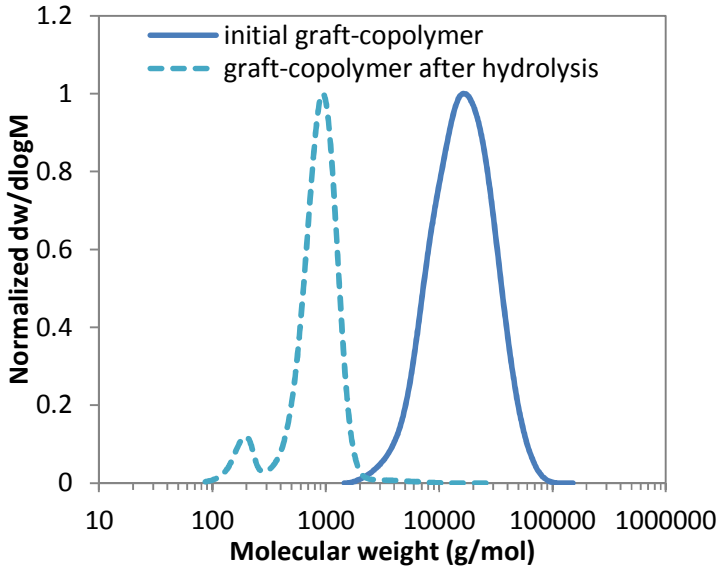

Figure 3.28. Size exclusion chromatograms of the PEG grafted copolymer before and after degradation in KOH solution (0.1 M in MeOH) at 40 °C, (SEC, $CHCl_3$).

Aiming at following the degradation of the grafted copolymer more gradually, degradation experiments were also investigated in phosphate buffer solution (PBS) at pH = 7.4 at 37 °C, a more suitable biological mimic, and samples were taken at different time points for 49 days. The hydrolyzed copolymer samples were then investigated using SEC analysis to observe changes in the molecular weight distributions which would indicate a degradation process occurring. This experiment revealed, as expected, that the degradation under these conditions was slower with 7 days required to observe initial signs of degradation. Indeed, after 7 days the appearance of small peaks at low molecular weights (200 - 2000 g/mol) was observed, of which the intensities increased after 11 and 49 days revealing that the degradation of the graft copolymer was occurring gradually under these conditions (Figure 3.29). The observation of a significantly increased rate of hydrolysis confirmed that the addition of hydrophilic functional groups *via* post-polymerization modification of the

copolymer drastically affected the properties and behavior of the material investigated in this study, highlighting the wide range of applications targeted for such functional degradable materials.

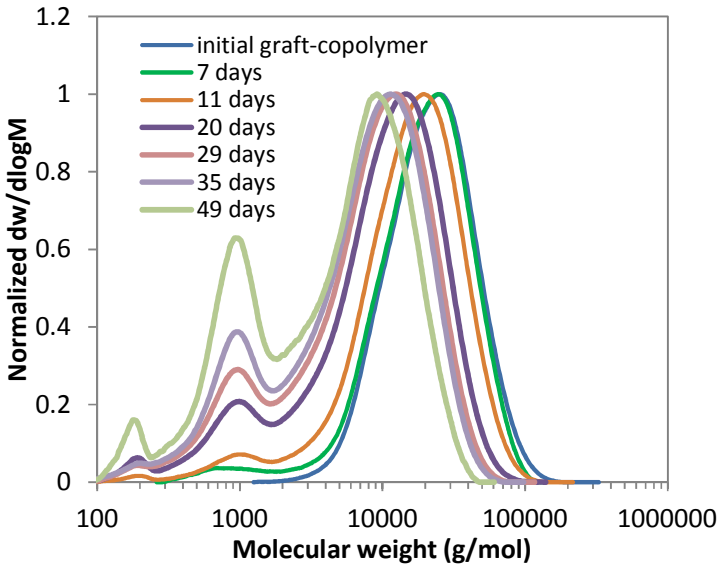

Figure 3.29. Size exclusion chromatograms of the PEG-grafted copolymer during its degradation in PBS, pH = 7.40, at 37 °C for different time points, (SEC, $CHCl_3$).

After demonstrating the successful degradation of the PEG-grafted copolymer in PBS medium, the degraded fractions of the copolymer were investigated using MALDI-TOF (matrix-assisted laser desorption/ionization – time-of-flight) mass spectrometry in an attempt to characterize the oligomers left after degradation and identify how the degradation of the copolymer was occurring. In an initial analysis, a sample of the copolymer hydrolyzed in PBS at 37 °C for 7 days was studied. For this sample, the MALDI-TOF mass spectrometry analysis revealed the presence of various and broad distributions, between 800 and 3000 g/mol, which could not be characterized. It was hypothesized that the degradation of the grafted copolymer after 7 days was not significantly long enough to produce enough oligomers which could easily fly and be of suitable size for detection by the instrument. Instead, the various and board distributions observed were hypothesized, and assigned to the remaining non-hydrolyzed main grafted copolymer, which remains a challenge to be

accurately analyzed by a mass spectrometry technique. A similar analysis was later performed on a sample having undergone degradation for 15 days. After this length of time the amount of oligomers should be sufficient to be detected by MALDI-TOF mass spectrometry analysis, as surmised from the degradation observed by SEC (Figure 3.29). Under these conditions, it was noted that the different broad distributions previously observed were replaced by a smaller and more defined single distribution between molecular weight values of 800 to 1100 g/mol. Analysis of this distribution led to the identification of the oligomers to be the PEG-grafted functionality still attached to the vinyl repeat unit *via* the triazole linkage suggesting that the degradation was indeed occurring through the fragmentation of the ester repeat unit of the copolymer introduced from the rROP of MDO of the vinyl bromobutanoate repeat unit (Figure 3.30).

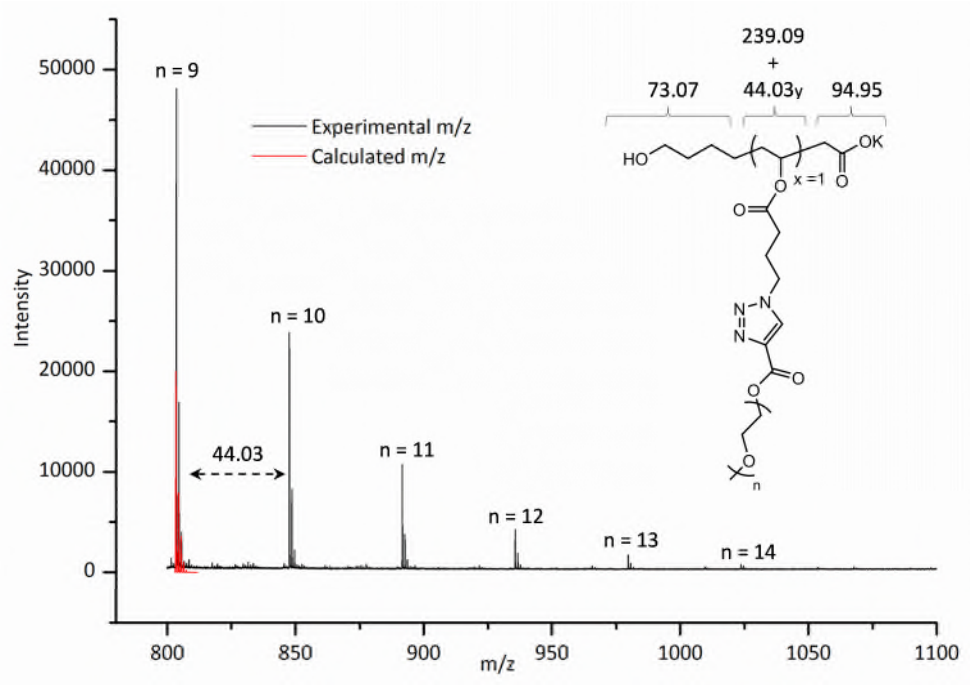

Figure 3.30. MALDI-TOF mass spectrometry spectrum of the PEG-grafted copolymer of poly(MDO-*co*-VN_3) after 15 days of hydrolysis in PBS at 37 °C.

Additionally, it was observed that the distribution of the oligomers was composed of signals with a spacing of 44.03 m/z between neighbouring peaks which corresponds to one unit of

ethylene glycol. This also suggested that the remaining oligomers were also composed of different length of PEG-grafted segments on the vinyl repeat units (Figure 3.30). This pattern was observed as a consequence of the use of the commercially available poly(ethylene glycol) methyl ether as the starting polymer reagent for the synthesis of the functional PEG-alkyne. These commercial polymers are often supplied with average molecular weights and therefore contained different DPs (n), in this case with values of 9, 10, 11, 12, 13 and 14. This observation was also confirmed with the good correlation between the experimental m/z values with the calculated m/z values for each DP respectively (Table 3.6).

Table 3.6. Theoretical and observed m/z values of the PEG-grafted copolymer of poly(MDO-*co*-VN_3) after 15 days of hydrolysis in PBS at 37 °C.

n	Experimental m/z [a]	Calculated m/z
9	803.53	803.35
10	847.57	847.37
11	891.61	891.40
12	935.65	935.42
13	979.71	979.45

[a] determined by MALDI-TOF mass spectrometry analysis using dithranol as matrix, sodium trifluoroacetate as the cationization agent and spherical dendrimers 500 – 1800 g/mol as standard calibrants.

While using MALDI-TOF mass spectrometry analysis strongly suggested that the degradation of the grafted copolymer was occurring *via* the fragmentation of the ester repeat units from the main polymer backbone, it should be noted that potential other degradations *via* the fragmentation of the two other ester units from the side pendent chains could potentially also occur. These specific degradation products were not observed by MALDI-TOF mass spectrometry as they may lead to oligomers which cannot fly as well or be detectable by the spectrometer.

3.4 Conclusions

The synthesis of vinyl bromobutanoate, a novel vinyl acetate derived monomer bearing a bromine pendent group in order to increase the functionality of the common polymer poly(VAc), is demonstrated. The homopolymerization and copolymerization of VBr with MDO using the RAFT/MADIX polymerization technique led to the controlled formation of well-defined polymers as proven by SEC analysis and ^{1}H NMR spectroscopy, and containing pendent functional groups available for further modification. The ratio of MDO could be tuned to produce degradable polymers containing different degrees of ester repeat units as a way to increase the degradability of the targeted final material. Additionally, the successful post-polymerization modification of the polymers was proven using azidation and cycloaddition reactions to deliver polymers with additional functionalities with no effect on the defined and controlled nature of the process reported. The degradation of the copolymer was confirmed by hydrolysis experiments which have shown that the rate of degradation could be tuned by simply varying the amount of MDO incorporated in the copolymer as well as by incorporating hydrophilic functional groups on the polymer by post-polymerization modifications. These results illustrate the great potential in using the vinyl bromobutanoate monomer as a novel route towards the synthesis of functional and degradable polymers from cyclic ketene acetal monomers. The incorporation of the bromine group opens almost limitless possibilities for functionalization on such copolymers to target a wider range of properties and applications.

3.5 Experimental Section

3.5.1 Materials

Vinyl acetate (99%), 4-bromobutyric acid (98%), palladium acetate ($Pd(OAc)_2$, 98%), potassium hydroxide (KOH, 90%) and sodium azide (NaN_3, 97%) were purchased from Sigma-Aldrich and used as received, unless otherwise mentioned. Alumina, activated basic (Al_2O_3: Sigma-Aldrich, Brockmann I, standard grade, ~ 150 mesh, 58 Å), magnesium sulfate ($MgSO_4$: anhydrous, Fisher Scientific, LR grade) were used as received. The following solvents were used as received; dichloromethane (CH_2Cl_2: VWR International, AR grade), *N*,*N*-dimethylformamide (DMF: Sigma-Aldrich, HPLC grade). The following monomers were de-inhibited before use by distillation over CaH_2; vinyl acetate (VAc: Sigma-Aldrich, > 99%, distillation pressure: 0.015 atm, 90-92 °C), vinyl chloroacetate (VClAc: Alfa Aesar, 99%). 2-Methylene-1,3-dioxepane (MDO) was synthesized using the previously described method of Bailey *et al*.[65] and the CTA *O*-hexyl *S*-methyl 2-propionylxhanthate (CTA 1) was synthesized using the procedure described in Chapter 2.[45]

3.5.2 Characterization

^{1}H Nuclear Magnetic Resonance (NMR) spectra were recorded at 400 or 300 MHz in $CDCl_3$ on a Bruker DPX-400/300 spectrometer at 298 K. ^{13}C NMR spectra were recorded at 125 or 100 MHz in $CDCl_3$ on a Bruker DPX-500 spectrometer at 298 K. Chemical shifts are reported as δ in parts per million (ppm) and referenced to the chemical shift of the residual solvent resonances ($CDCl_3$ ^{1}H: δ = 7.26 ppm; ^{13}C: δ = 77.16 ppm). Size exclusion chromatography (SEC) analyses were performed on a system composed of a Varian 390-LC-Multi detector suite using a Varian Polymer Laboratories guard column (PLGel 5 μM, 50 × 7.5 mm), two mixed-D Varian Polymer Laboratories columns (PLGel 5μM, 300 × 7.5 mm)

and a PLAST RT autosampler. Detection was conducted using a differential refractive index (RI) and an ultraviolet (UV) detector set to 280 nm. The analyses were performed in $CHCl_3$ (HPLC grade) at 303 K and containing 2% triethyl amine (TEA) at a flow rate of 1.0 mL/min. Polystyrene (PS) (162 – 2.4 × 10^5 g/mol) or poly(methyl methacrylate) (PMMA) (200 – 1.0 × 10^6 g/mol) standards were used for calibration. Molecular weights and dispersities were determined using Cirrus v3.3 SEC software. IR spectroscopy was carried out using a Perkin Elmer Spectrum 100 FT-IR. 16 scans from 600 to 4000 cm^{-1} were taken, and the spectra corrected for background absorbance. . DLS analyses were performed on a Malvern Zetasizer Nano ZS instrument operating at 25 °C with a 4 Mw He-Ne 633 nm laser module. Measurements were made at an angle of 173° (back scattering), and results were analyzed using Malvern DTS 6.32 software. All determinations were made in triplicate unless otherwise stated (with 10 measurements recorded for each run). SLS experiments were performed at angles of observation ranging from 20° up to 150° with an ALV CG3 spectrometer operating at λ_0 = 633 nm and at 20 ± 1 °C. Solutions (1 mg·mL^{-1}) were filtered through 0.45 μm nylon filters prior to analysis. Data were collected in duplicate with 100 s run times. Calibration was achieved with filtered toluene and the background was measured with filtered solvent (NaCl 0.1 M). The aggregation number, N_{agg} of the self-assemblies was calculated using the REPES algorithm.[66] MALDI-TOF mass spectra were recorded on a Bruker Daltonics Ultraflex and an Autoflex MALD-TOF mass spectrometer in positive ion TOF detection mode performed using an acceleration voltage of 25 kV. Solutions in THF of dithranol as matrix (30 mg/mL), sodium or potassium trifluoroacetate as ionization agents (2 mg/mL) and analyte (1 mg/mL) were mixed prior to being spotted on the MALDI plate and air-dried. The samples were measured in reflector ion mode and calibrated by comparison to SpheriCal (Polymer Factory) single molecular weight standards (500 – 1800 g/mol).

3.5.3 Monomer synthesis

A solution of 4-bromobutanoic acid (15.50 g, 92.8 mmol), KOH (0.52 g, 9.28 mmol)

and $Pd(OAc)_2$ (1.04 g, 4.64 mmol) in vinyl acetate (VAc) (79.90 g, 928 mmol) was stirred at 60 °C for 16 h. The solution was then filtered over celite and thoroughly washed with petroleum ether 40-60 °C in order to remove the excess of catalyst. The excess of vinyl acetate and solvent (petroleum ether) were evaporated under reduced pressure using rotary evaporation. The crude product was purified and isolated by column chromatography (Silica, 100% CH_2Cl_2) before being dried over anhydrous $MgSO_4$, then reduced to dryness using rotary evaporation to yield to a colourless liquid (12.2 g, 63.2 mmol, 68%). ^{1}H NMR ($CDCl_3$, ppm) δ: 7.26 (dd, COOC*H*CH_2, 1H, $^3J_{H\text{-}H}$ = 13.9 Hz, $^3J_{H\text{-}H}$ = 7.5 Hz), 4.89 (dd, COOCHC*H*H, 2H, $^3J_{H\text{-}H}$ = 13.8 Hz, $^2J_{H\text{-}H}$ = 1.84 Hz), 4.58 (dd, COOCHCH*H*, 2H, $^3J_{H\text{-}H}$ = 5.9 Hz, $^2J_{H\text{-}H}$ = 1.7 Hz), 3.47 (t, CH_2CH_2Br, 2H, $^3J_{H\text{-}H}$ = 6.1 Hz), 2.60 (t, CH_2CH_2COOCH, 2H, $^3J_{H\text{-}H}$ = 7.2 Hz), 2.22 (m, $CH_2CH_2CH_2$Br, 2H, $^3J_{H\text{-}H}$ = 6.4 Hz). ^{13}C NMR ($CDCl_3$, ppm) δ: 186.8 (CH_2CHCOO), 141.3 (CH_2CHCOO), 98.2 (CH_2CHCOO), 34.1 ($CH_2CH_2CH_2$Br), 32.9 ($CH_2CH_2CH_2$Br), 27.5 ($CH_2CH_2CH_2$Br). Anal. Calcd for $C_6H_9BrO_2$: C, 37.33%; H, 4.70%. Found: C, 36.99%; H, 4.65%.

3.5.4 Homopolymerization of VBr

In an inert environment, VBr (0.60 g, 3.10 mmol), CTA 1 (8.20 mg, 3.10×10^{-2} mmol), AIBN (0.50 mg, 3.10×10^{-4} mmol) were placed into an ampoule and sealed. The resulting solution was stirred and heated to 60 °C for 16 h before the polymerization was quenched by plunging the ampoule into an ice bath. An aliquot was taken prior to precipitation in order to determine the monomer conversion using ^{1}H NMR spectroscopy. The polymer was dissolved in $CHCl_3$ and precipitated several times in hexane, collected and dried under vacuum at room temperature overnight. ^{1}H NMR ($CDCl_3$, ppm) δ: 5.09-4.72 ppm (m, CH_2CH backbone, 1H), 4.58 (m, SCOCH_2CH_2 end-group, 2H), 3.69 (m, CH_3CCOCH end-group. 3H), 3.49 (m, BrCH_2CH_2CO, 2H,), 2.48 (m, COCH_2CH_2Br, 2H,), 2.17 (m,

$BrCH_2CH_2CH_2$, 2H), 1.98-1.60 (m, $CHCH_2OCO$ backbone, 1H, $CH_3OCOCHCH_3$ end-group, 1H, $CH_3OCOCHCH_3$ end-group, 3H, $OCH_2CH_2CH_2$ end-group, 2H), 1.46-1.13 (m, $CH_2CH_2CH_2CH_3$ end-group, 2H, $CH_2CH_2CH_2CH_3$ end-group, 2H, $CH_2CH_2CH_2CH_3$ end-group, 2H), 0.91 (m, $CH_2CH_2CH_2CH_3$ end-group, 3H). Conversion by ^{1}H NMR spectroscopy: VBr conv. = 35%, M_n (SEC, $CHCl_3$) = 5.2 kg/mol, $Đ_M$ = 1.20, M_n (^{1}H NMR) = 5.9 kg/mol.

3.5.5 Copolymerization of MDO and VBr

Prior to polymerization VBr and MDO monomers were dried and distilled over CaH_2 before being degassed by 3 freeze pump thaw cycles. In an inert environment, MDO (0.126 g, 1.10 mmol), VBr (0.50 g, 2.60 mmol), CTA 1 (9.20 mg, 3.70×10^{-2} mmol), AIBN (0.610 mg, 3.70×10^{-3} mmol) and benzene (15% w/w) were placed into an ampoule and sealed. The resulting solution was stirred and heated to 60 °C for 9 h before the polymerization was quenched by plunging the ampoule into an ice bath. An aliquot was taken prior to precipitation in order to determine the monomer conversions using ^{1}H NMR spectroscopy. The polymer was dissolved in a small amount of $CHCl_3$ and precipitated several times in hexane until no further monomer residue was observed. The colorless solid was dried under vacuum overnight. ^{1}H NMR ($CDCl_3$, ppm) δ: 5.28-4.64 (m, CH_2CHOCO backbone, 1H), 4.58 (t, $SCOCH_2CH_2$ end-group, 2H, $^3J_{H\text{-}H}$ = 5.8 Hz), 4.16-3.91 (m, $COOCH_2CH_2CH_2$ backbone, 2H), 3.69 (m, CH_3CCOCH end-group. 3H), 3.50 (m, $BrCH_2CH_2CH_2CO$, 2H), 3.18 (m, $COOCH_2CH_2CH_2SC$, 2H), 2.65-2.15 (m, $CHCOOCH_2CH_2$ backbone, 2H, $COCH_2CH_2Br$, 2H), 2.17 (m, $BrCH_2CH_2CH_2$, 2H), 1.98-1.40 (m, $CHCH_2OCO$ backbone, 1H, $CH_2CHOCOCH_2$ backbone, 2H, $CH_3OCOCHCH_3$ end-group, 1H, $CH_3OCOCHCH_3$ end-group, 3H), 1.46-1.13 (m, $CH_2CH_2CH_2CH_3$ end-group, 2H, $CH_2CH_2CH_2CH_3$ end-group, 2H, $CH_2CH_2CH_2CH_3$ end-group, 2H, $CH_2COOCH_2CH_2CH_2$, 2H), 0.91 (m, $CH_2CH_2CH_2CH_3$ end-group,

3H). ^{13}C NMR ($CDCl_3$, ppm) δ: 216.1 (S*C*SOCH$_2$CH$_2$CH$_2$ end-group), 176.3 (CH$_3$O*C*OCHCH$_3$ end-group), 174.3 (O*C*OCH$_2$CH$_2$CH$_2$Br), 170.9 (*C*OOCH$_2$CH$_2$CH$_2$ backbone), 100.0 (CH$_2$*C*OCH$_2$CH$_2$CH$_2$ ring-retained), 71.3 (CH$_2$*C*HOCOCH$_2$CH$_2$CH$_2$Br), 64.7 (COO*C*H$_2$CH$_2$CH$_2$ backbone), 51.3 (*C*H$_3$OCOCHCH$_3$ end-group), 39.1 (COOCH$_2$*C*H$_2$CH$_2$ backbone), 33.4 (OCOCH$_2$*C*H$_2$CH$_2$Br), 32.1 (OCOCH$_2$CH$_2$*C*H$_2$Br), 29.8 (OCO*C*H$_2$CH$_2$CH$_2$Br), 28.3 (COOCH$_2$CH$_2$*C*H$_2$ backbone), 17.9 (CH$_3$OCOCH*C*H$_3$ end-group), 14.2 (CH$_2$CH$_2$CH$_2$*C*H$_3$ end-group). Conversion by ^{1}H NMR spectroscopy: VBr conv. = 24%, MDO conv. = 19%, M_n (SEC, $CHCl_3$) = 3.7 kg/mol, $Đ_M$ = 1.44, M_n (^{1}H NMR) = 4.8 kg/mol.

3.5.6 Chain growth experiments

Poly(VBr) was synthesized according to the procedure described previously, (M_n (^{1}H NMR) = 4.1 kg/mol, M_n (SEC, $CHCl_3$) = 3.4 kg/mol, $Đ_M$ = 1.20). Homopolymer poly(VBr) (0.50 g, 0.14 mmol), VAc (0.15 g, 1.74 mmol), AIBN (0.40 mg, 2.43×10^{-3} mmol) were dissolved in benzene (40 wt%) and placed into a sealed ampoule before being degassed by 3 freeze pump thaw cycles. The polymer mixture was then heated at 60 °C for 5 h to afford the diblock poly(VBr)-*b*-poly(VAc). The polymer was purified by precipitation into cold hexane three times and dried *in vacuo*, M_n (SEC, $CHCl_3$) = 6.8 kg/mol, M_n (^{1}H NMR, $CDCl_3$) = 9.12 kg/mol, $Đ_M$ = 1.24.

3.5.7 Post-polymerization modifications using azidation

Poly(MDO-*co*-VBr) was synthesized according to the procedure previously described, (M_n (^{1}H NMR) = 8.9 kg/mol, M_n (SEC, $CHCl_3$) = 4.5 kg/mol, $Đ_M$ = 1.53). Copolymer poly(MDO-*co*-VBr) (0.21 g, 0.35 mmol) was dissolved in DMF (10 mL) and NaN_3 (0.07 g, 1.05 mmol) was added to the mixture before being stirred at room temperature for 3 days. DMF was removed under vacuum and the polymer was re-dissolved in a small amount of

toluene before being precipitated into cold hexane. The polymer was dried *in vacuo*, M_n (^{1}H NMR, $CDCl_3$) = 4.5 kg/mol, M_n (SEC, $CHCl_3$) = 4.8 kg/mol, $Đ_M$ = 1.50. ^{1}H NMR ($CDCl_3$, ppm), δ: 5.28-4.72 (m, CH_2CHOCO backbone, 1H), 4.58 (t, $SCOCH_2CH_2$ end-group, 2H, $^3J_{H\text{-}H}$ = 5.8 Hz), 4.17-3.95 (m, $COOCH_2CH_2CH_2$ backbone, 2H), 3.67 (m, CH_3OCOCH end-group, 3H), 3.41 (m, $N_3CH_2CH_2CH_2$, 2H), 2.65-2.50 (m, $CHCOOCH_2CH_2CH_2$, 2H), 2.41 (m, $N_3CH_2CH_2CH_2$, 2H), 2.03-1.63 (m, $N_3CH_2CH_2CH_2$), 1.60-1.48 (m, CH_2CHOCO backbone, 2H), 1.45-1.12 (m, $COOCH_2CH_2CH_2$ backbone, 2H, m, $SCOCH_2CH_2CH_2$ end-group, 2H, m, $CH_2CH_2CH_3$ end-group, 2H, m, $CH_2CH_2CH_3$ end-group, 2H), 0.91 (m, $CH_2CH_2CH_3$ end-group, 3H). FTIR, ν/cm^{-1}: 2954 (C-H alkyl chains), 2095 (N_3 azide stretch), 1724 (C=O carbonyl stretch), 1441 (C-H stretch), 1252 (C-O stretch).

3.5.8 Post-polymerization modifications using 1,3-dipolar cycloaddition

Poly(MDO-*co*-VN_3) was synthesized using the procedure previously described, (M_n (^{1}H NMR) = 10.1 kg/mol), M_n (SEC, $CHCl_3$) = 6.9 kg/mol, $Đ_M$ = 1.57). The azide copolymer, poly($MDO_{0.24}$-*co*-$VN_{3(0.76)})_{50}$ (0.17 g, 0.61 mmol) was dissolved in DMF (1.5 mL) and ethyl propiolate (0.06 g, 0.61 mmol) was added. The mixture was stirred for 15 min before being heated to 80 °C for 48 h. The solvent was removed under vacuum and the polymer was re-dissolved in a small amount of $CHCl_3$ before being recovered by precipitation in hexane and dried *in vacuo*, M_n (SEC, $CHCl_3$) = 8.4 kg/mol, $Đ_M$ = 1.53. ^{1}H NMR ($CDCl_3$, ppm), δ: 8.45-8.27 (m, NNC*H*C triazole, 1H), 5.43-4.66 (m, CH_2CHOCO backbone, 1H), 4.51 (m, CH_2CH_2NCH pendent group, 2H), 4.30 (m, CH_3CH_2OCO pendent group, 2H), 4.15-3.92 (m, $COOCH_2CH_2CH_2$ backbone, 2H), 3.68 (s, CH_3OCOCHend-group, 3H), 2.60-2.48 (m, CH_2COOCH_2 backbone, 2H), 2.40-2.00 (m, $COCH_2CH_2CH_2N$ pendent group, 2H, m, $COCH_2CH_2CH_2N$ pendent group, 2H), 1.98-1.47 (m, $COOCH_2CH_2CH_2CH_2$ backbone, 2H, m $COOCH_2CH_2CH_2CH_2$ backbone, 2H, $COOCH_2CH_2CH_2CH_2$, 2H, $CH_2CHOCOCH_2$

backbone, 2H), 1.33 (m, C*H*$_3$CH$_2$OCO pendent group, 3H), 0.91 (m, CH$_2$CH$_2$CH$_2$CH$_2$C*H*$_3$ end-group, 3H).

3.5.9 Degradation experiments

In a typical experiment, 500 mg of copolymer was placed in a 10 mL vial and dissolved in a small amount (0.5 mL) of CH_2Cl_2. A solution of KOH in methanol (0.1M, 6 mL) was then added to the vial and stirred at 40 °C. Samples were taken at different time points and the solvents were removed under vacuum. The polymer residues were re-dissolved in $CHCl_3$ and filtered in order to remove the residual salt and the solution was analyzed by SEC ($CHCl_3$).

3.6 References

(1) Staudinger, H. *Rubber Chem. Technol.* **1939**, *12*, 117.

(2) Gauthier, M. A.; Gibson, M. I.; Klok, H.-A. *Angew. Chem. Int. Ed.* **2009**, *48*, 48.

(3) Günay, K. A.; Theato, P.; Klok, H.-A. In *Functional Polymers by Post-Polymerization Modification*; Wiley-VCH Verlag GmbH & Co. KGaA: 2012, p 1.

(4) Justynska, J.; Hordyjewicz, Z.; Schlaad, H. *Polymer* **2005**, *46*, 12057.

(5) Justynska, J.; Schlaad, H. *Macromol. Rapid Commun.* **2004**, *25*, 1478.

(6) Chujo, Y.; Sada, K.; Saegusa, T. *Macromolecules* **1990**, *23*, 2636.

(7) Canary, S. A.; Stevens, M. P. *J. Polym. Sci., Part A: Polym. Chem.* **1992**, *30*, 1755.

(8) Canadell, J.; Fischer, H.; De With, G.; van Benthem, R. A. T. M. *J. Polym. Sci., Part A: Polym. Chem.* **2010**, *48*, 3456.

(9) Ladmiral, V.; Mantovani, G.; Clarkson, G. J.; Cauet, S.; Irwin, J. L.; Haddleton, D. M. *J. Am. Chem. Soc.* **2006**, *128*, 4823.

(10) Truong, V. X.; Ablett, M. P.; Gilbert, H. T. J.; Bowen, J.; Richardson, S. M.; Hoyland, J. A.; Dove, A. P. *Biomater. Sci.* **2014**, *2*, 167.

(11) Binder, W. H.; Sachsenhofer, R. *Macromol. Rapid Commun.* **2007**, *28*, 15.

(12) Kato, M.; Kamigaito, M.; Sawamoto, M.; Higashimura, T. *Macromolecules* **1995**, *28*, 1721.

(13) Chiefari, J.; Chong, Y. K.; Ercole, F.; Krstina, J.; Jeffery, J.; Le, T. P. T.; Mayadunne, R. T. A.; Meijs, G. F.; Moad, C. L.; Moad, G.; Rizzardo, E.; Thang, S. H. *Macromolecules* **1998**, *31*, 5559.

(14) Moad, G.; Rizzardo, E. *Macromolecules* **1995**, *28*, 8722.

(15) Albertsson, A.-C.; Varma, I. K. *Biomacromolecules* **2003**, *4*, 1466.

(16) Uhrich, K. E.; Cannizzaro, S. M.; Langer, R. S.; Shakesheff, K. M. *Chem. Rev.* **1999**, *99*, 3181.

(17) Woodruff, M. A.; Hutmacher, D. W. *Prog. Polym. Sci.* **2010**, *35*, 1217.

(18) Seyednejad, H.; Ghassemi, A. H.; van Nostrum, C. F.; Vermonden, T.; Hennink, W. E. *J. Control. Release* **2011**, *152*, 168.

(19) Dash, T. K.; Konkimalla, V. B. *J. Control. Release* **2012**, *158*, 15.

(20) Ulery, B. D.; Nair, L. S.; Laurencin, C. T. *J. Polym. Sci. Pol. Phys.* **2011**, *49*, 832.

(21) Yu, Y.; Zou, J.; Cheng, C. *Polym. Chem.* **2014**, *5*, 5854.

(22) Pounder, R. J.; Dove, A. P. *Polym. Chem.* **2010**, *1*, 260.

(23) Williams, C. K. *Chem. Soc. Rev.* **2007**, *36*, 1573.

(24) Jérôme, C.; Lecomte, P. *Adv. Drug Deliv. Rev.* **2008**, *60*, 1056.

(25) Riva, R.; Schmeits, S.; Stoffelbach, F.; Jerome, C.; Jerome, R.; Lecomte, P. *Chem. Commun.* **2005**, 5334.

(26) Carrot, G.; Hilborn, J. G.; Trollsås, M.; Hedrick, J. L. *Macromolecules* **1999**, *32*, 5264.

(27) Hvilsted, S. *Polym. Int.* **2012**, *61*, 485.

(28) Campos, J. M.; Ribeiro, M. R.; Ribeiro, M. F.; Deffieux, A.; Peruch, F. *Eur. Polym. J.* **2013**, *49*, 4025.

(29) Li, G.; Lamberti, M.; Pappalardo, D.; Pellecchia, C. *Macromolecules* **2012**, *45*, 8614.

(30) Wilson, J. A.; Hopkins, S. A.; Wright, P. M.; Dove, A. P. *Macromolecules* **2015**, *48*, 950.

(31) Wurth, J. J.; Shastri, V. P. *J. Polym. Sci., Part A: Polym. Chem.* **2013**, *51*, 3375.

(32) Bailey, W. J.; Ni, Z.; Wu, S. R. *Macromolecules* **1982**, *15*, 711.

(33) Agarwal, S. *Polym. J.* **2006**, *39*, 163.

(34) Jin, S.; Gonsalves, K. E. *Macromolecules* **1997**, *30*, 3104.

(35) Bailey, W. J.; Endo, T.; Gapud, B.; Lin, Y.-N.; Ni, Z.; Pan, C.-Y.; Shaffer, S. E.; Wu, S.-R.; Yamazaki, N.; Yonezawa, K. *J. Macromol. Sci. A.* **1984**, *21*, 979.

(36) Undin, J.; Illanes, T.; Finne-Wistrand, A.; Albertsson, A.-C. *Polym. Chem.* **2012**, *3*, 1260.

(37) Undin, J.; Finne-Wistrand, A.; Albertsson, A.-C. *Biomacromolecules* **2014**, *15*, 2800.

(38) Undin, J.; Finne-Wistrand, A.; Albertsson, A.-C. *Biomacromolecules* **2013**, *14*, 2095.

(39) Agarwal, S. *Polym. Chem.* **2010**, *1*, 953.

(40) Roberts, G. E.; Coote, M. L.; Heuts, J. P. A.; Morris, L. M.; Davis, T. P. *Macromolecules* **1999**, *32*, 1332.

(41) Maji, S.; Mitschang, F.; Chen, L.; Jin, Q.; Wang, Y.; Agarwal, S. *Macromol. Chem. Phys.* **2012**, *213*, 1643.

(42) Maji, S.; Zheng, M.; Agarwal, S. *Macromol. Chem. Phys.* **2011**, *212*, 2573.

(43) Agarwal, S. *Polym. J.* **2007**, *39*, 163.

(44) Kobben, S.; Ethirajan, A.; Junkers, T. *J. Polym. Sci., Part A: Polym. Chem.* **2014**, *52*, 1633.

(45) Hedir, G. G.; Bell, C. A.; Ieong, N. S.; Chapman, E.; Collins, I. R.; O'Reilly, R. K.; Dove, A. P. *Macromolecules* **2014**, *47*, 2847.

(46) Agarwal, S.; Kumar, R.; Kissel, T.; Reul, R. *Polym. J.* **2009**, *41*, 650.

(47) Allaoua, I.; Goi, B. E.; Obadia, M. M.; Debuigne, A.; Detrembleur, C.; Drockenmuller, E. *Polym. Chem.* **2014**, *5*, 2973.

(48) Marvel, C. S.; DePierri, W. G. *J. Polym. Sci.* **1958**, *27*, 39.

(49) Chênevert, R.; Pelchat, N.; Morin, P. *Tetrahedron Asymmetry* **2009**, *20*, 1191.

(50) Murray, R. E.; Lincoln, D. M. *Catal. Today* **1992**, *13*, 93.

(51) Liu, X.; Coutelier, O.; Harrisson, S.; Tassaing, T.; Marty, J.-D.; Destarac, M. *ACS Macro Lett.* **2014**, *4*, 89.

(52) Hiemenz, P. C.; Lodge, T. P. *Polymer Chemistry, Second Edition*; Taylor & Francis, 2007.

(53) Chinai, S. N.; Scherer, P. C.; Levi, D. W. *J. Polym. Sci.* **1955**, *17*, 117.

(54) Gruendling, T.; Junkers, T.; Guilhaus, M.; Barner-Kowollik, C. *Macromol. Chem. Phys.* **2010**, *211*, 520.

(55) Lu, A.; Smart, T. P.; Epps, T. H.; Longbottom, D. A.; O'Reilly, R. K. *Macromolecules* **2011**, *44*, 7233.

(56) Manders, B. G.; Smulders, W.; Aerdts, A. M.; van Herk, A. M. *Macromolecules* **1997**, *30*, 322.

(57) Van Der Meer, R.; Linssen, H. N.; German, A. L. *J. Polym. Sci., Part A: Polym. Chem.* **1978**, *16*, 2915.

(58) Plikk, P.; Tyson, T.; Finne-Wistrand, A.; Albertsson, A.-C. *J. Polym. Sci., Part A: Polym. Chem.* **2009**, *47*, 4587.

(59) Lutz, J.-F. *Angew. Chem. Int. Ed.* **2008**, *47*, 2182.

(60) Becer, C. R.; Hoogenboom, R.; Schubert, U. S. *Angew. Chem. Int. Ed.* **2009**, *48*, 4900.

(61) Li, Z.; Seo, T. S.; Ju, J. *Tetrahedron Lett.* **2004**, *45*, 3143.

(62) Obadia, M. M.; Colliat-Dangus, G.; Debuigne, A.; Serghei, A.; Detrembleur, C.; Drockenmuller, E. *Chem. Commun.* **2015**, *51*, 3332.

(63) Truong, V. X.; Dove, A. P. *Angew. Chem. Int. Ed.* **2013**, *52*, 4132.

(64) Knop, K.; Hoogenboom, R.; Fischer, D.; Schubert, U. S. *Angew. Chem. Int. Ed.* **2010**, *49*, 6288.

(65) Bailey, W. J.; Ni, Z.; Wu, S.-R. *J. Polym. Sci., Part A: Polym. Chem.* **1982**, *20*, 3021.

(66) Jakeš, J. *Collect. Czech. Chem. Commun.* **1995**, *60*, 1781.

4 Controlling the synthesis of degradable vinyl polymers by RAFT/MADIX polymerization

4.1 Abstract

In this chapter, the copolymerization of MDO and VAc is further investigated using a different chain transfer agent, *p*-methoxyphenyl xanthate (CTA 4), in an attempt to increase the degree of control and identify the cause of loss of control previously noted in Chapters 2 and 3 which was observed as an increase of the dispersity when higher conversions and amounts of MDO were targeted. Towards this aim, the homopolymerization of MDO was also investigated using CTA 4 and compared with the CTAs previously used in Chapters 2, 3. Investigation using ^{13}C NMR spectroscopy analyses of the homopolymer and the copolymer, poly(MDO-*co*-VAc) were performed to show that the loss of control was resulting from the fragmentation of the Z-group of the xanthate polymer chain-end and the subsequent formation of carbonodithioate groups which led to terminated polymer chains unable to be further grown. The use of CTA 4 was found to reduce this effect and therefore improve the copolymerization of MDO with VAc.

The work presented in this chapter is resulting from the collaborative work with Dr Craig A. Bell from the groups of Prof. Andrew P. Dove and Prof. Rachel K. O'Reilly. All the copolymerizations presented in this chapter were performed and analyzed by Dr Craig A. Bell.

4.2 Introduction

As introduced in the previous Chapters, the radical ring-opening polymerization (rROP) of cyclic ketene acetal (CKA) monomers has in recent years been re-invented as a simple approach to incorporate degradable ester repeat units into conventional vinyl polymers *via* the copolymerization of CKAs with vinyl monomers.[1-5] While most of these copolymerizations have been performed using conventional free radical polymerization techniques, the use of controlled polymerization methods in such systems has been increasingly studied to obtain degradable vinyl polymers with narrow dispersities and control over the molecular weights.[5-9] Delplace and co-workers investigated the copolymerization of 2-methylene-1,3-dioxepane (MDO, the seven-membered ring **CKA 1**), with poly(ethylene glycol) methyl acrylate (PEGMA), methyl methacrylate (MMA) and acrylonitrile (AN) using the Nitroxide-Mediated Polymerization (NMP) as the controlled polymerization technique.[8,10] The controlled aspect of their copolymerization was confirmed by low dispersity values of the final copolymers, typically $Đ_M$, < 1.4. However, only small amounts of the MDO monomer were used in the initial feed (20 and 40 mol%) suggesting that the controlled polymerization for higher MDO content remained challenging. Wei and co-workers also investigated the use of NMP with 2,2,6,6-tetramethyl-1-piperidinyloxy (TEMPO) to attempt to control the homopolymerization of MDO.[11,12] Some promising results suggested the controlled nature of the process, as seen by the increase in molecular weights ($M_n \leq 8.5$ kg/mol) while maintaining lower dispersities (typically $Đ_M < 2$). These experiments were again limited to low MDO monomer conversions and the use of higher reaction temperatures which often led to multimodal SEC traces for the final poly(MDO). In Chapters 2 and 3, the rROP of MDO, was investigated alongside its copolymerization with vinyl acetate, VAc, and vinyl bromobutanoate, VBr, using the reversible addition-fragmentation chain-transfer polymerization/macromolecular

design by interchange of xanthates (RAFT/MADIX) to form well-defined copolymers of poly(MDO-*co*-VAc) and poly(MDO-*co*-VBr) with control over the molecular weights and narrow dispersities, typically $Đ_M$, < 1.6.[6,7] While the controlled aspect of each copolymerization was confirmed by the retention of the xanthate chain-end group on the copolymer, as seen by size exclusion chromatography (SEC) and ^{1}H NMR spectroscopy analyses, a broadening of the dispersities was observed when higher conversions and amount of MDO were targeted, suggesting loss of control under these conditions.

The broadening of the dispersities and the loss of control in RAFT polymerization reactions can often be observed when the choice of Z and R groups of the chain transfer agent (CTA) is not ideal for the monomer system investigated (less activated monomers *vs*. activated monomers).[13,14] As previously mentioned in Chapter 1, the nature of the Z group of the CTA has a significant effect on the polymerization as it affects the stability of the thiocarbonyl group and hence the stability of the radical intermediate in the main equilibrium of the RAFT polymerization (Scheme 4.1). An efficient balance must be reached between the Z group stability and the radical intermediate formed during the equilibrium in order to allow both fragmentation of the chain ends and propagation of the polymer chains to occur and allow the growth of the polymer. Failing to achieve such balance can lead to a higher amount of termination reactions resulting from the higher radical concentration occurring in the process which lead to a loss of control of the polymerization. Xanthates have been found to be ideal candidates for the controlled polymerization of less activated monomers, such as VAc and *N*-vinyl pyrrolidone (NVP), as they contain a stabilizing Z group which maintains a good balance between the fragmentation and propagation steps, thus leading to good control of the polymerization process.

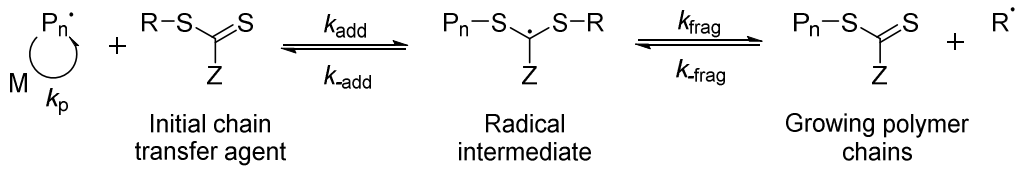

Scheme 4.1. Schematic representation of the equilibrium mechanism for RAFT polymerization using a chain transfer agent, where P_n is the growing polymer chain with a polymerization degree of n, and M being the monomer.

While the choice of Z group in xanthates as CTAs has widely been investigated, [15,16] a less common effect which can lead to a loss of control in RAFT/MADIX polymerization reactions was recently reported by Dommanget and co-workers. [17] In their study, the RAFT/MADIX technique was applied to the polymerization of ethylene in an attempt to produce well-define polyethylene samples with narrow dispersities and controlled molecular weights. To this aim, two xanthates, *O*-ethyl xanthate and *O*-methyl xanthate, were used to mediate the reaction as ethylene was considered a non-activated monomer. Initial results indicated the successful mediation of the polymerization as seen by the low dispersity values obtained for the polymers ($Đ_M$ = 1.40 - 1.90) after 1, 3 and 7 h of reaction in comparison with much larger values of up to 10 obtained when the polymerizations were performed in the absence of chain transfer agent. The control nature of their polymerizations was also confirmed by the characteristic signals of the xanthate polymer chain-ends observed by ^{1}H NMR spectroscopy analysis and the successful ability to chain extend the polyethylene sample with VAc to for block polymers. However, further analysis of the polymers by ^{1}H NMR spectroscopy analysis and SEC analysis revealed that upon reaction time above 4 h, they observed a broadening of the dispersities and a deviation of the correlation between the observed molecular weights, M_n^{obs}, and theoretical molecular weights, M_n^{theo}, which contradicted their initial conclusions. It was therefore proposed that the occurring mechanism involving the fragmentation of the Z group from the xanthate chain-end where the presence of unstable radicals, such as

ethyl radicals, combined with the similar unstability of polyethylene radicals were favouring a side fragmentation in a way that carbonodithioate functional group was generated, causing the termination of the polymer chains (Scheme 4.2).

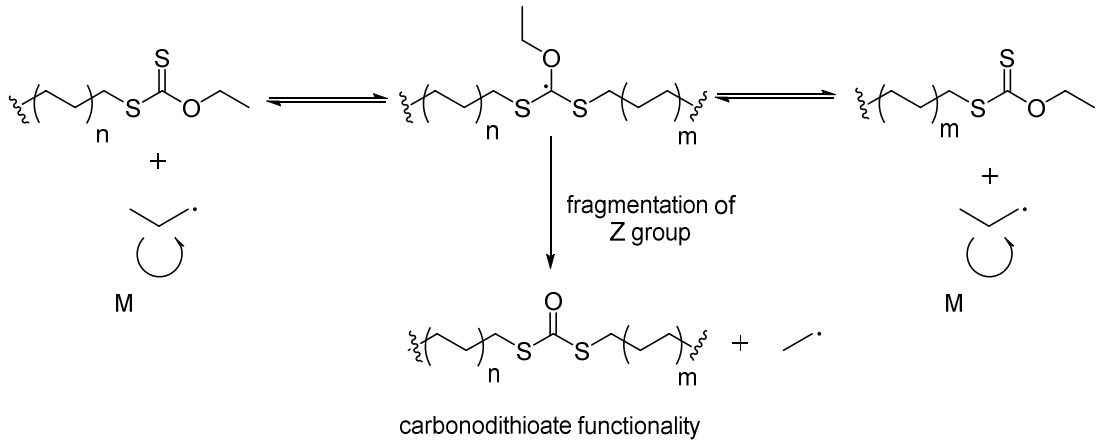

Scheme 4.2. Schematic representation of the side fragmentation of the Z group observed in the polymerization of ethylene mediated by RADFT/MADIX, as reported by Dommanget and co-workers.[17]

Inspired by the work of Dommanget and co-workers, the hypothesis that the Z group fragmentation phenomenon could be occurring in the rROP of MDO was postulated. Indeed, the incorporation of the unstable primary leaving group adjacent to the xanthate could force the xanthate radical to also fragment *via* the Z group side reaction. This side reaction could therefore explain the loss of control for the rROP of MDO using the RAFT/MADIX polymerization, previously observed in Chapters 2 and 3.

In this chapter, the improved copolymerization of VAc and MDO using *p*-methoxyphenyl xanthate, CTA 4, was investigated and used to explain the broadening of the dispersities previously obtained as a consequence of the loss of xanthate *via* the fragmentation of the Z group mechanism. The homopolymerization of MDO was also performed in an attempt to assess its controlled nature *via* the RAFT/MADIX polymerization technique.

4.3 Results and discussion

4.3.1 Choice of chain transfer agent: *p*-methoxyphenyl xanthate (CTA 4)

Aiming to reduce the loss of control observed for the copolymerization of MDO and VAc, which was assumed to be obtained as a consequence of the Z-group fragmentation process previously reported by Dommanget and co-workers,[17] a suitable xanthate CTA which would not stabilize a radical through the proposed Z group fragmentation mechanism was sought, such as one where the Z group would contain a phenyl group. Having such phenyl group would reduce the hypothesized Z group fragmentation as a consequence of the higher stability of the phenyl radical in comparison with the alkyl radicals, and thus allow the polymerization to proceed mainly *via* the conventional fragmentation of the dormant polymer chains and therefore maintain control of the polymerization process. After a literature search on the type of xanthates previously used for the polymerization of less activated monomers, *p*-methoxyphenyl xanthate (CTA 4, Scheme 4.3), reported by Stenzel and co-workers for the controlled polymerization of VAc over a wide range of molecular weights (M_w = 1 – 50 kg/mol) with low dispersity values, was selected as an ideal candidate.[18]

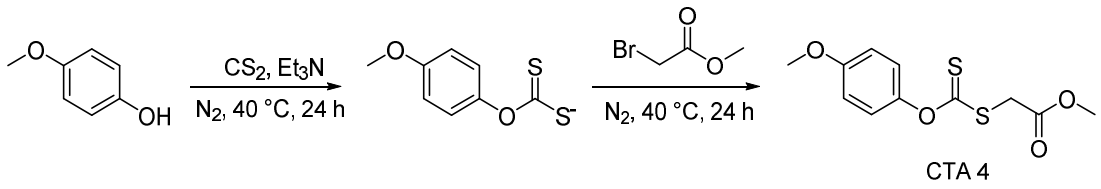

Scheme 4.3. Schematic representation of the synthetic approach used to obtain *p*-methoxyphenyl xanthate, CTA 4, which is further employed in the homopolymerization and copolymerization of MDO with VAc *via* RAFT/MADIX polymerization.

The synthesis of CTA 4 was performed in two steps using a similar procedure as the one previously reported by Stenzel and co-workers [18] where *p*-methoxyphenol (1 eq.) was reacted with carbon disulfide (1 eq.) and triethylamine (1 eq.) to obtain the

p-methoxyphenol carbonodithioate intermediate salt which was then reacted with methyl bromoacetate (1 eq.) to successfully yield *p*-methoxyphenyl xanthate, CTA 4, after column chromatography purification, as confirmed by ^{1}H NMR spectroscopy analysis (Figure 4.1).

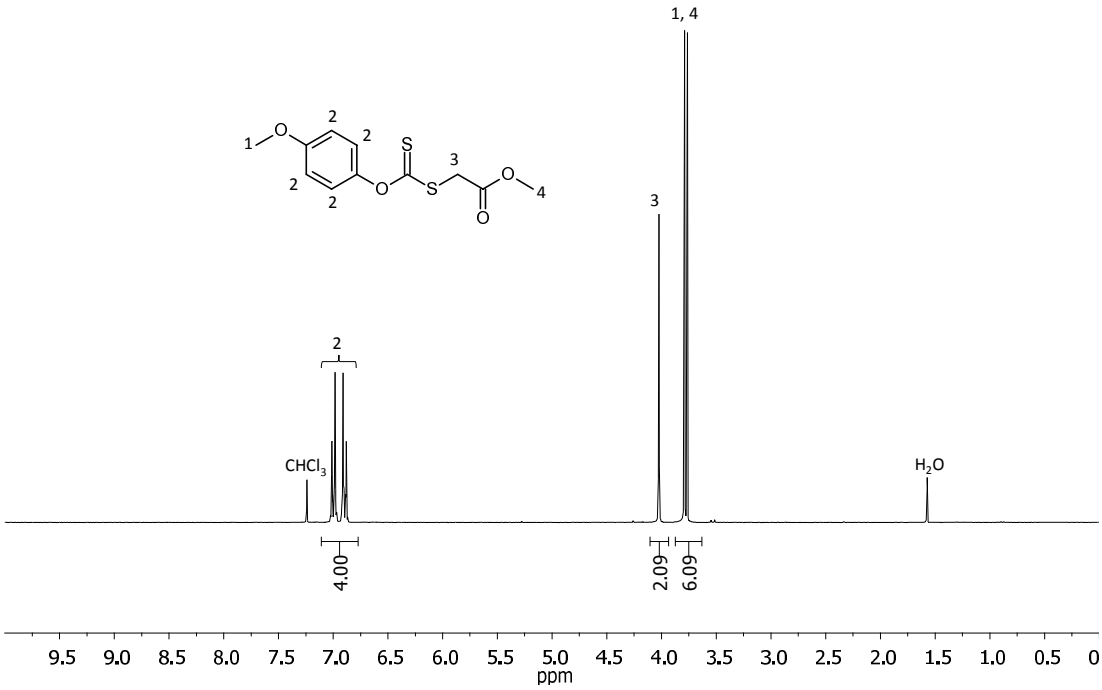

Figure 4.1. ^{1}H NMR spectrum of *p*-methoxyphenly xanthate, CTA 4, (400 MHz, $CDCl_3$).

4.3.2 Copolymerization of VAc and MDO using CTA 4 as the chain transfer agent

In an attempt to confirm the suitability of CTA 4 to mediate the copolymerization of VAc and MDO, initial experiments were carried out using the same conditions previously described in Chapter 2.[7] Two copolymerization reactions were performed in benzene (15 wt% to prevent the increase in apparent viscosity of the mixture) with 2,2′-azobis(2-methylpropionitrile), AIBN, as the radical initiator, stirred at 60 °C for 24 h with monomer/initiator feed ratios of $[MDO]_0/[VAc]_0/[AIBN]_0/[CTA\ 4]_0$ = 30:70:0.1:1 and $[MDO]_0/[VAc]_0/[AIBN]_0/[CTA\ 4]_0$ = 70:30:0.1:1 (Scheme 4.4).

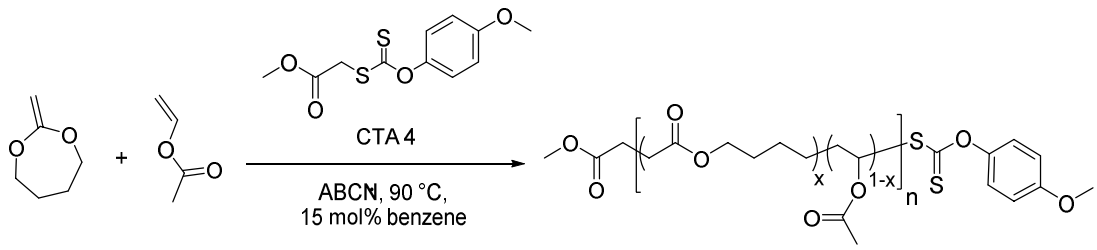

Scheme 4.4. Schematic representation of the synthesis of poly(MDO-*co*-VAc) copolymers by RAFT/MADIX polymerization using CTA 4 as the chain transfer agent.

After quenching the polymerization by plunging the ampoule containing the mixture into an ice bath, ^{1}H NMR spectroscopy analysis of each copolymerization revealed low monomer conversions with 17% and 12% reached for the lower amount of MDO targeted and 7% and 4% for the higher amount for VAc and MDO respectively. The obtained low monomer conversions were attributed to the low fragmentation rate of the polymer-bond xanthate, which was in turn considered to be a result of the high stability of the phenyl radicals. As such, the fragmentation/propagation steps are inhibited and the RAFT equilibrium is shifted towards the dormant species. Aiming at increasing the fragmentation rate and targeting higher conversions, the initiator AIBN was replaced with 1,1′-azobis(cyclohexanecarbonitrile), ABCN, as it was previously reported to be an efficient radical initiator for polymerizations at higher temperatures.[19] Using ABCN, the copolymerization of MDO and VAc were then performed at 90 °C, in benzene (15 wt%) with different monomer feed ratios, namely 10, 30, 50, and 70 mol% in MDO aiming at assessing copolymerizations with both higher and lower MDO content (Table 4.1).

Table 4.1. Characterization data for the copolymerization of VAc and MDO using CTA 4 as the chain transfer agent for different initial monomer feeds.

Time (h)	Monomer feed [VAc:MDO]	VAc conv.[a] (%)	MDO conv.[a] (%)	Polymer compo.[a] [VAc:MDO]	M_n (SEC) [b] (kg/mol)	M_n theo [c] (kg/mol)	M_n obs [d] (kg/mol)	$Đ_M$ [b]
4	90:10	58	51	93:07	8.1	5.4	8.2	1.38
15	70:30	65	41	72:21	7.9	5.6	8.2	1.35
15	50:50	55	30	66:34	7.2	4.4	6.5	1.32
24	30:70	55	29	46:54	5.7	4.2	6.3	1.43

[a] determined by ^{1}H NMR spectroscopy, [b] obtained by SEC analysis in $CHCl_3$, [c] theoretical molecular weight based on monomer conversion (^{1}H NMR spectroscopy), [d] observed molecular weight obtained by ^{1}H NMR spectroscopy end-group analysis.

Under these conditions, the reaction times were required to be longer, 4 to 24 h to reach monomer conversions above 50%, as the content of MDO increased in the polymerization mixture, which could be explained by the lower fragmentation rate of the new xanthate from the dormant polymer chains that have an MDO repeat unit adjacent to the xanthate (Figure 4.2). These kinetic features were similarly observed by d'Ayala and co-workers for the copolymerization of VAc with 5,6-benzo-2-methylene-1,3-dioxepane (BMDO, an analogue CKA monomer) using the RAFT/MADIX polymerization.[20]

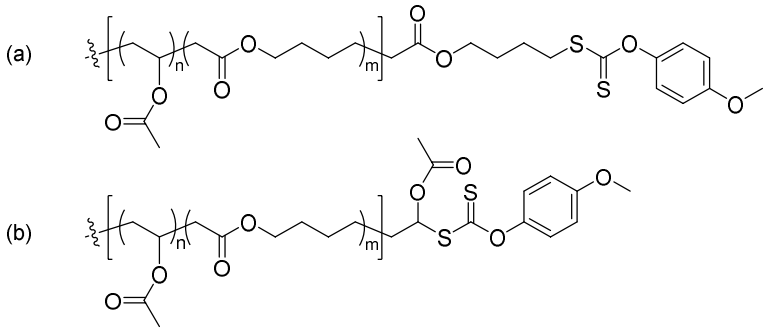

Figure 4.2. Schematic representation of a copolymer chain having (a) MDO repeat unit adjacent to the xanthate and (b) VAc repeat unit adjacent to the xanthate.

Analyses using ^{1}H NMR spectroscopy revealed that higher conversions (compared to results obtained using AIBN) were successfully reached with values of 58 - 65% and 51 - 29% for VAc and MDO, respectively. SEC analyses confirmed the controlled nature of the polymerization as seen by the low dispersity values obtained, $Đ_M$ = 1.38 - 1.55. These values were found to be lower that the previous results obtained when CTA 1 was used in Chapter 2 suggesting an improvement in the control of the copolymerization. The controlled aspect of these copolymerizations was also confirmed by the good agreement between the UV trace of the SEC at λ = 280 nm (absorbing wavelength of xanthates) and the RI trace confirming the presence of the xanthate chain-end throughout the whole distribution (Figure 4.3). However, it should also be noted that as the content of MDO increases in the copolymerization mixture, the UV traces were found to shift towards the higher molecular weights region suggesting that some termination reactions occurred resulting in the loss of the xanthate chain-end and the formation of a lower molecular weight polymers with no xanthate ends.

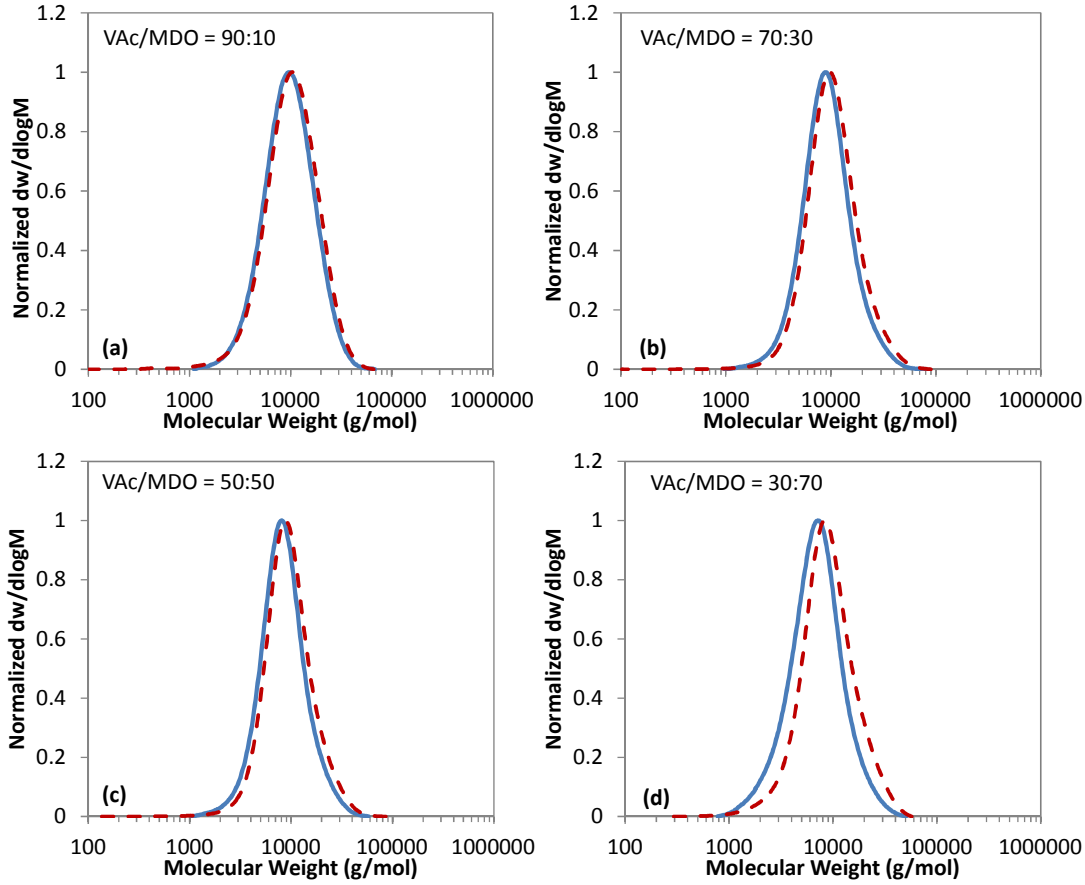

Figure 4.3. Size exclusion chromatograms of poly(MDO-*co*-VAc) obtained by the RAFT/MADIX polymerization using CTA 4 as the chain transfer agent with different initial monomer feeds of VAc/MDO: (a) 90/10 mol% , (b) 70/30 mol%, (c) 50/50 mol% and (d) 30/70 mol%, (SEC, $CHCl_3$), dashed lines indicate molecular weight distribution from the UV detection at λ = 280 nm.

Analyses using ^{1}H NMR spectroscopy on all copolymers revealed the retention of the xanthate chain-ends as seen by the characteristic resonances at δ = 6.90 - 7.00 ppm and δ = 3.80 ppm corresponding to the aromatic group and the methoxy group from the xanthate chain ends, respectively, suggesting the suitability of CTA 4 to mediate the copolymerization (Figure 4.4). The observed molecular weight, M_n^{obs}, was calculated by integration of the signal from the protons from the VAc and MDO polymer backbone at δ = 4.80 - 5.20 ppm and δ = 4.20 ppm, respectively, and referenced to the signal of the aromatic xanthate group at δ = 6.90 - 7.00 ppm.

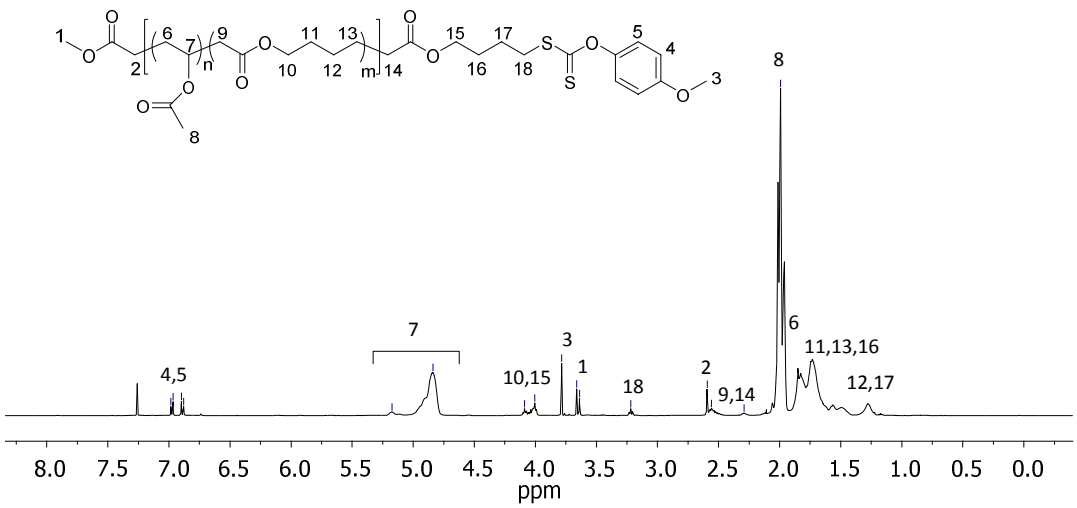

Figure 4.4. ^{1}H NMR spectrum of poly(MDO-*co*-VAc) obtained using the RAFT/MADIX polymerization with CTA 4 as the chain transfer agent, (400 MHz, $CDCl_3$).

As in the previous chapters, the theoretical molecular weights, M_n^{theo}, were determined from the monomer conversion obtained by ^{1}H NMR spectroscopy analysis on the aliquots obtained before precipitation in hexane. The values of M_n^{obs} were found to be in good agreement with the molecular weights obtained by SEC, M_n^{SEC}. Nevertheless, the M_n^{obs} values were found to always be higher compared to M_n^{theo}, suggesting that some termination reactions still occurred during the polymerization. Further analysis using ^{1}H NMR spectroscopy on the copolymers was performed to show that as the VAc content in the copolymers decreases, the intensity of the VAc peak at δ = 5.00 ppm also decreases. Similarly, the intensity of the peak associated with MDO at δ = 4.20 ppm was also found to increase (Figure 4.5). It can also be observed that at higher MDO content, the intensity of the VAc-MDO diad signal at δ = 5.2 ppm increases and the intensity of the VAc-VAc diad signal at δ = 4.9 ppm decreases, which suggests the successful incorporation of higher MDO content in the copolymer backbone. However, as the content of MDO increases, a signal at δ = 6.70

ppm appears and was found to increase as the MDO content in the final polymer increases.

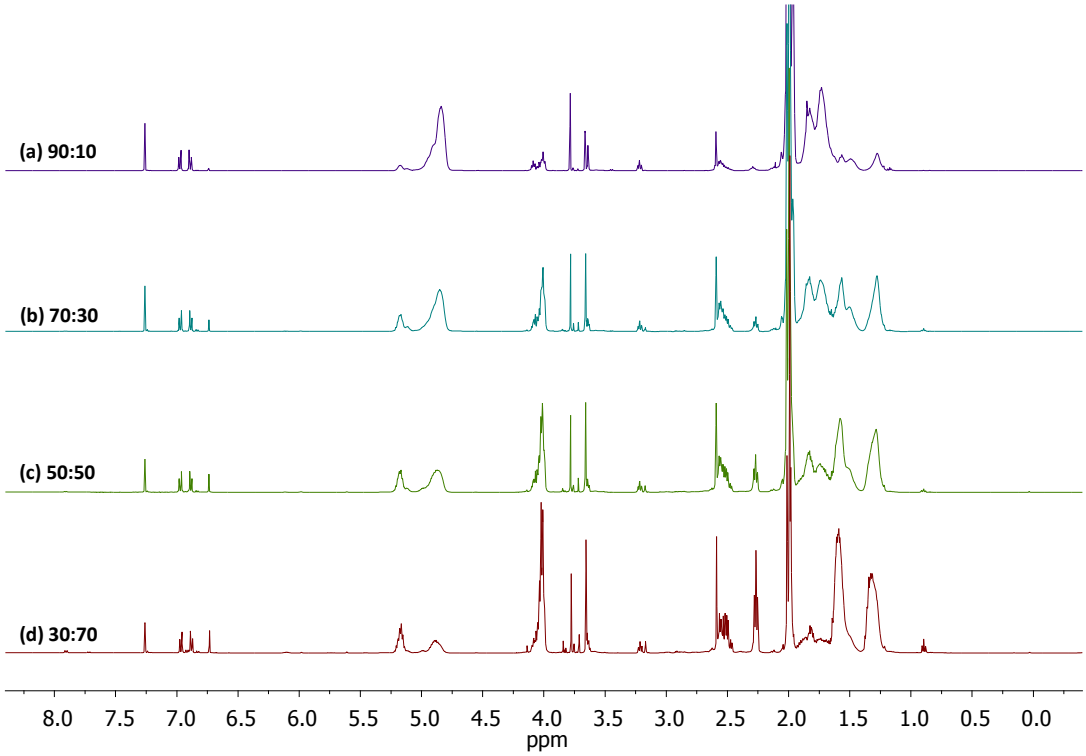

Figure 4.5. ^{1}H NMR spectra comparison of all the poly(MDO-*co*-VAc) copolymers obtained using CTA 4 as the chain transfer agent starting with different monomer feeds (a) 90:10, (b) 70:30, (c) 50:50 and (d) 30:70, VAc:MDO, (400 MHz, $CDCl_3$).

This signal was hypothesized to appear as a consequence of the proposed Z group fragmentation which would lead to the formation of a *p*-methoxyphenyl radical that could reinitiate or terminate the polymer chains. As previously discussed in Chapter 2 for the same system, where the copolymerization of MDO and VAc was performed using CTA 1 as the chain transfer agent and AIBN as the radical initiator, peaks at $\delta = 0.90$ and 3.65 ppm were observed which were shown to be characteristic of the 1,4- and 1,7-hydrogen side reactions occurring for the rROP of MDO, thus leading to branching abstraction of the polymer.[21,22] While there was no evidence of the methine proton, expected at $\delta = 3.00$ ppm, corresponding to the VAc adjacent to the xanthate chain-end, however there was a peak at $\delta = 3.2$ ppm that is consistent with the CH_2

resonance from MDO adjacent to a xanthate. This observation would suggest that all dormant polymer chains have the xanthate attached to a terminal MDO unit, not to a VAc unit, which would be a result of the slow fragmentation rate from the MDO alkyl chain to form a reactive radical species and is in agreement with the observations by Dommanget *et al*. in the RAFT/MADIX-mediated copolymerization of ethylene. [23,24]

Furthermore, ^{13}C NMR spectroscopy analysis was performed to confirm the retention of the xanthate chain-ends *via* their characteristic signals observed at δ = 114, 123, 148, and 158 ppm for the aromatic group protons, as well as at δ = 56 ppm for the methoxy end-group. As discussed in Chapters 2 and 3, the ring retention side reactions which can often occur during the rROP of MDO, [25,26] were assessed on this new copolymerization by ^{13}C NMR spectroscopy analysis. However, no acetal peak, expected at δ = 100 ppm (Figure 4.6), could be observed confirming that no ring-retained MDO was contained in the copolymer backbone (similarly to the results obtained in Chapter 2).

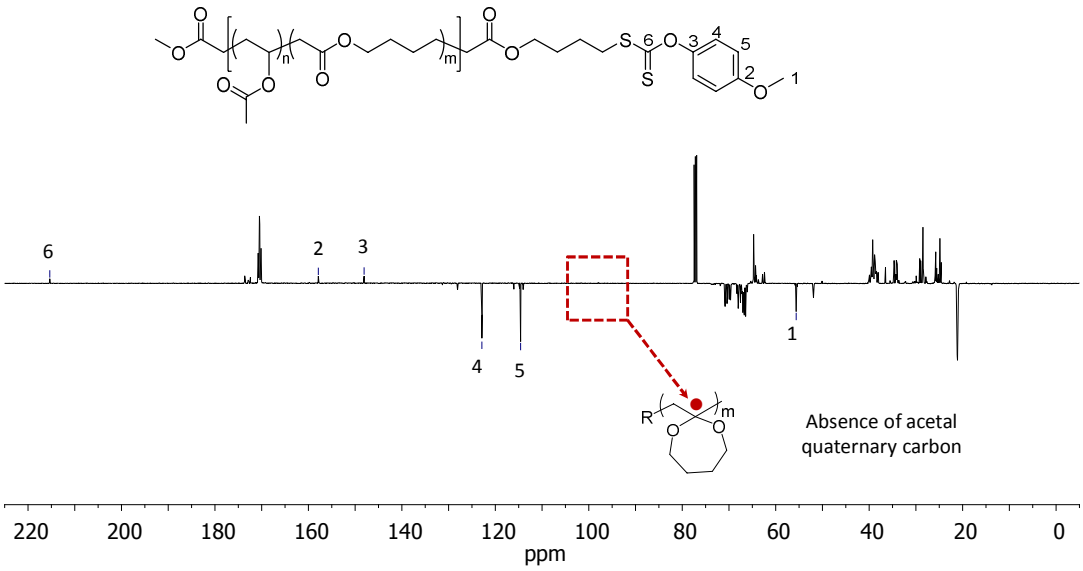

Figure 4.6. ^{13}C NMR spectrum of poly(MDO-*co*-VAc) synthesized by RAFT/MADIX polymerization using CTA 4 as the chain transfer agent, (125 MHz, $CDCl_3$). The highlighted area shows the region where the acetal signal would appear, if there had been ring-retention during the rROP of MDO.

While the copolymerization of MDO and VAc using CTA 4 as the chain transfer agent was found to still show some sign of termination reactions, the results obtained by SEC analysis and ^{1}H NMR spectroscopy also suggested an improvement in the control of the reaction. Indeed, lower dispersity values, $Đ_M$ = 1.38 - 1.43, were achieved for copolymerization with higher MDO content and higher monomer conversions reached when compared with the previous results obtained in Chapter 2 ($Đ_M$ = 1.52 - 1.55) where CTA 1, *O*-hexyl-*S*-methyl 2-propionylxanthate was used on the same system, suggesting an improvement of the control of the polymerization

4.3.3 Homopolymerization of MDO using CTA 4 as the chain transfer agent

Following on from the improved copolymerization of MDO and VAc using *p*-methoxyphenyl xanthate as the chain transfer agent, the homopolymerization of MDO was also instigated using CTA 4 and ABCN in order to assess the suitability of this chain transfer agent and the initiator to control the RAFT polymerization of MDO (Scheme 4.5).

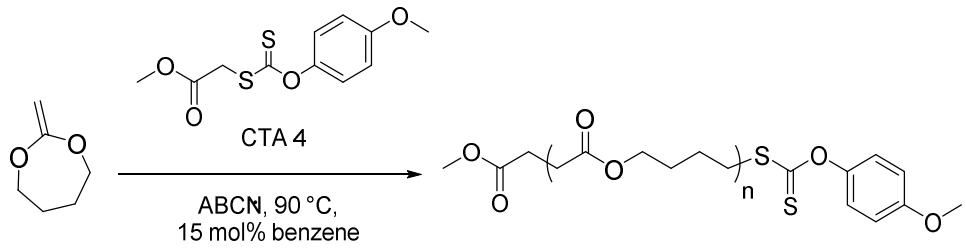

Scheme 4.5. Schematic representation of the homopolymerization of MDO using RAFT/MADIX polymerization with CTA 4 as the chain transfer agent.

The polymerization reactions were carried out employing the same optimized conditions used for the copolymerization of MDO and VAc (see paragraph 4.3.2), such that $[MDO]_0/[ABCN]_0/[CTA\ 4]_0$ = 100:0.1:1 in the presence of benzene (15 wt%) for 16, 24, and 48 h at 90 °C. Unsurprisingly, ^{1}H NMR spectroscopy revealed

an increase in MDO monomer conversion, namely 5%, 16%, and 28%, as the polymerization reaction time increased (Table 4.2).

Table 4.2. Characterization data for the RAFT/MADIX homopolymerization of MDO using CTA 4 as the chain transfer agent, at different reaction times.

Time (h)	MDO conv.[a] (%)	$M_n^{SEC\ b}$ (kg/mol)	$M_n^{theo\ c}$ (kg/mol)	$M_n^{obs\ d}$ (kg/mol)	$Đ_M$ [b]
16	5	1.7	0.9	1.4	1.19
24	16	2.5	1.8	2.7	1.30
48	28	3.4	3.2	4.0	1.39

[a] determined by ^{1}H NMR spectroscopy, [b] obtained by SEC analysis in $CHCl_3$, [c] theoretical molecular weight based on monomer conversion, [d] observed molecular weight obtained by ^{1}H NMR spectroscopy end-group analysis.

Further analysis using ^{1}H NMR spectroscopy on the final polymer confirmed the presence of the xanthate chain-end as seen by the characteristic signals at δ = 6.90 - 7.00 ppm and 3.75 ppm corresponding to the phenyl and methoxy groups, respectively (Figure 4.7).

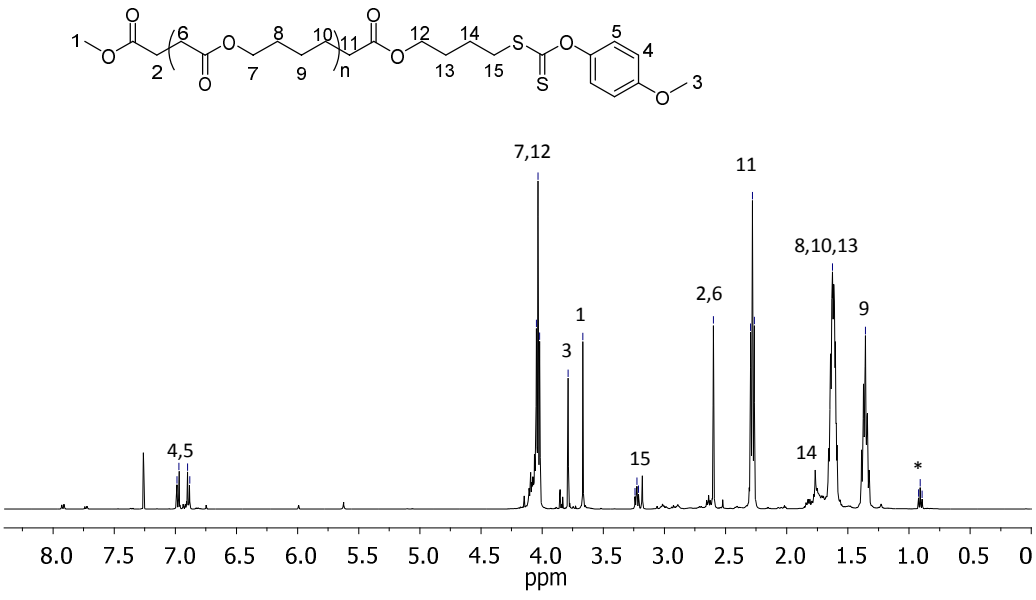

Figure 4.7. ^{1}H NMR spectrum of poly(MDO) obtained *via* RAFT/MADIX polymerization using CTA 4 as the chain transfer agent, (400 MHz, $CDCl_3$), * indicates signals derived from the 1,4- and 1,7-hydrogen side-reactions.

The observed molecular weights, M_n^{obs}, of poly(MDO) were found to be close to the molecular weights obtained by SEC, M_n^{SEC}, as in the case of the copolymer. However, some termination reactions were also observed as suggested by the higher M_n^{obs} values compared to the M_n^{theo} values. Further analysis using SEC showed the monomodal molecular weight distribution which was found to broaden as the reaction time increased from 16 to 48 h (Figure 4.8). The dispersities, $Đ_M$, of the homopolymers were found to be relatively low with values between 1.19 and 1.39 suggesting the controlled nature of the process (Table 4.2).

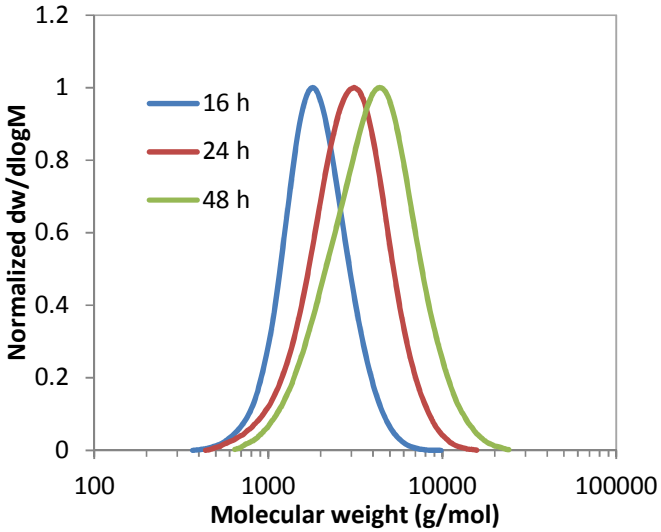

Figure 4.8. Size exclusion chromatograms of poly(MDO) obtained by RAFT/MADIX polymerization using CTA 4 for different reaction times of 16, 24 and 48 h, (SEC, $CHCl_3$).

Additionally, analysis of the poly(MDO) sample obtained after 24 h revealed good correlation between the SEC RI and UV traces (λ = 280 nm) suggesting the retention of the phenyl group of the xanthate chain-end across the whole distribution (Figure 4.9). However, similar to the copolymer with a higher amount of MDO (Figure 4.3d), a small shift of the UV trace to higher molecular weights was observed, indicating the presence of "dead" polymer chains that do not have the xanthate chain-end group and therefore suggesting a certain degree of loss of control.

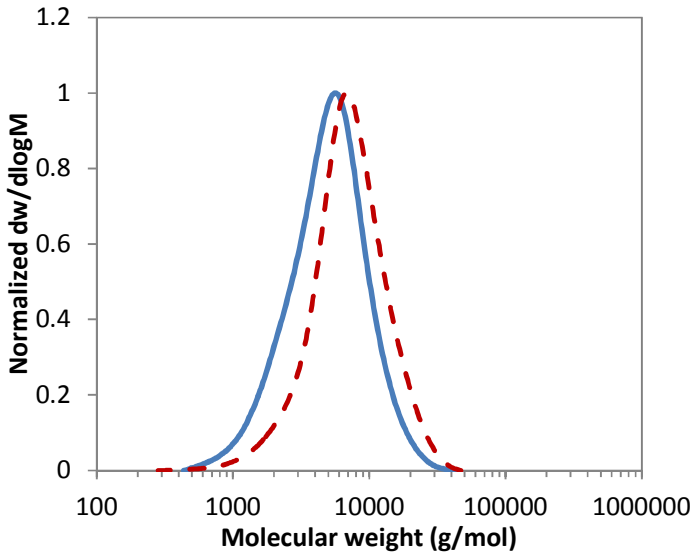

Figure 4.9. Size exclusion chromatogram of the homopolymer, poly(MDO), obtained after 24 h of RAFT/MADIX polymerization using CTA 4 as the chain transfer agent, (SEC, $CDCl_3$), dashed lines indicate molecular weight distribution from the UV detection at λ = 280 nm.

The results obtained by SEC analysis and ^{1}H NMR spectroscopy on the homopolymer samples of poly(MDO) synthesized using the RAFT/MADIX technique highligted many characteristics of a polymerization controlled with low dispersities values and defined molecular weights obtained. Nevertheless, when higher monomers conversion were targeted (typically above 20%) the occurrence of termination reactions was found to occur and hence limited the control nature of the process suggesting that mediated the polymerization of MDO was also remaining challenging when using the RAFT/MADIX polymerization approach.

4.3.4 Chain extension attempts

As previously shown for the copolymerizations in Chapters 2 and 3, the chain extension of the homopolymer, poly(MDO), was performed in an attempt to assess the controlled nature of the process. In an initial experiment, the extension of poly(MDO) with VAc was attempted, where the homopolymer obtained after 24 h, was dissolved in benzene (40 wt%) followed by the addition of VAc and ABCN prior

to being degassed by three freeze-pump-thaw cycles. The amount of benzene for the polymerization was increased in comparison with the amount previously used in order to fully solubilize the homopolymer. The chain extension polymerization was then conducted at 90 °C for 5 h. Unfortunately, this chain extension was found to be unsuccessful as seen by the bimodal SEC trace of the isolated polymer. The two molecular weight distributions observed were attributed to two homopolymers, poly(MDO) and poly(VAc), with the latter forming during the polymerization reaction (Figure 4.10). This result suggests that despite having some retention of the xanthate chain-ends on the homopolymer, poly(MDO), the chain extension from the precipitated poly(MDO) could not be accessed to form block polymers as a consequence of the low fragmentation of the MDO repeat unit adjacent to the xanthate which tends to disfavoured the addition of another monomer to the growing chain and instead terminate the polymer chains.

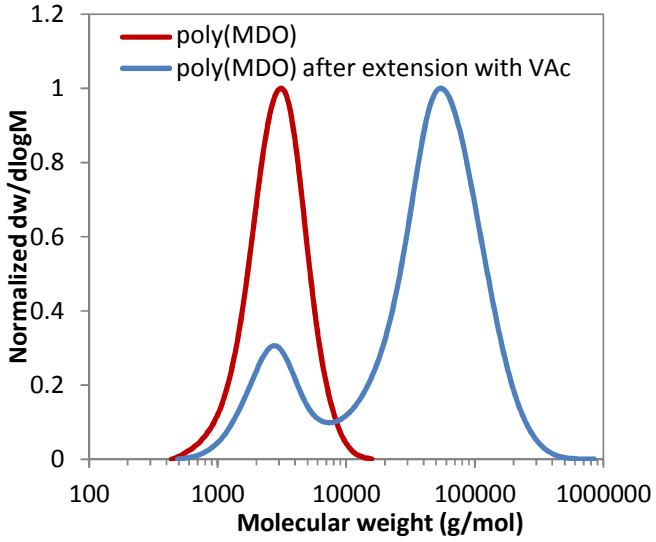

Figure 4.10. Size exclusion chromatograms of the attempted chain extension of poly(MDO) with VAc (SEC, $CHCl_3$).

Following on from these results, further experiments where the chain extension was performed on the non-precipitated poly(MDO) were carried out. In the first step, the

homopolymerization of MDO was performed using the same conditions as before for 24 h, before quenching by placing the reaction vessel in an ice bath. An aliquot of the polymerization mixture was taken for ^{1}H NMR spectroscopy and SEC analyses. In a second step, VAc and ABCN dissolved in benzene (40 wt%) were added to the polymerization mixture which was then degassed by three freeze-pump thaw cycles. The polymerization was allowed to proceed for a further 4 h at 90 °C. The final polymer was precipitated and was analysed by both ^{1}H NMR spectroscopy and SEC analyses. Under these conditions, the chain extension of poly(MDO) with VAc was found to be more successful, as seen by the shift of the molecular weight distribution to higher molecular weights (Figure 4.11), as well as by the appearance of signals at δ = 5.25 - 4.80 ppm on the ^{1}H NMR spectrum corresponding to the VAc being incorporated in the block copolymer, as previously observed in the ^{1}H NMR spectra of the copolymers (Figures 4.4 and 4.5).

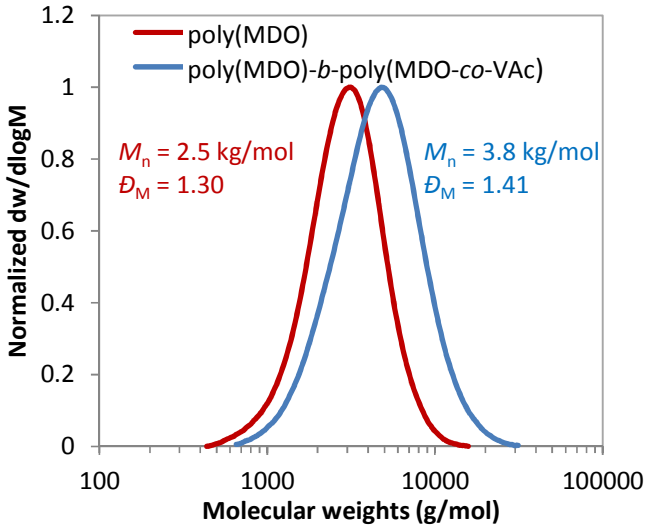

Figure 4.11. Size exclusion chromatograms of poly(MDO) before and after chain extension with VAc, without precipitation of the initial first block, to form poly(MDO)-*b*-poly(MDO-*co*-VAc), (SEC, $CHCl_3$).

However, as the extension was done on the non-precipitated poly(MDO) the final block copolymer obtained was poly(MDO)-*b*-poly(MDO-*co*-VAc) as the mixture contained both

unreacted MDO and VAc monomers, both available for polymerization. This experiment therefore suggests that despite of the termination reactions occurring at the early stages of the homopolymerization of MDO, the retention of the xanthate on some polymer chains makes chain growth possible and hence confirms the initial controlled nature of the polymerization of MDO using RAFT/MADIX.

4.3.5 Homopolymerization of MDO: comparison with other CTAs

Aiming at investigating the hypothesis that the suppression of fragmentation of the xanthate radical intermediate *via* the Z group can be achieved by using a phenyl Z group, three other xanthates were tested on the homopolymerization of MDO (Figure 4.12). These CTAs were previously introduced in Chapter 2 for the initial investigations in copolymerizing MDO and VAc.

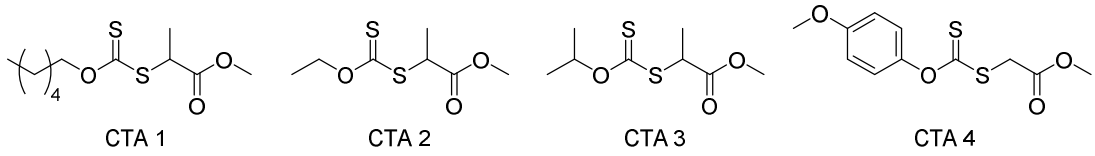

Figure 4.12. Schematic representation of the chemical structures of the different CTAs used for the homopolymerization of MDO.

The use of CTA 1, *O*-hexyl-*S*-methyl 2-propionylxanthate, and CTA 2, *O*-ethyl-*S*-methyl 2-propionyl xanthate, were used primarily as a control based on their previous results in mediating the copolymerization of MDO and VAc,[7] or the homopolymerization of VAc, respectively.[27,28] On the other hand, the use of CTA 3, *O*-isopropyl-*S*-methyl 2-propionyl xanthate, was investigated as the presence of the isopropyl Z group should increase the Z group fragmentation process as it is expected to form a more stable secondary alkyl radical. Homopolymerizations of MDO mediated with CTAs 1 to 4 were carried out such that $[MDO]_0/[ABCN]_0/[CTA]_0$ = 50:0.1:1 for 24 h at 60 °C, with the exception of CTA 4 which was reacted at 90 °C as

very low conversion was observed at 60 °C after 4 h of polymerization (Table 4.3) as a consequence of the low fragmentation rate of the xanthate from the dormant polymer chain.

Table 4.3. Characterization data for the homopolymerization of MDO using CTAs 1, 2, 3, and 4 as the chain transfer agents.

CTA	MDO conv.[a] (%)	M_n^{SEC} [b] (kg/mol)	M_n^{theo} [c] (kg/mol)	M_n^{obs} [d] (kg/mol)	$Đ_M$ [b]
1	20	4.2	1.4	1.7	1.55
2	22	2.8	1.5	6.0	1.58
3	21	5.2	1.4	9.5	1.90
4	2	-	0.4	-	-
4*	17	2.8	1.1	1.7	1.44

[a] determined by ^{1}H NMR spectroscopy, [b] obtained by SEC analysis in $CHCl_3$, [c] theoretical molecular weight based on monomer conversion, [d] observed molecular weight obtained by ^{1}H NMR spectroscopy end-group analysis, * homopolymerization conducted at 90 °C.

^{1}H NMR spectroscopy analyses revealed monomer conversions between 17 and 22% for all four xanthates (Table 4.3). The number-average molecular weights obtained by SEC analysis, M_n^{SEC}, were found to vary from 2.8 to 5.2 kg/mol for similar MDO monomer conversions. The final dispersities of the homopolymers were found to be similar when CTA 1, 2, and 4 were used ($Đ_M \approx 1.44$ - 1.58), however in the case of CTA 3 a much higher value of 1.90 was observed suggesting poorer control of the homopolymerization when this CTA was used. This observation could be explained by the fact that despite producing a slightly more stable radical and having similar electron donating effect when compared to the hexyl and ethyl radicals, the steric hindrance of the iso-propyl radical could also have an effect on the addition fragmentation equilibrium and therefore have a larger inhibition rate leading to further termination side reactions and a broadening of the dipsersity.[18] Additionally, as previously observed when the polymerization of MDO was carried out for 16, 24 and 48 h, using CTA 4 and carried out at 90 °C, the polymerization was leading to lower dispersity, $Đ_M = 1.44$, suggesting that a better control of the process was performed.

These results highlighted the fact that changing the nature of the xanthate Z group from less electron donating (CTA 1, 2 and 3) to more electron donating (CTA 4) was leading to different degree of control with the latest showing the most promising results in controlling the polymerization of MDO using the RAFT/MADIX technique.

4.3.6 Confirmation of Z group fragmentation

As mentioned in section 4.2, Dommanget and co-workers attributed the loss of control of the RAFT/MADIX polymerization of ethylene to the Z group fragmentation occurring as a consequence of the poor stability of the Z group radical and the unstable polyethylenyl radical, as confirmed by the presence of carbonodithioate moieties in their polyethylene.[17] Aiming at investigating this phenomenon in the case of the RAFT/MADIX polymerization of MDO, an in-depth investigation of the poly(MDO) obtained from the four different CTAs was carried out using ^{13}C NMR spectroscopy analysis. Initially, the analyses confirmed the retention of the xanthate chain-end on the polymers when CTAs 1, 2, and 4 were used, as seen by the presence of signals at δ = 214 ppm corresponding to the carbonyl group of the respective xanthate chain-ends (red dot, Figure 4.13). However it should be noted that in the case of CTA 3, this signal was not observed which suggests that under the conditions employed the polymer synthesised did not contain the xanthate end-group, thus confirming the formation of "dead" chains, and therefore resulting in the poorly controlled polymerization, as previously mentioned.

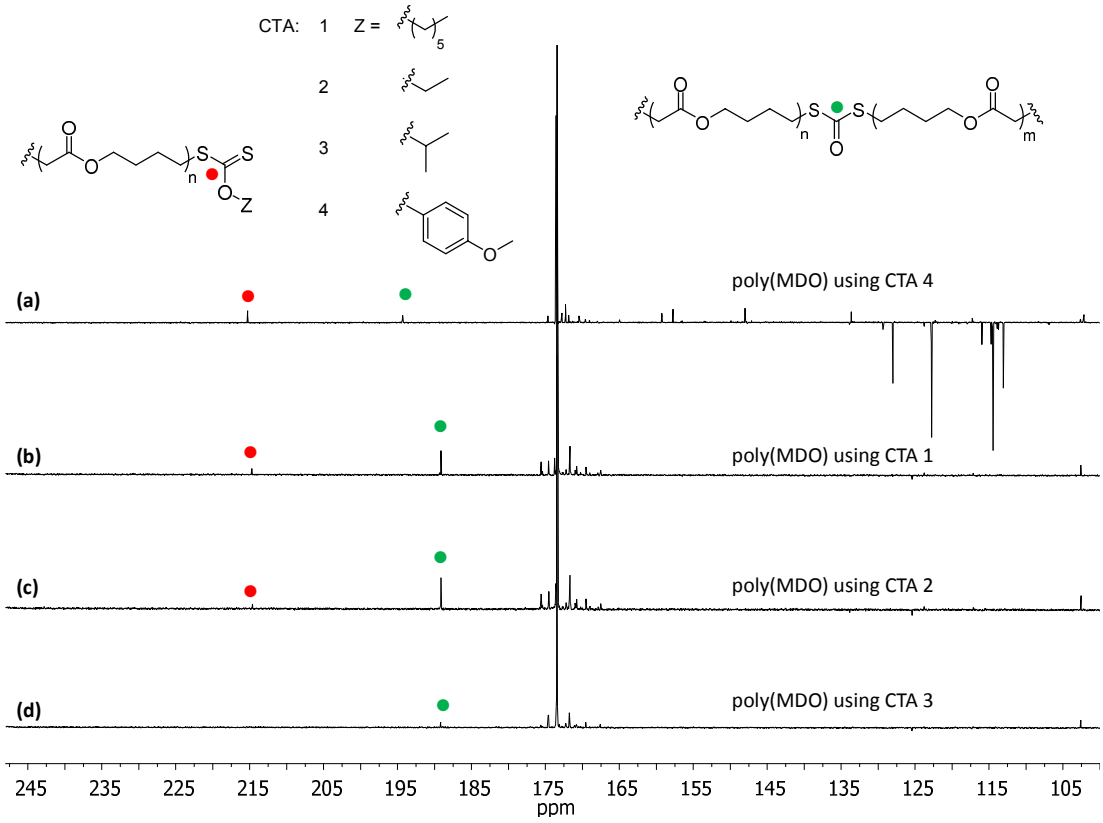

Figure 4.13. ^{13}C NMR spectra of poly(MDO) obtained by RAFT/MADIX polymerization using (a) CTA 4, (b) CTA 1, (c) CTA 2 and (d) CTA 3 as the chain transfer agents, (125 MHz, $CDCl_3$).

Further investigation of the spectra also revealed the presence of a resonance at δ = 189 – 195 ppm (green dot, Figure 4.13) which corresponds to the carbon of the carbonodithioate moities, as previously reported by Katritzky and co-workers, as well as Copeland and co-workers.[22,23] The presence of this carbonodithioate signal on all ^{13}C NMR spectra confirmed the original hypothesis that the Z group fragmentation indeed occurs during the RAFT/MADIX polymerization of MDO, as illustarted in Scheme 4.6. This fragmentation of the Z group and the subsequent formation of carbonodothioate functionalities led to termination of the polymer chains and loss of control, as observed by the broadening of the polymer distributions seen in Chapters 2 and 3.

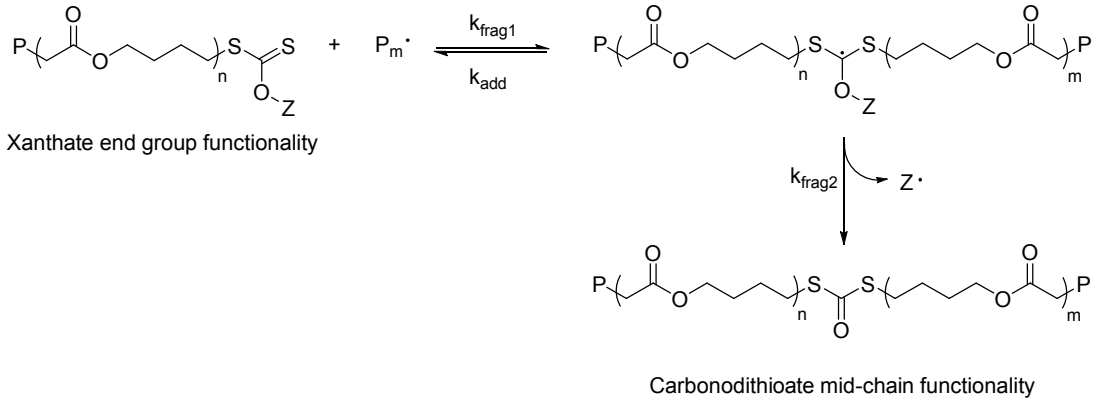

Scheme 4.6. Schematic rearrangement and Z group fragmentation occurring during the polymerization of MDO in the presence of xanthates, leading to the formation of carbonodithioate groups.

While a loss of control was observed for the polymerizations of MDO using CTA 1 – 4 as previously seen by the increase in molecular weight distributions (section 4.3.5), ^{13}C NMR spectroscopy analyses allowed the clear evidence of the carbonodithioate mid-chain functionality presence on the polymer backbone. The detection of this functional group on all ^{13}C NMR spectra confirmed the plausibility of the Z group fragmentation mechanism to also occur during the rROP of MDO while using the RAFT/MADIX polymerization technique.

4.4 Conclusions

In conclusion, the copolymerization of MDO and VAc with *p*-methoxyphenyl xanthate, CTA 4, was investigated in an attempt to improve the control of the RAFT/MADIX polymerization, previously observed in Chapters 2 and 3. The use of CTA 4 was found to lead to copolymers of poly(MDO-*co*-VAc) with significantly enhanced control over their molecular weight and dispersities as seen by the lower $Đ_M$ values, 1.38 - 1.43, obtained while higher conversions of monomers could be reached, compared to the other hexyl, ethyl and isopropyl xanthates previously discussed. The homopolymerization of MDO using CTA 4 was also found to show indications of

control based on the results obtained by ^{1}H NMR spectroscopy and SEC analysis where characteristic signals of the xanthate chain ends and monomodal traces were observed respectively. A comparison of all the CTAs on the homopolymerization of MDO was also performed in order to confirm that *p*-methoxyphenyl xanthate was the best candidate to mediate the rROP of MDO using RAFT/MADIX polymerization where higher conversion could be reached. Furthermore, in-depth characterization using ^{13}C NMR spectroscopy on all the homopolymers, poly(MDO), mediated with the different xanthates revealed the presence of carbonodithioate functionalities which suggested that the loss of control observed when higher content and conversions of MDO were targeted resulted from the Z group fragmentation occurring during the polymerization, similarly to the previous work reported by Dommanget and co-workers for a different monomer (ethylene). This work demonstrates the limitation to the fully control the synthesis of degradable vinyl polymers *via* the use of MDO and xanthates as chain transfer agents for the polymerization of such monomer using the RAFT/MADIX technique.

4.5 Experimental

4.5.1 Materials and methods

The following chemicals were used as received; alumina, activated basic (Al_2O_3: Sigma-Aldrich, Brockmann I, standard grade, ~ 150 mesh, 58 Å), carbon disulfide (CS_2: Fisher Scientific, AR grade), magnesium sulfate ($MgSO_4$: anhydrous, Fisher Scientific, LR grade), methyl bromoacetate (MBA: Sigma-Aldrich, 97%), silica gel (SiO_2: Apollo Scientific, 40-63 μm), sodium hydroxide (NaOH: Fisher Scientific, > 99%), sodium hydride (NaH: Sigma-Aldrich, 60 wt% dispersion in mineral oil), triethylamine (Et_3N: Fisher Scientific, > 99%). The following solvents were used as received; acetone (VWR International, AR grade), chloroform ($CHCl_3$: VWR

International, AR grade), d-chloroform ($CDCl_3$: Apollo, > 99%), benzene (C_6H_6, Sigma-Aldrich, > 99.7%), toluene ($CH_3C_6H_5$, Sigma-Aldrich > 99.7%), dichloromethane (CH_2Cl_2: VWR International, AR grade), hexane (Sigma-Aldrich, HPLC grade), ethyl acetate (EtOAc: Fisher Scientific, LR grade). 2,2′-Azobis(2-methylpropionitrile) (AIBN: Molekula) and 1,1′-azobis(cyclohexanecarbonitrile) (ABCN: Sigma-Aldrich, 98%) were recrystallized from acetone prior to use. Vinyl acetate (VAc: Sigma-Aldrich, ≥ 99%) was dried and vacuum distilled over CaH_2 to remove the inhibitor and residual water. 2-Methylene-1,3-dioxepane (MDO) was synthesized using the previously described method of Bailey *et al.*[29] then dried and vacuum distilled over CaH_2. *O*-Hexyl-*S*-methyl 2-propionylxanthate (CTA 1) was synthesized as described in Chapter 2. *O*-Ethyl-*S*-ethyl 2-propionylxanthate (CTA 2) was synthesized using the previously described method of Skey *et al.*[30]

4.5.2 Characterization methods

Nuclear magnetic resonance (^1H and ^{13}C NMR) spectra were recorded at 400 MHz and 125 MHz, respectively, in $CDCl_3$ on a Bruker DPX-400/500 spectrometer at 298 K. Chemical shifts are reported as δ in parts per million (ppm) and referenced to the chemical shift of the residual solvent resonances ($CDCl_3$ ^1H: δ = 7.26 ppm; ^{13}C: δ = 77.16 ppm). The resonance multiplicities are described as s (singlet), d (doublet), t (triplet), q (quartet) or m (multiplet). Size exclusion chromatography (SEC) analyses were performed on a system composed of a Varian 390-LC-Multi detector using a Varian Polymer Laboratories guard column (PLGel 5 μM, 50 × 7.5 mm), two mixed D Varian Polymer Laboratories columns (PLGel 5μM, 300 × 7.5 mm) and a PLAST RT autosampler. Detection was conducted using a differential refractive index (RI) and an ultraviolet (UV) detector set to 280 nm. The analyses were performed in $CHCl_3$ containing 0.5% w/w triethylamine (Et_3N) at a flow rate of 1.0 mL/min at 313

K. Polystyrene (PS) (162 - 2.4 × 10^5 g/mol) standards were used to calibrate the system. Molecular weights and dispersities were determined using Cirrus v2.2 SEC software.

4.5.3 Synthesis of *p*-methoxyphenyl xanthate (CTA 4)

This synthesis is a modified version of the procedure published by Stenzel *et al*.[18] To a 1,000 mL Schlenk flask under N_2 was added carbon disulfide (250 mL, 4.16 mol) and *p*-methoxyphenol (15.0 g, 0.12 mol) and stirred at 40 °C until fully dissolved. Triethylamine (17 mL, 0.12 mol) was added and the reaction was stirred for 24 h. Methyl bromoacetate (11.4 mL, 0.12 mol) was added dropwise and the reaction was allowed to stir at 40 °C for 24 h whereby a precipitate formed. The unreacted carbon disulfide was then removed by vacuum transfer to leave a yellowish residue. This was then dissolved in 100 mL EtOAc, filtered to remove the Et_3N/HBr salts, and then washed with H_2O (100 mL), 1M NaOH (100 mL), 1M HCl (100 mL), H_2O (100 mL), and finally brine (100 mL). The organic phase was dried over anhydrous magnesium sulfate, filtered, and taken to dryness *in vacuo*. Column chromatography (silica gel, 100% toluene) afforded the target compound as a pale yellow oil (9.9 g, 29.5%). R_f (toluene) 0.2; HRMS *m/z* Theory: 295.0069 ($M\text{-}Na^+$); Found: 295.0077; Elemental analysis: Calculated for $C_{11}H_{12}O_4S_2$: C, 48.51%; H, 4.44%; Found: C, 48.21%; H, 4.38%. ^{1}H NMR (400 MHz, $CDCl_3$, ppm): δ 6.90 - 7.10 (Ar, 4H, $^3J_{H\text{-}H}$ = 9.0 Hz), 4.04 (s, SCH_2(C=O)O, 2H), 3.81 (s, (C=O)OCH_3, 3H), 3.80 (s, Ar-OCH_3, 3H). ^{13}C NMR (125 MHz, $CDCl_3$, ppm): δ 213.1 (O*C*SSCH_2), 168.1 (*C*OOCH_3), 157.9 (CH_3O*C*-Ar), 148.1 (Ar-*C*OCS), 122.7 (Ar-*C*HCH), 114.5 (Ar-CH*C*H), 55.6 (*C*H_3O-Ar), 53.0 (COO*C*H_3), 38.7 (*C*H_2C$OOCH_3$). FTIR (ν_{max}, cm^{-1}): 2954-2835 (C-H alkyl stretch), 1739 (C=O stretch), 1596 (C=C aromatic), 1168 (C-O stretch), 1035 (C-S stretch).

4.5.4 General procedure for the synthesis of poly(MDO-*co*-VAc) using CTA 4

In an inert environment, VAc (1.55 g, 18 mmol), MDO (0.228 g, 2.0 mmol), CTA 4 (55.5 mg, 0.2 mmol), ABCN (4.9 mg, 2.0×10^{-2} mmol) and benzene (15 wt%) were placed into an ampoule and sealed. The solution was subjected to three freeze-pump-thaw cycles before backfilling with argon. The resulting solution was stirred and heated to 90 °C for 4 h before the polymerization was quenched by plunging the ampoule into an ice bath. An aliquot was taken prior to precipitation to determine conversion by ^{1}H NMR spectroscopy ($CDCl_3$ was pre-treated by passing through basic Al_2O_3 to remove any acids present). The polymer was then dissolved in $CHCl_3$ and precipitated several times into hexane until no further monomer residue was observed. The final light yellow solid was dried under vacuum at room temperature for 24 h. ^{1}H NMR (400 MHz, $CDCl_3$, ppm): δ 6.90 - 7.10 (dd, Ar end-group, 4H, $^3J_{H\text{-}H}$ = 9.0 Hz), 5.30 - 4.75 (m, CH_2CHOCO backbone, 1H), 4.15 - 3.95 (m, $CH_2COOCH_2CH_2$ backbone, 2H), 3.76 (m, Ar-OCH_3 end-group, 3H), 3.60 (s, CH_3OCOCH_2 end-group, 3H), 3.26 (m, CH_2SCSO end-group, 2H), 2.60 - 2.10 (m, CH_3OCOCH_2 end-group, 2H, $CH_2COOCH_2CH_2$ backbone, 2H), 2.05 - 1.95 (m, $OCOCH_3$ backbone, 3H, CH_2CHOCO backbone, 2H), 1.90 - 1.20 (m, $COOCH_2CH_2CH_2$ backbone, 2H, $COOCH_2CH_2CH_2CH_2$ backbone, 2H, $COOCH_2CH_2CH_2CH_2$ backbone, 2H). Conversion: VAc = 58%, MDO = 51%. M_n (^{1}H NMR, $CDCl_3$) = 8.2 kg/mol, M_n (SEC, $CHCl_3$) = 8.1 kg/mol, $Đ_M$ = 1.38.

4.5.5 General procedure for the synthesis of poly(MDO) using CTA 4

In an inert environment, MDO (2.28 g, 20 mmol), CTA 4 (55.5 mg, 0.2 mmol), ABCN (4.9 mg, 2.0×10^{-2} mmol) and benzene (15 wt%) were placed into an ampoule and sealed. The solution was subjected to three freeze-pump-thaw cycles and then backfilled with argon. The resulting solution was stirred and heated to 90 °C for 24 h

before the polymerization was quenched by plunging the ampoule into an ice bath. An aliquot was taken prior to precipitation to determine the conversion by ^{1}H NMR spectroscopy ($CDCl_3$ was pre-treated by passing through basic Al_2O_3 to remove any acids present). The polymer was then dissolved in $CHCl_3$ and precipitated several times into hexane until no further monomer residue was observed. The final light yellow solid was dried under vacuum at room temperature for 24 h. ^{1}H NMR (400 MHz, $CDCl_3$, ppm): δ 6.90 - 7.10 (dd, Ar end-group, 4H, $^{3}J_{H\text{-}H}$ = 9.1 Hz), 4.15 - 3.95 (m, $CH_2COOCH_2CH_2$ backbone, 2H), 3.76 (s, Ar-OCH_3 end-group, 3H), 3.60 (s, CH_3OCOCH_2 end-group, 3H), 3.26 (m, CH_2SCSO end-group, 2H), 2.65 - 2.50 (m, CH_3OCOCH_2 end-group, 2H, $CH_2COOCH_2CH_2$ backbone, 2H), 2.35 – 2.25 (m, $CH_2COOCH_2CH_2CH_2CH_2S$ backbone, 2H), 2.05 - 1.50 (m, $CH_2COOCH_2CH_2CH_2$ backbone, 2H, $CH_2COOCH_2CH_2CH_2CH_2$ backbone, 2H), 1.45 - 1.25 (m, $CH_2COOCH_2CH_2CH_2CH_2$ backbone, 2H), 0.90 (m, $CH_3CH_2CH_2$ from branches, 3H). Conversion: MDO = 16%. M_n (^{1}H NMR, $CDCl_3$) = 2.7 kg/mol, M_n (SEC, $CHCl_3$) = 2.5 kg/mol, $Đ_M$ = 1.30.

Use of the general procedure for the synthesis of poly(MDO) using CTA 1. ^{1}H NMR (400 MHz, $CDCl_3$, ppm): δ 4.58 (m, $SCOCH_2CH_2$ end-group, 2H), 4.15 - 3.95 (m, $CH_2COOCH_2CH_2$ backbone, 2H), 3.60 (s, CH_3OCOCH end-group, 3H), 3.25 - 2.90 (m, $CH_2SCSOCH_2$ end-group, 2H), 2.45 - 2.25 (m, $CH_2COOCH_2CH_2$ backbone, 2H), 1.80 - 1.50 (m, CH_2CH_2SCSO end-group, 2H, $CH_2COOCH2CH_2CH_2$ backbone, 2H, $CH_2COOCH_2CH_2CH_2CH_2$ backbone, 2H), 1.50 - 1.10 (m, $CH_2COOCH_2CH_2CH_2CH_2$ backbone, 2H, $CH_3OCOCHCH_3$ end-group, 3H, $SCSOCH_2(CH_2)_4CH_3$ end-group, 2H), 0.90 (m, $CH_3CH_2CH_2$ from branches, 3H, $SCSOCH_2(CH_2)_4CH_3$ end-group, 3H). Conversion: MDO = 20%. M_n (^{1}H NMR, $CDCl_3$) = 1.7 kg/mol, M_n (SEC, $CHCl_3$) = 4.2 kg/mol, $Đ_M$ = 1.55.

Use of the general procedure for the synthesis of poly(MDO) using CTA 2. ^{1}H NMR (400 MHz, $CDCl_3$, ppm): δ 4.58 (m, SCOCH_2CH$_3$ end-group, 2H), 4.15 - 3.95 (m, $CH_2COOCH_2CH_2$ backbone, 2H), 3.60 (s, CH_3OCOCH end-group, 3H), 3.25 - 2.90 (m, CH_2SCSOCH$_2$ end-group, 2H), 2.45 - 2.25 (m, CH_2COOCH$_2$CH$_2$ backbone, 2H), 1.80 - 1.50 (m, CH_2CH$_2$SCSO end-group, 2H, CH$_2$COOCH2CH_2CH$_2$ backbone, 2H, $CH_2COOCH_2CH_2CH_2CH_2$ backbone, 2H), 1.50 - 1.10 (m, CH$_2$COOCH$_2$CH$_2$CH_2CH$_2$ backbone, 2H, CH$_3$OCOCHCH_3 end-group, 3H), 0.90 (t, CH_3CH$_2$CH$_2$ from branches, 3H, SCSOCH$_2$CH_3 end-group, 3H). Conversion: MDO = 22%. M_n (^{1}H NMR, $CDCl_3$) = 6.0 kg/mol, M_n (SEC, $CHCl_3$) = 2.8 kg/mol, $Đ_M$ = 1.58.

Use of the general procedure for the synthesis of poly(MDO) using CTA 3. ^{1}H NMR (400 MHz, $CDCl_3$, ppm): δ 4.60 (m, SCOCH(CH$_3$)$_2$ end-group, 1H), 4.15 - 3.95 (m, $CH_2COOCH_2CH_2$ backbone, 2H), 3.60 (s, CH_3OCOCH end-group, 3H), 3.25 - 2.90 (m, CH_2SCSOCH$_2$ end-group, 2H), 2.45 - 2.25 (m, CH_2COOCH$_2$CH$_2$ backbone, 2H), 2.35 - 1.50 (m, CH_2CH$_2$SCSO end-group, 2H, CH$_2$COOCH2CH_2CH$_2$ backbone, 2H, $CH_2COOCH_2CH_2CH_2CH_2$ backbone, 2H), 1.50 - 1.10 (m, CH$_2$COOCH$_2$CH$_2$CH_2CH$_2$ backbone, 2H, CH$_3$OCOCHCH_3 end-group, 3H, SCOCH(CH$_3$)$_2$ end-group, 6H), 0.90 (m, CH_3CH$_2$CH$_2$ from branches, 3H). Conversion: MDO = 21%. M_n (^{1}H NMR, $CDCl_3$) = 9.5 kg/mol, M_n (SEC, $CHCl_3$) = 5.2 kg/mol, $Đ_M$ = 1.90.

4.5.6 Typical procedure for the chain extension of poly(MDO) with VAc

In a first step, poly(MDO) was synthesized according to the procedure described above and an aliquot was taken from the polymerization mixture for ^{1}H NMR spectroscopy and SEC analyses. M_n (^{1}H NMR, $CDCl_3$) = 2.7 kg/mol, M_n (SEC, $CHCl_3$) = 2.5 kg/mol, $Đ_M$ = 1.30. The non-precipitated poly(MDO) was left in the ampoule and VAc (0.10 g, 1.16 mmol), ABCN (0.20 mg, 1.75×10^{-6} mmol) and benzene (40 wt%) were added to the polymerization mixture. The ampoule was degassed by three freeze-pump-thaw cycles and the polymerization was carried out at 90 °C for 5 h to afford the diblock poly(MDO)-*b*-

poly(MDO-*co*-VAc). The polymer was purified by precipitations into hexane and dried *in vacuo*. ^{1}H NMR (400 MHz, $CDCl_3$, ppm): δ 6.90 - 7.10 (dd, Ar end-group, 4H, $^{3}J_{H\text{-}H}$ = 9.0 Hz), 5.30 - 4.75 (m, CH_2CHOCO backbone, 1H), 4.15 - 3.95 (m, $CH_2COOCH_2CH_2$ backbone, 2H), 3.76 (s, Ar-OCH_3 end-group, 3H), 3.60 (s, CH_3OCOCH_2 end-group, 3H), 3.26 (m, CH_2SCSO end-group, 2H), 2.60 - 2.10 (m, CH_3OCOCH_2 end-group, 2H, $CH_2COOCH_2CH_2$ backbone, 2H), 2.05 - 1.95 (m, $OCOCH_3$ backbone, 3H, CH_2CHOCO backbone, 2H), 1.90 - 1.20 (m, $COOCH_2CH_2CH_2$ backbone, 2H, $COOCH_2CH_2CH_2CH_2$ backbone, 2H, $COOCH_2CH_2CH_2CH_2$ backbone, 2H). Conversion: VAc = 10%. M_n (^{1}H NMR, $CDCl_3$) = 3.7 kg/mol, M_n (SEC, $CHCl_3$) = 3.8 kg/mol, $Đ_M$ = 1.41.

4.6 References

(1) Undin, J.; Finne-Wistrand, A.; Albertsson, A.-C. *Biomacromolecules* **2013**, *14*, 2095.

(2) Agarwal, S. *Polym. J.* **2006**, *39*, 163.

(3) Agarwal, S.; Kumar, R.; Kissel, T.; Reul, R. *Polym. J.* **2009**, *41*, 650.

(4) Sun, L. F.; Zhuo, R. X.; Liu, Z. L. *J. Polym. Sci., Part A: Polym. Chem.* **2003**, *41*, 2898.

(5) Kobben, S.; Ethirajan, A.; Junkers, T. *J. Polym. Sci., Part A: Polym. Chem.* **2014**, *52*, 1633.

(6) Hedir, G. G.; Bell, C. A.; O'Reilly, R. K.; Dove, A. P. *Biomacromolecules* **2015**, *16*, 2049.

(7) Hedir, G. G.; Bell, C. A.; Ieong, N. S.; Chapman, E.; Collins, I. R.; O'Reilly, R. K.; Dove, A. P. *Macromolecules* **2014**, *47*, 2847.

(8) Delplace, V.; Harrisson, S.; Tardy, A.; Gigmes, D.; Guillaneuf, Y.; Nicolas, J. *Macromol. Rapid Commun.* **2014**, *35*, 484.

(9) Tardy, A.; Delplace, V.; Siri, D.; Lefay, C.; Harrisson, S.; de Fatima Albergaria Pereira, B.; Charles, L.; Gigmes, D.; Nicolas, J.; Guillaneuf, Y. *Polym. Chem.* **2013**, *4*, 4776.

(10) Delplace, V.; Tardy, A.; Harrisson, S.; Mura, S.; Gigmes, D.; Guillaneuf, Y.; Nicolas, J. *Biomacromolecules* **2013**, *14*, 3769.

(11) Wei, Y.; Connors, E. J.; Jia, X.; Wang, C. *J. Polym. Sci., Part A: Polym. Chem.* **1998**, *36*, 761.

(12) Wei, Y.; Connors, E. J.; Jia, X.; Wang, B. *Chem. Mater.* **1996**, *8*, 604.

(13) Chiefari, J.; Mayadunne, R. T. A.; Moad, C. L.; Moad, G.; Rizzardo, E.; Postma, A.; Thang, S. H. *Macromolecules* **2003**, *36*, 2273.

(14) Keddie, D. J.; Moad, G.; Rizzardo, E.; Thang, S. H. *Macromolecules* **2012**, *45*, 5321.

(15) Nakabayashi, K.; Mori, H. *Eur. Polym. J.* **2013**, *49*, 2808.

(16) Harrisson, S.; Liu, X.; Ollagnier, J.-N.; Coutelier, O.; Marty, J.-D.; Destarac, M. *Polymers* **2014**, *6*, 1437.

(17) Dommanget, C.; D'Agosto, F.; Monteil, V. *Angew. Chem. Int. Ed.* **2014**, *53*, 6683.

(18) Stenzel, M. H.; Cummins, L.; Roberts, G. E.; Davis, T. P.; Vana, P.; Barner-Kowollik, C. *Macromol. Chem. Phys.* **2003**, *204*, 1160.

(19) Teertstra, S. J.; Chen, E.; Chan-Seng, D.; Otieno, P. O.; Hicks, R. G.; Georges, M. K. *Macromol. Symp.* **2007**, *248*, 117.

(20) d'Ayala, G. G.; Malinconico, M.; Laurienzo, P.; Tardy, A.; Guillaneuf, Y.; Lansalot, M.; D'Agosto, F.; Charleux, B. *J. Polym. Sci., Part A: Polym. Chem.* **2014**, *52*, 104.

(21) Jin, S.; Gonsalves, K. E. *Macromolecules* **1997**, *30*, 3104.

(22) Agarwal, S. *Polym. Chem.* **2010**, *1*, 953.

(23) Dommanget, C.; D'Agosto, F.; Monteil, V. *Angew. Chem.* **2014**, *53*, 6683.

(24) Rizzardo, E.; Moad, G.; Thang, S. *Handbook of RAFT Polymerization*; Wiley-VCH, 2008.

(25) Maji, S.; Zheng, M.; Agarwal, S. *Macromol. Chem. Phys.* **2011**, *212*, 2573.

(26) Grabe, N.; Zhang, Y.; Agarwal, S. *Macromol. Chem. Phys.* **2011**, *212*, 1327.

(27) Brown, S. L.; Perrier, S.; Rayner, C. M.; Cooper, A.; Graham, S.; Rannard, S. *Chem. Commun.* **2007**, 2145.

(28) Barner-Kowollik, C.; Davis, T. P.; Stenzel, M. H. *Chem. Commun.* **2004**, 1546.

(29) Bailey, W. J.; Ni, Z.; Wu, S.-R. *J. Polym. Sci., Part A: Polym. Chem.* **1982**, *20*, 3021.

(30) Skey, J.; O'Reilly, R. K. *Chem. Commun.* **2008**, 4183.

5 Degradable copolymers with tuneable thermoresponsive properties by copolymerization of MDO and novel oligo (ethylene glycol) methyl ether vinyl acetate derived monomers

5.1 Abstract

In this Chapter, the synthesis of a new oligo (ethylene glycol) vinyl acetate derived monomer, di(ethylene glycol) methyl ether vinyl acetate (MeO_2VAc), is reported through the reaction between 2-[2-(2-methoxyethoxy)ethoxy] acetic acid and vinyl acetate (VAc) using the palladium-catalyzed vinyl exchange reaction previously introduced in Chapter 3. The homopolymerization of MeO_2VAc using the RAFT/MADIX polymerization technique leads to the formation of novel water-soluble polymers with defined dispersities and controlled molecular weights. Furthermore, the copolymerization of MeO_2VAc with 2-methylene-1,3-dioxepane (MDO) is also reported producing a range of novel functional, degradable and water-soluble copolymers of poly(MDO-*co*-MeO_2VAc). The copolymer composition was able to be tuned to vary the amount of ester repeat units in the polymer backbone and hence change the degradable properties of the polymer, while maintaining a good control of the final copolymers' molecular weights. The incorporation of different amounts of MeO_2VAc repeat units in the copolymer backbone was also found to significantly influence the solubility behavior of the copolymers as revealed by the different thermoresponsive properties achieved. Indeed, polymers with a lower critical solution temperature (LCST) were obtained with tunable values of between 4 °C and 80 °C achieved by varying the final copolymer composition. The concept was also applied to two other monomers, ethylene glycol methyl ether vinyl acetate (MeOVAc) and tri(ethylene glycol) methyl ether vinyl acetate (MeO_3VAc), containing a shorter and longer oligo (ethylene glycol) unit (1 and 3 respectively) which were also able to form degradable copolymers with similar tunable thermoresponsive properties.

5.2 Introduction

In the last decade "smart" polymers containing thermoresponsive properties have been widely investigated as a consequence of their great potential in nanotechnology and biomedical applications.[1-6] These polymers display a phase transition behavior dependent on the temperature to which they are exposed; the phase transition observed can either be an upper critical solution temperature (UCST) or a lower critical solution temperature (LCST).[3,7] The use of water-soluble polymers exhibiting an LCST in aqueous media has been seen as a promising tool in the biomedical field where they can be used as smart bioactive surfaces, for selective bioseparation, drug delivery and as a tissue engineering scaffold.[8-10] Below the LCST, the polymer chains will be soluble and adopt an extended coils confirmation whereas above the LCST the polymer chains become insoluble and will transition into a globular confirmation.[7,11] These transitions are commonly used to release drugs and/or small molecules when such polymers are used in nano-structures.[9,12,13] Among the most common LCST exhibiting thermoresponsive polymers, poly(*N*-isopropylacrylamide), poly(NIPAm), has attracted significant attention as a consequence of the close proximity of its LCST to body temperature (32 °C).[9,14-19] Although poly(NIPAm) has been widely applied and studied, the questionable toxicity of the *N*-isopropylacrylamide monomer, and subsequent polymer, has highlighted the need to find new non-toxic alternatives.[20] To this aim, Lutz and co-workers initially developed a range of biocompatible and thermoresponsive polymers based on the copolymerization of di(ethylene glycol) acrylate based monomers of 2-(2'-methoxyethoxy)ethyl methacrylate (MEO_2MA) and oligo(ethylene glycol) methacrylate (OEGMA) using atom transfer radical polymerization (ATRP) as the controlled polymerization technique.[21] In their studies, the composition of the copolymers could be successfully modified to target poly(MEO_2MA-*co*-OEGMA) samples with LCST properties close to body temperature when the copolymers contained 5% OEGMA in its polymer backbone. Many other studies followed this approach to use

different oligo(ethylene glycol) acrylate monomers including: 2-methoxyethoxy methacrylate (MEMA), tri(ethylene glycol) methyl ether methacrylate (MeO_3MA) and $(OEGMA)_n$ having different oligo(ethylene glycol) repeat units within the monomers, to create biocompatible copolymers with tunable thermoresponsive properties with LCST varying from 10 to 90 °C.[22-28] While all these studies were successful in the formation of copolymers with LCST properties, only a few reports were focused on the degradable properties of these polymers.[29] Indeed, while the main polymer backbone is composed of carbon-carbon bonds, the degradability of acrylate polymers can only proceed *via* the cleavage of the ester functionalities within the acrylate pendent groups.[30] To overcome this issue, Lutz *et al*. copolymerized MEO_2MA and OEGMA with 5,6-benzo-2-methylene-1,3-dioxepane (BMDO, **CKA 2**), a cyclic ketene acetal (CKA) able to introduce ester repeat units into the polymer backbone after radical ring-opening polymerization (rROP) of the CKA monomer.[29] The presence of the ester repeats units in the polymer backbone enabled the incorporation of carbon-oxygen bonds, which are able to be cleaved under hydrolytic or enzymatic degradation conditions. While the successful formation of degradable, LCST exhibiting polymers was confirmed, many later studies have highlighted that the copolymerization of CKA with acrylate or methylacrylate monomers failed to produce copolymers with efficient distribution of degradable density as a consequence of the great difference between the reactivity ratios of acrylates and CKA monomers.[31,32] Therefore, there is a need to design new copolymers that could contain both sufficient distribution of degradable density in the polymer backbone and contain interesting functional groups which can lead to the incorporation of thermoresponsive properties. In Chapters 2 and 3, the successful copolymerization of 2-methylene-1,3-dioxepane (MDO, **CKA 1**), the non-aromatic version of BMDO, with vinyl acetate (VAc) and vinyl bromobutanoate (VBr) was presented using the reversible addition-fragmentation chain transfer polymerization (RAFT) technique as a successful route towards the synthesis of well-defined and controlled

functional degradable copolymers of poly(MDO-*co*-VAc) and poly(MDO-*co*-VBr).[33,34] While the use of vinyl bromobutanoate as a new vinyl acetate derived monomer led to copolymers containing pendent bromine functional groups, the introduction of hydrophilic properties in the copolymers could only be achieved *via* post-polymerization modifications using azidation and "click" chemistry with a PEG functional alkyne to make the final copolymer hydrophilic.[34] Inspired by this result, the hypothesis that hydrophilic properties could directly be incorporated in the copolymer, through the use of a new vinyl acetate derived monomer containing oligo(ethylene glycol) groups, was postulated. The synthesis of such vinyl acetate derived monomers has recently been improved and optimized by Drockenmuller and co-workers who performed the reaction between vinyl acetate and corresponding acids in the presence of a palladium catalyst and successfully created new vinyl acetate derived monomers in good yield.[35,36] This approach was later used in other studies by other groups including Destarac and co-workers to create a new range of polymers where desired properties can be targeted by designing specific novel vinyl monomers.[34-37]

In this Chapter, the synthesis of a new type of oligo(ethylene glycol) monomer, di(ethylene glycol) methyl ether vinyl acetate (MeO_2VAc), a vinyl acetate derived form of MeO_2MA monomer is introduced. Its homopolymerization, along with its copolymerization with MDO, is shown to produce well-defined and functional degradable thermoresponsive copolymers *via* the RAFT/MADIX polymerization technique. Additionally, we demonstrate that both degradability and thermoresponsive properties can be tuned by varying the amount of MDO in the final copolymers to create degradable copolymers exhibiting a phase separation at different temperature varying from 4 °C to 80 °C. The reported approach opens up a new method to obtain thermoresponsive polymers showing good degradability and phase separation properties close to body temperature as well as potentially being biocompatible.

5.3 Results and Discussion

5.3.1 Synthesis of di(ethylene glycol) methyl ether vinyl acetate (MeO_2VAc)

Inspired by the results presented in Chapter 3 for the post-polymerization modifications of poly(MDO-*co*-VBr) using azidation and 1,3-dipolar cycloaddition with PEG(alkyne) to incorporate hydrophilicity, the idea of incorporating similar properties through a different approach was made. A hypothesis was made that a new monomer, which will introduce hydrophilic properties directly into the copolymer backbone, could be achieved without the requirement of post-polymerization modifications was investigated. To this end, the synthesis of a hydrophilic vinyl monomer, from the reaction between the commercially available 2-[2-(2-methoxyethoxy)ethoxy] acetic acid and vinyl acetate using the palladium vinyl exchange methodology previously investigated in Chapter 3, was investigated (Scheme 5.1).

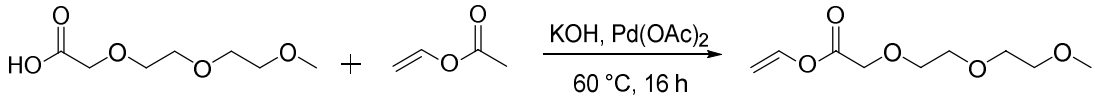

Scheme 5.1. Schematic representation of the palladium catalyzed reaction between 2-[2-(2-methoxyethoxy)ethoxy] acetic acid and vinyl acetate to prepare the monomer di(ethylene glycol) methyl ether vinyl acetate, MeO_2VAc.

This approach was aimed at introducing a short oligo (ethylene glycol) segment into the new vinyl monomer that will enhance the hydrophilicity of the final polymer following polymerization. The vinyl exchange reaction was performed for 16 h using 0.05 eq. of $Pd(OAc)_2$ as catalyst and 10 eq. of vinyl acetate (both relative to the carboxylic acid, 2-[2-(2-methoxyethoxy)ethoxy] acetic acid) at 60 °C. After purification using column chromatography and distillation the desired pure monomer was obtained with relatively good yield (61%). The successful formation of di(ethylene glycol) methyl ether vinyl acetate, MeO_2VAc, was confirmed by ^{1}H NMR spectroscopy, ^{13}C NMR spectroscopy and elemental analysis (Figures 5.1 and 5.2).

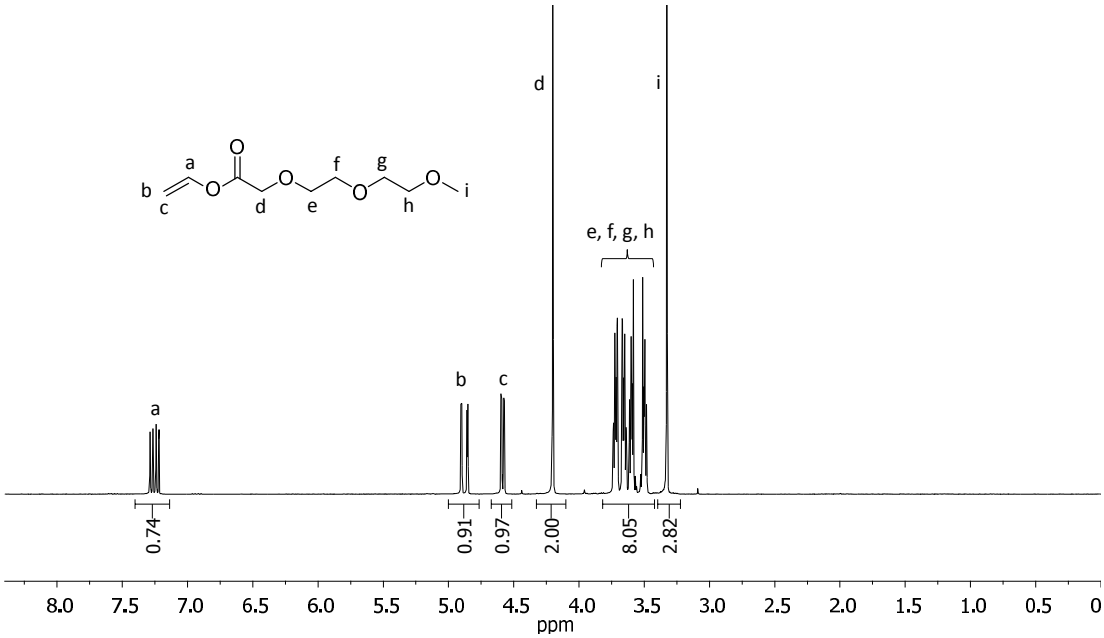

Figure 5.1. ^{1}H NMR spectrum of di(ethylene glycol) methyl ether vinyl acetate, MeO_2VAc, synthesized by palladium catalyzed vinyl exchange reaction between 2-[2-(2-methoxyethoxy)ethoxy] acetic acid and vinyl acetate (300 MHz, $CDCl_3$).

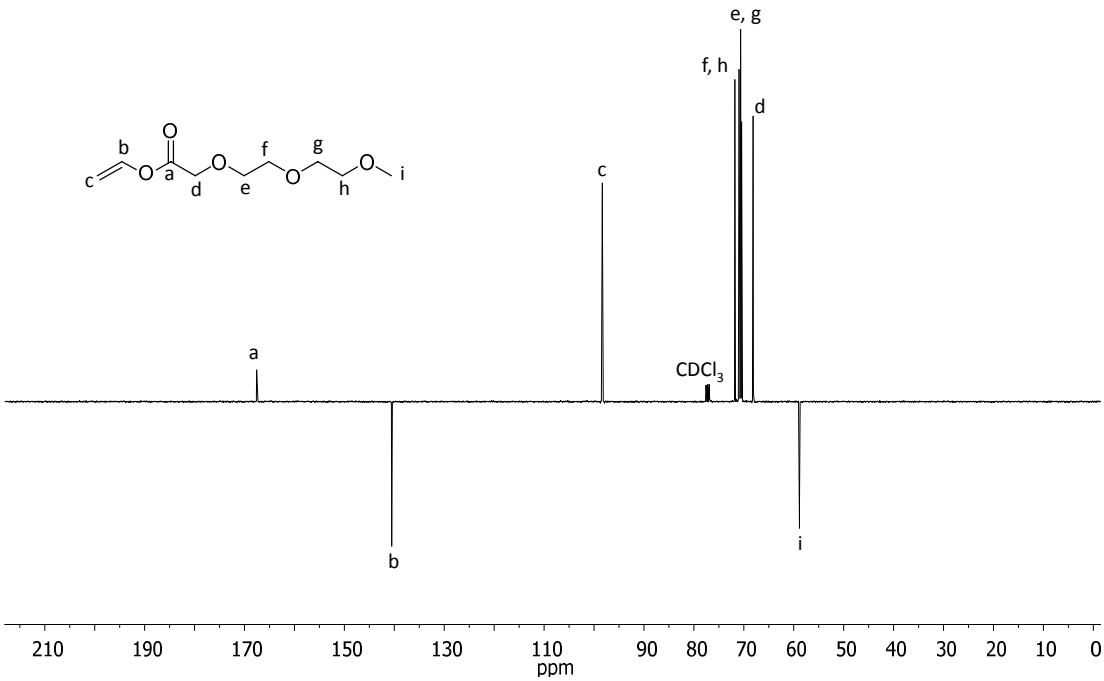

Figure 5.2. ^{13}C NMR spectrum of di(ethylene glycol) methyl ether vinyl acetate, MeO_2VAc, synthesized by palladium catalyzed vinyl exchange reaction between 2-[2-(2-methoxyethoxy)ethoxy] acetic acid and vinyl acetate (100 MHz, $CDCl_3$).

5.3.2 Homopolymerization of MeO_2VAc using RAFT/MADIX

Following on from the successful synthesis of di(ethylene glycol) methyl ether vinyl acetate (MeO_2VAc), and in order to confirm that the monomer could be polymerized using the RAFT/MADIX polymerization technique, the homopolymerization of MeO_2VAc was initially performed in bulk at 90 °C for different reaction times using 1,1'-azobis-(cyclohexanocarbonitrile) (ABCN) and *O*-*p*-methoxyphenyl xanthate, CTA 4, as the chain transfer agent, such that $[MeO_2VAc]_0/[ABCN]_0/[CTA\ 4]_0$ = 100:0.1:1 (Scheme 5.2). The choice of the CTA and ABCN as the chain transfer agent and the initiator respectively were made as a consequence of the previous results presented in Chapter 4 where they were found to show successful control of the copolymerization of MDO and VAc.

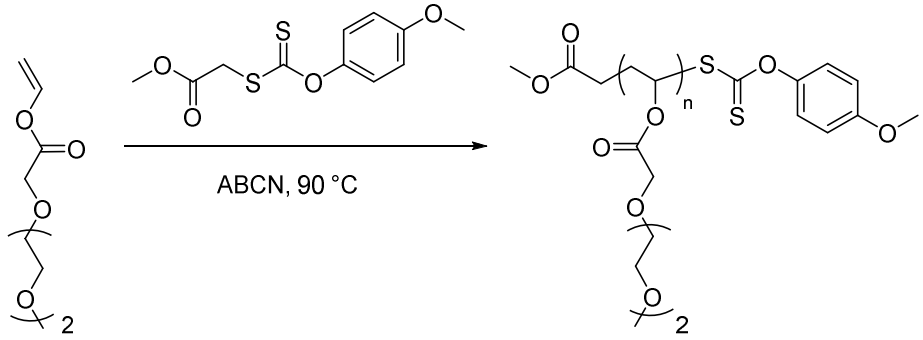

Scheme 5.2. Schematic representation of the homopolymerization of di(ethylene glycol) methyl ether vinyl acetate, MeO_2VAc, using RAFT/MADIX polymerization and CTA 4 as the chain transfer agent.

Under these conditions, the polymerization of MeO_2VAc resulted in the formation of poly(MeO_2VAc) with monomodal traces and low dispersities, $Đ_M$, with values between 1.13 and 1.53 when analyzed by size exclusion chromatography (SEC) suggesting the controlled nature of the polymerization (Figure 5.3).

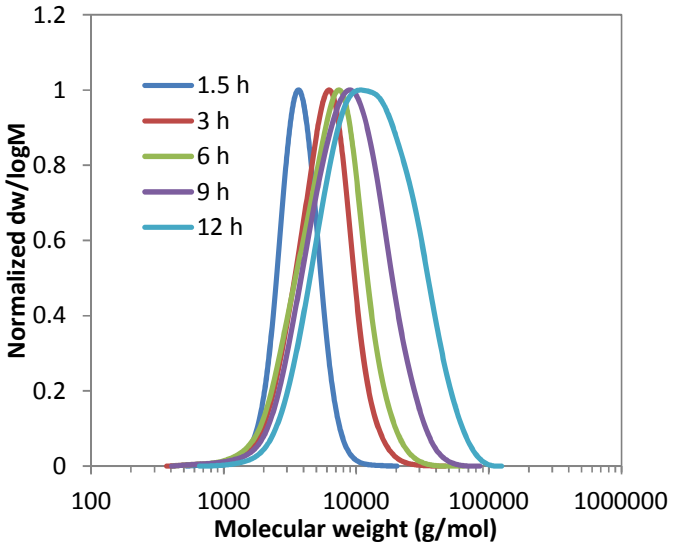

Figure 5.3. Size exclusion chromatograms of poly(MeO_2VAc) obtained by the RAFT/MADIX polymerization with CTA 4 as the chain transfer agent for different reaction times, (SEC, $CHCl_3$).

Further analysis using ^1H NMR spectroscopy revealed a significant increase in monomer conversions throughout the polymerization with conversions of 13, 30, 38, 53 and 68% obtained for reaction times of 1.5, 3, 6, 9 and 12 h respectively (Table 5.1). The increase in conversion was also confirmed by the shift in the molecular weight distributions observed by SEC analysis for the different polymerization times. The controlled aspect of the polymerization of MeO_2VAc was further observed in the good correlation between the UV trace (λ = 280 nm, characteristic wavelength of xanthates) and RI trace obtained by SEC analysis on the polymer obtained after 6 h confirming the presence of the xanthate chain-end on the final polymer throughout the molecular weight distribution (Figure 5.4).

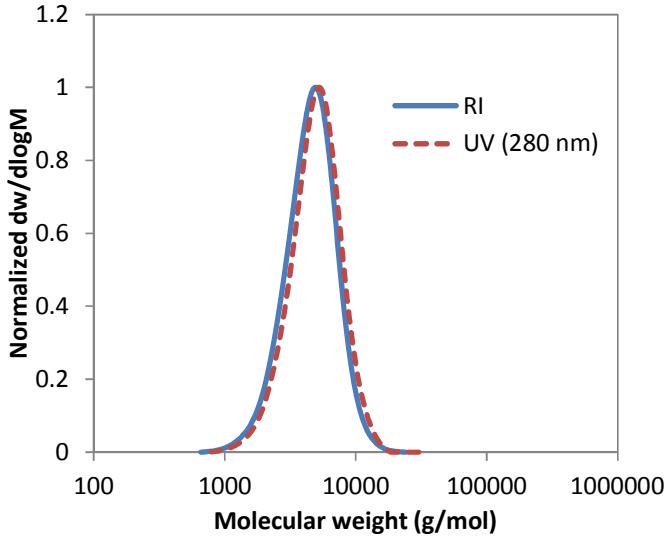

Figure 5.4. Size exclusion chromatograms of poly(MeO_2VAc) synthesized using RAFT/MADIX polymerization after 6 h; blue trace using RI detection and red dashed trace using UV detection at λ = 280 nm, (SEC, $CHCl_3$).

Table 5.1. Characterization data for the homopolymerization of MeO_2VAc for different polymerization time points.

Time (h)	MeO_2VAc conv.[a] (%)	M_n [SEC b] (kg/mol)	M_n [theo. c] (kg/mol)	M_n [obs. d] (kg/mol)	$Đ_M$ [b]
1.5	15	3.5	3.1	3.7	1.13
3	30	4.8	6.1	7.8	1.28
6	38	5.3	7.8	9.2	1.39
9	53	6.7	10.8	12.4	1.53
12	68	9.3	13.3	17.8	1.73

[a] conversions determined by ^{1}H NMR spectroscopy ($CDCl_3$), [b] obtained by SEC analysis in $CHCl_3$, [c] theoretical molecular weight based on monomer conversion (^{1}H NMR spectroscopy), [d] observed molecular weight obtained by ^{1}H NMR spectroscopy end-group analysis.

It should be noted that for a reaction time of 12 h the polymer displayed a much increased dispersity of 1.73 which suggested the presence of some termination reactions occurring and thus resulted in some loss of control over the process. This observation could be explained by the chain transfer reactions that tend to occur during the bulk vinyl acetate polymerizations which results in a broadening of the molecular weight distribution.[38]

Additionally, the controlled nature of the polymerization was confirmed by ^{1}H NMR spectroscopic analysis where the characteristic resonances of the xanthate aromatic group at

δ = 7.00 – 6.90 ppm were observed, suggesting a good retention of the xanthate chain-ends onto the polymer chains (Figure 5.5). The observed number-average molecular weights of the polymers, $M_n^{obs.}$, were obtained by ^{1}H NMR spectroscopic analysis through comparison of the integrals of the signals from the MeO_2VAc polymer backbone at δ = 5.10 – 4.70 ppm and the xanthate aromatic resonance at δ = 7.00 – 6.90 ppm (Figure 5.5). The theoretical molecular weights, $M_n^{theo.}$, were based on the monomer conversions obtained by ^{1}H NMR spectroscopic analysis performed on the crude polymers solution. The values of $M_n^{theo.}$ and $M_n^{obs.}$ were found to be in good agreement throughout the polymerization process indicating the good control of the polymerization, however above a reaction time of 9 h, a deviation could be observed which could suggest that some termination reactions were occurring when higher MeO_2VAc monomer conversion was reached.

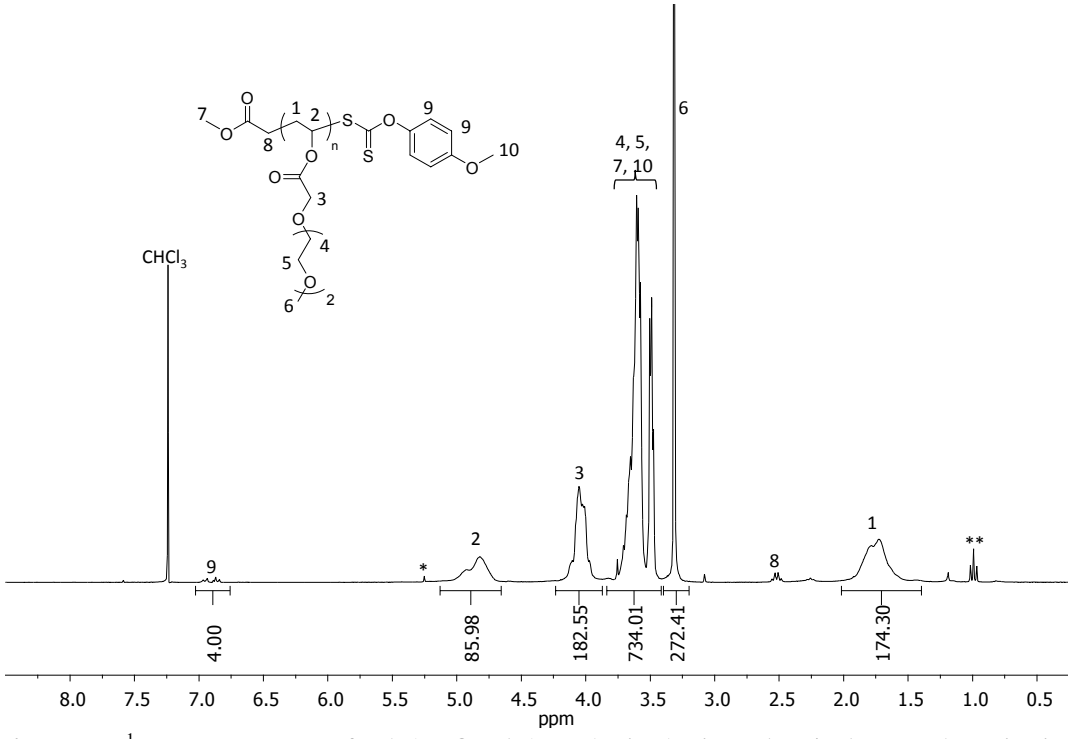

Figure 5.5. ^{1}H NMR spectrum of poly(MeO_2VAc) synthesized using RAFT/MADIX polymerization and CTA 4 as the chain transfer agent, (300 MHz, $CDCl_3$), * indicates residual dichloromethane traces and ** residual hexane traces.

5.3.3 Copolymerization of MDO and MeO_2VAc using RAFT/MADIX

Following on from the results obtained in Chapters 2 and 3, and with a view towards the synthesis of degradable and hydrophilic copolymers, the copolymerization of MDO and $VMeO_2Ac$ was investigated. Using the RAFT/MADIX polymerization technique, an initial copolymerization was performed such that $[MeO_2VAc]_0/[MDO]_0/[ABCN]_0/[CTA\ 4]_0$ = 70:30:0.1:1, and was carried for 9 h at 90 °C (Scheme 5.3).

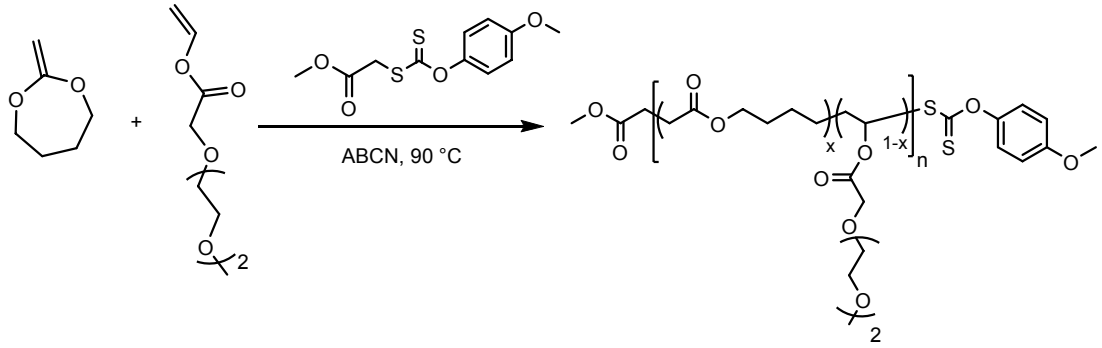

Scheme 5.3. Schematic representation of the copolymerization of MDO and MeO_2VAc using the RAFT/MADIX polymerization process and CTA 4 as the chain transfer agent.

From this initial experiment, a well-defined copolymer of poly(MDO-*co*-MeO_2VAc) was synthesized as evidenced by the monomodal trace and low dispersity, $Đ_M$ = 1.40, obtained by SEC analysis (Figures 5.6 and 5.7). The UV trace for the copolymer recorded at λ = 280 nm also remained monomodal and in good agreement with the RI detection trace, which confirmed the presence of the xanthate chain-end attached to the end of the polymer backbone (Figure 5.6).

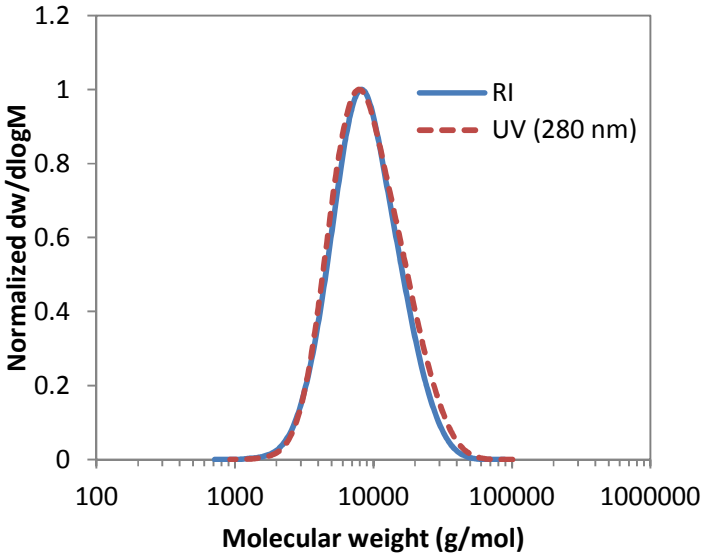

Figure 5.6. Size exclusion chromatograms of poly(MDO-*co*-MeO_2VAc) obtained by the RAFT/MADIX polymerization after 9 h, blue trace using RI detection and red dashed trace using UV detection at λ = 280 nm, (SEC, $CHCl_3$).

Further analysis on the crude polymer mixture obtained after 9 h using ^{1}H NMR spectroscopy revealed monomer conversions of 43% and 21% for MeO_2VAc and MDO respectively. ^{1}H NMR analysis on the final copolymer revealed a good correlation between $M_n^{theo.}$ and $M_n^{obs.}$ (Table 5.2). The theoretical molecular weights, $M_n^{theo.}$, was based on conversion of both MDO and MeO_2VAc and the observed molecular weights, $M_n^{obs.}$, was obtained by integration of the protons from the MeO_2VAc and MDO polymer backbone at δ = 5.30 – 4.80 ppm and δ = 2.55 ppm respectively, and referenced to the characteristic resonance of the phenyl protons from the xanthate end-group at δ = 7.00 - 6.90 ppm (Figure 5.8). Further analysis using ^{1}H NMR spectroscopy revealed a final composition of 82 mol% in MeO_2VAc and 18 mol% in MDO. These initial copolymerization results indicated both the suitability of MDO and MeO_2VAc to copolymerize as well as the suitability of CTA 4 to mediate the reaction.

In an attempt to study the kinetics of the copolymerization of MeO_2VAc and MDO, a detailed study was conducted in which samples were taken after 2, 4, 7, 9, 12 and 16 h

and analyzed by ^{1}H NMR spectroscopy and SEC analysis. The conditions used were the same as previously, where $[MeO_2VAc]_0/[MDO]_0/[ABCN]_0/[CTA\ 4]_0$ = 70:30:0.1:1. From this study, poly(MDO-*co*-MeO_2VAc) samples with controlled characteristics were successfully synthesized, as seen by the good correlation between $M_n^{theo.}$ and M_n^{SEC} and the low dispersity values ($Đ_M$ = 1.23-1.50, Table 5.2 and Figure 5.7) throughout the polymerization. However, as previously observed in Chapter 4, the values of $M_n^{obs.}$ were found to be consistently higher than the $M_n^{theo.}$ values during the copolymerization process which suggested that some termination reactions were occurring during the process. Further investigations using ^{1}H NMR spectroscopy showed the increase in monomer conversion during the study where values of 57% and 38% were reached for MeO_2VAc and MDO respectively after 16 h.

Table 5.2. Characterization data for the copolymerization of MDO and MeO_2VAc (initial monomer feed 30/70 mol% MDO/ MeO_2VAc) for different polymerization time points.

Time (h)	MeO_2VAc conv.[a] (%)	MDO conv.[a] (%)	Polymer comp.[a] [MeO_2VAc: MDO]	M_n^{SEC} [b] (kg/mol)	$M_n^{theo.}$ [c] (kg/mol)	$M_n^{obs.}$ [d] (kg/mol)	$Đ_M$ [b]
2	17	13	75:25	4.9	2.9	6.3	1.23
4	27	16	79:21	5.9	4.5	8.0	1.27
7	42	25	78:22	7.5	6.8	10.7	1.36
9	45	28	77:23	7.7	7.4	12.2	1.40
12	52	31	80:20	8.2	8.4	12.6	1.43
16	57	38	78:22	7.6	9.4	11.3	1.50

[a] determined by ^{1}H NMR spectroscopy ($CDCl_3$), [b] obtained by SEC analysis in $CHCl_3$, [c] theoretical molecular weight based on monomer conversion (^{1}H NMR spectroscopy), [d] observed molecular weight obtained by ^{1}H NMR spectroscopy end-group analysis.

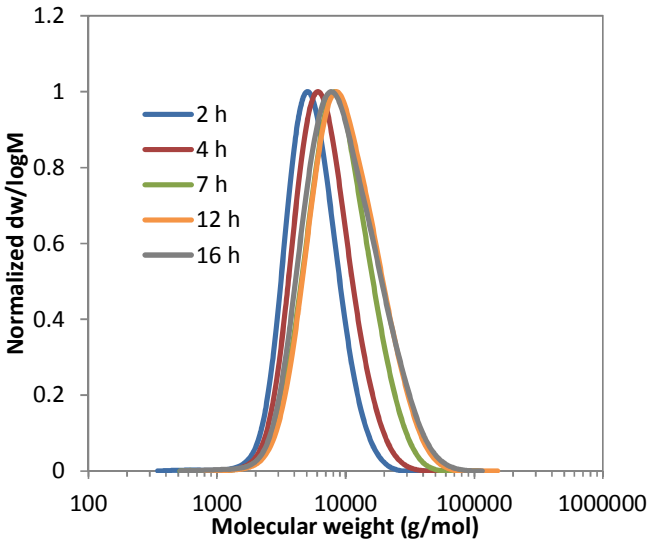

Figure 5.7. Size exclusion chromatograms of poly(MDO-*co*-MeO_2VAc) (70/30 mol%) at different polymerization times (SEC, $CHCl_3$).

Further investigation using ^1H NMR spectroscopy on the copolymers revealed the presence of resonance at δ = 0.90 ppm (Figure 5.8), which has previously been assigned to the side-chain reactions that result from the 1,4- and 1,7-hydrogen abstraction or backbiting reaction during the rROP of MDO.

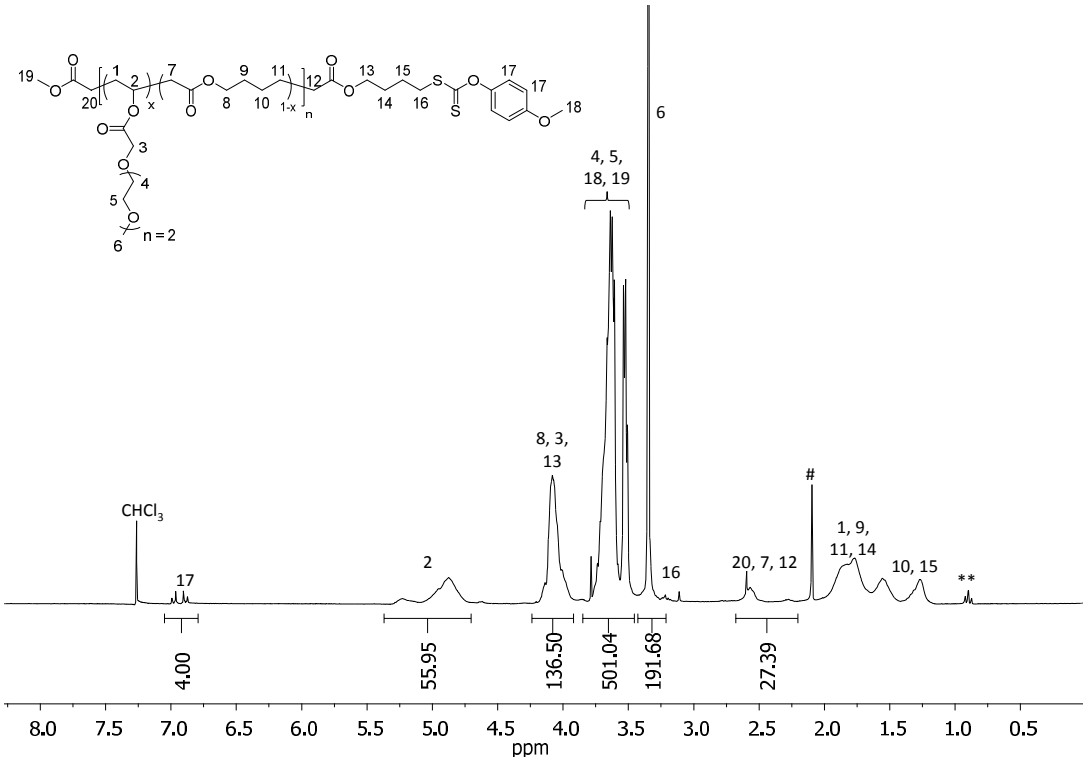

Figure 5.8. ^{1}H NMR spectrum of poly(MDO-*co*-MeO_2VAc) synthesized using RAFT/MADIX polymerization and CTA 4 as the chain transfer agent, (300 MHz, $CDCl_3$),** branches resulting from the 1,4- and 1,7-hydrogen abstraction, # residual acetone.

Additionally, ^{13}C NMR spectroscopic analysis was conducted on the copolymers to confirm the presence of the aromatic xanthate end-group with characteristic aromatic signals observed at δ = 114, 123, 148 and 158 ppm. Furthermore, the presence of a small peak at δ = 100 ppm corresponding to the quaternary carbon signal suggested the presence of some ring-closed species within the polymer backbone as previously observed in Chapters 2 and 3 (Figure 5.9).

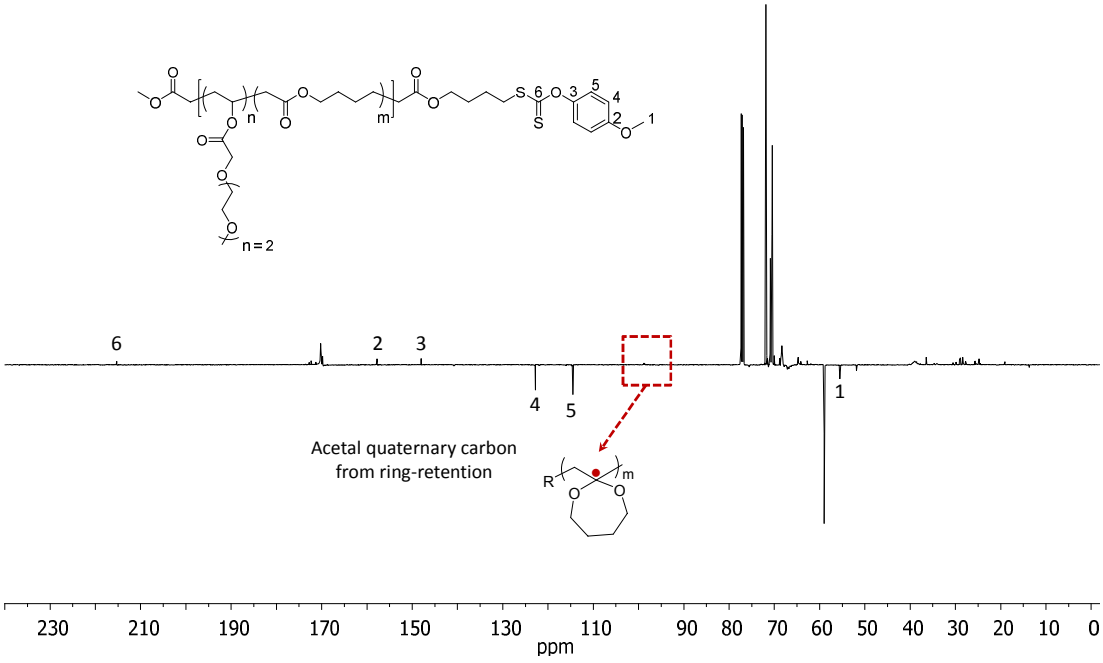

Figure 5.9. ^{13}C NMR spectrum of poly(MDO-*co*-MeO_2VAc) using the RAFT/MADIX polymerization process, the red point indicates a small portion of MDO ring-retained in the copolymer, (125 MHz, $CDCl_3$)

5.3.4 Solubility and thermoresponsive behavior

Polymers containing oligo (ethylene glycol) functionality, either within the polymer backbone or as pendent chains, have been widely studied and used in the biomedical field as a consequence of their interesting properties including biocompatibility, non-toxicity and high solubility in an aqueous environment.[3,26,39] Following the successful formation of poly(MeO_2VAc) and poly(MDO-*co*-MeO_2VAc) using the RAFT/MADIX polymerization, and aiming to investigate the polymer behavior in an aqueous environment, attempts to dissolve poly(MeO_2VAc) and poly(MDO-*co*-MeO_2VAc) samples in nanopure water (18 MΩ/cm) at a concentration of 5 mg/mL were performed. In both cases, the polymer and copolymer were found to be directly soluble in water suggesting that the hydrophilic properties introduced into the polymer backbone *via* a single polymerization step using the new oligo(ethylene glycol) vinyl acetate derived monomer had imparted solubility. Further analysis using Dynamic Light Scattering (DLS) suggested the presence of unimers in the

solution, as seen by the small sized population detected by DLS, as a hydrodynamic diameter, D_h, of ≈ 7 nm (Figure 5.10). Some additional large populations could also be observed, yet only in the intensity signal and therefore in a very low concentration, which were presumably obtained as a consequence of aggregation of polymers chains in solutions. Further analysis by Static Light Scattering (SLS) analysis revealed a small hydrodynamic radius, R_h, of 1.7 and 2.7 nm and small aggregation number, N_{agg}, of 1.4 and 3.3 for poly(MeO_2VAc) and poly(MDO-*co*-MeO_2VAc) respectively, which suggested that the polymers in solution were predominantly unimeric.

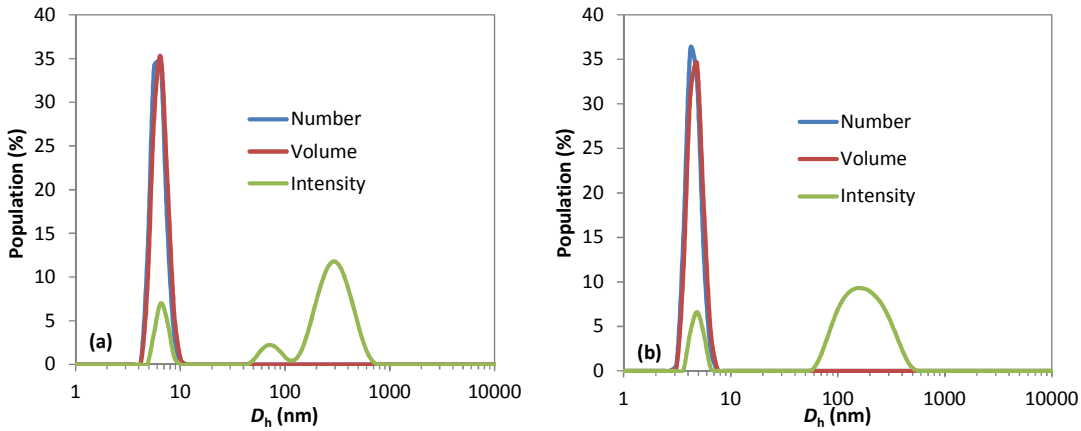

Figure 5.10. Dynamic light scattering traces for the solutions obtained from the direct dissolution of (a) poly(MeO_2VAc) and (b) poly(MDO-*co*-MeO_2VAc) in water at a concentration of 5 mg/mL.

Various studies on hydrophilic poly(ethylene glycol) copolymers (mainly on acrylates: poly(MEO_2MA) or poly(MEO_3MA) have highlighted the variation in solubility of the copolymers when the solution temperature was modified.[23,24,27,29] For the majority of them, at low temperatures the polymers showed good water solubility but became insoluble at higher temperatures when the specific lower critical solution temperature is reached. The change of solubility for such polymers is based on the hydrogen-bonding interactions between the water and polymer. At low temperatures these interactions are dominant and the polymer chains are elongated, flexible and in the form of extended coils in the medium, however as the temperature is increased these interactions become unfavorable and the polymer chains

will collapsed into a globule conformation.[7,27] This change results in the physical change of the polymer shifting from being dissolved in the solution to precipitating out. While many studies report this phase transition as LCST, in this Chapter it will be referred as "cloud point" instead. The cloud point is commonly defined as the temperature at which the solution transition from transparent to opaque for a given solution concentration whereas the LCST usually refers to the lowest point on a temperature *vs*. composition phase diagram.[40]

Aiming at further investigating the solubility and the potential thermoresponsivity of poly(MeO_2VAc) and poly(MDO-*co*-MeO_2VAc), the solutions were analyzed by turbidimetry using a UV-vis spectrophotometer to determine their cloud points. The measurements were performed at a detection wavelength of 550 nm from 10 to 90 °C at a heating rate of 1 °C/min. Under these conditions, the homopolymer poly(MeO_2VAc) was found to remain soluble for a wide range of temperatures (from 10 to 80 °C). However, above 80 °C, there was a significant reduction in the solubility as seen by the sharp decrease in transmittance measured, revealing that the polymer was reaching its cloud point and was becoming insoluble in water above this temperature (Figure 5.11, blue line).

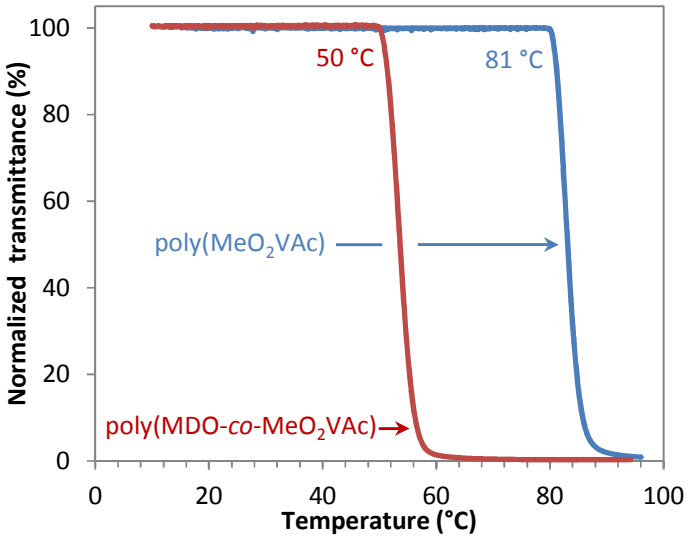

Figure 5.11. Plots of normalized transmittance *vs*. temperature obtained by turbidimetry analysis on the solution of poly(MeO_2VAc) (blue line) and poly(MDO-*co*-MeO_2VAc) (red line), containing 80 mol% MeO_2VAc, in water at a concentration of 5 mg/mL.

Similarly, the solubility of poly(MDO-*co*-MeO_2VAc) containing 80 mol% MeO_2VAc in the polymer backbone was found to decrease at a markedly lower temperature range, with a sharp decrease in the measured transmittance observed at 50 °C, again implying that the copolymer had reached its cloud point (Figure 5.11, red line). These temperature dependent solubility changes for both poly(MeO_2VAc) and poly(MDO-*co*-MeO_2VAc) confirm that the polymers synthesized in this Chapter did exhibit both hydrophilic and thermoresponsive properties with specific cloud point.

5.3.5 Parameters influencing the phase separation

Various studies on thermoresponsive polymers have highlighted the possibility of having reversible or irreversible phase separation.[25,27,41] For a system with a reversible phase transition, the heating and cooling behaviors are similar, whereas for a system with an irreversible phase transition, heating and cooling behavior are different and a hysteresis effect is observed.[25,41] Amongst the most common thermoresponsive polymer, poly(NIPAm) is now well-known to suffer from a significant hysteresis effect observed as a consequence of the additional intramolecular and intermolecular HN···O=C hydrogen bonding interactions which reduced the re-hydration rate of the polymer during the cooling process.[16,27] Conversely, poly(ethylene glycol) based polymers are found to exhibit a reversible phase transition as a consequence of the absence of strong hydrogen bonding interactions within the polymer structure which prevent the re-hydration process.[25,27] To investigate potential hysteresis for the copolymers, poly(MDO-*co*-MeO_2VAc), further turbidimetry experiments were performed to identify the potential changes in the phase transition upon heating/cooling. Turbidimetry experiments with three heating/cooling cycles were run over the temperature range of 15 to 80 °C at a detection wavelength of 550 nm with a rate of 1.0 °C/min. In all three cycles, no evidence of hysteresis could be observed as seen by the good overlap of the heating and cooling traces suggesting that the phase transition of

poly(MDO-*co*-MeO_2VAc) was reversible (Figure 5.12). Interestingly this feature was similar to the previously reported poly(ethylene glycol) acrylate analogue copolymers and also suggested that the reversible phase transition in the poly(MDO-*co*-MeO_2VAc) solution was observed as a consequence of the absence of strong hydrogen bonding interactions and therefore the polymer can undergo efficient re-hydration during the cooling process.[25,27]

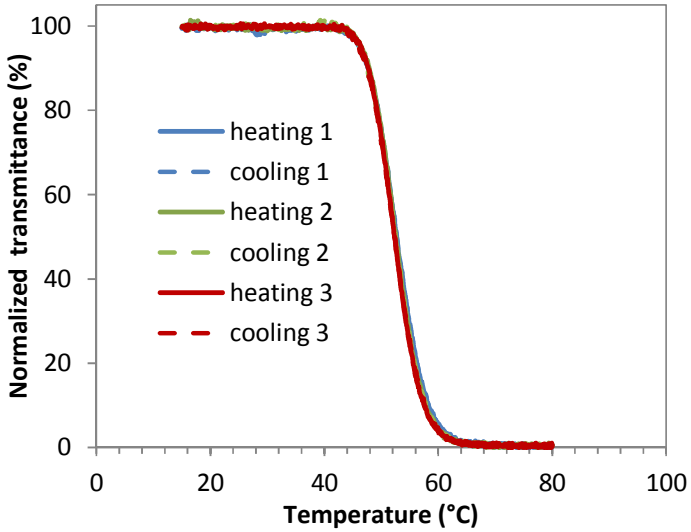

Figure 5.12. Plot of the normalized intensity of transmitted laser light *vs* temperature for the solution of poly(MDO-*co*-MeO_2VAc) (80 mol% MeO_2VAc in the polymer) measured for three heating/cooling cycles, in water at a concentration 5 mg/mL.

It is widely accepted that the LCST phase separation of thermoresponsive polymers can change depending on various parameters including solution concentration, polymer molecular weight, tacticity, and composition, or medium of the solution use.[3,7] In an attempt to study the influence of these parameters on the cloud points of the copolymers, different studies were performed. Initially, the copolymer composition of poly(MDO-*co*-MeO_2VAc) was varied with different incorporations of MeO_2VAc in the final backbone, ranging from 95 mol% to 47 mol% by altering the monomer feed ratios during the RAFT/MADIX polymerization of MDO and MeO_2VAc (Table 5.3). Turbidimetry experiments across a temperature range of 10 to 95 °C were carried out on these copolymers with the exception of the copolymer containing 47 mol% in MeO_2VAc. This was measured manually using a

thermocouple in an ice bath owing to the phase transition occurring below the minimum temperature attainable by the UV-vis instrument. In all cases, the thermoresponsive properties were confirmed by the significant decrease in transmittance when the cloud points were reached (Figure 5.13, left). A wide range of cloud points were obtained, with values ranging between 5 °C and 81 °C observed depending on the content of MeO_2VAc incorporated in the copolymer (Table 5.3). As expected, the cloud point values were found to increase linearly as the $VMeO_2Ac$ content in the copolymer was increased; the increase in hydrophilicity in the final copolymer when MeO_2VAc content is increased in turn increasing the solubility of the polymer and hence shifting the phase transition towards higher values (Figure 5.13, right). Moreover, as the content of MeO_2VAc in the copolymers was increased, the cloud points were found to increase towards the phase transition temperatures of the homopolymer, poly(MeO_2VAc).

Table 5.3. Characterization data for the copolymers of poly(MDO-*co*-MeO_2VAc), containing different amounts of MDO, and their associated cloud points in solution (5 mg/mL).

Polymer comp.[a] [MeO_2VAc: MDO]	M_n SEC [b] (kg/mol)	M_n theo. [c] (kg/mol)	M_n obs [d] (kg/m.ol)	$Đ_M$ [b]	Cloud point (°C) [e]
100:0	6.7	10.8	12.4	1.53	83
95:5	6.8	8.1	15.5	1.64	76
89:11	4.5	6.4	8.1	1.49	60
80:20	5.4	7.6	9.7	1.54	51
71:29	4.3	6.4	7.2	1.49	36
67:33	5.4	5.9	9.4	1.51	26
53:47	5.5	5.2	7.1	1.62	4*

[a] determined by ^{1}H NMR spectroscopy ($CDCl_3$), [b] obtained by SEC analysis in $CHCl_3$, [c] theoretical molecular weight based on monomer conversion (^{1}H NMR spectroscopy), [d] observed molecular weight obtained by ^{1}H NMR spectroscopy end-group analysis, [e] measured by turbidimetry (*obtained manually).

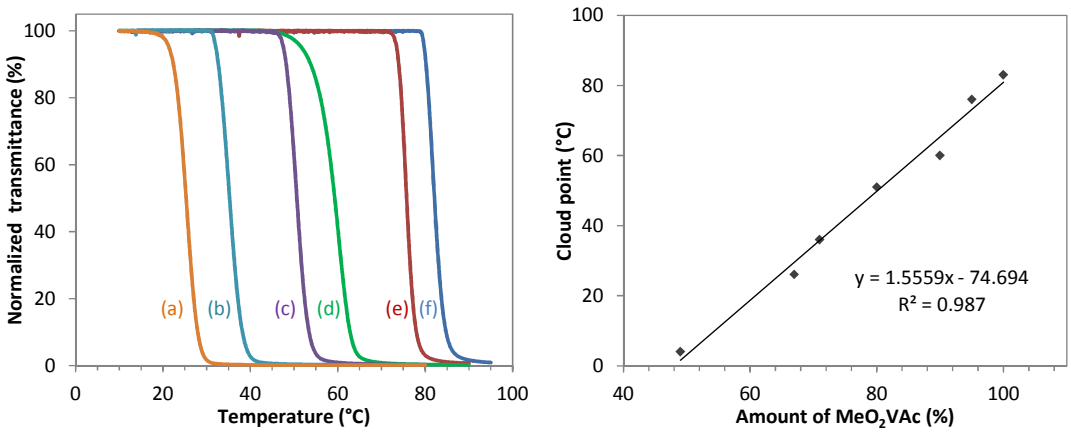

Figure 5.13. (Left) Intensity of the normalized transmitted laser light *vs*. temperature for poly(MDO-*co*-MeO_2VAc) copolymers of various compositions (a) 67 mol%, (b) 71 mol%, (c) 80 mol%, (d) 89 mol%, (e) 95 mol% and (f) 100 mol% of MeO_2VAc, at a concentration of 5 mg/mL in water, (right) effect of MeO_2VAc content on cloud point values.

These observations confirmed that the formation of new hydrophilic copolymers of poly(MDO-*co*-MeO_2VAc) presented interesting thermoresponsive properties, with their cloud points easily tuned from low to high temperatures simply by varying the ratio of monomers contained in the final copolymers.

The influence of the poly(MDO-*co*-MeO_2VAc) copolymer concentration on the phase transition temperature was also investigated using turbidimetry experiments. Solutions were prepared using the same poly(MDO-*co*-MeO_2VAc) sample to obtain different solutions with concentrations of 0.5, 1, 1.5, 2.5, 5 and 10 mg/mL which were subsequently analyzed using the UV-Vis spectrometer from 10 to 95 °C (Figure 5.14). Under such conditions, the "cloud point" was found to significantly change depending on the concentration of the polymer solutions: for the lowest concentration, 0.5 mg/mL, the cloud point was found to be 72 °C whereas the more concentrated solution, 10 mg/mL, had the lowest cloud point of 48 °C. The change in phase separation temperature was found to be more pronounced for lower concentrations of 0.5 to 1.5 mg/mL, with cloud point values of 72, 66 and 56 °C obtained respectively. At the other end of the spectrum, concentrations of 10, 5 and 2.5 mg/mL were found to have very similar cloud points of 47 – 52 °C suggesting that experiments needed to

be carried with a solution concentration of at least 2.5 mg/mL in order to obtain accurate cloud point measurements. These observations could be explained by the fact that at lower concentrations, the amount of polymer in the solution does not favor the formation of intermolecular aggregations between polymer chains in the solution which are required to produce a phase transition. If the aggregation density is not significantly high, increased temperatures will be required to enhance the interactions between polymer chains and lead to a precipitation of the polymer and hence the formation of a cloudy solution. However, for higher polymer concentrations, the amount of polymer in the solution is sufficient to easily trigger polymer chains to aggregate at a lower temperature, observed in the lower temperature the phase transition. This phenomenon has also been previously observed for different thermoresponsive polymers including poly(NIPAm), poly(α-peptoid)s and (oligo ethylene glycol) methacrylate based polymers.[42-44]

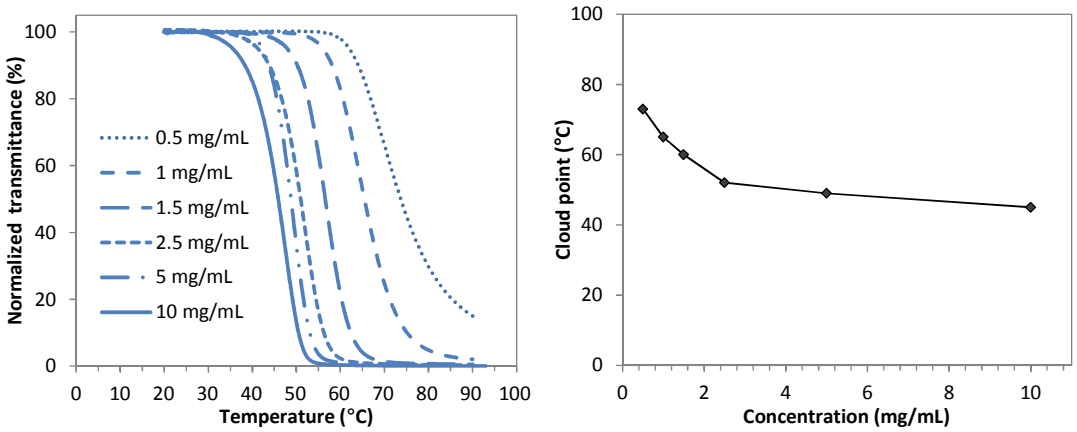

Figure 5.14. (left) Plots of normalized transmittance *vs*. temperature for poly(MDO-*co*-MeO_2VAc) containing 80 mol% in MeO_2VAc for different polymer solution concentrations of 0.5 to 10 mg/mL, (right) cloud points, in water, as a function of polymer concentrations.

The polymer chain-length of thermoresponsive polymers has often been reported as another parameter which could affect the temperature of the phase transition, and hence also affect the observed LCST values. Indeed, studies on poly(NIPAm) reported that varying LCST values could be observed for polymers having different molecular weights.[43,45] In order to

investigate the effect of the poly(MDO-*co*-MeO_2VAc) polymer chain-length on the cloud point values, a series of copolymers targeting different DPs were synthesized such that the final content of $VMeO_2Ac$ in the polymer backbone was similar (81 - 83 mol%) in order to avoid the aforementioned cloud point changes as a result of polymer composition. Copolymers with different degrees of polymerization, DP, were successfully synthesized and characterized by ^1H NMR spectroscopy and SEC analysis (Table 5.4), and molecular weights of 3.9, 5.1, 6.1 and 8.5 kg/mol were obtained for DP 15, 38, 55 and 117 respectively. Turbidimetry experiments on the four different molecular weight copolymers were conducted from 15 to 95 °C at a concentration of 5 mg/mL and a heating rate of 1.0 °C/min. Under these conditions, the DP of the copolymers were found to have a very small effect on the value of the cloud points, as seen by the similarity of the heating curves obtained for the solutions of the four different DPs (Figure 5.15). This result suggested that the final molecular weight of the copolymers was not influencing the phase transition temperature of the solution. Interestingly, a similar observation was also obtained by Lutz *et al*. for the study of the thermoresponsive copolymer poly(MEO_2MA-*co*-OEGMA), which further confirmed the similarity of the copolymers presented in this chapter to the well-known poly(ethylene) glycol acrylate or methacrylate analogues.[25]

Table 5.4. Characterization data for the copolymers of poly(MDO-*co*-MeO_2VAc) with different DPs of 15, 38, 55, 117, containing similar amounts of $VMeO_2Ac$, and their associated LCST values in solution (5 mg/mL).

DP [a]	Polymer comp.[a] [MeO_2VAc: MDO]	M_n SEC [b] (kg/mol)	M_n theo. [c] (kg/mol)	M_n obs. [d] (kg/mol)	$Đ_M$ [b]	Cloud point (°C)
15	83:17	3.9	2.7	3.5	1.45	52
38	82:18	5.1	7.1	8.8	1.55	54
55	80:20	6.1	10.3	11.7	1.62	56
117	83:17	8.5	22.0	25.2	1.91	58

[a] determined by ^{1}H NMR spectroscopy ($CDCl_3$), [b] obtained by SEC analysis in $CHCl_3$, [c] theoretical molecular weight based on monomer conversion (^{1}H NMR spectroscopy), [d] observed molecular weight obtained by ^{1}H NMR spectroscopy end-group analysis.

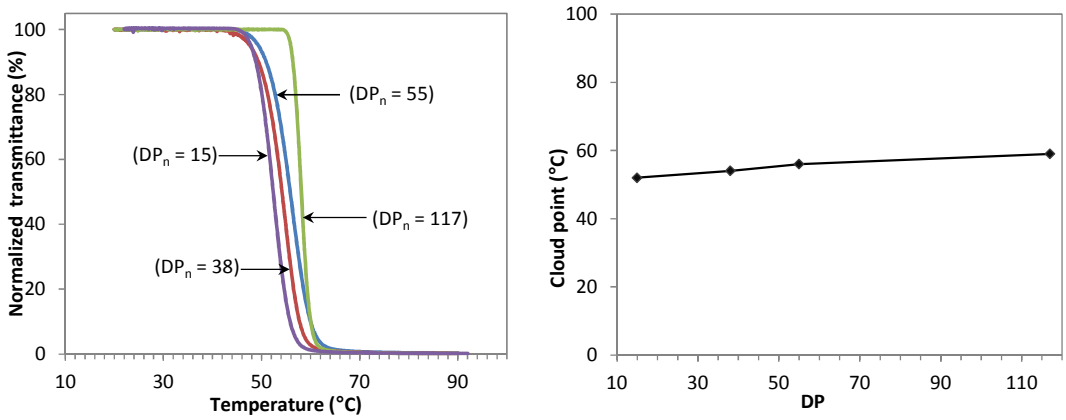

Figure 5.15. (left) Plots of normalized transmittance *vs*. temperature obtained for poly(MDO-*co*-MeO_2VAc) copolymers (5 mg/mL) in water containing 83 - 81 mol% of MeO_2VAc and having different molecular weights M_n, DP = 15; M_n = 3.9 kDa, DP = 38; M_n = 5.1 kDa, DP = 55; M_n = 6.1 kDa, DP = 117; M_n = 8.5 kDa and (right) cloud points as a function of the copolymer DP.

5.3.6 Synthesis of other oligo-vinyl acetate derived monomers

Following the successful results previously observed for the copolymers, poly(MDO-*co*-MeO_2VAc), where thermoresponsive properties were achieved and successfully tuned by simply varying the MeO_2VAc content in the final copolymers, the assumption that the length of the oligo(ethylene glycol) functional group contained in the vinyl acetate derived monomer could also have an influence on the cloud point was probed. Indeed, various reports regarding the methacrylate and acrylate versions of the polymers highlighted the possibility of tuning the LCST when the length of the oligo(ethylene glycol) acrylates and

methacrylate monomer was increased or decreased.[26,27] Motivated by these results, the synthesis of two other monomers was investigated with a shorter and a longer version of the vinyl oligo(ethylene glycol) chain derived acetate monomer, MeO_2VAc. Their synthesis was produced using the palladium vinyl reactions between vinyl acetate and 2-(2-methoxyethoxy) acetic acid or 2-2-[2-(2-methoxyethoxy)ethoxy]ethoxy acetic acid (Scheme 5.4), performed at 60 °C for 16 h. It should be noted that the reagent 2-2-[2-(2-methoxyethoxy)ethoxy]ethoxy acetic acid was not commercially available and was therefore synthesized by the oxidation of tetra(ethylene glycol) monomethyl ether (TEGME) using potassium permanganate ($KMnO_4$). The successful synthesis of both monomers was then confirmed by ^1H and ^{13}C NMR spectroscopy (Figures 5.16 – 5.19) with yields, after purification by column chromatography and distillation, of 58 and 26% obtained for ethylene glycol methyl ether vinyl acetate (MeOVAc) and tri(ethylene glycol) methyl ether vinyl acetate (MeO_3VAc) respectively. The lower yield observed in the case of the MeO_3VAc monomer was obtained as a consequence of the difficulty in the purification steps using distillation requiring higher temperatures which were found to lead to a degradation of the monomer as seen by the change in color from colorless to brown under such conditions.

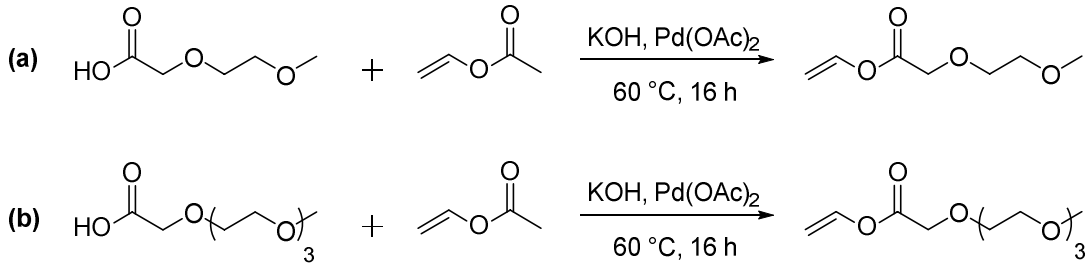

Scheme 5.4. Schematic representation of the palladium catalyzed reaction between (a) 2,2-(methoxyethoxy) acetic acid and VAc to prepare the monomer MeOVAc, and (b) 2-2-[2-(2-methoxyethoxy)ethoxy]ethoxy acetic acid and VAc to prepare the monomer MeO_3VAc.

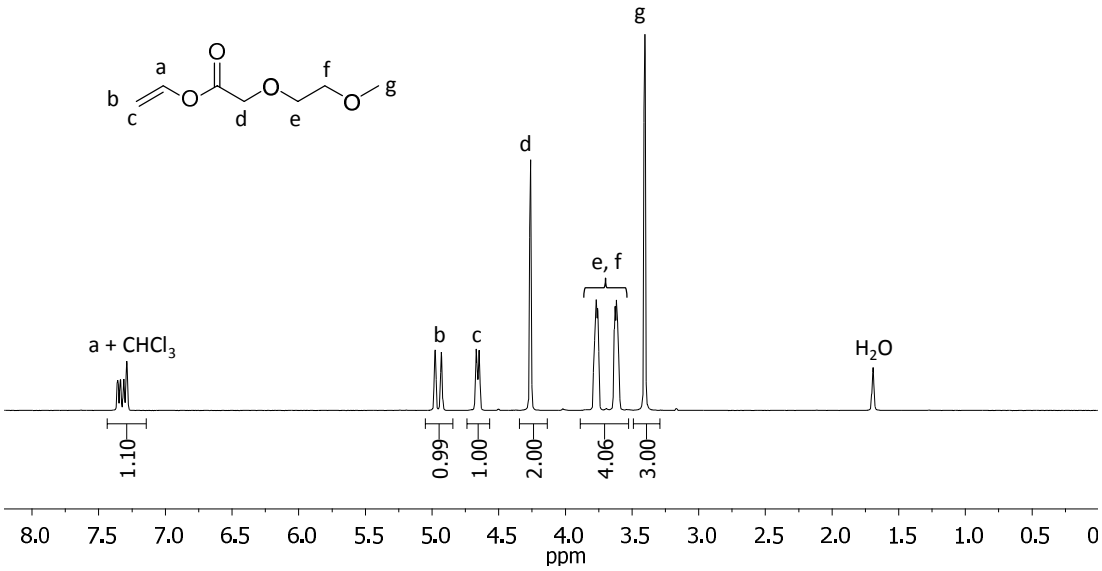

Figure 5.16. ^{1}H NMR spectrum of ethylene glycol methyl ether vinyl acetate, MeOVAc, synthesized by the palladium catalyzed vinyl exchange reaction between 2,2-(methoxy)ethoxy acetic acid and vinyl acetate (400 MHz, $CDCl_3$).

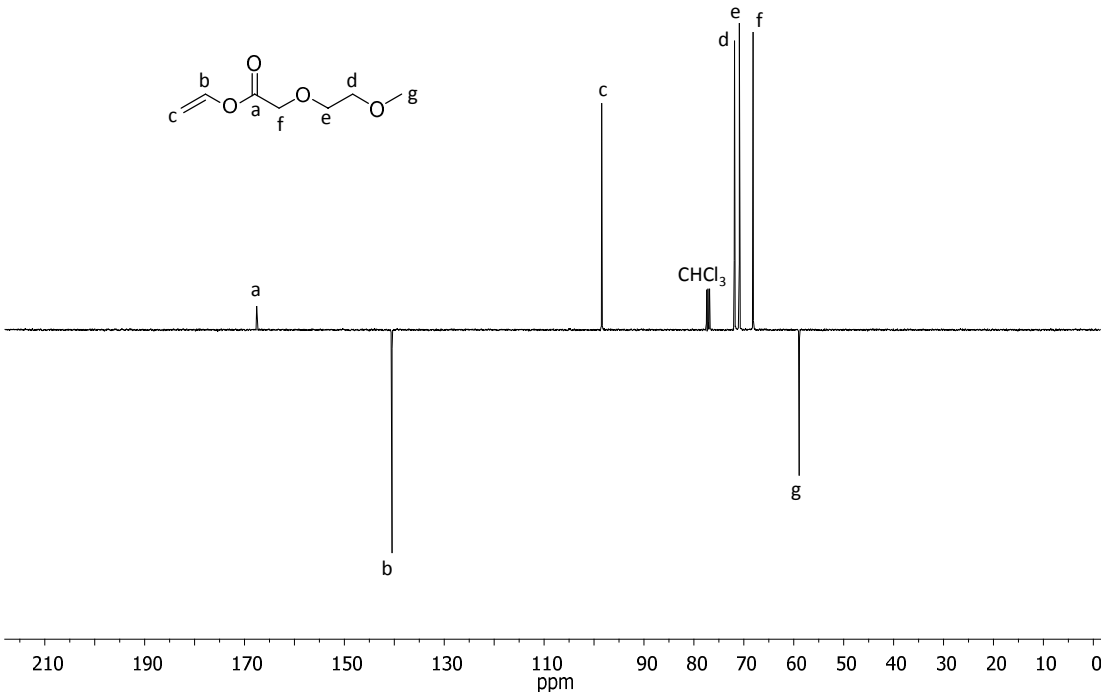

Figure 5.17. ^{13}C NMR spectrum of ethylene glycol methyl ether vinyl acetate, MeOVAc, synthesized by palladium catalysed vinyl exchange reaction between 2,2-(methoxy)ethoxy acetic acid and vinyl acetate (100 MHz, $CDCl_3$).

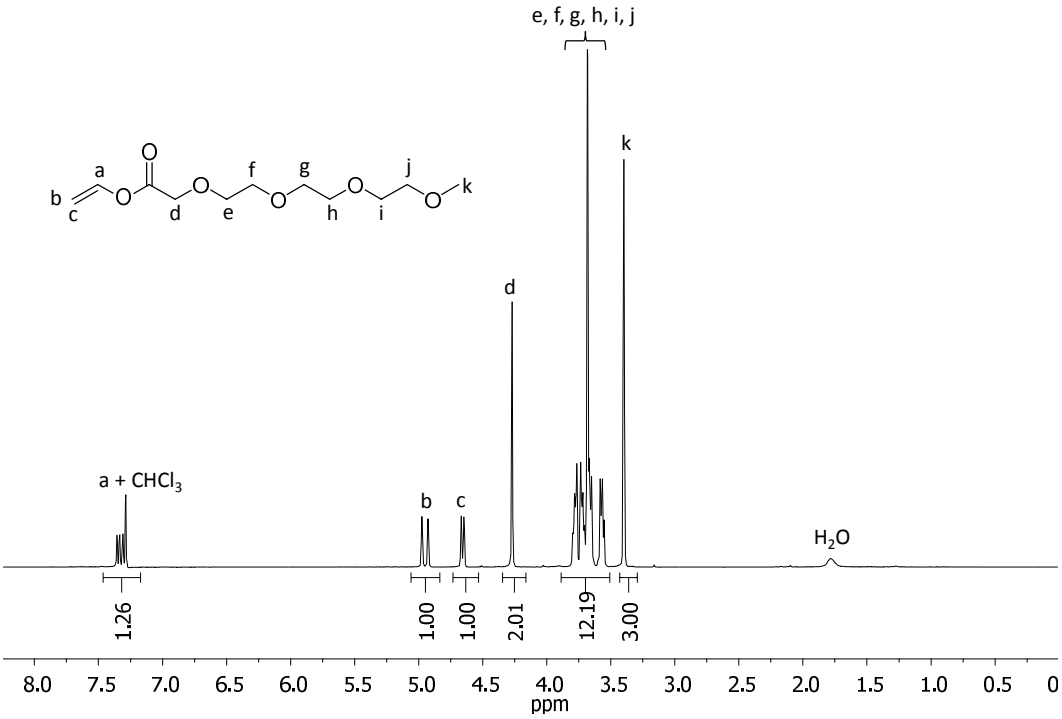

Figure 5.18. ^{1}H NMR spectrum of tri(ethylene glycol) methyl ether vinyl acetate, $VMeO_3Ac$, synthesized by palladium catalyzed vinyl exchange reaction between 2-2-[2-(2-methoxyethoxy)ethoxy]ethoxy acetic acid and vinyl acetate (400 MHz, $CDCl_3$).

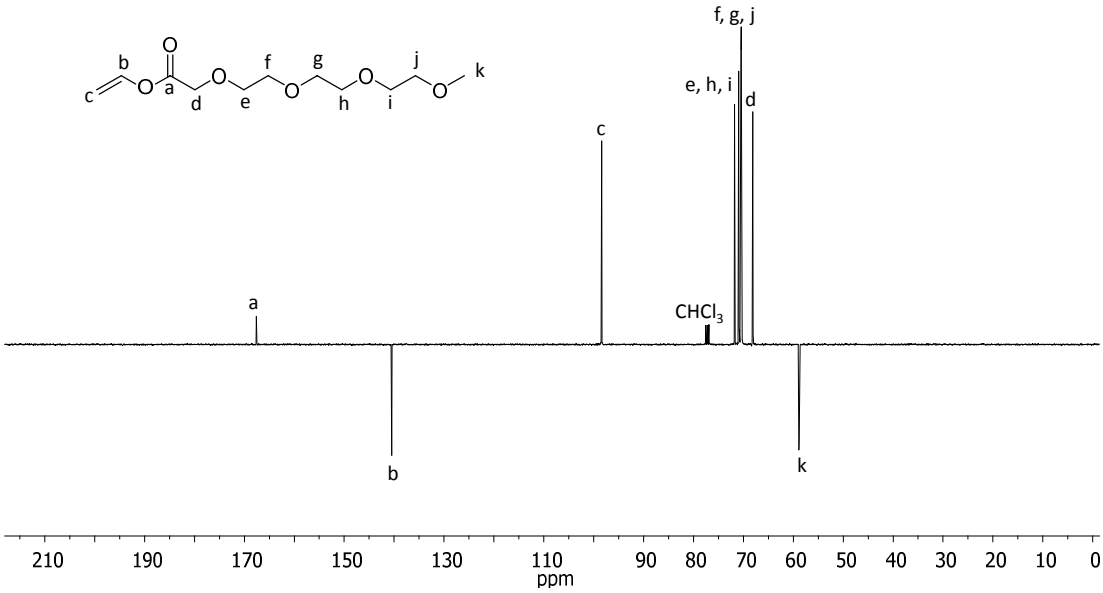

Figure 5.19. ^{13}C NMR spectrum of tri(ethylene glycol) methyl ether vinyl acetate, $VMeO_3Ac$, synthesized by palladium catalyzed vinyl exchange reaction between 2-2-[2-(2-methoxyethoxy)ethoxy]ethoxy acetic acid and vinyl acetate (100 MHz, $CDCl_3$).

5.3.7 Polymerization and copolymerization of MeOVAc and MeO_3VAc

In order to confirm that the shorter and longer oligo (ethylene glycol) vinyl monomers could also produce hydrophilic and thermoresponsive polymers, the copolymerization of MeOVAc or MeO_3VAc with MDO was investigated using similar conditions as before, where CTA 4 was used as the chain transfer agent and ABCN as the radical initiator (Scheme 5.5).

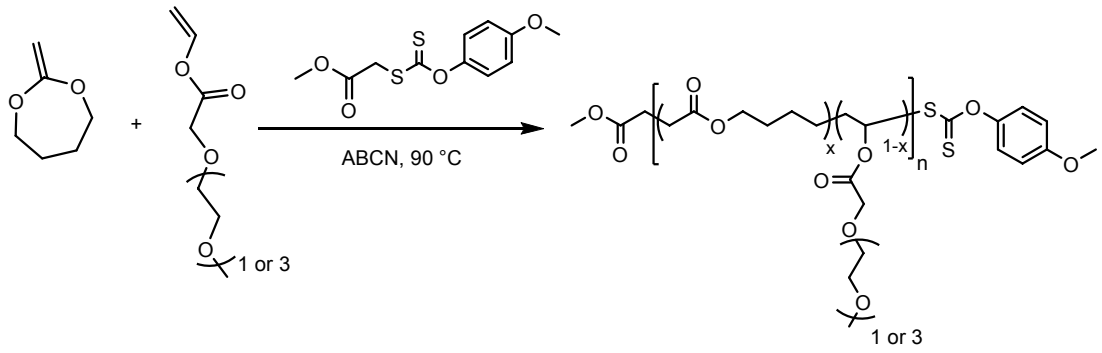

Scheme 5.5. Copolymerization of MDO with MeOVAc, or MeO_3VAc using the RAFT/MADIX polymerization process.

In an initial experiment, the polymerization of MeOVAc was performed for 4.5 h at 90 °C with CTA 4 as the chain transfer agent such that $[MeOVAc]_0/[ABCN]_0/[CTA\ 4]_0$ = 100:0.1:1. Under these conditions, the formation of poly(MeOVAc) was achieved as confirmed by ^1H NMR spectroscopy, in which resonances at δ = 7.10 – 6.90 ppm were observed, corresponding to the phenyl xanthate end-group suggesting CTA 4 was suitable of to mediate the polymerization of MeOVAc (Figure 5.21). SEC analysis confirmed this suitability with the synthesis of well-defined poly(MeOVAc) observed in the monomodal trace and low $Đ_M$ value observed (Table 5.5 and Figure 5.20). Similarly, two copolymerizations of MeOVAc with MDO were performed such that $[MeOVAc]_0/[MDO]_0/[ABCN]_0/[CTA\ 4]_0$ = 90:10:0.1:1 and $[MeOVAc]_0/[MDO]_0/[ABCN]_0/[CTA\ 4]_0$ = 80:20:0.1:1, with an aim towards producing copolymers of poly(MDO-*co*-MeOVAc) with different degrees of degradability and potentially different thermoresponsive behavior. The controlled nature of these

copolymerizations was again confirmed by the monomodal SEC traces observed (Figure 5.22) and the inclusion of the characteristic resonances associated with the xanthate end-group in the ^{1}H NMR spectral analyses (Figure 5.23).

Table 5.5. Characterization data for the polymers, poly(MeOVAc), poly(MDO-*co*-MeOVAc) and poly(MDO-*co*-MeO_3VAc) synthesized using RAFT/MADIX polymerization.

Initial monomer feed MeO_nVAc :MDO [a]	n	Time (h)	$VMeO_nAc$ conv.[a] (%)	MDO conv.[a] (%)	Polymer comp.[a] MeO_nVAc: MDO	M_n SEC [b] (kg/mol)	M_n theo. [c] (kg/mol)	M_n obs. [d] (kg/mol)	$Đ_M$ [b]
100:0	1	4.5	42	-	100:0	4.7	7.0	7.7	1.46
90:10	1	4.5	43	31	92:8	5.6	6.8	7.2	1.62
80:20	1	5.5	38	23	86:14	4.6	5.6	6.3	1.58
40:60	3	18	43	24	73:27	6.3	7.7	8.2	1.47

n is the number of oligo ethylene repeat unit in the monomers, [a] determined by ^{1}H NMR spectroscopy ($CDCl_3$), [b] obtained by SEC analysis in $CHCl_3$, [c] theoretical molecular weight based on monomer conversion (^{1}H NMR spectroscopy), [d] observed molecular weight obtained by ^{1}H NMR spectroscopy end-group analysis.

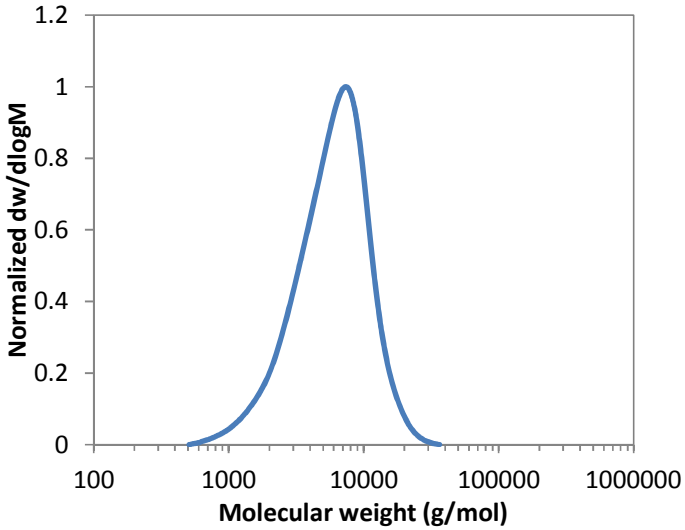

Figure 5.20. Size exclusion chromatogram of poly(MeOVAc) obtained after 4.5 h of RAFT/MADIX polymerization using CTA 4 as the chain transfer agent, (SEC, $CHCl_3$).

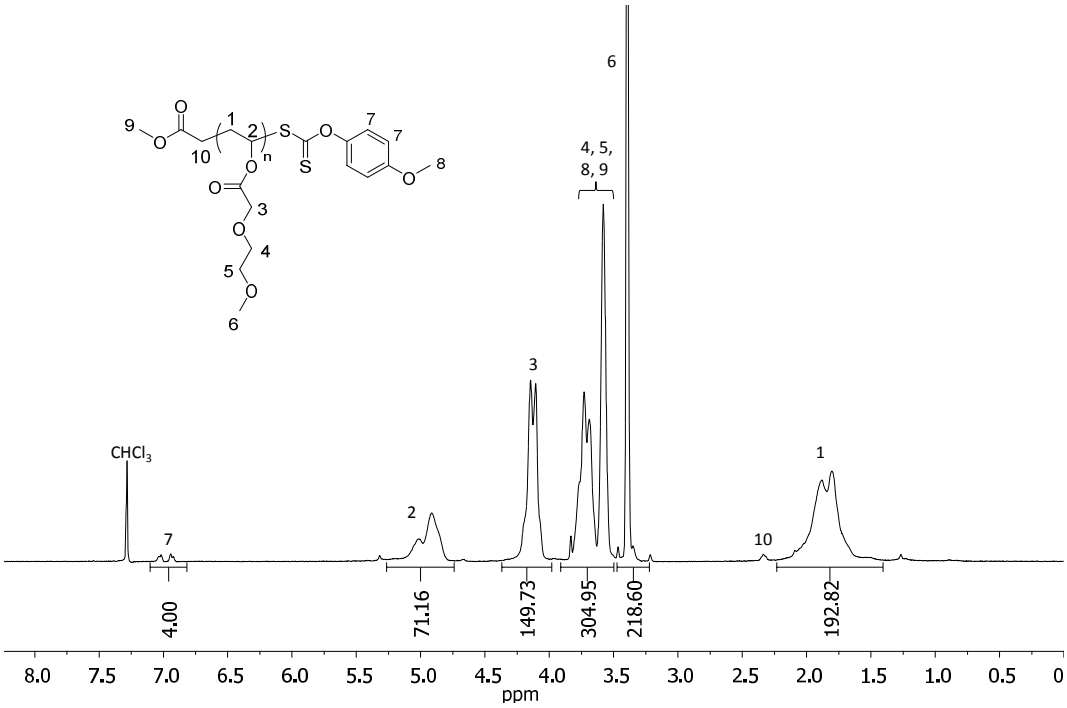

Figure 5.21. ^{1}H NMR spectrum of poly(MeOVAc) synthesized using RAFT/MADIX polymerization and CTA 4 as the chain transfer agent, (300 MHz, $CDCl_3$).

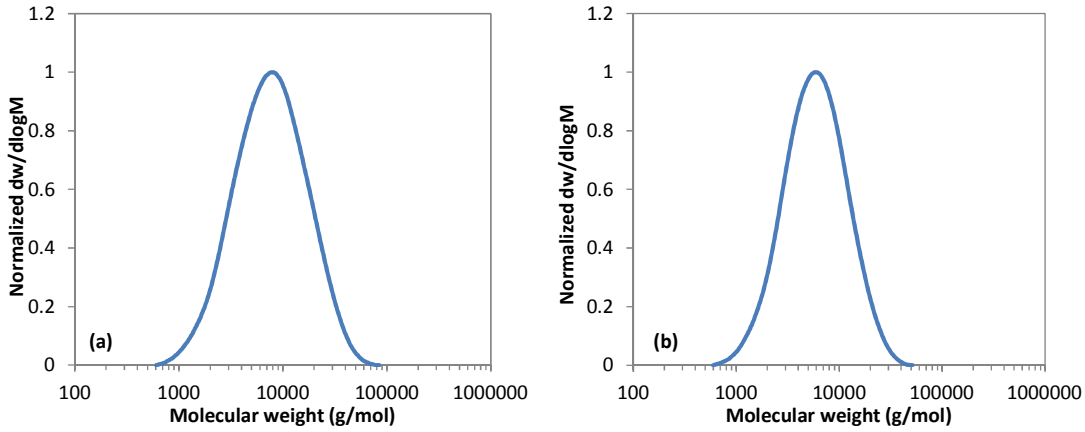

Figure 5.22. Size exclusion chromatograms of poly(MDO-*co*-MeOVAc) copolymers obtained by the RAFT/MADIX polymerization using CTA 4 as the chain transfer agent for different initial feeds of (a) 10/90 mol% and (b) 20/80 mol% MDO/MeOVAc, (SEC, $CHCl_3$).

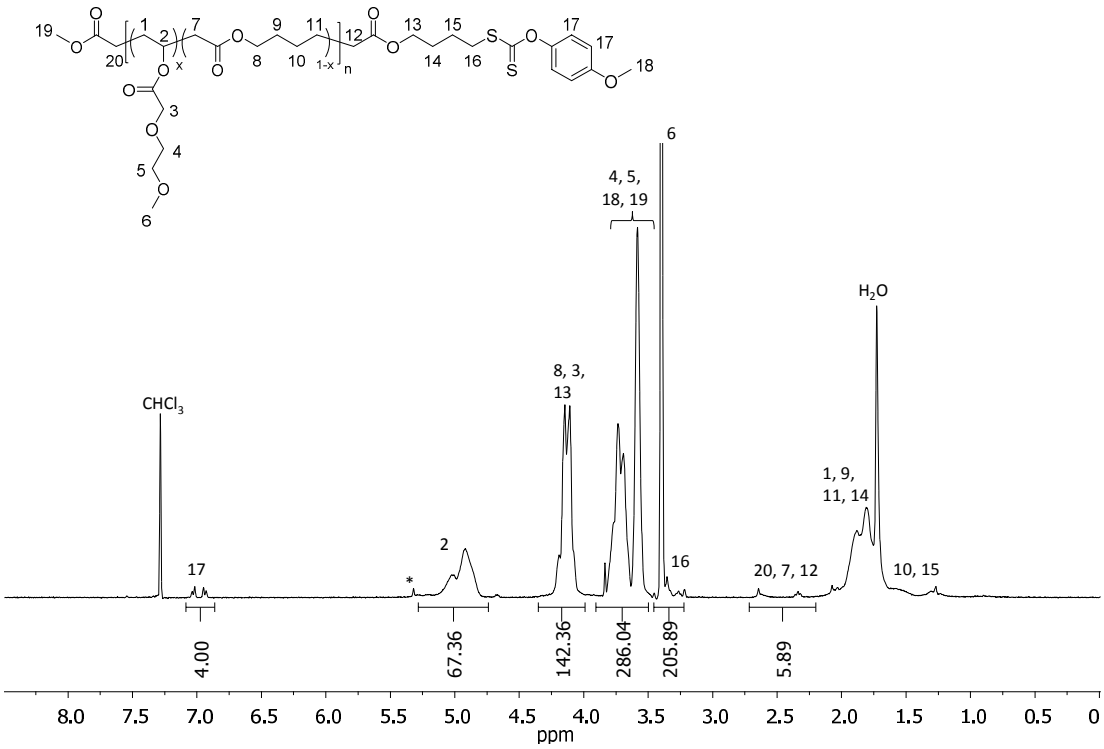

Figure 5.23. ^{1}H NMR spectrum of poly(MDO-*co*-MeOVAc) synthesized using the RAFT/MADIX polymerization and CTA 4 as the chain transfer agent, (300 MHz, $CDCl_3$), * residual dichloromethane.

Additionally, the copolymerization of MeO_3VAc with MDO was also carried out for 18 h at 90 °C with a monomer/initiator/CTA feed ratio of $[MeO_3VAc]_0/[MDO]_0/[ABCN]_0/[CTA\ 4]_0$ = 60:40:0.1:1. In comparison with the two other copolymerization of MeOVAc, the amount of MDO in the initial monomer feed was chosen to be higher, with a value of 40 mol%, as it was hypothesized that a too low amount of MDO in the polymerization mixture would produce a copolymer with a cloud point having a higher value above 100 °C and hence not experimentally measurable using UV-vis spectrophotometry. Similarly, based on the previous results obtained for the homopolymer of poly(MeO_2VAc) (Figure 5.11, cloud point = 83 °C), the homopolymerization of MeO_3VAc was not performed in this study as its cloud point would be significantly higher and therefore not experimentally measureable. Under the aforementioned copolymerization conditions, the successful synthesis of poly(MDO-*co*-MeO_3VAc), with defined molecular weights and a low dispersity, $Đ_M$ of 1.47, was confirmed

by ^{1}H NMR spectroscopy (Figure 5.25) and SEC analyses (Figure 5.24), with a final incorporation of 27 mol% in MDO in the backbone (Table 5.5).

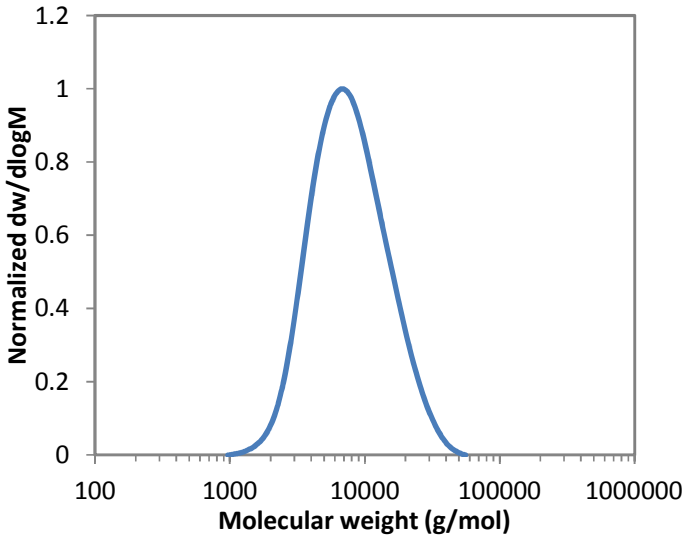

Figure 5.24. Size exclusion chromatogram of poly(MDO-*co*-MeO_3VAc) obtained by the RAFT/MADIX polymerization using CTA 4 as the chain transfer agent with an initial monomer feed of 73 mol% MeO_3VAc, (SEC, $CHCl_3$).

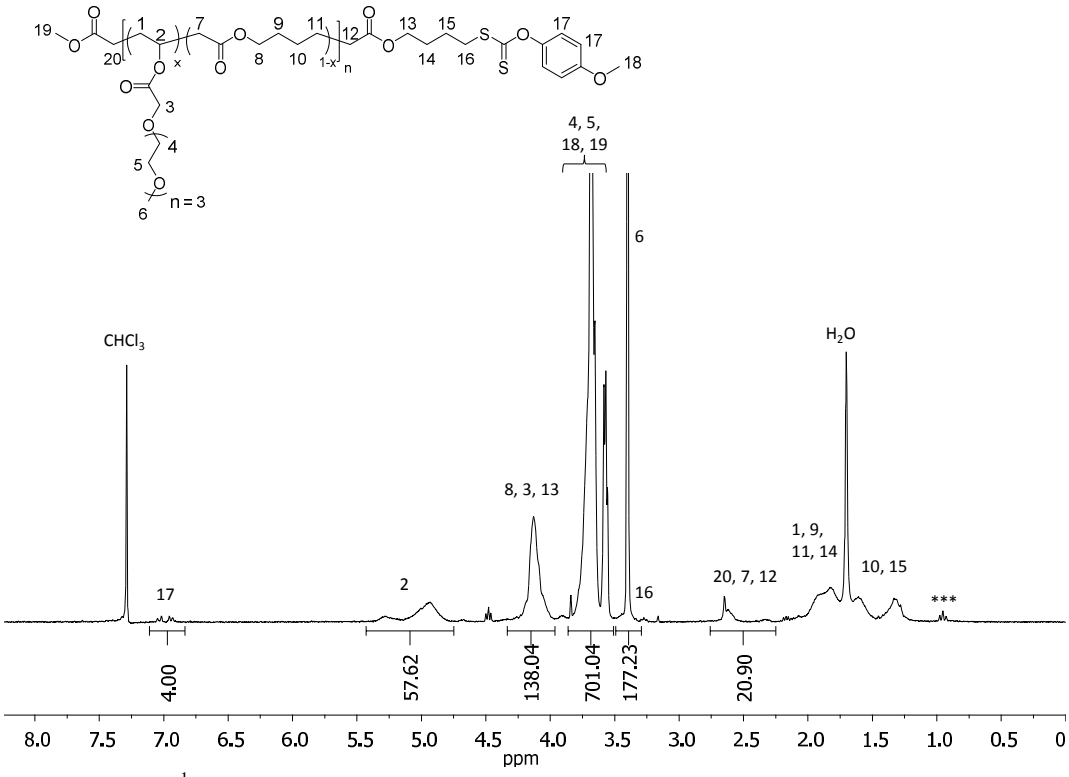

Figure 5.25. ^{1}H NMR spectrum of poly(MDO-*co*-MeO_3VAc) synthesized using RAFT/MADIX polymerization and CTA 4 as the chain transfer agent, (300 MHz, $CDCl_3$), *** residual hexane trace.

5.3.8 Solubility and comparison of the thermoresponsive behaviour

As in the previous copolymers investigated in section 5.3.4, all the samples of poly(MeOVAc), poly(MDO-*co*-MeOVAc) and poly(MDO-*co*-MeO_3VAc) were found to be directly soluble in aqueous medium and at room temperature. Analysis of each solution at a concentration of 5.0 mg/mL using DLS also suggested the presence of unimers as seen by the small sized populations which were observed in all the traces of each polymer solution (Figures 5.26 and 5.27). Additionally, similarly to the previous DLS results of the other copolymers, larger population were observed around 100 – 400 nm and were assigned to potential aggregation of polymer chains in each solution.

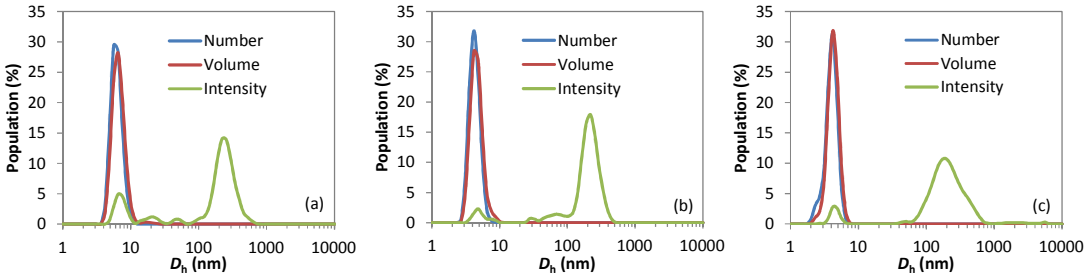

Figure 5.26. Dynamic light scattering traces of the solutions obtained from the direct dissolution of (a) poly(MeOVAc), (b) poly(MDO-*co*-MeOVAc) containing 92 mol% in MeOVAc and (c) poly(MDO-*co*-MeOVAc) containing 86 mol% in MeOVAc, in water at a concentration of 5 mg/mL.

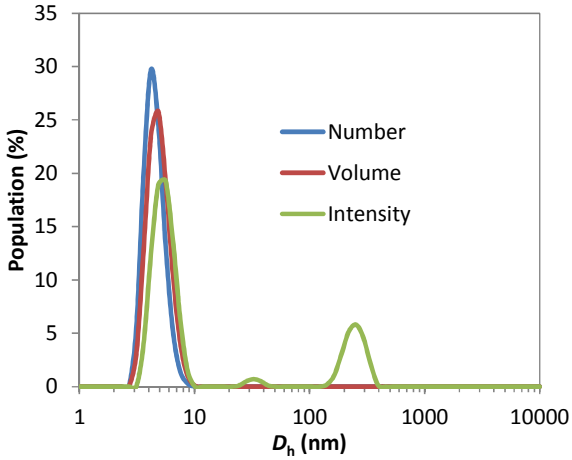

Figure 5.27. Dynamic light scattering traces of the solution obtained from the direct dissolution of poly(MDO-*co*-MeO_3VAc) containing 73 mol% in MeO_3VAc in water at a concentration of 5 mg/mL.

Further turbidimetry experiments were performed on the homopolymer poly(MeOVAc) and copolymers poly(MDO-*co*-MeOVAc) over a temperature range of 5 to 90 °C at a heating rate of 1.0 °C/min. Under these conditions, the solubility of the three samples was found to vary with temperature as seen by the net decrease in transmittance measured by the UV-vis instrument (Figure 5.28). Indeed, the homopolymer was found to exhibit a cloud point of 57 °C, which decreased to values of 44 and 29 °C for copolymers containing 92 and 84 mol% MeOVAc in the polymer backbone respectively. These observations suggest, similar to the case of poly(MDO-*co*-MeO_2VAc), that the thermo-responsive properties of the new polymer system, poly(MDO-*co*-MeOVAc), could also be tuned by simply changing the incorporation of MeOVAc in the final polymer backbone through varying the monomer feed ratio in the initial polymerization mixture.

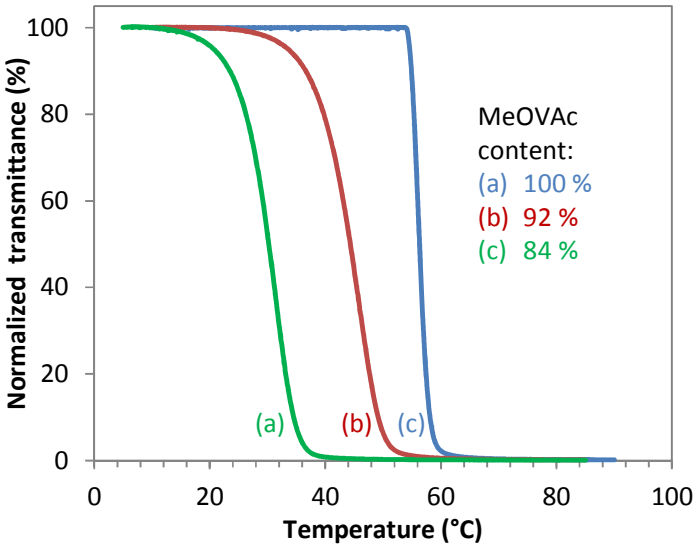

Figure 5.28. Plots of normalized transmittance *vs*. temperature obtained by turbidimetry analysis for the solution of (a) poly(MeOVAc) (b) poly(MDO-*co*-MeOVAc) containing 92 mol% in MeOVAc and (c) poly(MDO-*co*-MeOVAc) containing 84 mol% in MeOVAc, in water at a concentration of 5 mg/mL.

Additionally, comparison between the thermoresponsive properties of both homopolymers, poly(MeOVAc) and poly(MeO_2VAc), was made and revealed a difference of phase transition temperature, ΔT, of 26 °C for the two polymers with cloud points of 57 and 83 °C

respectively (Figure 5.29). This result further indicated that the phase transition temperature of the polymer in solution could also be easily tuned by adding or removing one oligo(ethylene glycol) repeat unit in the hydrophilic vinyl acetate derived monomers investigated in this Chapter. This observation was in good agreement with the previously results reported by Han *et al*. for the homopolymers of 2-(methoxyethoxy)ethyl methacrylate and 2-[2-(methoxyethoxy)ethoxy]ethyl methacrylate which yielded LCST values of 25 and 52 °C respectively.[23]

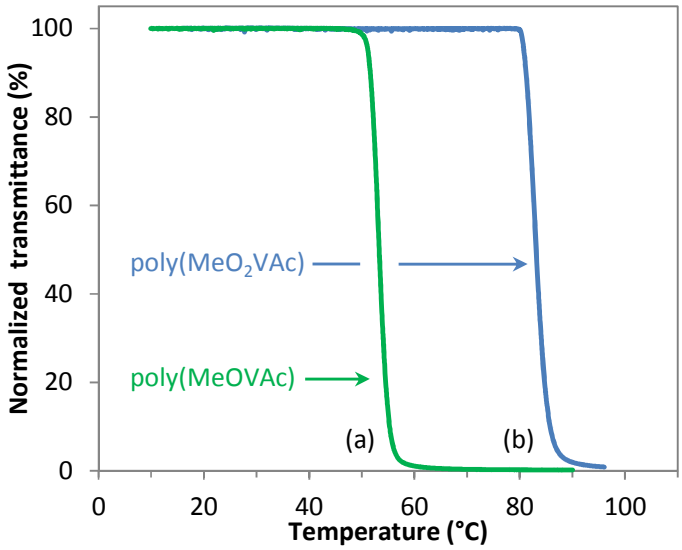

Figure 5.29. Plots of normalized transmittance *vs*. temperature obtained by turbidimetry analysis for the solution of (a) poly(MeOVAc) and (b) poly(MeO_2VAc), in water at a concentration of 5 mg/mL.

To further confirm the influence of the length of the oligo(ethylene glycol) unit on the phase transition temperature, a similar comparison was performed using copolymers of poly(MDO-*co*-MeOVAc), poly(MDO-*co*-MeO_2VAc) and poly(MDO-*co*-MeO_3VAc), all having a similar content of MeO_nVAc in their polymer backbones in order to avoid the aforestated effect of the copolymer compositions on thermo-responsive properties. For the copolymers of poly(MDO-*co*-MeOVAc) and poly(MDO-*co*-MeO_2VAc) containing 90 – 92 mol% of MeO_nVAc, the cloud points obtained by turbidimetric analysis were measured at 44 and

64 °C respectively (Figure 5.30), suggesting a difference of phase transition temperature, ΔT, of 20 °C, similar to the difference obtained for the two homopolymers (ΔT = 26 °C).

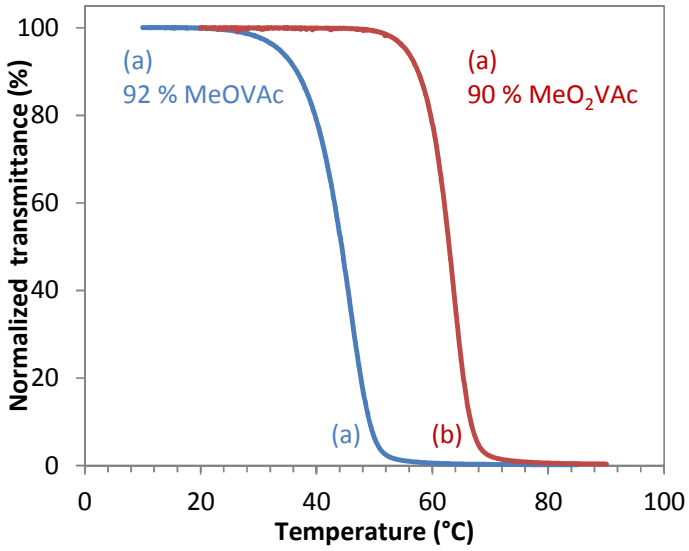

Figure 5.30. Plots of normalized transmittance *vs*. temperature obtained by turbidimetry analysis for the solution of (a) poly(MDO-*co*-MeOVAc) containing 92 mol% in MeOVAc and (b) poly(MDO-*co*-MeO_2VAc) containing 90 mol% in MeO_2VAc, in water at a concentration of 5 mg/mL.

Similarly, turbidimetry measurements of the copolymer of poly(MDO-*co*-MeO_2VAc) and poly(MDO-*co*-MeO_3VAc) containing 71 – 73 mol% of MeO_nVAc within their backbones revealed cloud points of 36 and 64 °C for the shorter and longer versions respectively (Figure 5.31) and hence showing a difference of phase transition of ΔT of 28 °C for this system. These results confirmed the versatility of the process reported in this Chapter to produce hydrophilic polymers and copolymers having tuneable thermoresponsive properties through varying the length of the oligo(ethylene glycol) functionality contained within the vinyl acetate derived monomers.

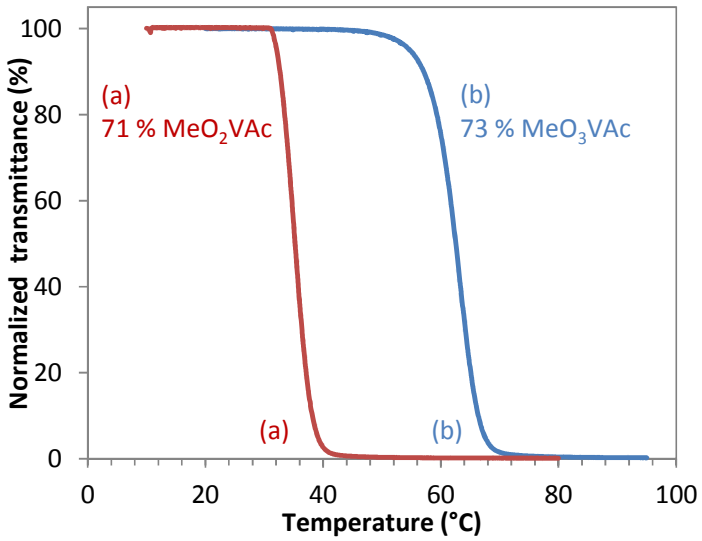

Figure 5.31. Plots of normalized transmittance *vs*. temperature obtained by turbidimetry analysis for the solution of (a) poly(MDO-*co*-MeO_2VAc) containing 71 mol% in MeO_2VAc and (b) poly(MDO-*co*-MeO_3VAc) containing 73 mol% in MeO_3VAc, in water at a concentration of 5 mg/mL.

5.3.9 Degradation experiments

Following on from the successful formation of hydrophilic polymers having tunable thermoresponsive properties, degradation experiments were performed on the copolymers of poly(MDO-*co*-MeOVAc) and poly(MDO-*co*-MeO_2VAc) in order to assess the degradability of the copolymers produced under different hydrolysis conditions. The degradability of poly(MDO-*co*-MeO_2VAc) was firstly investigated at 37 °C under basic conditions using a solution of potassium hydroxide in methanol (0.1 M). These hydrolysis conditions were previously used in Chapters 2 and 3 to successfully degrade poly(MDO-*co*-VAc) and poly(MDO-*co*-VBr) during a short period of exposure (typically 1 – 2 h) depending on the amount of MDO incorporated in the final copolymers. For such conditions, the successful degradation of poly(MDO-*co*-MeO_2VAc) containing 20 mol% of MDO was successfully monitored by the net decrease of the polymer's molecular weight observed by SEC analysis, confirming that the incorporation of MDO in the polymer backbone was affording degradability to the copolymers (Figure 5.32a). The degradation was also found to occur

rapidly with only 5 min in the basic solution required to fully hydrolyze the copolymer sample. Nevertheless, when the hydrolysis time was extended to 45 min, no further degradation could be observed by SEC analysis suggesting that all the degradable linkages introduced in the copolymers were cleaved during the first five minutes of the degradation (Figure 5.32b). This observation indicated that the increased hydrophilicity of the copolymers obtained using MeO_2VAc as a co-monomer with MDO was leading to a significant increase of the degradation rate when compared with other analogous copolymers containing hydrophobic properties and hence requiring longer hydrolysis times (Chapter 3).

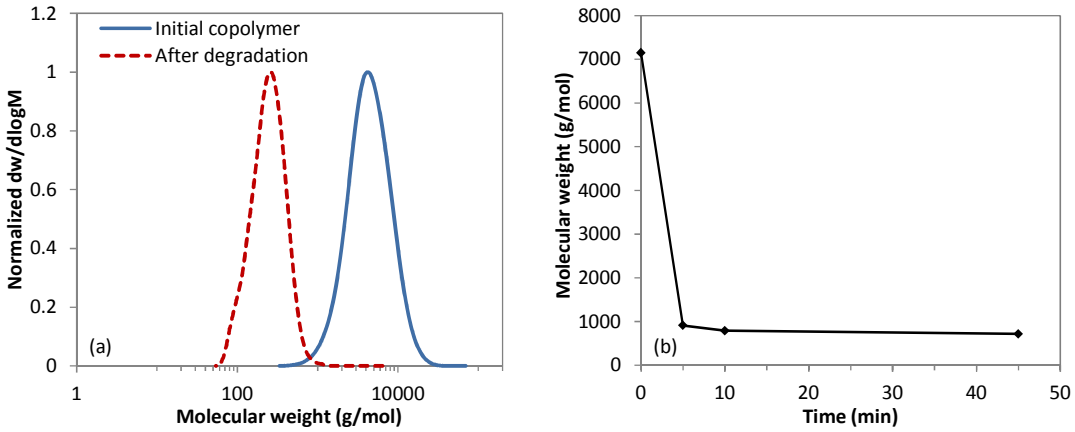

Figure 5.32. (a) Size exclusion chromatograms of poly(MDO-*co*-MeO_2VAc) before and after 10 min of degradation in methanolic potassium hydroxide (0.1 M), (SEC, $CHCl_3$) and (b) the decrease of molecular weight *versus* time of exposure.

Degradation of hydrophilic copolymers of a CKA monomer under enzymatic conditions have previously been reported by Agarwal and co-workers for the successful degradation of hydrophilic gels composed of vinyl cyclopropane (VCP), 2-methylene-4-phenyl-1,3-dioxolane (MPDL, **CKA 7**), a functionalized version of MDO) and oligo(ethylene glycol) methacrylate (OEGMA) monomers.[46] Under these biological conditions, the degradation of the gels was found to occur over 35 days confirming the cleavage of the ester repeat unit in the polymeric structure.

Aiming at investigating the degradation of the hydrophilic and thermo-responsive copolymers synthesised in this Chapter under enzymatic conditions, experiments were carried out with immobilized *Lipase* from *Candida antarctica* in order to study the degradation process under a more biological medium. In a first experiment, the degradation of two copolymers having similar thermoresponsive properties (cloud point ≈ 32 °C for a concentration of 5 mg/mL) was investigated. Poly(MDO-*co*-MeOVAc) containing 10 mol% MDO and poly(MDO-*co*-MeO_2VAc) containing 33 mol% MDO were dissolved in a phosphate buffer solution (PBS, pH = 7.4) and enzyme beads (*Lipase* immobilized from *Candida antarctica*, 200 U/g) were added to the mixture and stirred at room temperature for 6 days. The beads were changed every 24 h in order to keep the activity of enzyme in solution constant throughout the study. Under these conditions, the degradation successfully occurred, with net shift of the molecular weight distribution (as analysed by SEC) to lower values suggesting the formation of oligomers species in the solution for each copolymers (Figure 5.33).

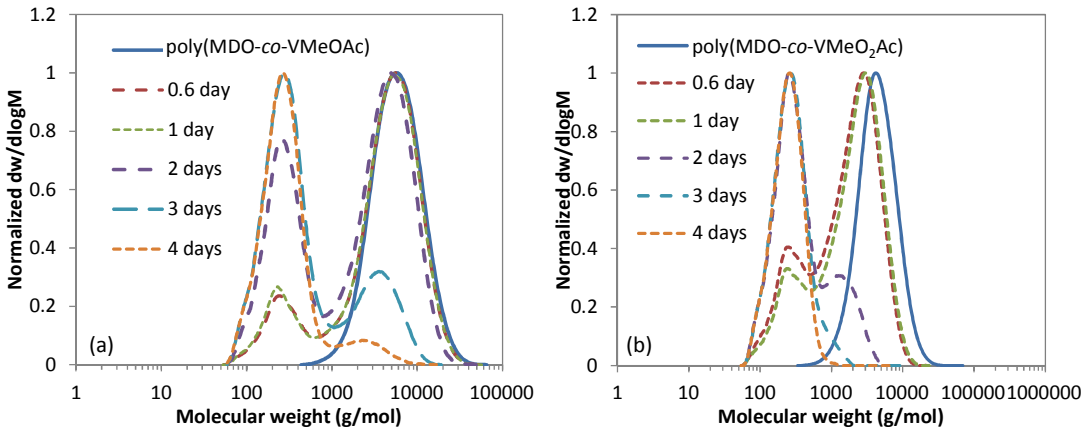

Figure 5.33. Size exclusion chromatograms of (a) poly(MDO-*co*-MeOVAc) and (b) poly(MDO-*co*-MeO_2VAc) during their enzymatic degradation, at 25 °C for different time points, (SEC, $CHCl_3$).

Further analysis on the degraded samples using SEC revealed that the degradation was faster in the case of poly(MDO-*co*-MeO_2VAc) with 3 days were required to fully degrade the sample in comparison to the 4 days needed for poly(MDO-*co*-MeOVAc) (Figure 5.34). This

observation was consistent with the fact that poly(MDO-*co*-MeO_2VAc) contains a larger amount of ester repeat units (33 mol%) in its polymer backbone compared to poly(MDO-*co*-MeOVAc) which has approximately three times less MDO in its backbone (10 mol%). This result further supports the possibility of tuning the rate of degradation of CKA copolymers by simply varying the copolymer compositions as previously investigated in Chapter 3 for the degradation of poly(MDO-*co*-VBr) where different rates of hydrolysis were similarly obtained.

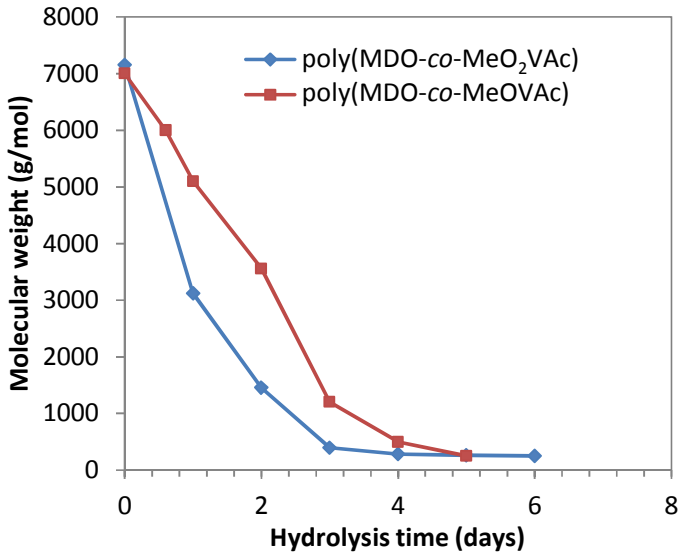

Figure 5.34. Molecular weight changes occurring during the hydrolysis of poly(MDO-*co*-MeOVAc) and poly(MDO-*co*-MeO_2VAc) at different time points, in a PBS/enzyme solution at 25 °C.

Recent work of Xu and co-workers investigated the degradation of co-assemblies of poly(ethylene glycol)-*b*-poly(lactide) (PEG-*b*-PLA) and poly(*N*-isopropylacrylamide)-*b*-poly(lactid acid) (PNIPAm-*b*-PLA) under enzymatic *proteinase K* degradation conditions at different temperatures.[47] In their study, different rates of degradation were successfully observed depending on whether the hydrolysis was performed below or above the LCST of PNIPAm. Above their LCST, the structure existed as collapsed particles and therefore hydrolysable bonds were protected from the *proteinase K* degradation, whereas below the LCST the particles were more soluble and the core permeable and therefore susceptible to

degradation. Aiming at investigating this behaviour, alteration of the degradation conditions were altered in order to study the degradation of poly(MDO-*co*-MeO_2VAc) containing 33 mol% MDO (cloud point ≈ 32 °C for a concentration of 5 mg/mL) at temperatures above and below its cloud point, at 25 and 37 °C respectively. Under these two different conditions, different rates of degradation could potentially be obtained: at 25 °C, poly(MDO-*co*-MeO_2VAc) would be fully soluble in the aqueous medium as it is be situated below its phase separation temperature, whereas at 37 °C the copolymer should phase separate with the medium and therefore be insoluble in the medium. Nevertheless, when the experiment was performed, SEC analysis revealed the full degradation of both samples after 3 days regardless of the hydrolysis being performed at 25 or 37 °C (Figure 5.35). This result suggested that under these enzyme conditions, the phase separation of the copolymer did not affect the rate at which the samples were degrading. While these results were found to be inconclusive, it is hypothesised that, with correct optimization of the degradation conditions, it would be possible to sufficiently reduce the degradation rate to a level in which the state of the polymer would have an impact (below or above the cloud point). Further optimization experiments would confirm this hypothesis.

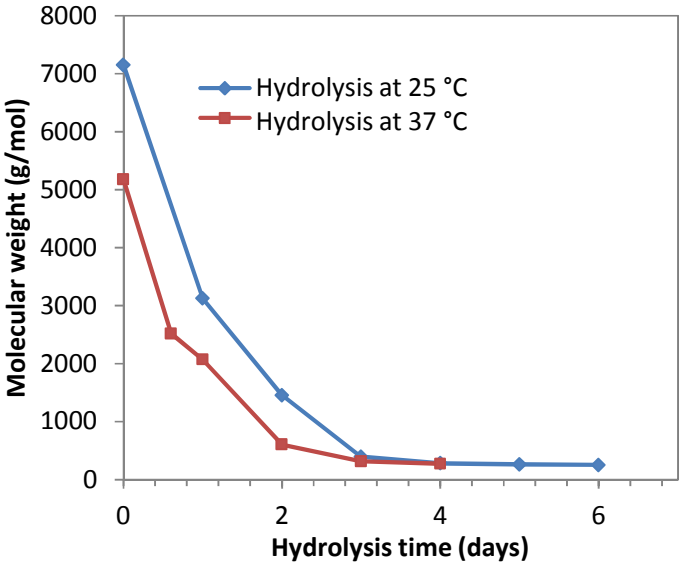

Figure 5.35. Molecular weight changes occurring during the hydrolysis of two poly(MDO-*co*-MeO_2VAc) at 33% MeO_2VAac samples at different time points, in a PBS/enzyme solution at 25 and 37 °C.

5.4 Conclusions

In this Chapter, the synthesis of a new type of hydrophilic vinyl acetate derived monomer was demonstrated though the use of a palladium vinyl exchange reaction between VAc and 2-[2-(2-methoxyethoxy)ethoxy] acetic acid, to yield di(ethylene glycol) methyl ether vinyl acetate (MeO_2VAc) as confirmed by ^{1}H and ^{13}C NMR spectroscopy. The homopolymerization and copolymerization of MeO_2VAc with MDO using the RAFT/MADIX polymerization technique was found to produce polymers and copolymers with controlled molecular weights as confirmed by SEC and ^{1}H NMR spectroscopic analyses. Further analysis using turbidimetry revealed the presence of a cloud point for both the homopolymer of poly(MeO_2VAc) and copolymers of poly(MDO-*co*-MeO_2VAc). Interestingly, the thermoresponsive properties were found to be easily tuned by varying the copolymer composition to yield to polymers with cloud point values ranging from 4 to 83 °C. The concept was further extended to two other monomers, MeOVAc and MeO_3VAc, containing a shorter or longer oligo(ethylene glycol) functionality within the monomer, to produce polymers with similar thermoresponsive properties as seen by the presence of phase

separations between 29 and 63 °C depending on the concentration of MeO_nVAc introduced in the polymer backbone. Additionally, hydrolysis experiments on these copolymers under basic and enzymatic conditions confirmed the successful degradation of these novel hydrophilic and thermoresponsive polymers, a parameter which has been sparsely investigated in the literature despite the vast range of thermoresponsive polymers currently available.

5.5 Experimental Section

5.5.1 Materials

The following reagents were used as received: vinyl acetate (VAc: Sigma-Aldrich, > 99%), 2-[2-(2-methoxyethoxy)ethoxy] acetic acid ($C_6H_{12}O_5$: VWR International, AR grade), 2-(2-methoxyethoxy) acetic acid ($C_4H_8O_4$: Sigma-Aldrich, technical grade), tetra(ethylene glycol) monomethyl ether (TEGME: Sigma-Aldrich, technical grade), potassium hydroxide (KOH: Fisher Scientific, 90%), palladium acetate ($Pd(OAc)_2$, Sigma-Aldrich, 98%), potassium permanganate ($KMnO_4$, Sigma-Aldrich, > 99%), magnesium sulfate ($MgSO_4$: anhydrous, Fisher Scientific, LR grade), silica gel (SiO_2: Apollo Scientific, 40 – 63 μm). 1,1'-azobis-(cyclohexanocarbonitrile) (ABCN: Sigma-Aldrich, 98%) was recrystallized from methanol prior to use. The following solvents were used as received: dichloromethane (DCM: VWR International, AR grade), ethyl acetate (EtOAc, Fisher Scientific, LT grade), tetrahydrofuran (THF, VWR International, AR grade), hexane (C_6H_{14}, Sigma-Aldrich, HPLC grade) and methanol (CH_3OH, Fisher Scientific, LT grade), Diethyl ether (VWR International, AR grade). The enzyme used for the degradation- *Lipase,* immobilized from *Candida antarctica* (Sigma-Aldrich, beads > 2 U/mg) were used as received and kept at a low temperature (5 °C) prior use. 2-Methylene-1,3-dioxepane (MDO) was synthesized using the previously described method of Bailey *et al.*,[48] the chain

transfer agent *p*-methoxyphenyl xanthate (CTA 4) was synthesized using the procedure described in Chapter 4.[49] The water used for the dissolution of the polymers for LCST measurements was purified using an ion exchange cartridge (18.2 MΩ/cm).

5.5.2 Characterization

Nuclear magnetic resonance (^{1}H and ^{13}C NMR) spectra were recorded at 400 MHz, 100 (or 125) MHz, respectively, in $CDCl_3$ on a Bruker DPX-400 spectrometer at 298 K. Chemical shifts are reported as δ in parts per million (ppm) and referenced to the chemical shift of the residual solvent resonances ($CDCl_3$ ^{1}H: δ = 7.26 ppm; ^{13}C: δ = 77.16 ppm). Size exclusion chromatography (SEC) analysis was performed on a system composed of a Varian 390-LC-Multi detector suite using a Varian Polymer Laboratories guard column (PLGel 5 μM, 50 × 7.5 mm), two mixed-D Varian Polymer Laboratories columns (PLGel 5 μM, 300 × 7.5 mm) and a PLAST RT autosampler. Detection was conducted using a differential refractive index (RI) and an ultraviolet (UV) detector set to λ = 280 nm. The analyses were performed at 313 K in $CHCl_3$ (HPLC grade) containing 0.5% w/w triethyl amine (TEA) at a flow rate of 1.0 mL/min. Polystyrene (PS) (162 – 2.4 × 10^5 g/mol) standards were used for calibration. Molecular weights and dispersities were determined using Cirrus v3.3 SEC software. DLS analysis was performed on a Malvern Zetasizer Nano ZS instrument operating at 25 °C with a 4 Mw He-Ne 633 nm laser module. Measurements were made at an angle of 173° (back scattering), and results were analyzed using Malvern DTS 6.3 software. All determinations were made in triplicate unless otherwise stated (with 10 measurements recorded for each run). SLS experiments were performed at angles of observation ranging from 20° up to 150° with an ALV CG3 spectrometer operating at λ_0 = 633 nm and at 20 ± 1 °C. Solutions (1 mg/mL) were filtered through 0.45 μm nylon filters prior to analysis. Data were collected in duplicate with 100 s run times. Calibration was achieved with filtered toluene and the background was measured with filtered solvent (NaCl 0.1 M). The aggregation number, N_{agg} of the self-assemblies was calculated using the REPES algorithm.[50] All turbidimetric

analysis was performed at a concentration of 5.0 mg/mL, unless otherwise stated, by UV-visible spectrophotometry using an Agilent Cary 60/visible spectrophotometer. The absorbance was set at 550 nm and a heating rate of 1 °C/min was applied. The hysteresis investigation was performed at a concentration of 5.5 mg/mL by UV-visible spectrophotometry using a Perkin-Elmer Lambda 35 UV-visible spectrophotometer fitted with a Peltier heating and cooling system at a heating and cooling rate of 1 °C/min and performed at a wavelength of 500 nm. Data was normalized between 0 and 100, plotted in terms of transmittance (%), and the cloud point was defined as the temperature at which the normalized transmittance equals 50%.

5.5.3 Procedure for the synthesis of MeO_2VAc monomer

A solution of 2-[2-(2-methoxyethoxy)ethoxy] acetic acid (32.02 g, 179.7 mmol), KOH (1.0 g, 17.8 mmol) and $Pd(OAc)_2$ (2.0 g, 8.90 mmol) in vinyl acetate (VAc) (153.30 g, 1780.9 mmol) was stirred at 60 °C for 16 h. The solution was then filtered over celite and thoroughly washed with diethyl ether (100 mL) in order to remove the excess of catalyst. The excess of vinyl acetate and solvent (diethyl ether) were evaporated under reduced pressure using rotary evaporation. The crude product was purified and isolated by column chromatography (Silica, 7:3, EtOAc/hexane) before being dried over anhydrous $MgSO_4$, and then reduced to dryness using rotary evaporation, to yield to a pale brown liquid. R_f (EtOAc/hexane 7:3) 0.46. The monomer was further purified by vacuum distillation (0.3 mmHg / 130 °C) to yield a colorless liquid (22.3 g, 109.30 mmol, 61%). ^{1}H NMR (400 MHz, $CDCl_3$, ppm) δ: 7.26 (dd, COOC*H*CH_2, 1H, $^3J_{H\text{-}H}$ = 13.8 Hz, $^3J_{H\text{-}H}$ = 7.7 Hz), 4.90 (dd, COOCHC*H*H, 1H, $^3J_{H\text{-}H}$ = 13.8 Hz, $^2J_{H\text{-}H}$ = 1.7 Hz), 4.60 (dd, COOCHCH*H*, 1H, $^3J_{H\text{-}H}$ = 6.3 Hz, $^2J_{H\text{-}H}$ = 1.8 Hz), 4.20 (s, OCOC*H*$_2$O, 2H), 3.74 – 3.48 (m, (C*H*$_2$C*H*$_2$O)$_2$, 8H), 3.33 (s, $CH_2CH_2OCH_3$, 3H). ^{13}C NMR (100 MHz, $CDCl_3$) δ: 167.8 (CH_2CHOCO), 140.5 (CH_2CHCOO), 98.3 (CH_2CHCOO), 70.9 – 70.4 (CH_2CH_2O), 68.1 ($OCOCH_2O$), 58.9

($CH_2CH_2OCH_3$). Elemental analysis: Calculated for $C_9H_{16}O_5$: C, 52.93%; H, 7.90%. Found: C, 52.09%; H, 7.98%. FTIR (ν_{max}, cm^{-1}): 2995 (C-H alkyl stretch), 1772 (C=O stretch), 1646 (C-O stretch), 1116 (C-O-C stretch), 950 (C-H bending).

5.5.4 General procedure for the homopolymerization of MeO_2VAc

In an inert environment, MeO_2VAc (0.30 g, 1.47 mmol), CTA 4 (4.30 mg, 0.015 mmol), ABCN (0.50 mg, 2.04×10^{-3} mmol) were placed into an ampoule and sealed. The solution was subjected to a further three freeze-pump-thaw cycles and backfilled with nitrogen. The resulting solution was stirred and heated to 90 °C for 6 h before the polymerization was quenched by plunging the ampoule into an ice bath. An aliquot was taken prior to precipitation for monomer conversion analysis by ^{1}H NMR spectroscopy. The polymer was dissolved in a small amount of DCM (0.50 mL) and precipitated several times into hexane until no further monomer residue was observed. The light yellow solid was dried under vacuum at room temperature for 24 h. ^{1}H NMR (400 MHz, $CDCl_3$, ppm) δ: 7.10 – 6.90 (dd, Ar, 4H, $^3J_{H\text{-}H}$ = 9.0 Hz), 5.10 – 4.72 (m, CH_2CH backbone, 1H), 4.20 – 3.80 (m, $OCOCH_2(OCH_2CH_2)_2$ side chain, 2H), 3.75 – 3.45 (m, $(CH_2CH_2O)_2$ side chain, 2H, $(CH_2CH_2O)_2$ side chain, 2H, CH_3OCOCH_2 end-group, 3H, Ar-OCH_3, 3H), 2.50 (m, CH_3OCOCH_2 end-group, 2H), 3.45 – 3.30 (m, $(CH_2CH_2O)_2CH_3$ side chain, 3H), 1.95 – 1.60 (m, CH_2CH backbone, 2H). Conversion: MeO_2VAc = 38%. M_n (^{1}H NMR, $CDCl_3$) = 9.2 kg/mol, M_n (SEC, $CHCl_3$) = 5.3 kg/mol, $Đ_M$ = 1.39.

5.5.5 General procedure for the copolymerization of MDO and MeO_2VAc

In an inert environment, MeO_2VAc (0.50 g, 2.45 mmol), MDO (0.11 g, 0.96 mmol), CTA 4 (9.90 mg, 3.6×10^{-2} mmol) and ABCN (0.80 mg, 3.27×10^{-3} mmol) were placed into an ampoule and sealed. The resulting solution was subjected to a further three freeze-pump-thaw cycles and then backfilled with nitrogen. The resulting solution was stirred and heated

to 90 °C for 9 h before the polymerization was quenched by plunging the ampoule into an ice bath. An aliquot was taken prior precipitation for conversion analysis by ^{1}H NMR spectroscopy. The polymer was dissolved in a small amount of DCM (0.20 mL) and precipitated several times into hexane until no further monomer residue was observed. The final light yellow solid was dried under vacuum at room temperature for 24 h. ^{1}H NMR (400 MHz, $CDCl_3$, ppm) δ: 7.10 – 6.90 (dd, Ar, 4H, $^{3}J_{H\text{-}H}$ = 8.9 Hz), 5.25 – 4.75 (m, CH_2CH backbone, 1H), 4.20 – 3.80 (m, $OCOCH_2(OCH_2CH_2)_2$, 2H, $COOCH_2CH_2CH_2$ backbone, 4H), 3.75 – 3.45 (m, $(CH_2CH_2O)_2$ side chain, 2H, $(CH_2CH_2O)_2$ side chain, 2H, CH_3OCOCH_2 end-group, 3H, Ar-OCH_3, 3H), 3.45 – 3.25 (m, $(CH_2CH_2O)_2CH_3$ side chain, 3H, CH_2CH_2SCSO end-group, 2H), 2.60 – 2.15 (m, CH_3OCOCH_2 end-group, 2H, $CH_2COOCH_2CH_2$ backbone, 2H), 1.95 – 1.45 (m, $CHCH_2$ backbone, 2H, $COOCH_2CH_2CH_2CH_2$ backbone, 2H, $COOCH_2CH_2CH_2CH_2$ backbone, 2H, $CH_2CH_2CH_2SCS$ end-group, 2H), 1.45 – 1.10 (m, $COOCH_2CH_2CH_2CH_2$, 2H, CH_2CH_2SCS end-group, 2H). Conversions: MeO_2VAc = 45%, MDO = 28%. M_n (^{1}H NMR, $CDCl_3$) = 12.2 kg/mol, M_n (SEC, $CHCl_3$) = 7.7 kg/mol, $Đ_M$ = 1.40.

5.5.6 Procedure for the synthesis of MeOVAc monomer

A solution of 2-(2-methoxyethoxy) acetic acid (32.02 g, 187.9 mmol), KOH (1.0 g, 17.8 mmol) and $Pd(OAc)_2$ (2.0 g, 8.90 mmol) in vinyl acetate (VAc) (161.3 g, 1873.4 mmol) was stirred at 60 °C for 16 h. The solution was filtered over celite and thoroughly washed with diethyl ether (100 mL) in order to remove the excess of catalyst. The excess of vinyl acetate and solvent (diethyl ether) were evaporated under reduced pressure using rotary evaporation. The crude product was purified and isolated by column chromatography (Silica, 7:3, EtOAc/hexane) before being dried over anhydrous $MgSO_4$, and then reduced to dryness using rotary evaporation to yield to a pale brown liquid. R_f (EtOAc/hexane 7:3) 0.38. The monomer was further purified by vacuum distillation (0.3 mmHg / 90 °C) to yield a colorless

liquid (17.5 g, 109.25 mmol, 58%). ^{1}H NMR (400 MHz, $CDCl_3$, ppm) δ: 7.33 (dd, COOC*H*CH_2, 1H, $^{3}J_{H\text{-}H}$ = 13.0 Hz, $^{3}J_{H\text{-}H}$ = 6.0 Hz), 4.95 (dd, COOCHC*H*H, 1H, $^{3}J_{H\text{-}H}$ = 13.9 Hz, $^{2}J_{H\text{-}H}$ = 1.7 Hz), 4.62 (dd, COOCHCH*H*, 1H, $^{3}J_{H\text{-}H}$ = 6.2 Hz, $^{2}J_{H\text{-}H}$ = 1.7 Hz), 4.24 (s, OCOC*H*$_2$O, 2H), 3.74 (m, C*H*$_2$CH$_2$O, 2H), 3.60 (m, CH$_2$C*H*$_2$O, 2H), 3.38 (m, CH$_2$CH$_2$OC*H*$_3$, 3H). ^{13}C NMR (100 MHz, $CDCl_3$) δ: 167.6 (CH$_2$CH*C*OO), 140.5 (CH$_2$*C*HCOO), 98.5 (*C*H$_2$CHCOO), 71.9 (*C*H$_2$CH$_2$O), 70.9 (CH$_2$*C*H$_2$O), 68.1 (COO*C*H$_2$O), 58.9 (CH$_2$CH$_2$O*C*H$_3$). FTIR (ν_{max}, cm^{-1}): 2990 (C-H alkyl stretch), 1774 (C=O stretch), 1648 (C-O stretch), 1125 (C-O-C stretch), 952 (C-H bending). Elemental analysis: Calculated for $C_7H_{12}O_4$: C, 52.49%; H, 7.55%; Found: C, 52.30%; H, 7.57%.

5.5.7 Procedure for the synthesis of MeO_3VAc monomer

The monomer MeO_3VAc was synthesized in a two steps procedure. In the first step, 2-2-[2-(2-methoxyethoxy)ethoxy]ethoxy acetic acid was formed as follows: A solution of tetra(ethylene glycol) monomethyl ether (TEGME) (10.4 g, 49.9 mmol), KOH (5.4 g, 96.4 mmol) and potassium permanganate ($KMnO_4$) (15.2 g, 96.4 mmol) in distilled water (1000 mL) was stirred at 0 °C for 2 h. The brown solution was left to stir for a further 16 h at room temperature. The solution was filtered on a Büchner filter, in order to remove the $KMnO_4$ salt, and reduced to ¾ of its original volume using rotary evaporation. The solution was acidified to pH = 2 using HCl (1 M) and the desired product was extracted from the water phase against DCM (200 mL). The solution was dried over anhydrous $MgSO_4$, and then reduced to dryness using rotary evaporation to yield to a colorless liquid (6.1 g, 27.4 mmol, 55%). ^{1}H NMR (400 MHz, $CDCl_3$, ppm) δ: 11.30 (s, CH$_2$COO*H*, 1H), 4.15 (s, C*H*$_2$COOH, 2H), 3.74 – 3.48 (m, C*H*$_2$C*H*$_2$O, 12H), 3.38 (s, CH$_2$CH$_2$OC*H*$_3$, 3H). ^{13}C NMR (100 MHz, $CDCl_3$) δ: 171.3 (CH$_2$*C*OOH), 71.9 – 70.9 (*C*H$_2$*C*H$_2$O), 68.4 (COO*C*H$_2$O), 58.5 (CH$_2$CH$_2$O*C*H$_3$). In the second step, $VMeO_3Ac$ was synthesized as follows: A solution of 2-2-[2-(2-methoxyethoxy)ethoxy]ethoxy acetic acid (4.1 g, 18.4 mmol), KOH (0.10 g, 0.18

mmol) and $Pd(OAc)_2$ (0.20 g, 0.89 mmol) in vinyl acetate (VAc) (16.0 g, 185.8 mmol) was stirred at 60 °C for 16 h. The solution was filtered over celite and thoroughly washed with diethyl ether (10 mL) in order to remove the excess of catalyst. The excess of vinyl acetate and solvent (diethyl ether) were evaporated under reduced pressure using rotary evaporation. The crude product was purified and isolated by column chromatography (Silica, 7:3, EtOAc/hexane), before being dried over anhydrous $MgSO_4$, and reduced to dryness using rotary evaporation to yield to a colorless liquid, (1.2 g, 4.82 mmol, 26%). R_f (EtOAc/hexane 7:3) 0.51. ^{1}H NMR (400 MHz, $CDCl_3$, ppm) δ: 7.28 (dd, COOC*H*CH_2, 1H, $^3J_{H\text{-}H}$ = 13.9 Hz, $^3J_{H\text{-}H}$ = 7.2 Hz), 4.95 (dd, COOCHC*H*H, 1H, $^3J_{H\text{-}H}$ = 13.8 Hz, $^2J_{H\text{-}H}$ = 1.7 Hz), 4.65 (dd, COOCHCH*H*, 1H, $^3J_{H\text{-}H}$ = 6.5 Hz, $^2J_{H\text{-}H}$ = 1.7 Hz), 4.20 (s, OCOC*H*$_2$O, 2H), 3.78 – 3.50 (m, C*H*$_2$C*H*$_2$O, 12H), 3.38 (s, $CH_2CH_2OCH_3$, 3H). ^{13}C NMR (100 MHz, $CDCl_3$) δ: 167.4 (CH_2CHCOO), 140.7 (CH_2CHCOO), 98.1 (CH_2CHCOO), 70.9 – 70.6 (CH_2CH_2O), 68.5 ($COOCH_2O$), 58.5 ($CH_2CH_2OCH_3$). FTIR (ν_{max}, cm^{-1}): 2991 (C-H alkyl stretch), 1776 (C=O stretch), 1647 (C-O stretch), 116 (C-O-C stretch), 948 (C-H bending). Elemental analysis: Calculated for $C_{11}H_{20}O_6$: C, 53.22%; H, 8.12%; Found: C, 52.15%; H, 8.13%.

5.5.8 General procedure for the homopolymerization of MeOVAc

In an inert environment, MeOVAc (0.50 g, 3.10 mmol), CTA 4 (8.50 mg, 0.031 mmol), ABCN (0.76 mg, 3.10× 10^{-3} mmol) were placed into an ampoule and sealed. The solution was subjected to a further three freeze-pump-thaw cycles and backfilled with nitrogen. The resulting solution was stirred and heated to 90 °C for 4.5 h before the polymerization was quenched by plunging the ampoule into an ice bath. An aliquot was taken prior to precipitation for monomer conversion analysis by ^{1}H NMR spectroscopy. The polymer was dissolved in a small amount of DCM (0.50 mL) and precipitated several times into hexane until no further monomer residue was observed. The light yellow solid was dried under vacuum at room temperature for 24 h. ^{1}H NMR (400 MHz, $CDCl_3$, ppm) δ: 7.10 – 6.90 (dd,

Ar, 4H, $^{3}J_{H\text{-}H}$ = 9.0 Hz), 5.10 – 4.80 (m, CH_2CH backbone, 1H), 4.20 – 3.80 (m, $OCOCH_2OCH_2CH_2$ side chain, 2H), 3.75 – 3.45 (m, CH_2CH_2O side chain, 2H, CH_2CH_2O side chain, 2H, CH_3OCOCH_2 end-group, 3H, Ar-OCH_3, 3H), 3.45 – 3.30 (m, $CH_2CH_2OCH_3$ side chain, 3H), 2.50 (m, CH_3OCOCH_2 end-group, 2H), 1.95 – 1.60 (m, CH_2CH backbone, 2H). Conversion: MeOVAc = 42%. M_n (^{1}H NMR, $CDCl_3$) = 7.7 kg/mol, M_n (SEC, $CHCl_3$) = 4.7 kg/mol, $Đ_M$ = 1.46.

5.5.9 General procedure for the copolymerization of MDO and MeOVAc

In an inert environment, MeOVAc (0.40 g, 2.50 mmol), MDO (0.03 g, 0.26 mmol), CTA 4 (7.50 mg, 2.6 × 10^{-2} mmol) and ABCN (0.68 mg, 2.78 × 10^{-3} mmol) were placed into an ampoule and sealed. The resulting solution was subjected to a further three freeze-pump-thaw cycles and then backfilled with nitrogen. The resulting solution was stirred and heated to 90 °C for 4.5 h before the polymerization was quenched by plunging the ampoule into an ice bath. An aliquot was taken prior to precipitation for conversion analysis by ^{1}H NMR spectroscopy. The polymer was dissolved in a small amount of DCM (0.50 mL) and precipitated several times into hexane until no further monomer residue was observed. The final light yellow solid was dried under vacuum at room temperature for 24 h. ^{1}H NMR (400 MHz, $CDCl_3$, ppm) δ: 7.10 – 6.90 (dd, Aromatic, 4H, $^{3}J_{H\text{-}H}$ = 9.0 Hz), 5.25 – 4.75 (m, CH_2CH backbone, 1H), 4.20 – 3.80 (m, $OCOCH_2OCH_2CH_2$ side chain, 2H, $COOCH_2CH_2CH_2$ backbone, 2H), 3.75 – 3.45 (m, CH_2CH_2O side chain, 2H, CH_2CH_2O side chain, 2H, CH_3OCOCH_2 end-group, 3H, Aromatic-OCH_3, 3H), 3.45 – 3.25 (m, $CH_2CH_2OCH_3$ side chain, 3H, CH_2CH_2SCSO end-group, 2H), 2.60 – 2.15 (m, CH_3OCOCH_2 end-group, 2H, $CH_2COOCH_2CH_2$ backbone, 2H), 1.95 – 1.45 (m, $CHCH_2$ backbone, 2H, $COOCH_2CH_2CH_2CH_2$ backbone, 2H, $COOCH_2CH_2CH_2CH_2$ backbone, 2H, $CH_2CH_2CH_2SCS$ end-group, 2H), 1.45 – 1.10 (m, $COOCH_2CH_2CH_2CH_2$, 2H, CH_2CH_2SCS end-group, 2H).

Conversions: MeOVAc = 43%, MDO = 31%. M_n (^{1}H NMR, $CDCl_3$) = 7.2 kg/mol, M_n (SEC, $CHCl_3$) = 5.6 kg/mol, $Đ_M$ = 1.62.

5.5.10 General procedure for the copolymerization of MDO and MeO_3VAc

In an inert environment, MeO_3VAc (0.40 g, 1.61 mmol), MDO (0.12 g, 1.05 mmol), CTA 4 (7.20 mg, 2.66×10^{-2} mmol) and ABCN (0.66 mg, 2.70×10^{-3} mmol) were placed into an ampoule and sealed. The resulting solution was subjected to a further three freeze-pump-thaw cycles and backfilled with nitrogen. The resulting solution was stirred and heated to 90 °C for 18 h before the polymerization was quenched by plunging the ampoule into an ice bath. An aliquot was taken prior precipitation for conversion analysis by ^{1}H NMR spectroscopy. The polymer was dissolved in a small amount of DCM (0.50 mL) and precipitated several times into hexane until no further monomer residue was observed. The final light yellow solid was dried under vacuum at room temperature for 24 h. ^{1}H NMR (400 MHz, $CDCl_3$, ppm) δ: 7.10 – 6.90 (dd, Ar, 4H, $^3J_{H\text{-}H}$ = 9.0 Hz), 5.25 – 4.75 (m, CH_2CH backbone, 1H), 4.20 – 3.80 (m, $OCOCH_2OCH_2CH_2$ side chain, 2H, $COOCH_2CH_2CH_2$ backbone, 2H), 3.75 – 3.45 (m, $(CH_2CH_2O)_3$ side chain, 2H, $(CH_2CH_2O)_3$ side chain, 2H, CH_3OCOCH_2 end-group, 3H, Ar-OCH_3, 3H), 3.45 – 3.25 (m, $(CH_2CH_2O)_3CH_3$ side chain, 3H, CH_2CH_2SCSO end-group, 2H), 2.60 – 2.15 (m, CH_3OCOCH_2 end-group, 2H, $CH_2COOCH_2CH_2$ backbone, 2H), 1.95 – 1.45 (m, $CHCH_2$ backbone, 2H, $COOCH_2CH_2CH_2CH_2$ backbone, 2H, $COOCH_2CH_2CH_2CH_2$ backbone, 2H, $CH_2CH_2CH_2SCS$ end-group, 2H), 1.45 – 1.10 (m, $COOCH_2CH_2CH_2CH_2$, 2H, CH_2CH_2SCS end-group, 2H). Conversions: MeO_3VAc = 43%, MDO = 24%. M_n (^{1}H NMR, $CDCl_3$) = 8.2 kg/mol, M_n (SEC, $CHCl_3$) = 6.3 kg/mol, $Đ_M$ = 1.47.

5.5.11 Degradation experiments

The initial degradation in basic methanol was performed as follows: 500 mg of copolymer was placed in a 10 mL vial and a solution of KOH in methanol (0.1 M, 6 mL) was then added to the vial and stirred at 40 °C. Samples were taken a different time points and the solvent was removed under vacuum. The polymer residues were re-dissolved in $CHCl_3$ and filtered in order to remove the residual salt, and analyzed by SEC in $CHCl_3$. The degradation under enzymatic conditions was performed as follows: 500 mg copolymer was placed in a 10 mL vial and 10 mL of a phosphate buffer solution (PBS, pH = 7.4) was added to dissolve the sample. Enzymes beads (*Lipase* immobilized from *Candida antarctica* , 0.10 g) were added to the polymer solution and stirred at either 25 or 37 °C. In order to keep the enzymes activities constant throughout the experiment, the beads were replaced every 24 h. Samples were taken a different time points and the solvent (PBS solution) was removed by freeze-drying for 16 h. The polymer residues were re-dissolved in $CHCl_3$ and filtered in order to remove the residual salt, and analyzed by SEC in $CHCl_3$.

5.6 References

(1) Alarcon, C. d. l. H.; Pennadam, S.; Alexander, C. *Chem. Soc. Rev.* **2005**, *34*, 276.

(2) Alexander, C.; Shakesheff, K. M. *Adv. Mater. (Weinheim, Ger.)* **2006**, *18*, 3321.

(3) Roy, D.; Brooks, W. L. A.; Sumerlin, B. S. *Chem. Soc. Rev.* **2013**, *42*, 7214.

(4) Uhlig, K.; Wischerhoff, E.; Lutz, J.-F.; Laschewsky, A.; Jaeger, M. S.; Lankenau, A.; Duschl, C. *Soft Matter* **2010**, *6*, 4262.

(5) Gota, C.; Okabe, K.; Funatsu, T.; Harada, Y.; Uchiyama, S. *J. Am. Chem. Soc.* **2009**, *131*, 2766.

(6) Ward, M. A.; Georgiou, T. K. *Polymers* **2011**, *3*, 1215.

(7) Phillips, D. J.; Gibson, M. I. *Polym. Chem.* **2015**, *6*, 1033.

(8) Moughton, A. O.; O'Reilly, R. K. *Chem. Commun.* **2010**, *46*, 1091.

(9) Gil, E. S.; Hudson, S. M. *Prog. Polym. Sci.* **2004**, *29*, 1173.

(10) Kikuchi, A.; Okano, T. *Prog. Polym. Sci.* **2002**, *27*, 1165.

(11) Taylor, L. D.; Cerankowski, L. D. *J. Polym. Sci., Part A: Polym. Chem.* **1975**, *13*, 2551.

(12) Sershen, S.; West, J. *Adv. Drug Deliv. Rev.* **2002**, *54*, 1225.

(13) Chilkoti, A.; Dreher, M. R.; Meyer, D. E.; Raucher, D. *Adv. Drug Deliv. Rev.* **2002**, *54*, 613.

(14) Scarpa, J. S.; Mueller, D. D.; Klotz, I. M. *J. Am. Chem. Soc.* **1967**, *89*, 6024.

(15) Schild, H. G. *Prog. Polym. Sci.* **1992**, *17*, 163.

(16) Blackman, L. D.; Wright, D. B.; Robin, M. P.; Gibson, M. I.; O'Reilly, R. K. *ACS Macro Lett.* **2015**, *4*, 1210.

(17) Dai, S.; Ravi, P.; Tam, K. C. *Soft Matter* **2009**, *5*, 2513.

(18) Vogt, A. P.; Sumerlin, B. S. *Soft Matter* **2009**, *5*, 2347.

(19) De, P.; Gondi, S. R.; Sumerlin, B. S. *Biomacromolecules* **2008**, *9*, 1064.

(20) Cooperstein, M. A.; Canavan, H. E. *Biointerphases* **2013**, *8*, 19.

(21) Lutz, J.-F.; Hoth, A. *Macromolecules* **2006**, *39*, 893.

(22) Becer, C. R.; Hahn, S.; Fijten, M. W. M.; Thijs, H. M. L.; Hoogenboom, R.; Schubert, U. S. *J. Polym. Sci., Part A: Polym. Chem.* **2008**, *46*, 7138.

(23) Han, S.; Hagiwara, M.; Ishizone, T. *Macromolecules* **2003**, *36*, 8312.

(24) Yamamoto, S.-I.; Pietrasik, J.; Matyjaszewski, K. *J. Polym. Sci., Part A: Polym. Chem.* **2008**, *46*, 194.

(25) Lutz, J.-F.; Akdemir, Ö.; Hoth, A. *J. Am. Chem. Soc.* **2006**, *128*, 13046.

(26) Mertoglu, M.; Garnier, S.; Laschewsky, A.; Skrabania, K.; Storsberg, J. *Polymer* **2005**, *46*, 7726.

(27) Lutz, J.-F. *J. Polym. Sci., Part A: Polym. Chem.* **2008**, *46*, 3459.

(28) Boyer, C.; Whittaker, M. R.; Luzon, M.; Davis, T. P. *Macromolecules* **2009**, *42*, 6917.

(29) Lutz, J.-F.; Andrieu, J.; Üzgün, S.; Rudolph, C.; Agarwal, S. *Macromolecules* **2007**, *40*, 8540.

(30) Pierre, T. S.; Chiellini, E. *J. Bioact. Compat. Polym.* **1986**, *1*, 467.

(31) Kobben, S.; Ethirajan, A.; Junkers, T. *J. Polym. Sci., Part A: Polym. Chem.* **2014**, *52*, 1633.

(32) Agarwal, S. *Polym. J.* **2007**, *39*, 163.

(33) Hedir, G. G.; Bell, C. A.; Ieong, N. S.; Chapman, E.; Collins, I. R.; O'Reilly, R. K.; Dove, A. P. *Macromolecules* **2014**, *47*, 2847.

(34) Hedir, G. G.; Bell, C. A.; O'Reilly, R. K.; Dove, A. P. *Biomacromolecules* **2015**, *16*, 2049.

(35) Allaoua, I.; Goi, B. E.; Obadia, M. M.; Debuigne, A.; Detrembleur, C.; Drockenmuller, E. *Polym. Chem.* **2014**, *5*, 2973.

(36) Obadia, M. M.; Colliat-Dangus, G.; Debuigne, A.; Serghei, A.; Detrembleur, C.; Drockenmuller, E. *Chem. Commun.* **2015**, *51*, 3332.

(37) Liu, X.; Coutelier, O.; Harrisson, S.; Tassaing, T.; Marty, J.-D.; Destarac, M. *ACS Macro Lett.* **2014**, *4*, 89.

(38) Harrisson, S.; Liu, X.; Ollagnier, J.-N.; Coutelier, O.; Marty, J.-D.; Destarac, M. *Polymers* **2014**, *6*, 1437.

(39) Tasaki, K. *J. Am. Chem. Soc.* **1996**, *118*, 8459.

(40) Schmaljohann, D. *Adv. Drug Deliv. Rev.* **2006**, *58*, 1655.

(41) Wang, X.; Qiu, X.; Wu, C. *Macromolecules* **1998**, *31*, 2972.

(42) Lahasky, S. H.; Hu, X.; Zhang, D. *ACS Macro Lett.* **2012**, *1*, 580.

(43) Kujawa, P.; Segui, F.; Shaban, S.; Diab, C.; Okada, Y.; Tanaka, F.; Winnik, F. M. *Macromolecules* **2006**, *39*, 341.

(44) Trzcinska, R.; Szweda, D.; Rangelov, S.; Suder, P.; Silberring, J.; Dworak, A.; Trzebicka, B. *J. Polym. Sci., Part A: Polym. Chem.* **2012**, *50*, 3104.

(45) Xia, Y.; Yin, X.; Burke, N. A. D.; Stöver, H. D. H. *Macromolecules* **2005**, *38*, 5937.

(46) Shi, Y.; Schmalz, H.; Agarwal, S. *Polym. Chem.* **2015**, *6*, 6409.

(47) Xu, Y.; Ma, R.; Zhang, Z.; He, H.; Wang, Y.; Qu, A.; An, Y.; Zhu, X. X.; Shi, L. *Polymer* **2012**, *53*, 3559.

(48) Bailey, W. J.; Ni, Z.; Wu, S.-R. *J. Polym. Sci., Part A: Polym. Chem.* **1982**, *20*, 3021.

(49) Bell, C. A.; Hedir, G. G.; O'Reilly, R. K.; Dove, A. P. *Polym. Chem.* **2015**, *6*, 7447.

(50) Jakeš, J. *Collect. Czech. Chem. Commun.* **1995**, *60*, 1781.

6 Amphiphilic Block Copolymer Self-Assemblies of Poly(NVP)-*b*-poly(MDO-*co*-vinyl esters): Tunable Dimensions and Functionalities

6.1 Abstract

In this chapter the copolymerization of vinyl acetate (VAc) and 2-methylene-1,3-dioxepane (MDO) using a macro-xanthate CTA, poly(*N*-vinylpyrrolidone) is studied, resulting in the formation of amphiphilic block copolymers of poly(NVP)-*b*-poly(MDO-*co*-VAc). The behavior of the block copolymers in water was investigated and resulted in the formation of self-assembled nanoparticles consisting of a hydrophobic core and a hydrophilic corona. The size of the resultant nanoparticles was able to be tuned with variation of the hydrophilic and hydrophobic segments of the core and corona by using different macro-CTAs and changing the incorporation of the monomer composition in the copolymers. The concept was further applied to the vinyl acetate derivative monomer vinyl bromobutanoate (VBr), previously studied in Chapter 3, to create a block copolymer able to undergo post-polymerization reactions resulting in the formation of fluorescently-labelled nanoparticles after self-assembly.

6.2 Introduction

In recent years, there has been significant interest in the development of amphiphilic block copolymers using controlled radical polymerization (CRP) techniques.[1-10] Amphiphilic block copolymers can self-assemble in aqueous medium in order to minimize the unfavourable hydrophobic interactions between the hydrophobic block of the polymer and water medium.[8,9,11] A major part of the increasing interest in amphiphilic block copolymers results from the wide range of applications where they can be used, such as drug delivery, coatings, nanoparticle synthesis or colloidal stabilization.[12] Many of these applications are in the pharmaceutical and biomedical areas which therefore require the block copolymers to be biocompatible, non-toxic and biodegradable.[13-15] Numerous studies have reported the use of controlled polymerization techniques, such as ring-opening polymerization (ROP) combined with reversible-addition fragmentation chain transfer (RAFT) polymerization, to synthesize

well-defined amphiphilic diblock copolymers of hydrophobic poly(ε-caprolactone) (PCL) or poly(*D,L*-lactide) (PDLLA) and hydrophilic poly(*N*-isopropylacrylamide) (PNIPAAm) or poly(*N*-vinylpyrrolidone) (PNVP).[15-24] PCL and PDLLA are amongst the most common biodegradable polymers used in the biomedical field as a consequence of their excellent mechanical, thermal and biocompatible properties, and are commonly synthesized by ROP of the associated cyclic (di)lactones in the presence of a metal catalyst and an initiator.[25-31] Meanwhile, both PNIPAAm and PNVP are commonly synthesized by radical polymerization and have frequently been studied towards potential bioapplications as a consequence of their high solubility in water, good biocompatibility and low toxicity,[21,32-35] with PNVP further exhibiting good cryo-protectivity and antibiofouling properties.[36,37] In order to diversify the range of properties targeted for the biodegradable hydrophobic block, much effort has recently been focused on the addition of functional groups on the PCL or PDLLA polymer backbone by either synthesis of new functional ε-CL and *D,L*-lactide monomers, chain-end modifications *via* the incorporation of functional groups in the ROP initiator or by copolymerization of CL and *D,L*-lactide with other monomers.[24,38-42] Whilst these approaches have so far been successful in achieving incorporation of further functionalities, they have been shown to be limited as a consequence of arduous steps during functional monomer synthesis, poor functional group compatibilities, and/or a poor match in monomer reactivity ratios.[43-46] To overcome this issue, recent studies highlighted an alternative route whereby the radical ring-opening polymerization (rROP) of the 7-membered cyclic ketene acetal (CKA), 2-methylene-1,3-dioxepane (MDO, **CKA 1**), leads to a polymer with a structure very similar to the conventional PCL synthesized by ROP of ε-CL.[47,48] This alternative approach opens a new way of incorporating functionality into a PCL-like polymer backbone by copolymerization of MDO with other vinyl monomers.[48-58] In previous Chapters the copolymerization of MDO with different vinyl monomers (VAc, VBr) using the RAFT/MADIX polymerization technique was investigated as a route towards the synthesis

of well-defined and controlled functional copolymers of poly(MDO-*co*-vinyl esters).[59,60] Using the method previously described in Chapters 2 and 3 and by combining both rROP and the RAFT/MADIX polymerization technique, the synthesis of degradable functional amphiphilic block copolymers can now be achieved using a single technique, as briefly introduced in Chapter 2 where poly(NVP)-*b*-poly(MDO-*co*-VAc) were synthesized.

In this Chapter the synthesis of functional and degradable self-assemblies from the linear block copolymers of poly(NVP)-*b*-poly(MDO-*co*-VAc) obtained by the RAFT/MADIX copolymerization of MDO and vinyl acetate is further investigated. Additionally, the properties of the self-assemblies were found to be tunable by varying the lengths of the hydrophilic or hydrophobic segments to increase the particles' sizes as observed by Dynamic Light Scattering (DLS), Static Light Scattering (SLS) and Transmission Electron Microscopy (TEM) analyses. Extension of the concept to the new vinyl acetate derivative monomer, vinyl bromobutanoate (VBr), presented in Chapter 3, is also demonstrated as a new way of incorporating further functional pendent groups on the hydrophilic segment of the polymers, which can be modified *via* post-polymerization to incorporate fluorescent groups.

6.3 Results and Discussion

6.3.1 Synthesis of amphiphilic block copolymers

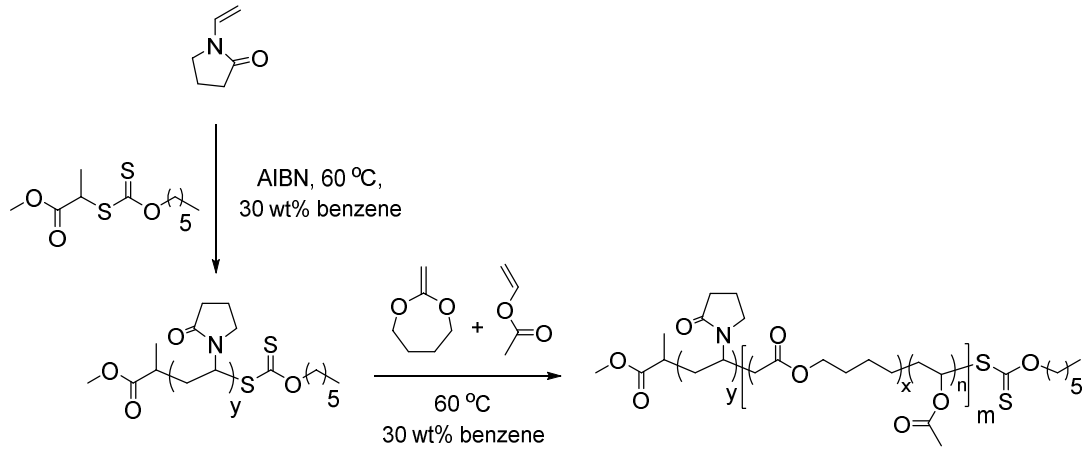

Scheme 6.1. Schematic representation of the synthetic approach used for the synthesis of amphiphilic block copolymer poly(NVP)-*b*-poly(MDO-*co*-VAc).

In order to obtain amphiphilic polymers, the synthesis of the block copolymers poly(NVP)-*b*-poly(MDO-*co*-VAc) was performed using the synthetic approach previously introduced in Chapter 2. The hydrophilic block was obtained by the RAFT/MADIX polymerization of NVP using *O*-hexyl *S*-methyl 2-propionylxanthate as the chain transfer agent (CTA 1) to synthesize a poly(NVP)$_{70}$ macro-CTA, (degree of polymerization, DP = 70, M_n^{SEC} = 5.3 kg/mol, $Đ_M$ = 1.18). This chain transfer agent was chosen following on from the previous results presented in Chapter 2 where CTA 1 was found to be able to mediate the initial copolymerization of MDO and VAc. The DP of the macro-CTA was calculated using ^{1}H NMR spectroscopy analysis on the polymer by integration of the proton signals of the NVP$_{ring}$ at δ = 3.50 – 2.20 ppm and referenced to the characteristic signal of the CH_2 protons adjacent to the xanthate end-group at δ = 4.50 ppm (Figure 6.1a). The macro-CTA, poly(NVP)$_{70}$ was further chain extended with a co-monomer mixture of MDO and VAc (10 mol% and 90 mol% respectively) leading to the formation of the hydrophobic second block copolymer of poly(MDO-*co*-VAc). The successful synthesis of poly(NVP)$_{70}$-*b*-

poly($MDO_{0.05}$-*co*-$VAc_{0.95}$)$_{60}$ (polymer **P1**) was proven by ^{1}H NMR spectroscopy and SEC analyses. ^{1}H NMR spectra revealed the successful extension of the macro-CTA with a copolymer of MDO and VAc as observed by the appearance of the characteristic signals at δ = 5.28 - 4.65 ppm and δ = 4.20 ppm corresponding to the VAc and MDO polymer backbone respectively (Figure 6.1b).

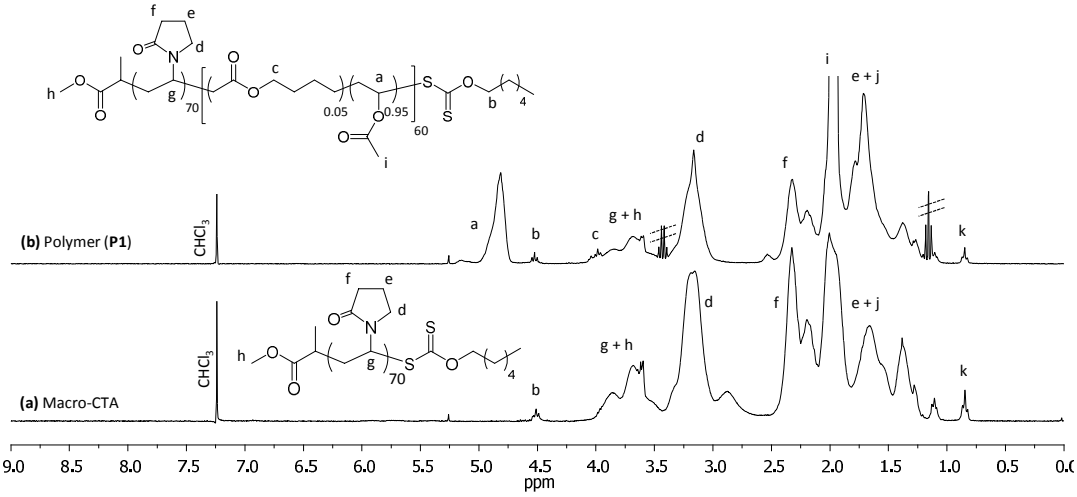

Figure 6.1. ^{1}H NMR spectra of (a) poly(NVP)$_{70}$ macro-CTA before (bottom) and after chain extension with MDO and VAc to form the block copolymer (b) poly(NVP)$_{70}$-*b*-poly($MDO_{0.05}$-*co*-$VAc_{0.95}$)$_{60}$, polymer **P1**, ($CDCl_3$, 300 MHz).

Additionally, the successful formation of the hydrophobic second block, poly(MDO-*co*-VAc) was confirmed by SEC analysis where the complete shift of the molecular weight distribution was observed after extension leading to a block copolymer with a molecular weight, M_n^{SEC} of 13.5 kg/mol, $Đ_M$ = 1.42 (Figure 6.2). The dispersity of the final block copolymer was found to increase from 1.18 to 1.42 after addition of the poly(MDO-*co*-VAc) second block. This can be explained by the fragmentation of the Z group previously investigated in Chapter 4 which tends to led to a lower degree of control during the copolymerization of MDO and VAc and hence a broadening of the dispersity of the final polymers.[61] Nevertheless, the observation of the xanthate signal at δ = 4.50 ppm on the ^{1}H

NMR spectrum (Figure 6.1) and the monomodality of the SEC trace after chain extension (Figure 6.2) suggested that a good degree of control was retained.

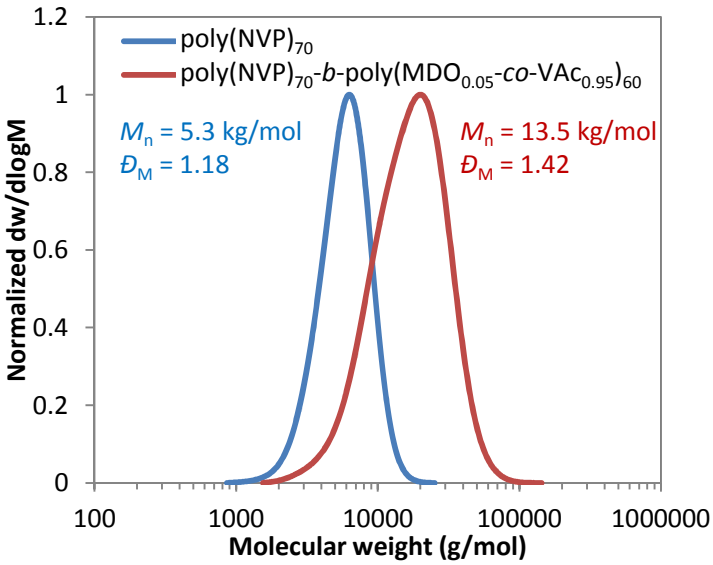

Figure 6.2. Size exclusion chromatograms of the poly(NVP)$_{70}$ macro CTA and poly(NVP)$_{70}$-*b*-poly(MDO$_{0.05}$-*co*-VAc$_{0.95}$)$_{60}$ diblock copolymer (polymer **P1**) (SEC DMF, PMMA used as standards).

The observed molecular weight by ^{1}H NMR spectroscopy, M_n^{obs}, was obtained by integration of the protons from the MDO and VAc polymer backbone at δ = 4.20 ppm and δ = 5.28 - 4.65 ppm respectively, relative to the characteristic resonance of the CH_2 proton adjacent to the xanthate group of the macro-CTA at δ = 4.50 ppm (Figure 6.1). A similar synthesis was performed where the initial monomer ratios of MDO and VAc were modified to 30 mol% and 70 mol% in order to produce a block copolymer containing a larger amount of degradable ester repeat units in the hydrophobic block (polymer **P2**). The successful synthesis of this other block copolymer was confirmed by SEC analysis (Figure 6.3) and ^{1}H NMR spectroscopy where the similar signals of MDO and VAc were observed as previously shown in Figure 6.1. This result confirmed that the final incorporation of ester repeat units in the hydrophobic block can be tuned by varying the monomer ratios used in order to produce polymers with different degrees of degradability.

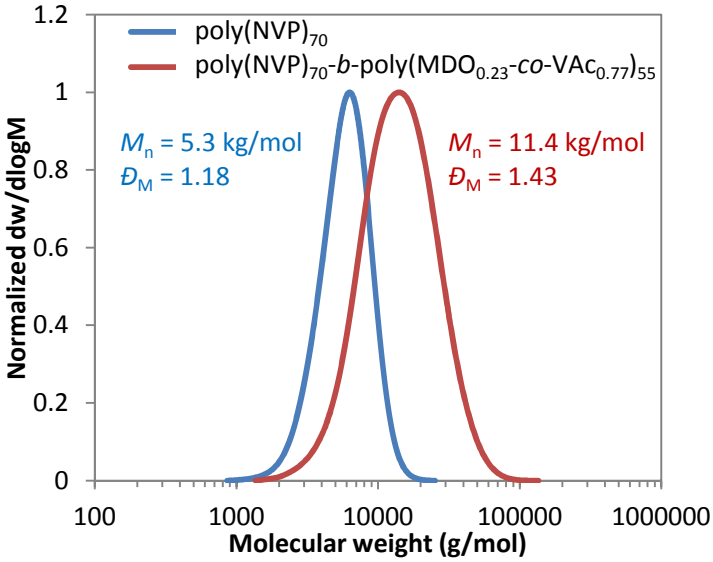

Figure 6.3. Size exclusion chromatograms of the poly(NVP)$_{70}$ macro CTA and poly(NVP)$_{70}$-*b*-poly(MDO$_{0.23}$-*co*-VAc$_{0.77}$)$_{55}$ diblock copolymer (polymer **P2**) (SEC DMF, PMMA used as standards).

Following on from these results, extension of the process of using the macro-NVP CTA to mediate the copolymerization of MDO and VAc was realized by the synthesis of different polymers where the size of the poly(NVP) macro-CTA (y) and the size of the hydrophobic block (x) were modified in order to obtain amphiphilic block copolymers of poly(NVP)$_y$-*b*-poly(MDO-*co*-VAc)$_x$ with different lengths of hydrophilic and hydrophobic segments.

The length of the hydrophilic block was altered by synthesizing three different poly(NVP) macro-CTAs with degrees of polymerization (DP) of 28, 43 and 87 respectively (polymers **P3**, **P4** and **P5**), leading to polymers with molecular weights, M_n^{SEC} of 1.80, 3.40 and 6.20 kg/mol respectively (Table 6.1, polymers **P3**, **P4** and **P5**, Figure 6.4). The three macro-CTAs were all chain extended with MDO and VAc to lead to three block copolymers of poly(NVP)-*b*-poly(MDO-*co*-VAc) with M_n^{SEC} after extension of 4.30, 5.70 and 8.40 kg/mol (polymers **P6**, **P7** and **P8** respectively) confirming the successful chain extension of the hydrophobic blocks from the initial hydrophilic poly(NVP) block (Figures 6.5-6.7).

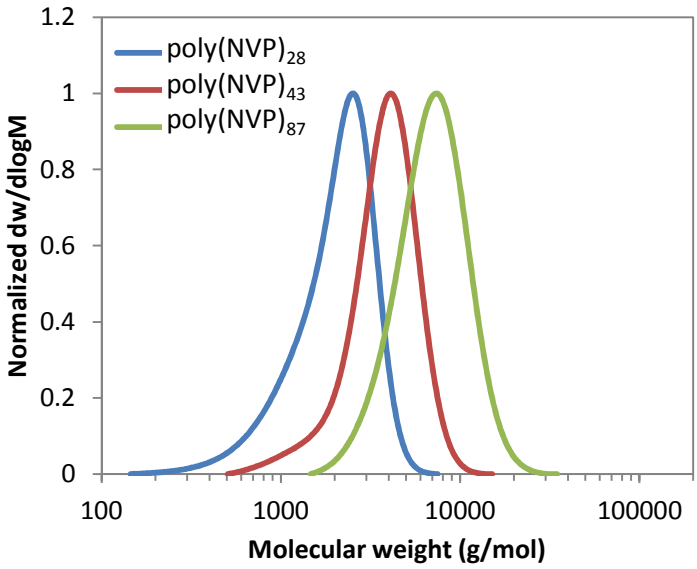

Figure 6.4. Size exclusion chromatograms of polymer **P3** (poly(NVP)$_{28}$), polymer **P4** (poly(NVP)$_{43}$) and polymer **P5** (poly(NVP)$_{87}$) obtained by the RAFT/MADIX polymerization using *O*-hexyl *S*-methyl 2-propionyl xanthate (CTA 1) as the chain transfer agent (SEC, DMF, PMMA used as standard).

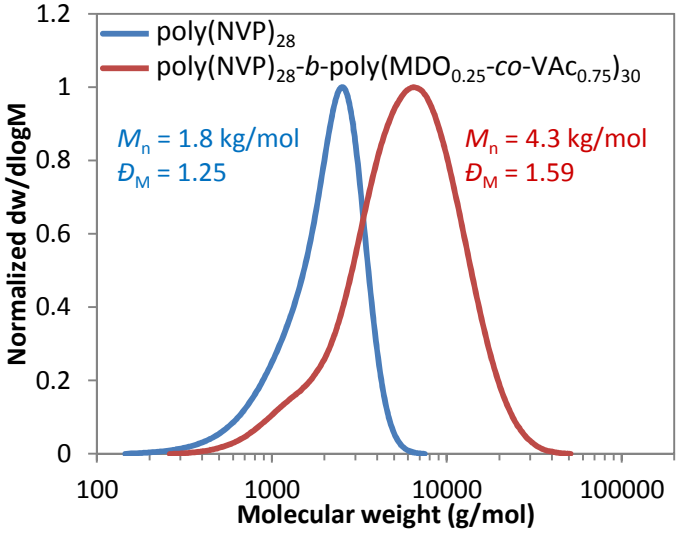

Figure 6.5. Size exclusion chromatograms of polymer **P3** (poly(NVP)$_{28}$) before and after chain extension with the co-monomer mixture of MDO and VAc to form polymer **P6** (poly(NVP)$_{28}$-*b*-poly(MDO$_{0.25}$-*co*-VAc$_{0.75}$)$_{30}$) (SEC, DMF, PMMA used as standard).

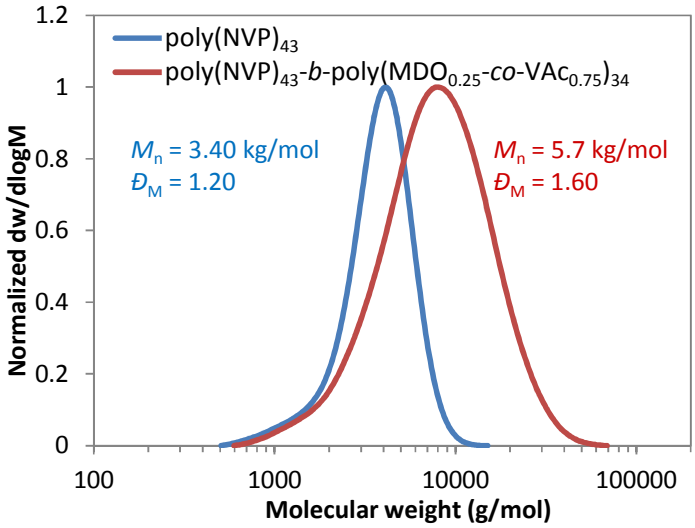

Figure 6.6. Size exclusion chromatograms of polymer **P4** (poly(NVP)$_{43}$) before and after chain extension with the co-monomer mixture of MDO and VAc to form polymer **P7** (poly(NVP)$_{43}$-*b*-poly(MDO$_{0.25}$-*co*-VAc$_{0.75}$)$_{34}$) (SEC, DMF, PMMA used as standard).

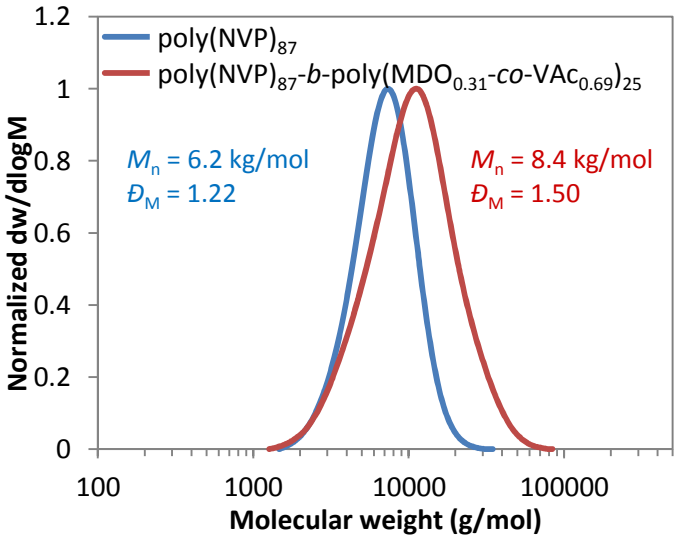

Figure 6.7. Size exclusion chromatograms of polymer **P5** (poly(NVP)$_{87}$) before and after chain extension with the co-monomer mixture of MDO and VAc to form polymer **P8** (poly(NVP)$_{43}$-*b*-poly(MDO$_{0.31}$-*co*-VAc$_{0.69}$)$_{25}$) (SEC, DMF, PMMA used as standard).

Table 6.1. Characterization data of the poly(NVP) and poly(NVP)-*b*-poly(MDO-*co*-VAc) diblock copolymers synthesized.

Entry	Polymer [a]	M_n^{SEC} [b] (kg/mol)	M_n^{theo} [c] (kg/mol)	$Đ_M$ [b]
P1	poly(NVP)$_{70}$-*b*-poly(MDO$_{0.05}$-*co*-VAc$_{0.95}$)$_{60}$	13.5	15.2	1.42
P2	poly(NVP)$_{70}$-*b*-poly(MDO$_{0.23}$-*co*-VAc$_{0.77}$)$_{55}$	11.4	13.1	1.43
P3	poly(NVP)$_{28}$	1.8	3.2	1.25
P4	poly(NVP)$_{43}$	3.4	5.1	1.20
P5	poly(NVP)$_{87}$	6.2	9.7	1.22
P6	poly(NVP)$_{28}$-*b*-poly(MDO$_{0.25}$-*co*-VAc$_{0.75}$)$_{30}$	4.3	6.2	1.59
P7	poly(NVP)$_{43}$-*b*-poly(MDO$_{0.25}$-*co*-VAc$_{0.75}$)$_{34}$	5.7	8.2	1.60
P8	poly(NVP)$_{87}$-*b*-poly(MDO$_{0.31}$-*co*-VAc$_{0.69}$)$_{25}$	8.4	12.1	1.50
P9	poly(NVP)$_{82}$	6.2	9.4	1.17
P10	poly(NVP)$_{82}$-*b*-poly(MDO$_{0.25}$-*co*-VAc$_{0.75}$)$_{20}$	11.2	12.2	1.34
P11	poly(NVP)$_{82}$-*b*-poly(MDO$_{0.26}$-*co*-VAc$_{0.74}$)$_{48}$	14.5	14.0	1.48
P12	poly(NVP)$_{82}$-*b*-poly(MDO$_{0.30}$-*co*-VAc$_{0.70}$)$_{95}$	19.5	18.4	1.72
P13	poly(NVP)$_{82}$-*b*-poly(MDO$_{0.25}$-*co*-VAc$_{0.75}$)$_{120}$	24.1	21.7	1.90

[a] DPs obtained by ^{1}H NMR spectroscopy in $CDCl_3$, [b] Measured by SEC DMF, PMMA used as standards, [c] theoretical molecular weight based on monomer conversion (^{1}H NMR spectroscopy).

In order to increase the hydrophobicity of the copolymer, four different copolymers, with varying hydrophobic block lengths were synthesized starting from the same macro-CTA, poly(NVP)$_{82}$ (polymer **P9**), M_n^{SEC} = 6.20 kg/mol, $Đ_M$ = 1.17. Chain extension of this macro CTA with MDO and VAc, yielded polymers **P10** – **P13** with poly(MDO-*co*-VAc) block lengths (DP) of 20, 48, 95 and 120 as calculated by ^{1}H NMR spectroscopy using the characteristic signals of the MDO and VAc repeat units at δ = 5.28 - 4.65 ppm and δ = 4.22 ppm, respectively, and compared with the signal of the xanthate chain end at δ = 4.50 ppm (similarly to Figure 6.1). Furthermore, the increase in hydrophobic block length was confirmed by the increase in M_n^{SEC} obtained from SEC analysis (Table 6.1 and Figure 6.8).

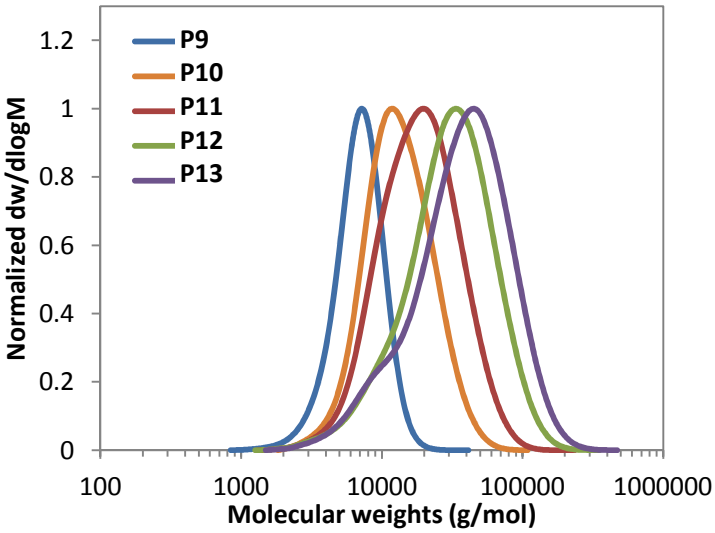

Figure 6.8. Size exclusion chromatograms of the chain extension of polymer **P9** (poly(NVP)$_{82}$) with MDO and VAc to form the diblock copolymers **P10 - P13** (poly(NVP)$_{82}$-*b*-poly(MDO-*co*-VAc)$_y$ where y = 20, 48, 95 and 120), (SEC DMF, PMMA used as standards).

Although the successful addition of the second block was proven by the net increase in molecular weight, it can be observed that the dispersities after chain extension increased as larger DPs were targeted. Indeed, dispersity values of 1.34, 1.48, 1.72 and 1.90 were obtained for polymers **P10 – P13,** respectively. The increase in dispersity can be attributed to the combination of two potential aspects as previously mentioned in Chapter 2. The first aspect deals with the use of controlled polymerization techniques to target higher DP polymers, which can often increase the dispersities of the final polymers as a consequence of the accumulation of irreversible termination reactions which tend to be more favoured when the ratio of $[Initiator]_0/[CTA]_0$ is increased.[62-64] The increase in dispersity could also be attributed to the loss of control during the polymerization of MDO using RAFT/MADIX polymerization. This aspect was also observed in the previous Chapters during the polymerization of MDO and VAc/VBr using RAFT/MADIX polymerization where fragmentation through the Z group was occurring as a consequence of the poor stability of the MDO primary radicals and the polymer growing radicals which led to the formation of a

carbonodithioate functionalities, hence producing "dead" polymer chains unable to be further extended.[61]

Nevertheless, the results obtained by ^{1}H NMR spectroscopy and SEC analyses confirm that the use of poly(NVP) as a xanthate macro-CTA for the copolymerization of MDO and VAc is suitable to achieve the synthesis of amphiphilic block copolymers of poly(NVP)-*b*-poly(MDO-*co*-VAc) while maintaining a certain degree of control during the polymerization process.

6.3.2 Formations of particles

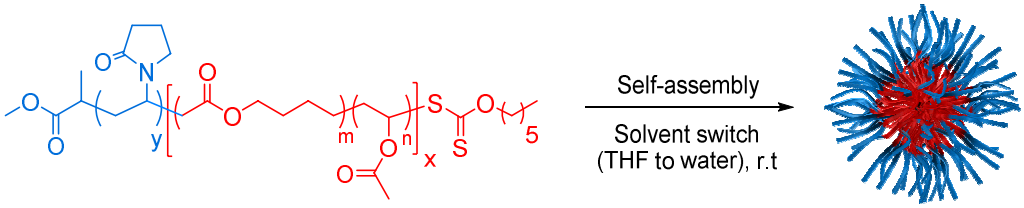

Scheme 6.2. Schematic representation of the self-assembly of poly(NVP)$_y$-*b*-poly(MDO-*co*-VAc)$_x$ using the solvent switch technique to form particles.

In order to investigate the self-assembly behaviour of the linear block copolymers in water, the solvent switch technique (from tetrahydrofuran (THF) to water) was employed, yielding particles composed of a poly(NVP) corona and a poly(MDO-*co*-VAc) core at a final concentration of 1.0 mg/mL (Scheme 6.2). The morphology of the particles formed was assessed by DLS and TEM analyses. DLS analysis of the particles formed from polymer **P1** revealed particles with a hydrodynamic diameter, D_h, of 26 nm and low polydispersity, PD, of 0.04. Particles formed from polymer **P2** displayed very similar results when analyzed by DLS, with a D_h of 27 nm and a PD of 0.075. The monomodal DLS traces (Figure 6.9) and low polydispersity indicates that the particles are well-defined and that a single particle population was obtained. TEM analysis confirmed the presence of spherical nanoparticles with similar profiles of 28 nm and 32 nm (Figures 6.10 and 6.11). The similar sizes obtained by DSL and TEM analyses was not surprising given that polymers **P1** and **P2** have the same

hydrophilic block length and similar overall hydrophobic block lengths. However, polymer **P1** contains only 5 mol% of MDO in the hydrophobic block whereas polymer **P2** contains 23 mol% of MDO. Therefore this observation shows that particles with different degrees of degradability can be synthesized, with little effect on the size or quality of the particles formed

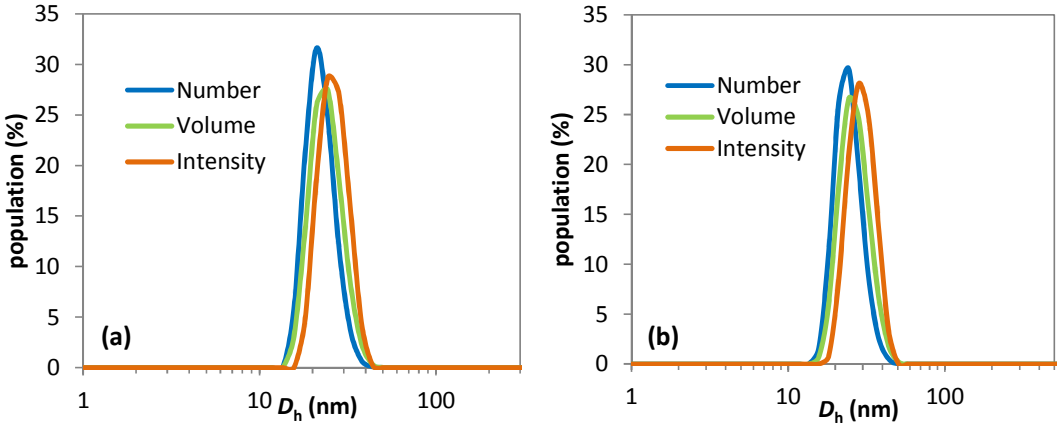

Figure 6.9. DLS traces of the particles formed from the amphiphilic block copolymer (a) polymer **P1** (poly(NVP)$_{70}$-*b*-poly(MDO$_{0.05}$-*co*-VAc$_{0.95}$)$_{60}$) and (b) polymer **P2** (poly(NVP)$_{70}$-*b*-poly(MDO$_{0.23}$-*co*-VAc$_{0.77}$)$_{55}$).

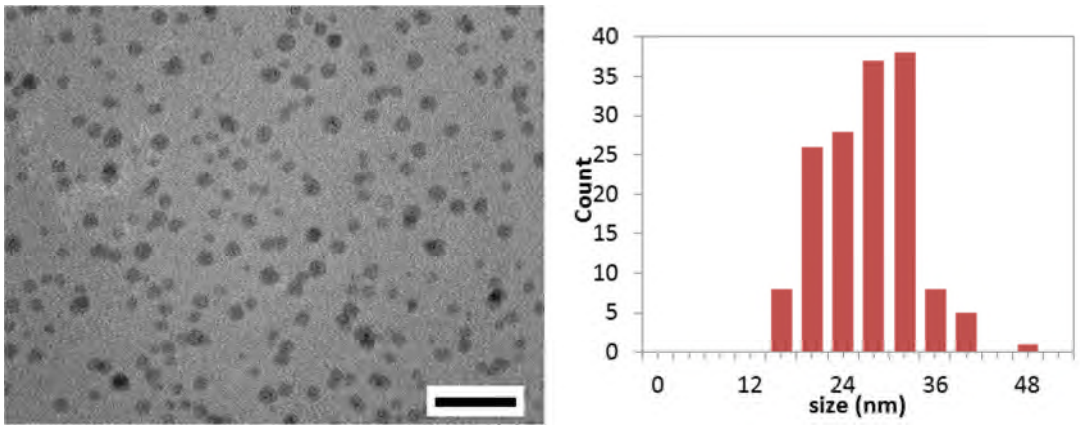

Figure 6.10. TEM image (left, scale bar = 100 nm) of particles formed from the amphiphilic block copolymer **P1** (poly(NVP)$_{70}$-*b*-poly(MDO$_{0.05}$-*co*-VAc$_{0.95}$)$_{60}$) and histogram showing the distribution of particle size (right).

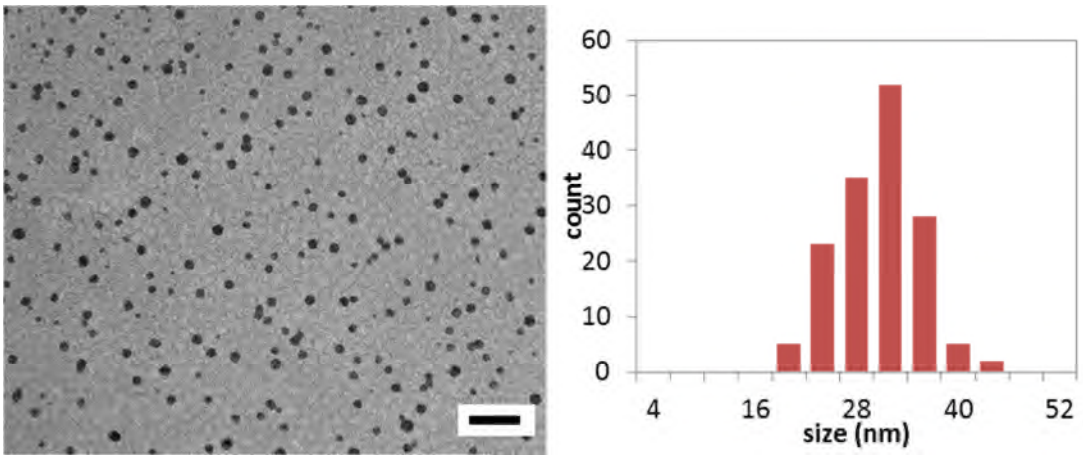

Figure 6.11. TEM image (left, scale bar = 100 nm) of particles formed from the amphiphilic block copolymer **P2** (poly(NVP)$_{70}$-*b*-poly(MDO$_{0.23}$-*co*-VAc$_{0.77}$)$_{55}$) and histogram showing the distribution of particle size (right).

6.3.3 Tuning the size of the particles by changing the hydrophobic and hydrophilic block lengths

It is widely accepted that the dimension of amphiphilic block copolymer self-assemblies is strongly dependent on the relative and overall volumes occupied by the hydrophobic and hydrophilic polymer chain segments which dictates the resulting morphology of the polymeric nanostructures.[11,65-67] In order to investigate the effect of changing the length of the hydrophilic block on polymer self-assembly, three different poly(NVP) macro-CTAs of increasing length (**P3** – **P5**) were used in the chain extension with MDO and VAc to yield three polymers (**P6** – **P8**) with varying hydrophilic lengths but similar hydrophobic block length and composition. The self-assembly of these three polymers was performed using the solvent switch method from THF to water as previously described. In all cases the formation of spherical particles was confirmed by DLS and TEM analyses (Figures 6.12 and 6.13). The hydrodynamic diameter, D_h, was found to increase as the hydrophilic poly(NVP) block length was increased. Indeed, DLS analysis revealed D_h values of 17 nm, 24 nm and 70 nm for particles formed from the block copolymer with hydrophilic length of poly(NVP)$_{28}$ (**P6**), poly(NVP)$_{43}$ (**P7**) and poly(NVP)$_{87}$ (**P8**) respectively (Table 6.2). The particles obtained from

P6 and **P7** were well-defined with a single monomodal distribution and fairly low polydispersities (PD) of 0.138 and 0.214 observed by DLS analysis (see Figure 6.12). However, in the case of polymer **P8**, which contains the longest poly(NVP) block, the polydispersity of the particles was found to be higher with a value of 0.842 as obtained by DLS analysis, which also revealed the presence of larger particles around 300 nm. This larger distribution was assumed to be a result of aggregations between smaller particles in the solution. Attempts to optimise the self-assembly conditions by reducing the concentration of the block copolymer in solution to 0.2 mg/mL did not reduce the formation of these aggregates.

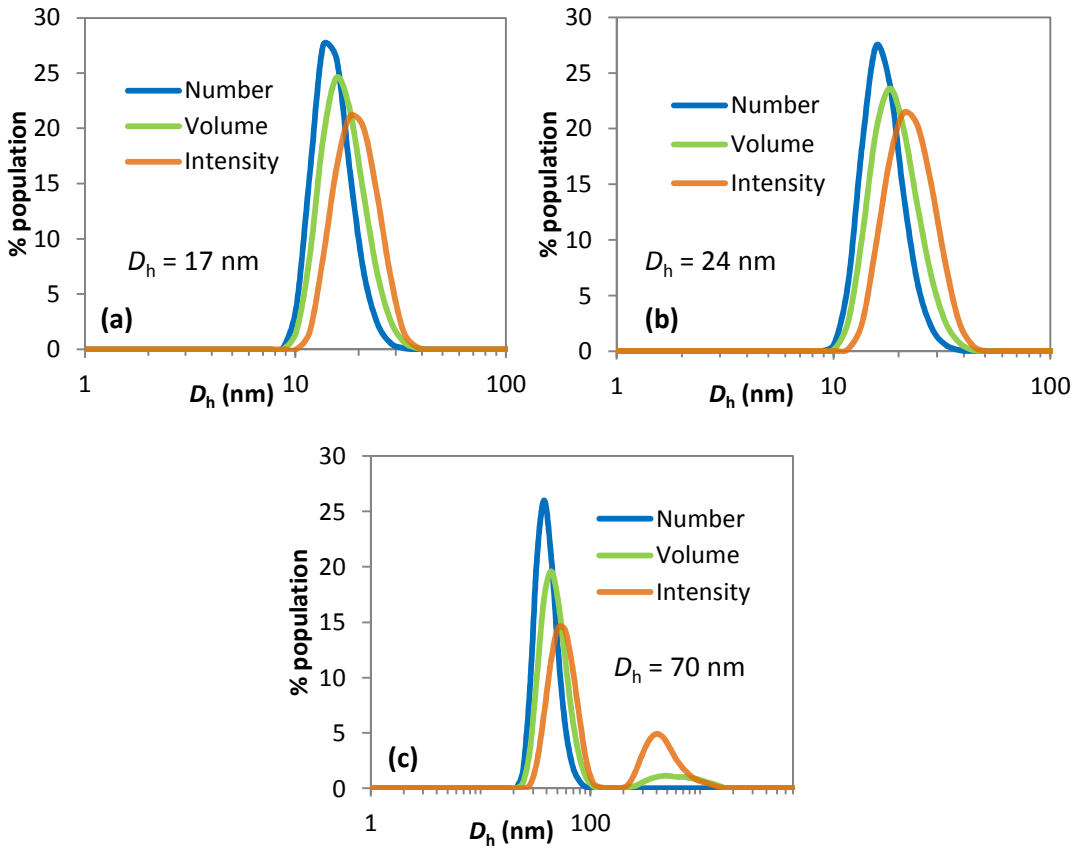

Figure 6.12. DLS traces of the particles formed from poly(NVP)-*b*-poly(MDO-*co*-VAc) using three different hydrophilic poly(NVP) macro-CTAs, (a) polymer **P6**, DP = 28 (b) polymer **P7**, DP = 43 and (c) polymer **P8**, DP = 87.

Further analysis using TEM revealed results in good agreement with the previous obtained by DLS analyses. Average diameter, D_{av}, values of 11 nm, 30 nm and 42 nm were observed for polymers **P6** to **P8**, respectively, confirming that the synthesis of spherical nanoparticles containing a larger hydrophilic corona-forming block could be obtained by using different size of poly(NVP) macro-CTA (Figure 6.13).

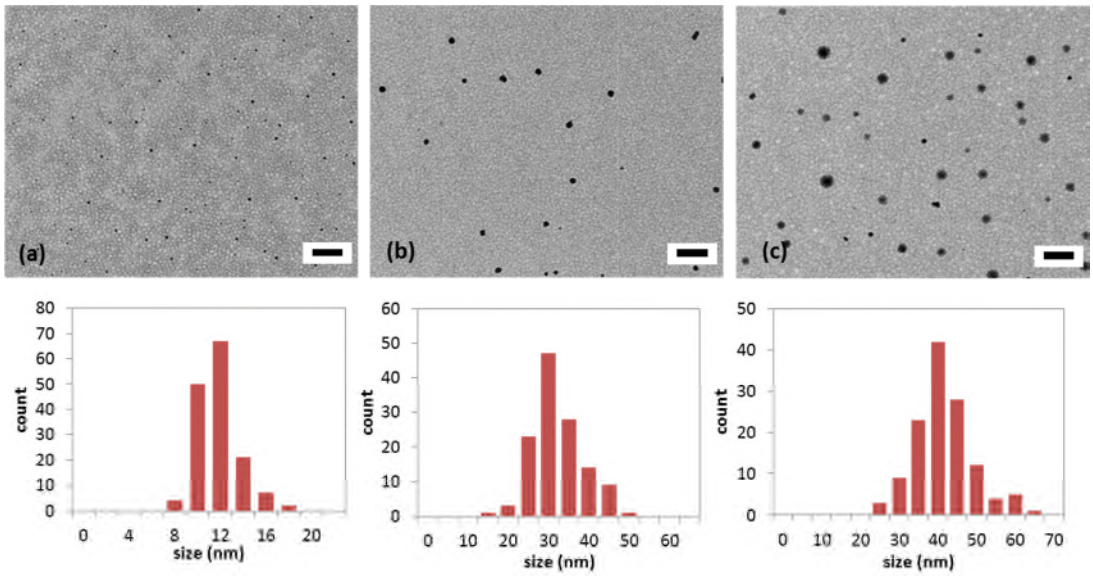

Figure 6.13. TEM images (top) of the particles formed from poly(NVP)-*b*-poly(MDO-*co*-VAc) using three different poly(NVP) macro-CTAs, (a) polymer **P6**, DP = 28 (b) polymer **P7**, DP = 43 and (c) polymer **P8**, DP = 87, (scale bar = 100 nm) and their histograms showing the distribution of particle size (bottom).

Table 6.2. Characteristic data of the particles obtained using the different block copolymers.

Entry	Polymer [a]	D_h (nm) [b]	PD [b]	D_{av} (nm) [c]	R_h (nm) [d]	N_{agg} [d]
P6	poly(NVP)$_{28}$-*b*-poly(MDO$_{0.25}$-*co*-VAc$_{0.75}$)$_{30}$	17	0.138	11	-	-
P7	poly(NVP)$_{43}$-*b*-poly(MDO$_{0.25}$-*co*-VAc$_{0.75}$)$_{34}$	24	0.214	30	-	-
P8	poly(NVP)$_{87}$-*b*-poly(MDO$_{0.31}$-*co*-VAc$_{0.69}$)$_{25}$	70	0.842	42	-	-
P10	poly(NVP)$_{82}$-*b*-poly(MDO$_{0.25}$-*co*-VAc$_{0.75}$)$_{20}$	20	0.175	18	12.6	182
P11	poly(NVP)$_{82}$-*b*-poly(MDO$_{0.26}$-*co*-VAc$_{0.74}$)$_{48}$	26	0.051	21	16.7	305
P12	poly(NVP)$_{82}$-*b*-poly(MDO$_{0.30}$-*co*-VAc$_{0.70}$)$_{95}$	33	0.106	26	18.7	391
P13	poly(NVP)$_{82}$-*b*-poly(MDO$_{0.25}$-*co*-VAc$_{0.75}$)$_{120}$	43	0.039	*	24.8	750

[a] DPs obtained by ^{1}H NMR spectroscopy in $CDCl_3$, [b] Measured by DLS, [c] Measured by analysis of TEM images (200 particles counted), [d] Obtained by SLS analysis, * not observed by TEM analysis.

In order to vary the particles' hydrophobic core size, chain extension of the same poly(NVP)$_{82}$ macro-CTA, M_n = 6.20 kg/mol, $Đ_M$ = 1.17 (polymer **P9**) was conducted to create four hydrophobic core-forming blocks with DPs of 20, 48, 95 and 120 (polymers **P10** to **P13**). The formation of particles with variable length of hydrophophic poly(MDO-*co*-VAc) blocks was confirmed using DLS and TEM analyses. As expected, the size of the particles was found to also increase with increasing the hydrophobic block length, as observed by DLS analysis showing D_h values of 20, 26, 33 and 43 nm, for polymers **P10** to **P13** respectively (Figures 6.14 and 6.15). The low dispersities and monomodal traces observed by DLS analysis indicated a single population of particles in each solution. The increase in size for these particles was not as significant as the results previously observed for the particles containing increasing hydrophilic blocks (Figure 6.12) as the overall size of the particles in solution is usually dictated by the hydrophilic corona of the self-assemblies.

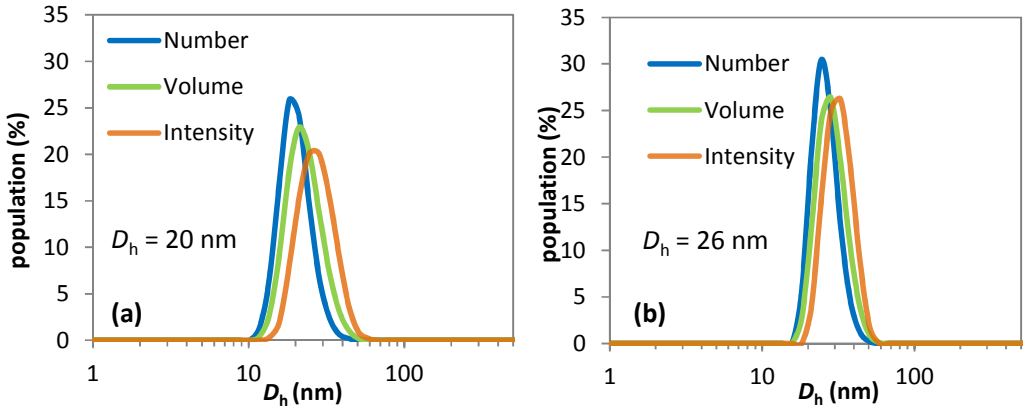

Figure 6.14. DLS traces of the particles formed from block copolymers with different hydrophobic block lengths (a) polymer **P10** (poly(NVP)$_{82}$-*b*-poly(MDO$_{0.25}$-*co*-VAc$_{0.75}$)$_{20}$) and (b) polymer **P11** (poly(NVP)$_{82}$-*b*-poly(MDO$_{0.26}$-*co*-VAc$_{0.74}$)$_{48}$).

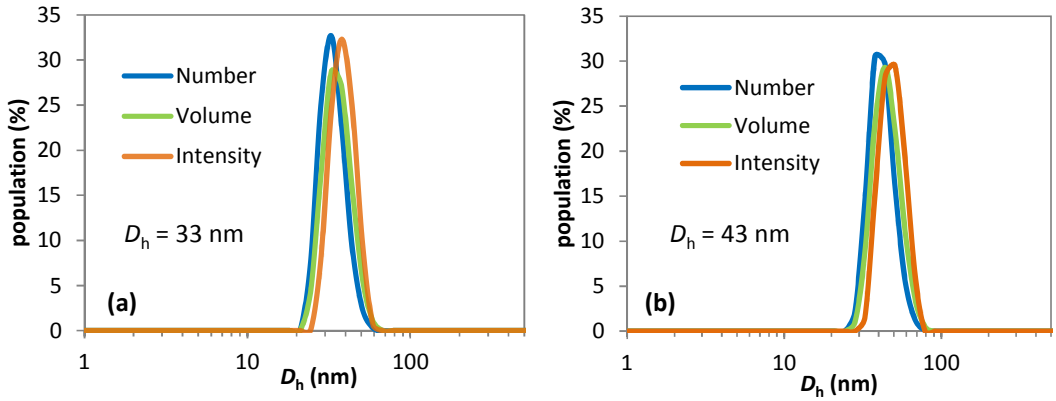

Figure 6.15. DLS traces of the particles formed from block copolymers with different hydrophobic block lengths (a) polymer **P12** (poly(NVP)$_{82}$-*b*-poly(MDO$_{0.30}$-*co*-VAc$_{0.70}$)$_{95}$) and (b) polymer **P13** (poly(NVP)$_{82}$-*b*-poly(MDO$_{0.25}$-*co*-VAc$_{0.75}$)$_{120}$).

While TEM analyses confirmed the presence of spherical particles, the effect of larger poly(MDO-*co*-VAc) hydrophobic block had on the size of the particle was not as noticable as when the hydrophilic block length was modified. Indeed for polymers **P10** – **P12**, average diameters, D_{av}, of 18, 21, and 26 nm were obtained indicating that the change in hydrophobic length did not significantly influence the size of the particles observed by TEM analysis (Figure 6.16). This suggests that the increase in the particles' core performed during this study was not sufficient enough to be observed by TEM analysis. Additionally in the case of

P13, with the longest hydrophobic block, the TEM images (Figure 6.17) showed an almost spherical morphology of lower contrast compared to the previous results observed. This result could be attributed to spherical self-assemblies and would confirm the DLS results previously described (Figure 6.15b).

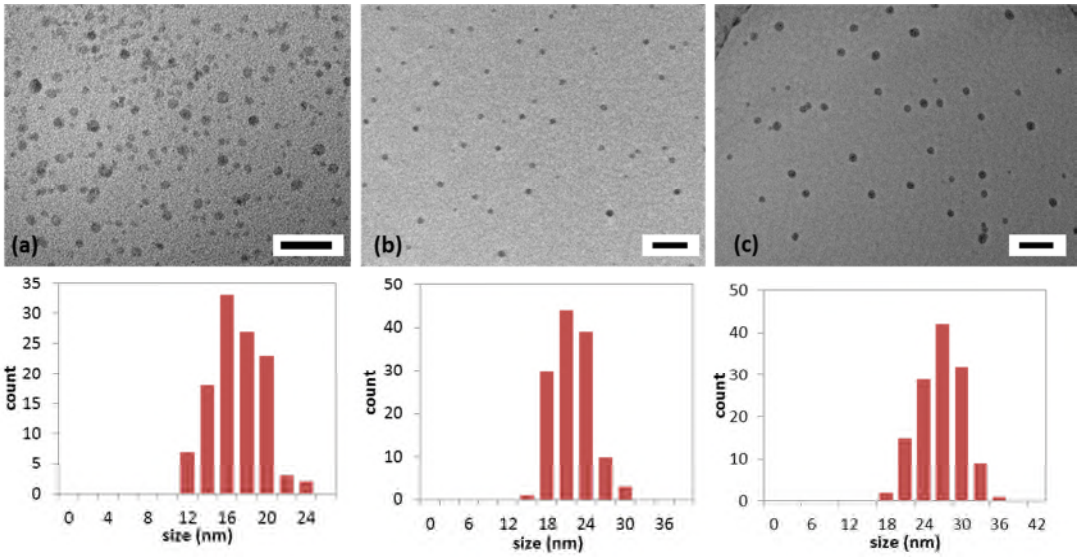

Figure 6.16. TEM images (bottom) of the particles formed from poly(NVP)-*b*-poly(MDO-*co*-VAc) with different hydrophobic block lengths (a) polymer **P10**, DP = 20, (b) polymer **P11**, DP = 48, and (c) polymer **P12**, DP = 95, (scale bar = 100 nm) their histograms showing the distribution of particle size (bottom).

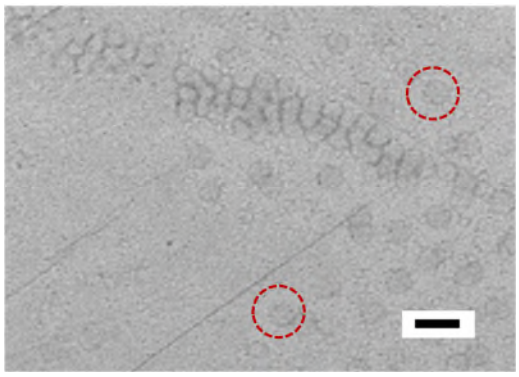

Figure 6.17. TEM images of the particles formed from poly(NVP)-*b*-poly(MDO-*co*-VAc) with a hydrophilic block of DP 120, polymer **P13**, (scale bar = 100 nm).

Following on from the TEM results obtained for polymers **P10** – **P13** and in order to confirm the change in particle size upon increasing hydrophobic block length, further investigations

using Static Light Scattering (SLS) were performed to determinate their hydrodynamic radius, R_h, and aggregation number, N_{agg}. From this analysis, R_h values were found to increase with increasing hydrophobic block length with R_h values of 12.6, 16.7, 18.7 and 24.8 nm being obtained for the particles formed from polymers **P10 – P 13**, respectively. This observation confirmed the results previously seen by DLS (Table 6.2). Additionally, N_{agg} values were also calculated for each solution and revealed a similar trend where N_{agg} of 182, 305, 391 and 750 were obtained for polymers **P10 – P13** indicating that the size of the particles were increased. While TEM analysis was not successful in confirming the changes in size for the particles obtained from **P10 –P13**, both DLS and SLS results suggest the expansion of these particle size when the hydrophobicity of the self-assemblies was increased by using different block lengths of poly(MDO-*co*-VAc).

6.3.4 Degradation studies

The degradation of amphiphilic block copolymers and their self-assemblies is of great interest as such polymers can be used as drug delivery vehicles in the biomedical field.[12,68] Various studies investigated the degradation of particles from such block copolymers under basic, acidic or enzymatic conditions and confirmed the degradable properties *via* SEC and/or DLS analyses.[69,70] Aiming at confirming the degradation of the poly(NVP)-*b*-poly(MDO-*co*-VAc) block copolymers, as well as the degradability of the self-assemblies previously formed, experiments were performed where the polymer samples and the self-assemblies were placed under different degradation conditions. In an initial experiment, the degradability of the poly(NVP)$_{82}$-*b*-poly(MDO$_{0.26}$-*co*-VAc$_{0.74}$)$_{40}$ block copolymer was investigated by the hydrolysis of the samples in a solution of potassium hydroxide (KOH, 0.1 M) in methanol at 40 °C. These conditions were previously used for the successful degradation of poly(MDO-*co*-VAc) and poly(MDO-*co*-VBr) in Chapters 2 and 3. Under these basic methanolic conditions and at 40 °C, the degradation of the block copolymer was

found to occur rapidly as seen by the decrease of the molecular weights of the sample on the SEC traces after only 15 min of hydrolysis (Figure 6.18). This decrease was assumed to be related to the degradation of the poly(MDO-*co*-VAc) block which contains degradable ester linkages along the backbone as a result of the rROP of MDO. The degradation was continued for another 15 minutes, but no further decrease in molecular weight could be observed. After 30 min, a comparison between the degraded block copolymer and the initial poly(NVP) macro-CTA was undertaken. After degradation, the remaining peak observed by SEC is likely to correspond to the initial hydrophilic poly(NVP) block suggesting that full degradation of the hydrophobic block was achieved as a consequence of the hydrolysis of the ester linkages introduced during the copolymerization.

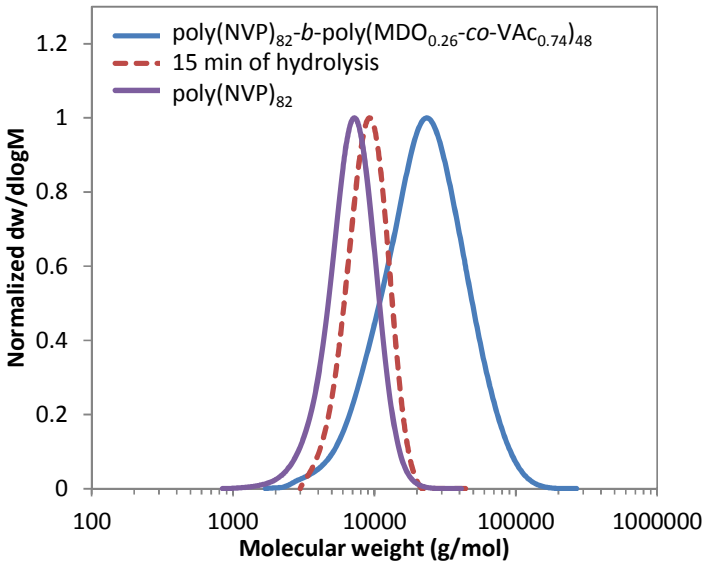

Figure 6.18. Size exclusion chromatograms of poly(NVP)$_{82}$-*b*-poly(MDO$_{0.26}$-*co*-VAc$_{0.74}$)$_{48}$ before and after degradation in KOH (0.1 M), methanol solution at 40 °C.

In order to follow the degradation of the block copolymers gradually, hydrolysis experiments in phosphate buffer solution (PBS) at pH = 7.4 and at 37 °C were conducted. These experiments revealed that no significant degradation had occurred after 6 and 50 days of exposure as no significant changes were observed in the molecular weight of the block

copolymers observed by SEC analysis (Figure 6.19). This observation revealed that despite introducing degradability in the core-forming block of the polymer, the hydrophilic block tends to reduce the rate of degradation of such polymers when exposed to the PBS solution. Nevertheless, as observed during the hydrolysis of the same sample in the presence of 0.1 M of KOH/MeOH, hypothesis that the degradation in PBS will occur but will require a longer time, as it was observed in Chapter 3 for the degradation of the PEG-grafted copolymer of poly(MDO-*co*-VBr).

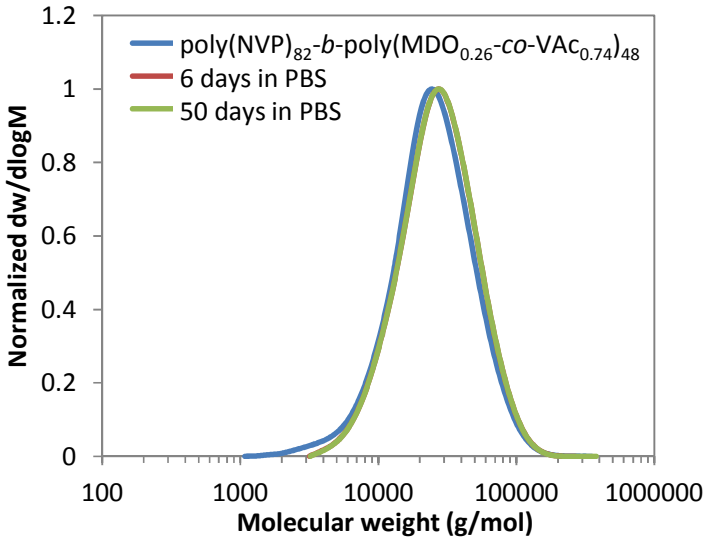

Figure 6.19. Size exclusion chromatograms of poly(NVP)$_{82}$-*b*-poly(MDO$_{0.26}$-*co*-VAc$_{0.74}$)$_{48}$ after degradation in PBS for 6 and 50 days at 37 °C.

In an attempt to investigate the degradation of the particles formed from the block copolymer poly(NVP)-*b*-poly(MDO-*co*-VAc), further experiments were carried out where the self-assembly of poly(NVP)$_{82}$-*b*-poly(MDO$_{0.26}$-*co*-VAc$_{0.74}$)$_{48}$ (polymer **P11**), was performed using the solvent switch technique from THF to as PBS solution. The self-assembly process under these conditions led to a particle solution in PBS with a concentration of 1.0 mg/mL. Under the PBS conditions, the amhiphilic block copolymer was found to form particles with a R_h of 36.7 nm as obtained by SLS analyses. The self-assemblies solution was the placed in an incubator at 37 °C and the stability of the particles over time was investigated by

monitoring the decrease in the aggregation, N_{agg} (Figure 6.20). After 28 days of incubation in the hydrolysis solution, a small decrease in N_{agg} was observed as seen by the reduction of the initial value of 146 to 126. Furthermore, when the hydrolysis was continued for a longer time, the aggregation number decreased to 29.5 after 152 days of hydrolysis confirming that the size of the particles were decreasing as a consequence of the degradation of the ester repeat units introduced in the core of the self-assemblies (Table 6.3).

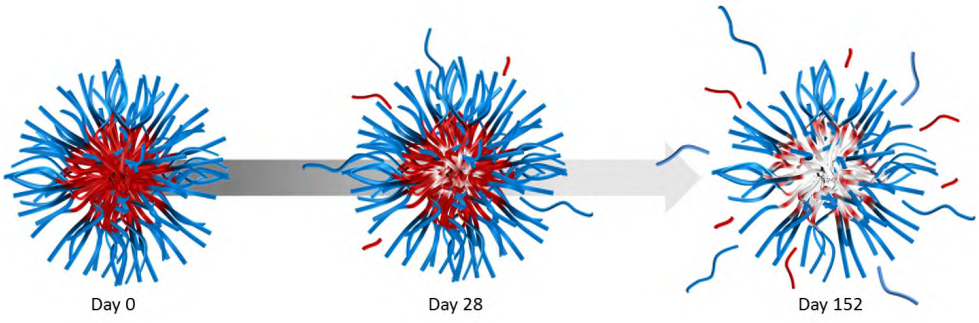

Figure 6.20. Schematic representation of the degradation occurring for the self-assemblies of poly(NVP)$_{82}$-*b*-poly(MDO$_{0.26}$-*co*-VAc$_{0.74}$)$_{48}$ in PBS medium and at 37 °C.

Table 6.3. Characteristic data of the particles after hydrolysis in PBS solution at 37 °C for different exposure times.

Hydrolysis time in PBS (Days)	R_h (nm)[a]	N_{agg}[a]
0	36.7	146
4	36.3	130
7	37.4	142
13	33.8	130
28	37.5	126
152	14.5	29.5

[a] Obtained by SLS analysis.

6.3.5 Extension of the concept to a vinyl acetate derivative monomer

Following on from the successful synthesis of degradable nanoparticles of poly(NVP)-*b*-poly(MDO-*co*-VAc), the concept was further investigated using vinyl bromobutanoate (VBr) as a functional substitute for VAc (Scheme 6.3). In Chapter 3 the copolymerization of VBr and MDO was introduced with a view towards the synthesis of functional degradable

copolymers bearing bromine functional pendent groups which can be modified *via* post-polymerization azidation and cycloaddition reactions.[60]

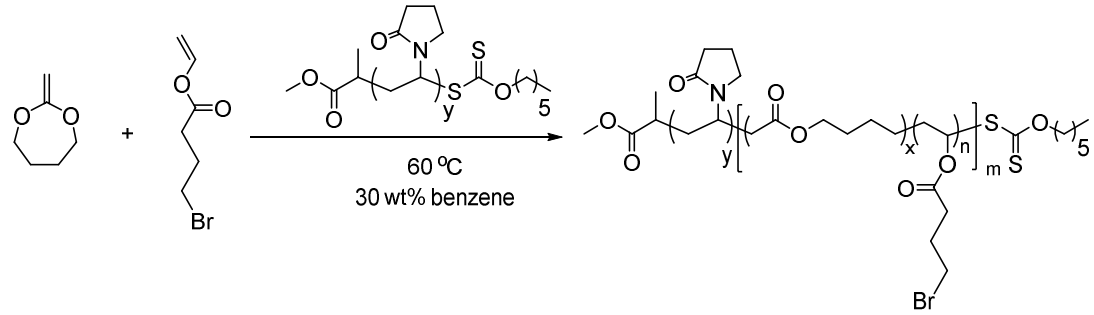

Scheme 6.3. Schematic representation of the synthesis of functional poly(NVP)-*b*-poly(MDO-*co*-VBr) using poly(NVP) as a macro-CTA.

Aiming at introducing the same bromine functional pendent groups in the amphiphilic block copolymer towards the formation of further functional self-assemblies the copolymerization of VBr and MDO using a poly(NVP)$_{58}$ macro-CTA, M_n^{SEC} = 4.30 kg/mol, $Đ_M$ = 1.19, was performed to form the functional block copolymer, poly(NVP)$_{58}$-*b*-poly(MDO$_{0.28}$-*co*-VBr$_{0.72}$)$_{40}$. The successful chain extension of the macro-CTA was proven by the net increase in molecular weight, as observed by SEC analysis, after addition of the hydrophobic poly(MDO-*co*-VBr) block to obtain a final block copolymer with a molecular weight, M_n^{SEC} of 10.2 kg/mol. The final dispersity, after chain extension, of 1.51 indicated that the polymerisation had proceeded with relatively good control (Figure 6.21).

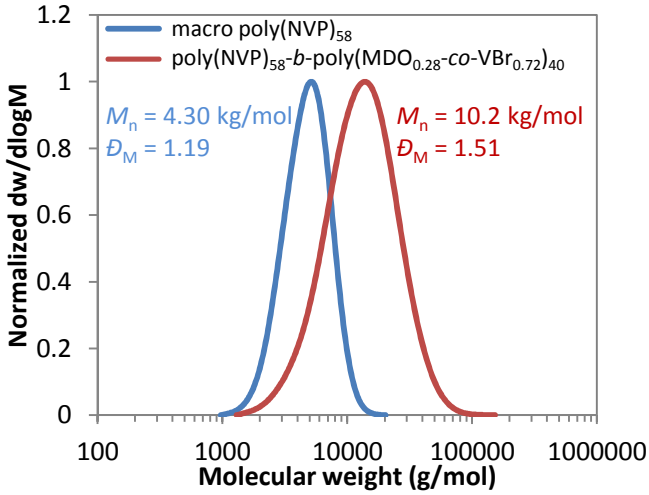

Figure 6.21. Size exclusion chromatograms of the chain extension of the poly(NVP)$_{58}$ macro-CTA with MDO and VBr to form the block copolymer: poly(NVP)$_{58}$-*b*-poly(MDO$_{0.28}$-*co*-VBr$_{0.72}$)$_{40}$ (SEC DMF, PMMA used as standards).

The self-assembly of poly(NVP)$_{58}$-*b*-poly(MDO$_{0.28}$-*co*-VBr$_{0.72}$)$_{40}$ was performed by using the solvent switch technique, from THF to water, previously used throughout this study to give a particle solution with a concentration of 1.0 mg/mL. DLS analysis confirmed the formation of particles with a D_h value of 28 nm (Figure 6.22), while the low polydispersity (0.202) obtained indicated a single population of the functional nanoparticle. TEM analysis was further carried out to confirm the presence of the particles where an average diameter, D_{av}, of 20 nm was obtained which was in good agreement with the DLS results (Figure 6.23).

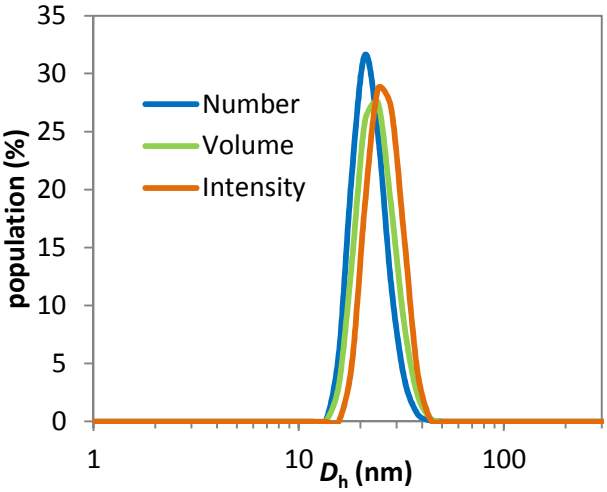

Figure 6.22. DLS traces of the particles formed from poly(NVP)$_{58}$-*b*-poly(MDO$_{0.28}$-*co*-VBr$_{0.72}$)$_{40}$.

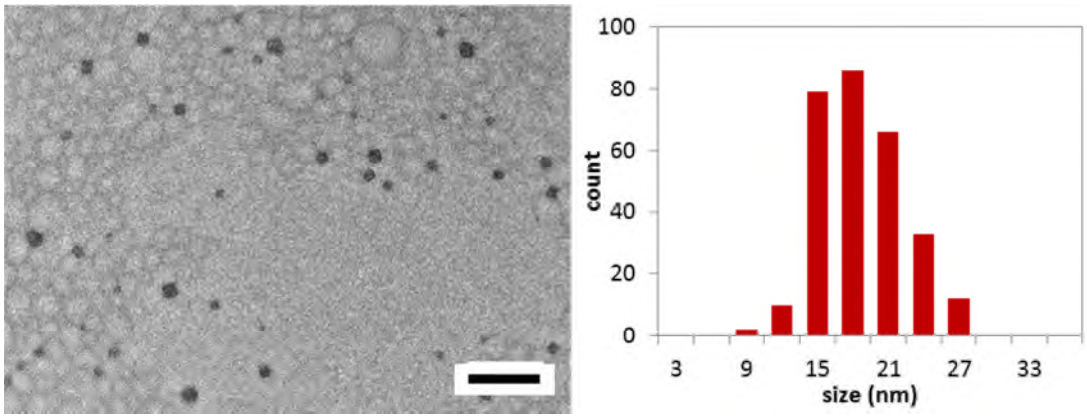

Figure 6.23. TEM image (left, scale bar = 100 nm) of particles formed from the amphiphilic block copolymer poly(NVP)$_{58}$-*b*-poly(MDO$_{0.28}$-co-VAc$_{0.72}$)$_{40}$ and histogram showing the distribution of sizes (right).

6.3.6 Post-polymerization of poly(NVP)$_{58}$-*b*-poly(MDO$_{0.28}$-*b*-VBr$_{0.72}$)$_{40}$

Inspired by the post-polymerization modification reactions performed in Chapter 3 on poly(MDO-*co*-VBr), and aiming to incorporate further functionality into the nanoparticles, post-polymerization reactions were performed using azidation and "click" chemistry (Scheme 6.4). In a first step, the conversion of the bromine pendent groups into azide groups was successfully performed using NaN_3 in DMF for 2 days, and confirmed by ^{1}H NMR spectroscopy analysis where a shift of the CH_2-Br characteristic signal at δ = 3.50 ppm to the CH_2-N_3 signal at δ = 3.40 ppm was observed (Figure 6.24a-b). These observations are in agreement with the changes in chemical shift previously observed for the azidation of poly(MDO-*co*-VBr) presented in Chapter 3.[60] In a second step, the "click" reaction between the azide-functional block copolymer and *N*-alkyne dithiomaleimide (1.1 eq) was conducted in THF, in the presence of CuI (0.1 eq) and *N*,*N*,*N*′,*N*′,*N*″-pentamethyldiethylenetriamine, PMDETA, (0.1 eq) for 2 hours at 35 °C. Dithiomaleimides (DTMs) are compounds which have been found to show high emissive fluorophore properties that can be used as interesting tools for fluorescent labelling of polymers.[71-74] After the "click" reaction, the dithiomaleimide functional block copolymer was recovered by several precipitations in diethyl ether in order to remove the excess of alkyne dithiomaleimide and the final polymer

was dried under vacuum overnight to yield a bright yellow solid. The successful "click" reaction was confirmed by ^{1}H NMR spectroscopy analysis where the appearance of the characteristic resonance at δ = 7.75 ppm, which corresponds to the triazole proton, was observed as well as the formation of new resonances at δ = 4.40, 3.25, 1.75-1.40 and 0.90 ppm from the characteristic CH_2 and CH_3 of the additional dithiomaleimide groups (Figure 6.24c).

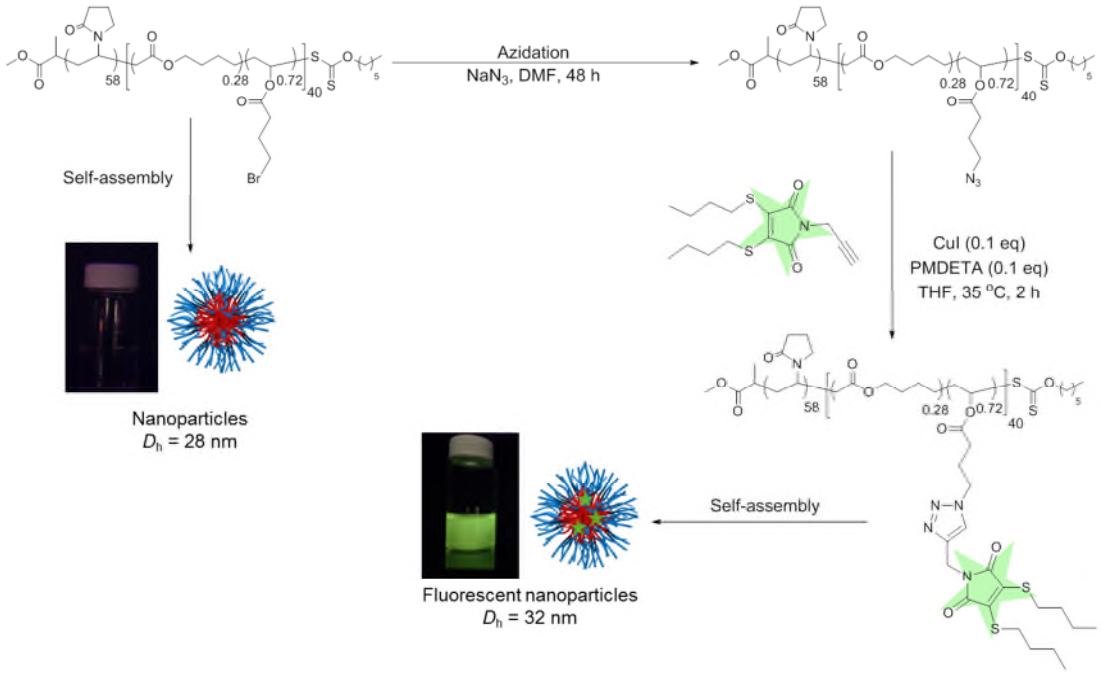

Scheme 6.4. Synthetic approach for the formation of fluorescently labelled particles by polymerization modification with the alkyne functional dithiomaleimide, followed by self-assembly.

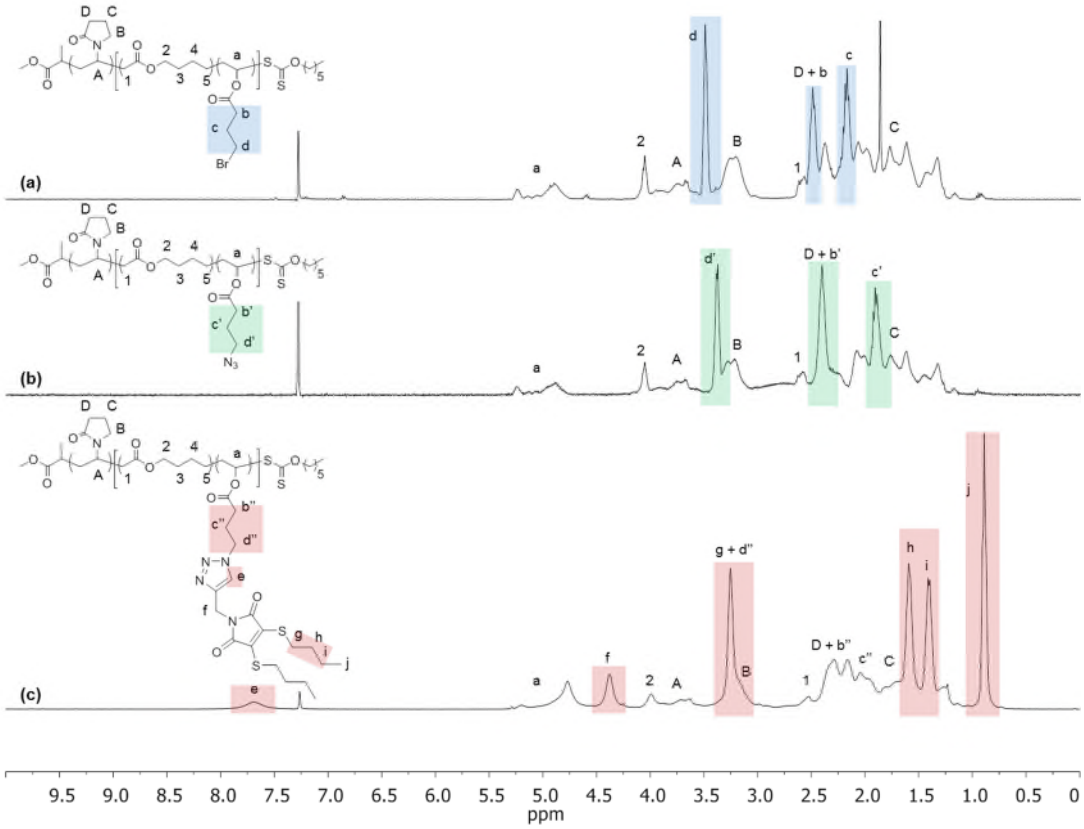

Figure 6.24. ^{1}H NMR spectra of the post-polymerization modification of the block copolymer, (a) poly(NVP)$_{58}$-*b*-poly(MDO$_{0.28}$-*co*-VBr$_{0.72}$),(b) after azidation with NaN_3 and (c) after click reaction with the functional dithiomaleimide. (400 MHz, $CDCl_3$).

The self-assembly of the dithiomaleimide functional block copolymer was then performed using the solvent switch technique to form a yellow solution in water containing particles (1.0 mg/ml) as confirmed by DLS analysis where D_h = 32 nm was observed, which is very similar to the size of the particles observed before functionalization (D_h = 28 nm). Nethertheless, the presence of larger, ill-defined aggregates in the solution was observed in both DLS analysis and TEM analysis (Figure 6.25), which was hypothesized to be the result of a change in the packing arrangement of the new dithiomalemide functionalized hydrophobic polymer chains.

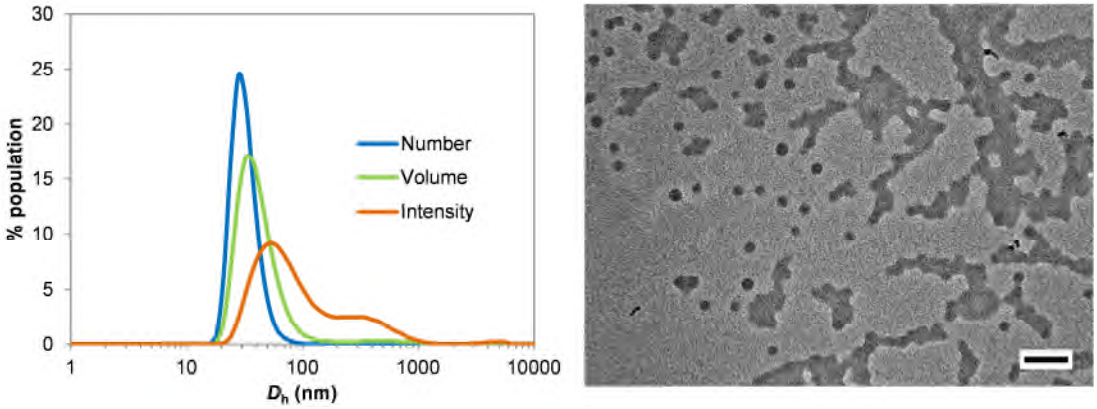

Figure 6.25. DLS trace (left) and TEM image (right, scale bar = 100 nm) of particles formed from poly(NVP)$_{58}$-*b*-poly(MDO$_{0.28}$-*co*-VN$_{3(0.72)}$)$_{40}$ after modification with the functional dithiomaleimide (left).

The functional self-assemblies solution was then analysed using fluorescent spectroscopy in order to identify the emission and excitation wavelengths of the solution and confirm whether or not the particle solution was presenting fluorescent properties. The fluorescence of the solution was confirmed by the excitation observed at λ = 419 nm and the following emission at λ = 533 nm (Figure 6.26). The copolymerization of VBr and MDO using a poly(NVP) macro-CTA, as well as the post-polymerization modifications to functionalize with a dithiomaleimide highlights the promising perspective of using the approach of this Chapter to create novel functional and degradable nanoparticles containing a fluorescent label.

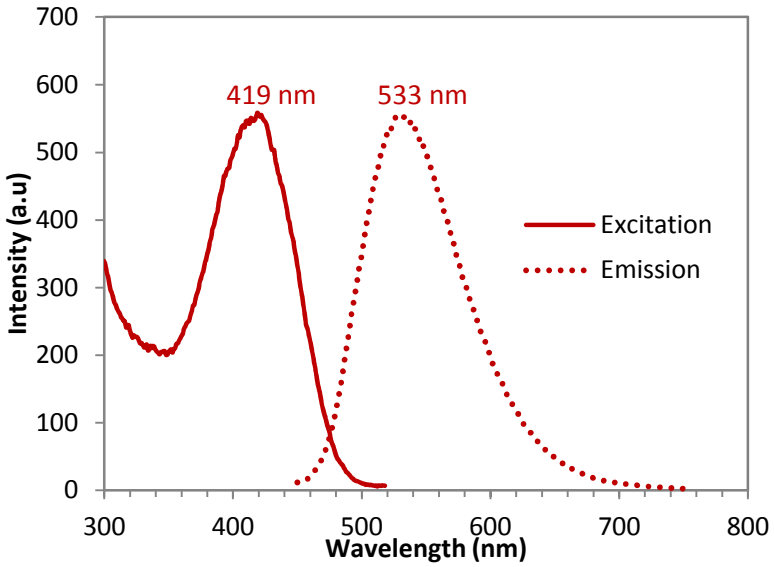

Figure 6.26. Excitation and emission spectra of the micelles in water obtained using the block copolymer after functionalization with the alkyne dithiomaleimide.

6.4 Conclusions

In this chapter, the synthesis of degradable, functional, amphiphilic block copolymers was investigated using the rROP of MDO and RAFT/MADIX polymerization with VAc in the presence of different poly(NVP) as macro chain transfer agents. The process was able to be tuned to obtain different amounts of ester repeat units in the hydrophobic backbone as a way of increasing the degradability. The self-assembly of these block copolymers in water was also demonstrated to form spherical nanoparticles, as seen by the results obtained by DLS and TEM. Further experiments where the hydrophilic and hydrophobic block lengths of the copolymers were modified highlighted the possibility of tuning the size of the particles where D_h, D_{av}, R_h and N_{agg} were found to increase as the length of either block was increased. Additionally, the degradability of the block copolymer was assessed by hydrolysis in both methanolic conditions and PBS, where a decrease of the molecular masses of the samples, observed by SEC, as well as a decrease in the $N_{agg,}$ calculated by SLS, confirmed the successful degradation of the hydrophobic part of the polymers. Finally, by applying this

concept to vinyl bromobutanoate, the successful synthesis of a new functional block copolymer of poly(NVP)-*b*-poly(MDO-*co*-VBr) was performed and was able to undergo successful post-polymerization modifications using azidation and "click" chemistry to incorporate a fluorescent tag into the polymer. Self-assembly of this polymer yielded fluorescent nanoparticles, as confirmed by the emission and excitation results obtained by fluorescent spectroscopy analysis. The concept of forming amphiphilic block polymers by combining both rROP and RAFT polymerization for the copolymerization of MDO and VAc/VBr opens a successful route towards the formation of nanoparticles for potential biomedical applications where labelling tags can be incorporated into the core of the particles.

6.5 Experimental section

6.5.1 Materials

The following monomers were purified before use by distillation over CaH_2; vinyl acetate (VAc: Sigma-Aldrich, > 99%; distillation pressure: 0.015 atm, 90-92 °C), *N*-vinylpyrrolidone (NVP: Sigma-Aldrich, > 98%; 0.015 atm, 90 °C). The following solvents were used as received; dichloromethane (DCM: VWR International, AR grade), *N*,*N*-dimethylformamide (DMF: Sigma-Aldrich, HPLC grade), ethyl acetate (EtOAc, Fisher Scientific, LT grade), tetrahydrofuran (THF, VWR International, AR grade). The following chemicals were used as received: 2,2'Azobis(2-methyl propionitrile) (AIBN, Sigma-Aldrich, > 98%), N-methyl morpholine (Sigma-Aldrich, > 98%, GC grade), methyl chloroformate (Sigma-Aldrich, > 98%), *N*,*N*,*N*′,*N*′,*N*″-pentamethyldiethylenetriamine (PMDETA, Sigma-Aldrich, 99%), copper iodide (CuI, Sigma-Aldrich, 99.5%), sodium azide (NaN_3, Sigma-Aldrich, 99%). 2-Methylene-1,3-dioxepane (MDO) was synthesized using the previously described method of Bailey *et al.*,[47] the CTA, *O*-hexyl *S*-methyl 2-propionylxanthate (CTA 1), and the monomer vinyl bromobutanoate (VBr) were synthesized

using the procedures described in Chapters 2 and 3, respectively.[59,60] The water used for self-assembly was purified using an ion exchange cartridge (18.2 MΩ·cm).

6.5.2 Characterization methods

Nuclear magnetic resonance (^{1}H and ^{13}C NMR) spectra were recorded at 400 MHz and 100 MHz, respectively, in $CDCl_3$ on a Bruker DPX-400 spectrometer at 298 K. Chemical shifts are reported as δ in parts per million (ppm) and referenced to the chemical shift of the residual solvent resonances ($CDCl_3$ ^{1}H: δ = 7.26 ppm; ^{13}C: δ = 77.16 ppm). Size exclusion chromatography (SEC) analyss was performed on a system composed of a Varian 390-LC-Multi detector using a Varian Polymer Laboratories guard column (PLGel 5 μM, 50 × 7.5 mm), two mixed D Varian Polymer Laboratories columns (PLGel 5 μM, 300 × 7.5 mm) and a PLAST RT autosampler. Detection was conducted using a differential refractive index (RI) and an ultraviolet (UV) detector set to 280 nm. The analyses were performed at 303 K in DMF (HPLC grade) containing 0.5% triethyl amine (TEA) at a flow rate of 1.0 mL/min. Poly(methyl methacrylate) (PMMA) (200 – 1.0 × 10^6 g/mol) standards were used for calibration. Molecular weights and dispersities were determined using Cirrus v3.3 SEC software. IR spectroscopy was carried out using a Perkin Elmer Spectrum 100 FT-IR. 16 scans from 600 to 4000 cm^{-1} were taken, and the spectra corrected for background absorbance. DLS analysis was performed on a Malvern Zetasizer Nano ZS instrument operating at 25 °C with a 4 Mw He-Ne 633 nm laser module. Measurements were made at an angle of 173° (back scattering), and results were analyzed using Malvern DTS 6.32 software. All determinations were made in triplicate unless otherwise stated (with 10 measurements recorded for each run). SLS experiments were performed at angles of observation ranging from 20° up to 150° with an ALV CG3 spectrometer operating at λ_0 = 633 nm and at 20 ± 1 °C. Solutions (1 mg/mL) were filtered through 0.45 μm nylon filters prior to analysis. Data were collected in duplicate with 100 s run times. Calibration was achieved with filtered

toluene and the background was measured with water. The hydrodynamic radius, R_h, and aggregation number, N_{agg} of the self-assemblies were calculated using the REPES algorithm[75] to calculate the relaxation time, τ. The values of τ for each measured angle were plotted against the square of the scattering wave vector, q, to identify the apparent diffusion coefficient, D, following the equation (1).

$$\tau^{-1} = q^2.D \qquad (1)$$

The Stokes-Einstein equation (2) was used to calculate the hydrodynamic radius, R_h, where η is the viscocity of the medium, k_B is the Boltzman's constent and T is the absolute temperature in Kelvin.

$$R_h = \frac{k_B.T}{6\pi.\eta.D} \qquad (2)$$

The partial Zimm plots were obtained from the SLS analysis and the aggregation number, N_{agg}, for each solution was determined using the equation (3) where c is the polymer concentration, R_g is the radius of gyration, M_w the apparent molecular weight of the particles, $R_{\theta,\,fast}$ is the Rayleigh ratio for the fast mode of the sample calculated using equation (5) and K is a constant calculated according to equation (4).

$$\frac{K.c}{R_{\theta,fast}} \approx \frac{q^2.{R_g}^2}{3M_{w,particle}} + \frac{1}{M_{w,particle}} \qquad (3)$$

$$K = \frac{4\pi^2 {n_{ref}}^2 \left(\frac{dn}{dc}\right)^2}{\lambda^4 N_A} \qquad (4)$$

Where n_{ref} is the refractive index of the reference (toluene), dn/dc is the calculated refractive index increment of the polymer solution, λ is the wavelength of the laser (633 nm) and N_A the Avogadro's number.

$$R_{\theta,fast} = A_{fast}(q)R_{\theta} = \frac{A_{fast}}{A_{fast} + A_{slow}}(q)\frac{I_{sample}(q) - I_{solvent}(q)}{I_{reference}(q)}R_{reference} \qquad (5)$$

Where A_{fast}(q) + A_{slow}(q) are the scattered intensity contribution at a given angle from the fast + slow mode of relaxation respectively as determined by DLS, I_{sample}, $I_{solvent}$ and $I_{reference}$ are the scattered intensities by the sample, the solvent and the reference at a given scattering wave vector, q, and $R_{reference}$ is the Rayleigh ratio of the reference solvent (toluene).

For each SLS analysis, the intensity of the scattering light, I_{sample}, was used to determine Kc/R_{θ} for each angle. It should be mentioned that if the R_h of the particles were less than 20 nm, the average value of Kc/R_{θ} over the angles analysed was equal to the inverse of the particles'molecular weight, $M_{wparticle}$, and was used to calculate the aggregation number, N_{agg}, using equation (6).

$$N_{agg} = \frac{M_{w,particle}}{M_{w,polymer}} \qquad (6)$$

TEM samples were prepared on graphene oxide (GO)-coated carbon grids which allows high contrast TEM images to be acquired without staining. As a typical preparation procedure, an aqueous drop of sample (5 μL, 1 mg/mL) was deposited on the grid and left to air dry. TEM observations were performed on a JEOL 2000FX electron microscope operating at an acceleration voltage of 200 keV. Fluorescence spectra were recorded using an Agilent CaryEclise fluorescence spectrometer.

6.5.3 Typical procedure for the synthesis of poly(NVP)$_{70}$ macro-CTA

The poly(NVP) macro-CTA was synthesized according to the previously reported procedure.[59] In a typical experiment NVP (1 g, 9.0 mmol), *O*-hexyl *S*-methyl 2-propionylxanthate (CTA 1) (0.047 g, 0.18 mmol), AIBN (2.95 mg, 0.018 mmol) and benzene (30 wt%) were introduced into an ampoule. The mixture was degassed by four freeze-pump-

thaw cycles, sealed under nitrogen and heated at 60 °C for 4.5 hours and then quenched in an ice bath. An aliquot was taken prior to precipitation in order to determine the monomer conversions using ^{1}H NMR spectroscopy. The poly(NVP) obtained was purified by several precipitations in diethyl ether until no further monomer residue could be observed by ^{1}H NMR spectroscopy. The sample was dried under vacuum overnight to yield a white solid. ^{1}H NMR (400 MHz, $CDCl_3$, ppm) δ: 4.58 (t, SCOCH_2CH$_2$ end-group, 2H, $^3J_{H\text{-}H}$ = 5.4 Hz), 4.16-3.50 (m, CH$_2$CHNCOCH$_2$ backbone, 1H, CH_3OCOCHCH$_3$ end-group, 3H), 3.45-2.65 (m, CHNCH_2CH$_2$CH$_2$ NVP$_{ring}$, 2H), 2.65-1.10 (m, NCH$_2$CH$_2$CH_2 NVP$_{ring}$, 2H, NCH$_2$CH$_2$CH$_2$ NVP$_{ring}$, 2H, CH$_2$CHNCH$_2$ backbone, 2H, CH$_2$CH_2CH$_2$CH$_3$ end-group, 2H, CH$_2$CH$_2$CH_2CH$_3$ end-group, 2H, CH$_2$CH_2CH$_2$CH$_3$ end-group, 2H), 0.90 (m, CH$_2$CH$_2$CH$_2$CH_3 end-group, 3H). Conversion by ^{1}H NMR spectroscopy: NVP conversion = 70%, M_n (SEC, DMF) = 5.3 kg/mol, $Đ_M$ = 1.18, M_n (^{1}H NMR) = 8.0 kg/mol.

6.5.4 Typical procedure for the synthesis of poly(NVP)$_{70}$-*b*-poly(MDO$_{0.23}$-*co*-VAc$_{0.77}$)$_{55}$

In a typical experiment, poly(NVP) macro-CTA (0.25 g, 0.074 mmol) was dissolved in benzene (30 wt%). MDO (0.25 g, 2.19 mmol), VAc (0.45 g, 5.22 mmol) and AIBN (1.2 mg, 0.0073 mmol) were added and stirred at room temperature until total dissolution. The mixture was introduced into an ampoule and degassed by four freeze-pump thaw cycles and sealed under nitrogen. The polymerization was carried out for 5 hours at 60 °C and then quenched in an ice bath. An aliquot was taken prior to precipitation in order to determine the monomer conversions using ^{1}H NMR spectroscopy. The block copolymer, poly(NVP)-*b*-poly(MDO-*co*-VAc), was dissolved in a small amount of CH_2Cl_2 (1 mL) and purified by several precipitations in diethyl ether. The sample was dried under vacuum overnight to yield a white solid. ^{1}H NMR (400 MHz, $CDCl_3$, ppm) δ: 5.30-4.75 (m, CH$_2$CHOCO backbone VAc, 1H), 4.58 (m, SCOCH_2CH$_2$ end-group, 2H), 4.16-3.90 (m, COOCH_2CH$_2$CH$_2$ backbone MDO, 2H), 3.90-3.45 (m, CH$_2$CHNCOCH$_2$ backbone NVP, 1H, CH_3OCOCHCH$_3$ end-

group, 3H), 3.45-2.75 (m, CHNCH_2CH$_2$CH$_2$ NVP$_{ring}$, 2H), 2.65-2.45 (m, CH_2COOCH$_2$CH$_2$ backbone MDO), 2.45-2.10 (m, CHNCH_2CH$_2$CH$_2$ NVP$_{ring}$, 2H, COOCH$_2$CH$_2$CH_2 backbone MDO, 2H), 2.10-1.80 (m, OCOCH_3 backbone VAc, 3H, CHNCH$_2$CH_2CH$_2$ NVP$_{ring}$, 2H, CH$_3$OCOCHCH$_3$ end-group, 1H, CH$_3$OCOCHCH_3 end-group, 3H), 1.45-1.10 (m, CH$_2$CH_2CH$_2$CH$_3$ end-group, 2H, CH$_2$CH$_2$CH_2CH$_3$ end-group, 2H, CH_2CH$_2$CH$_2$CH$_3$ end-group, 2H), 0.90 (m, CH$_2$CH$_2$CH$_2$CH_3 end-group, 3H). Conversions by ^{1}H NMR spectroscopy: VAc conversion = 38%, MDO conversion = 23%, M_n (SEC, DMF) = 13.2 kg/mol, $Đ_M$ = 1.49.

6.5.5 Typical procedure for the synthesis of poly(NVP)$_{58}$-*b*-poly(MDO$_{0.28}$-*co*-VBr$_{0.72}$)$_{40}$

In a typical experiment, poly(NVP) macro-CTA (0.10 g, 0.023 mmol) was dissolved in benzene (30 wt%) and MDO (0.10 g, 0.87 mmol), VBr (0.35 g, 1.81 mmol) and AIBN (1.2 mg, 0.0073 mmol) were added and stirred at room temperature until total dissolution. The mixture was introduced into an ampoule and degassed by four freeze-pump-thaw cycles and sealed under nitrogen. The polymerization was carried out for 4.5 hours at 60 °C and then quenched in an ice bath. An aliquot was taken prior to precipitation in order to determine the monomer conversions using ^{1}H NMR spectroscopy. The block copolymer, poly(NVP)-*b*-poly(MDO-*co*-VBr), was dissolved in a small amount of CH$_2$Cl$_2$ (1 mL) and purified by several precipitations in diethyl ether. The sample was dried under vacuum overnight to yield a white solid. ^{1}H NMR (400 MHz, CDCl$_3$, ppm) δ: 5.25-4.75 (m, CH$_2$CHOCO backbone VBr, 1H), 4.58 (m, SCOCH_2CH$_2$ end-group, 2H), 4.20-3.70 (m, COOCH_2CH$_2$CH$_2$ backbone MDO, 2H, m, CH$_2$CHNCOCH$_2$ backbone NVP, 1H, CH_3OCOCHCH$_3$ end-group, 3H), 3.60-3.40 (t, BrCH_2CH$_2$CH$_2$CO, 2H), 3.45-3.00 (m, CHNCH_2CH$_2$CH$_2$ NVP$_{ring}$, 2H), 2.65-2.45 (m, CH_2COOCH$_2$CH$_2$ backbone MDO, 2H), 2.45-2.10 (m, CHNCH_2CH$_2$CH$_2$ NVP$_{ring}$, 2H, COOCH$_2$CH$_2$CH_2 backbone MDO, 2H, m, BrCH$_2$CH$_2$CH_2CO, 2H), 2.10-1.80 (m, BrCH$_2$CH_2CH$_2$CO, 2H, m, OCOCH$_3$ backbone VAc, 3H, CHNCH$_2$CH$_2$CH$_2$ NVP$_{ring}$, 2H),

m, C*H*CH_2OCO backbone VBr, 1H, CH_3OCOC*H*CH_3 end-group, 1H, CH_3OCOCHC*H*$_3$ end-group, 3H), 1.45-1.10 (m, CH_2C*H*$_2CH_2CH_3$ end-group, 2H, CH_2CH_2C*H*$_2CH_3$ end-group, 2H, $CH_2CH_2CH_2CH_3$ end-group, 2H, $CH_2COOCH_2CH_2$C*H*$_2$, 2H), 0.90 (m, $CH_2CH_2CH_2$C*H*$_3$ end-group, 3H). Conversions by ^{1}H NMR spectroscopy: MDO conversion = 23%, VBr = 38%, M_n (SEC, DMF) = 10.2 kg/mol, $Đ_M$ = 1.51.

6.5.6 Typical procedure for the azidation of poly(NVP)$_{58}$-*b*-poly(MDO$_{0.28}$-*co*-VBr$_{0.72}$)$_{40}$

The starting polymer, poly(NVP)-*b*-poly(MDO-*co*-VBr) was synthesized according to the procedure previously described in section 6.5.5, M_n (SEC, DMF) = 10.2 kg/mol, $Đ_M$ = 1.51). Poly(NVP)-*b*-poly(MDO-*co*-VBr) (0.30 g, 0.029 mmol) was dissolved in DMF (12 mL) and NaN_3 (0.08 g, 1.23 mmol) was added to the mixture before being stirred at room temperature for 2 days. DMF was removed under vacuum and the polymer was re-dissolved in a small amount of toluene before being precipitated into cold hexane. The recovered polymer was dried *in vacuo*. ^{1}H NMR (400 MHz, $CDCl_3$, ppm) δ: 5.25-4.75 (m, CH_2C*H*OCO backbone$_{VN3}$, 1H), 4.58 (m, SCOC*H*$_2CH_2$ end-group, 2H), 4.20-3.70 (m, COOC*H*$_2CH_2CH_2$ backbone, 2H, m, CH_2C*H*NCOCH_2 backbone$_{NVP}$, 1H, C*H*$_3$OCOCHCH_3 end-group, 3H), 3.60-3.40 (t, BrC*H*$_2CH_2CH_2$CO, 2H), 3.45-3.00 (m, CHNC*H*$_2CH_2CH_2$ NVP$_{ring}$, 2H), 2.65-2.45 (m, C*H*$_2$COOCH_2CH_2 backbone, 2H), 2.45-2.10 (m, CHNC*H*$_2CH_2CH_2$ NVP$_{ring}$, 2H, COOCH_2CH_2C*H*$_2$ backbone, 2H, m, $N_3CH_2CH_2$C*H*$_2$CO, 2H), 2.10-1.80 (m, N_3CH_2C*H*$_2CH_2$CO, 2H, m, OCOCH_3 backbone, 3H, CHNC$H_2CH_2CH_2$ NVP$_{ring}$, 2H, m, C*H*CH_2OCO backbone, 1H, C*H*$_2$CHOCOCH_2 backbone, 2H, CH_3OCOC*H*CH_3 end-group, 1H, CH_3OCOCHC*H*$_3$ end-group, 3H), 1.45-1.10 (m, CH_2C*H*$_2CH_2CH_3$ end-group, 2H, CH_2CH_2C*H*$_2CH_3$ end-group, 2H, $CH_2CH_2CH_2CH_3$ end-group, 2H, $CH_2COOCH_2CH_2$C*H*$_2$, 2H), 0.90 (m, $CH_2CH_2CH_2$C*H*$_3$ end-group, 3H). M_n (SEC, DMF) = 11.1 kg/mol, $Đ_M$ = 1.53.

6.5.7 Synthesis of the alkyne-functional dithiomaleimide

The alkyne-functional dithiomaleimide was synthesized in a three step process. In the first step 3,4-bis(butylsulfanyl)-2,5-dihydro-1H-pyrrole-2,5-dione (i) was supplied by Dr Mathew Robin from Prof. Rachel O'Reilly's group, University of Warwick, and synthesized using the reported procedure.[71] In the second step, a solution of (i) (1.50 g, 5.49 mmol) and *N*-methylmorpholine (0.555 g, 5.49 mmol) in ethyl acetate (50 ml) was added to methyl chloroformate (0.570 g, 6.04 mmol). The solution was stirred at room temperature for 2 hours, before ethyl acetate (50 ml) was added and the organic layer washed with water (3 × 200 ml) and dried with $MgSO_4$. The solvent was removed *in vaccuo* to give the product, methyl 3,4-bis(butylsulfanyl)-2,5-dioxo-2,5-dihydro-1H-pyrrole-1-carboxylate (ii), as a dark yellow liquid (1.64 g, 90%). ^{1}H NMR (400 MHz, $CDCl_3$): δ 3.97 (s, C*H*$_3$OCON, 3H), 3.34 (t, SC*H*$_2$CH$_2$CH$_2$, 4H, $^3J_{H\text{-}H}$ = 7.5 Hz), 1.65 (quint, SCH$_2$C*H*$_2$CH$_2$, 4H, $^3J_{H\text{-}H}$ = 7.5 Hz), 1.45 (sext, SCH$_2$CH$_2$C*H*$_2$, 4H, $^3J_{H\text{-}H}$ = 7.5 Hz), 0.93 (t, CH$_2$CH$_2$C*H*$_3$, 6H, $^3J_{H\text{-}H}$ = 7.5 Hz); ^{13}C NMR (100 MHz, $CDCl_3$): δ 161.5 (CON*C*OC pyrrole), 151.2 (CH$_3$O*C*ON), 137.1 (CONCO*C* pyrrole), 54.3 (*C*H$_3$OCO), 32.5 (SCH$_2$*C*H$_2$CH$_2$), 31.7 (S*C*H$_2$CH$_2$CH$_2$), 21.7 (CH$_2$*C*H$_2$CH$_3$), 13.6 (CH$_2$CH$_2$*C*H$_3$). FTIR: λ_{max} / cm^{-1}, 1800 (C=O stretch), 1751 (C=O stretch maleimide), 1717 (C=O stretch maleimide); HR-MS: m/z found 354.0822, calc. 354.0804 ([M+Na]$^+$, 100%). In the third step, the alkyne-functional maleimide was obtained by dissolving (ii) (0.85 g, 2.56 mmol) in CH_2Cl_2 (85 ml) and propargyl amine (0.14 g, 2.54 mmol) was added to the solution and stirred for 5 hours at room temperature. After 5 hours, 0.85 g of silica was added and the mixture was stirred overnight. The solvent was removed *in vacuo* and the product was purified by column chromatography (19:1, petroleum ether: ethyl acetate) to yield a yellow liquid (0.68 g, 86%). ^{1}H NMR (400 MHz, $CDCl_3$): δ 4.25 (s, HCCC*H*$_2$N, 2H), 3.32 (t, SC*H*$_2$CH$_2$CH$_2$, 4H, $^3J_{H\text{-}H}$ = 7.5 Hz), 2.22 (s, *H*CCCH$_2$N, 1H), 1.62 (quint, SCH$_2$C*H*$_2$CH$_2$, 4H, $^3J_{H\text{-}H}$ = 7.5 Hz), 1.43 (sext, SCH$_2$CH$_2$C*H*$_2$, 4H, $^3J_{H\text{-}H}$ = 7.5 Hz), 0.91 (t, CH$_2$CH$_2$C*H*$_3$, 6H, $^3J_{H\text{-}H}$ = 7.5 Hz); ^{13}C NMR (100 MHz, $CDCl_3$) δ 163.0 (CON*C*OC

pyrrole), 137.5 (CONCO*C* pyrrole), 77.8 (*C*HCCH$_2$N), 72.1 (CH*C*CH$_2$N), 32.7 (SCH$_2$*C*H$_2$CH$_2$), 31.5 (S*C*H$_2$CH$_2$CH$_2$), 21.7 (CH$_2$*C*H$_2$CH$_3$), 13.5 (CH$_2$CH$_2$*C*H$_3$). FTIR: λ_{max} / cm^{-1}, 3285 (C≡CH stretch), 2960 (C-H stretch), 1800 (C=O stretch), 1770 (C=O stretch maleimide), 1702 (C=O stretch maleimide); HR-MS: m/z found 334.0908, calc. 334.0906 ([M+Na]$^+$, 100%).

6.5.8 Typical procedure for the "click" reaction between poly(NVP)-*b*-poly(MDO-*co*-VN$_3$) and the alkyne-functional dithiomaleimide

Poly(NVP)-*b*-poly(MDO-*co*-VN$_3$) was synthesized from the procedure described in section 6.5.6. Poly(NVP)-*b*-poly(MDO-*co*-VN$_3$) (0.25 g, 0.35 mmol) was dissolved in THF (20 mL) and PMDETA (73 μL, 0.035 mmol), Cu(I) (5 mg, 0.035 mmol) and the alkyne-functional dithiomaleimide (0.12 g, 0.38 mmol) were placed into an ampoule and sealed. The solution was then degassed by three freeze-pump-thaw cycles and the flask was re-filled with N$_2$. The mixture was stirred for 2 hours at 35 °C. After reaction, the solvent was removed under vacuum and the polymer was re-precipitated in diethyl ether in order to remove the excess of alkyne-functional dithiomaleimide. The modified copolymer was re-dissolved in CH$_2$Cl$_2$ and the copper species were removed using Cuprisorb beads overnight. The beads were removed via filtration and the polymer was precipitated in diethyl ether. ^{1}H NMR (400 MHz, CDCl$_3$, ppm) δ: 8.45-8.27 (m, NNC*H*C triazole, 1H), 5.25-4.75 (m, CH$_2$C*H*OCO backbone$_{Vinyl}$, 1H), 4.60-4.35 (s, C*H*$_2$N(CO)$_2$C=C dithiomaleimide$_{linkage}$, 2H, m, SCOC*H*$_2$CH$_2$ end-group, 2H), 4.20-3.70 (m, COOC*H*$_2$CH$_2$CH$_2$ backbone, 2H, m, CH$_2$C*H*NCOCH$_2$ backbone$_{NVP}$, 1H, C*H*$_3$OCOCHCH$_3$ end-group, 3H), 3.60-2.90 (m, CH$_2$CH$_2$C*H*$_2$-triazole, 2H, m, CHNC*H*$_2$CH$_2$CH$_2$ NVP$_{ring}$, 2H, m, CSC*H*$_2$CH$_2$CH$_2$CH$_3$ dithiomaleimide$_{end}$, 2H), 2.65-2.00 (m, C*H*$_2$COOCH$_2$CH$_2$ backbone, 2H, m, CHNC*H*$_2$CH$_2$CH$_2$ NVP$_{ring}$, 2H, COOCH$_2$CH$_2$C*H*$_2$ backbone, 2H), 2.00-1.20 (m, OCOCH$_3$ backbone, 3H, CHNCH$_2$CH$_2$CH$_2$ NVP$_{ring}$, 2H, m, C*H*CH$_2$OCO backbone, 1H, C*H*$_2$CHOCOCH$_2$ backbone, 2H, CH$_3$OCOC*H*CH$_3$ end-group,

1H, $CH_3OCOCHCH_3$ end-group, 3H, m, $CSCH_2CH_2CH_2CH_3$ dithiomaleimide$_{end}$, 2H, m, $CSCH_2CH_2CH_2CH_3$ dithiomaleimide$_{end}$, 2H, m, $CH_2CH_2CH_2CH_3$ end-group, 2H, $CH_2CH_2CH_2CH_3$ end-group, 2H, $CH_2CH_2CH_2CH_3$ end-group, 2H, $CH_2COOCH_2CH_2CH_2$, 2H), 0.90 (m, $CSCH_2CH_2CH_2CH_3$ dithiomaleimide$_{end}$, 3H, m, $CH_2CH_2CH_2CH_3$ end-group, 3H).

6.5.9 Self-assembly of polymers

The self-assembly of the diblock copolymers was performed using the solvent switch method. In a typical experiment, the polymer (10 mg) was dissolved in THF (1 mL) and water (10 mL) was slowly added at a rate of 0.6 mL/min under stirring. The solution was left stirring at room temperature for 3 days until the organic solvent was evaporated to yield a concentration solution of 1.0 mg/mL.

6.5.10 Degradation experiments

In a typical experiment, 500 mg of block copolymer was placed into a 14 mL vial and 10 mL of a solution of KOH in methanol (0.1 M) was then added to the vial and stirred at 37 °C. Samples (100 µL) were taken at different exposure times, freeze-dried and filtered in order to remove the residual salt before being analysed by SEC (DMF). The degradation in PBS was performed using similar conditions where 500 mg of block copolymer were placed in a 14 mL vial containing 10 mL of PBS solution (pH = 7.4). Samples (100 µL) were also taken at different exposure times, freeze-dried and filtered in order to remove the residual salt before being analysed by SEC (DMF). The degradation of the self-assemblies were performed by the direct formation of the nanoparticles in PBS (1.0 mg/mL) and placed in an incubator at 37 °C. SLS analysis of the nanoparticle solution was performed over time.

6.6 References

(1) Perrier, S.; Takolpuckdee, P. *J. Polym. Sci., Part A: Polym. Chem.* **2005**, *43*, 5347.

(2) Moad, G.; Rizzardo, E.; Thang, S. H. *Aust. J. Chem.* **2009**, *62*, 1402.

(3) Nicolas, J.; Guillaneuf, Y.; Lefay, C.; Bertin, D.; Gigmes, D.; Charleux, B. *Prog. Polym. Sci.* **2013**, *38*, 63.

(4) Hawker, C. J.; Bosman, A. W.; Harth, E. *Chem. Rev.* **2001**, *101*, 3661.

(5) Kamigaito, M.; Ando, T.; Sawamoto, M. *Chem. Rev.* **2001**, *101*, 3689.

(6) McCormick, C. L. *Stimuli-Responsive Water Soluble and Amphiphilic Polymers*; American Chemical Society: Washington, D.C., 2000; Vol. 780.

(7) Tsarevsky, N. V.; Sumerlin, B. S.; Chiefari, J.; Matyjaszewski, K. *Controlled Radical Polymerization: Materials*; American Chemical Society: Washington, D.C., 2015; Vol. 1188.

(8) Mai, Y.; Eisenberg, A. *Chem. Soc. Rev.* **2012**, *41*, 5969.

(9) Blanazs, A.; Armes, S. P.; Ryan, A. J. *Macromol. Rapid Commun.* **2009**, *30*, 267.

(10) Matyjaszewski, K.; Xia, J. *Chem. Rev.* **2001**, *101*, 2921.

(11) Zhang, L.; Eisenberg, A. *Polym. Adv. Technol.* **1998**, *9*, 677.

(12) Stenzel, M. H. *Chem. Commun.* **2008**, 3486.

(13) Albertsson, A.-C.; Varma, I. K. *Biomacromolecules* **2003**, *4*, 1466.

(14) Uhrich, K. E.; Cannizzaro, S. M.; Langer, R. S.; Shakesheff, K. M. *Chem. Rev.* **1999**, *99*, 3181.

(15) Oh, J. K. *Soft Matter* **2011**, *7*, 5096.

(16) Ramesh, K.; Mishra, A. K.; Patel, V. K.; Vishwakarma, N. K.; Biswas, C. S.; Paira, T. K.; Mandal, T. K.; Maiti, P.; Misra, N.; Ray, B. *Polymer* **2012**, *53*, 5743.

(17) Mishra, A. K.; Patel, V. K.; Vishwakarma, N. K.; Biswas, C. S.; Raula, M.; Misra, A.; Mandal, T. K.; Ray, B. *Macromolecules* **2011**, *44*, 2465.

(18) Lele, B. S.; Leroux, J. C. *Macromolecules* **2002**, *35*, 6714.

(19) You, Y.; Hong, C.; Wang, W.; Lu, W.; Pan, C. *Macromolecules* **2004**, *37*, 9761.

(20) Quan, C.-Y.; Wu, D.-Q.; Chang, C.; Zhang, G.-B.; Cheng, S.-X.; Zhang, X.-Z.; Zhuo, R.-X. *J. Phys. Chem. C* **2009**, *113*, 11262.

(21) Nese, A.; Li, Y.; Averick, S.; Kwak, Y.; Konkolewicz, D.; Sheiko, S. S.; Matyjaszewski, K. *ACS Macro Lett.* **2012**, *1*, 227.

(22) Debuigne, A.; Willet, N.; Jérôme, R.; Detrembleur, C. *Macromolecules* **2007**, *40*, 7111.

(23) Williams, R. J.; O'Reilly, R. K.; Dove, A. P. *Polym. Chem.* **2012**, *3*, 2156.

(24) Petzetakis, N.; Walker, D.; Dove, A. P.; O'Reilly, R. K. *Soft Matter* **2012**, *8*, 7408.

(25) Lecomte, P.; Jérôme, C. *Adv. Polym. Sci.* **2012**, *245*, 173.

(26) Dove, A. P. *Chem. Commun.* **2008**, 6446.

(27) Dutta, S.; Hung, W.-C.; Huang, B.-H.; Lin, C.-C. *Adv. Polym. Sci.* **2012**, *245*, 219.

(28) Labet, M.; Thielemans, W. *Chem. Soc. Rev.* **2009**, *38*, 3484.

(29) Dechy-Cabaret, O.; Martin-Vaca, B.; Bourissou, D. *Chem. Rev.* **2004**, *104*, 6147.

(30) Woodruff, M. A.; Hutmacher, D. W. *Prog. Polym. Sci.* **2010**, *35*, 1217.

(31) Yu, Y.; Zou, J.; Cheng, C. *Polym. Chem.* **2014**, *5*, 5854.

(32) Heskins, M.; Guillet, J. E. *J. Macromol. Sci. A.* **1968**, *2*, 1441.

(33) Oh, J. K.; Drumright, R.; Siegwart, D. J.; Matyjaszewski, K. *Prog. Polym. Sci.* **2008**, *33*, 448.

(34) Malonne, H.; Eeckman, F.; Fontaine, D.; Otto, A.; Vos, L. D.; Moës, A.; Fontaine, J.; Amighi, K. *Eur. J. Pharm. Biopharm.* **2005**, *61*, 188.

(35) Bruining, M. J.; Edelbroek-Hoogendoorn, P. S.; Blaauwgeers, H. G. T.; Mooy, C. M.; Hendrikse, F. H.; Koole, L. H. *J. Biomed. Mater. Res.* **1999**, *47*, 189.

(36) Liu, X.; Xu, Y.; Wu, Z.; Chen, H. *Macromol. Biosci.* **2013**, *13*, 147.

(37) Hira, S. K.; Mishra, A. K.; Ray, B.; Manna, P. P. *PLoS One* **2014**, *9*, e94309.

(38) Patterson, J. P.; Robin, M. P.; Chassenieux, C.; Colombani, O.; O'Reilly, R. K. *Chem. Soc. Rev.* **2014**, *43*, 2412.

(39) Jacquier, V.; Miola, C.; Llauro, M.-F.; Monnet, C.; Hamaide, T. *Macromol. Chem. Phys.* **1996**, *197*, 1311.

(40) Campos, J. M.; Ribeiro, M. R.; Ribeiro, M. F.; Deffieux, A.; Peruch, F. *Eur. Polym. J.* **2013**, *49*, 4025.

(41) Li, G.; Lamberti, M.; Pappalardo, D.; Pellecchia, C. *Macromolecules* **2012**, *45*, 8614.

(42) Wilson, J. A.; Hopkins, S. A.; Wright, P. M.; Dove, A. P. *Macromolecules* **2015**, *48*, 950.

(43) Williams, C. K. *Chem. Soc. Rev.* **2007**, *36*, 1573.

(44) Jérôme, C.; Lecomte, P. *Adv. Drug Deliv. Rev.* **2008**, *60*, 1056.

(45) Carrot, G.; Hilborn, J. G.; Trollsås, M.; Hedrick, J. L. *Macromolecules* **1999**, *32*, 5264.

(46) Korich, A. L.; Walker, A. R.; Hincke, C.; Stevens, C.; Iovine, P. M. *J. Polym. Sci., Part A: Polym. Chem.* **2010**, *48*, 5767.

(47) Bailey, W. J.; Ni, Z.; Wu, S.-R. *J. Polym. Sci., Part A: Polym. Chem.* **1982**, *20*, 3021.

(48) Jin, S.; Gonsalves, K. E. *Macromolecules* **1997**, *30*, 3104.

(49) Bailey, W. J.; Ni, Z.; Wu, S. R. *Macromolecules* **1982**, *15*, 711.

(50) Agarwal, S. *Polym. J.* **2006**, *39*, 163.

(51) Undin, J.; Illanes, T.; Finne-Wistrand, A.; Albertsson, A.-C. *Polym. Chem.* **2012**, *3*, 1260.

(52) Bailey, W. J.; Endo, T.; Gapud, B.; Lin, Y.-N.; Ni, Z.; Pan, C.-Y.; Shaffer, S. E.; Wu, S.-R.; Yamazaki, N.; Yonezawa, K. *J. Macromol. Sci. A.* **1984**, *21*, 979.

(53) Agarwal, S. *Polym. Chem.* **2010**, *1*, 953.

(54) Roberts, G. E.; Coote, M. L.; Heuts, J. P. A.; Morris, L. M.; Davis, T. P. *Macromolecules* **1999**, *32*, 1332.

(55) Sun, L. F.; Zhuo, R. X.; Liu, Z. L. *J. Polym. Sci., Part A: Polym. Chem.* **2003**, *41*, 2898.

(56) Maji, S.; Mitschang, F.; Chen, L.; Jin, Q.; Wang, Y.; Agarwal, S. *Macromol. Chem. Phys.* **2012**, *213*, 1643.

(57) Undin, J.; Finne-Wistrand, A.; Albertsson, A.-C. *Biomacromolecules* **2014**, *15*, 2800.

(58) Agarwal, S.; Kumar, R.; Kissel, T.; Reul, R. *Polym. J.* **2009**, *41*, 650.

(59) Hedir, G. G.; Bell, C. A.; Ieong, N. S.; Chapman, E.; Collins, I. R.; O'Reilly, R. K.; Dove, A. P. *Macromolecules* **2014**, *47*, 2847.

(60) Hedir, G. G.; Bell, C. A.; O'Reilly, R. K.; Dove, A. P. *Biomacromolecules* **2015**, *16*, 2049.

(61) Bell, C. A.; Hedir, G. G.; O'Reilly, R. K.; Dove, A. P. *Polym. Chem.* **2015**, *6*, 7447.

(62) Patel, V. K.; Vishwakarma, N. K.; Mishra, A. K.; Biswas, C. S.; Ray, B. *J. Appl. Polym. Sci.* **2012**, *125*, 2946.

(63) Yang, L.; Luo, Y.; Li, B. *J. Polym. Sci., Part A: Polym. Chem.* **2005**, *43*, 4972.

(64) Jakubowski, W.; Min, K.; Matyjaszewski, K. *Macromolecules* **2006**, *39*, 39.

(65) Yu, K.; Eisenberg, A. *Macromolecules* **1996**, *29*, 6359.

(66) Lin, L. Y.; Lee, N. S.; Zhu, J.; Nyström, A. M.; Pochan, D. J.; Dorshow, R. B.; Wooley, K. L. *J. Control. Release* **2011**, *152*, 37.

(67) Yu, K.; Zhang, L.; Eisenberg, A. *Langmuir* **1996**, *12*, 5980.

(68) Ding, Y.; Kang, Y.; Zhang, X. *Chem. Commun.* **2015**, *51*, 996.

(69) Lambermont-Thijs, H. M. L.; Heuts, J. P. A.; Hoeppener, S.; Hoogenboom, R.; Schubert, U. S. *Polym. Chem.* **2011**, *2*, 313.

(70) Hu, Y.; Jiang, Z.; Chen, R.; Wu, W.; Jiang, X. *Biomacromolecules* **2010**, *11*, 481.

(71) Robin, M. P.; Wilson, P.; Mabire, A. B.; Kiviaho, J. K.; Raymond, J. E.; Haddleton, D. M.; O'Reilly, R. K. *J. Am. Chem. Soc.* **2013**, *135*, 2875.

(72) Robin, M. P.; Mabire, A. B.; Damborsky, J. C.; Thom, E. S.; Winzer-Serhan, U. H.; Raymond, J. E.; O'Reilly, R. K. *J. Am. Chem. Soc.* **2013**, *135*, 9518.

(73) Mabire, A. B.; Robin, M. P.; Willcock, H.; Pitto-Barry, A.; Kirby, N.; O'Reilly, R. K. *Chem. Commun.* **2014**, *50*, 11492.

(74) Robin, M. P.; Raymond, J. E.; O'Reilly, R. K. *Mater. Horiz.* **2015**, *2*, 54.

(75) Jakeš, J. *Collect. Czech. Chem. Commun.* **1995**, *60*, 1781.

7 Conclusions and Future Work

7.1 Conclusions

In this thesis, the copolymerization of cyclic ketene acetals (CKA) and different vinyl monomers using a controlled polymerization technique has been reported, for the synthesis of degradable polymers containing different functionalities and properties. In the first approach, the copolymerization of the 7-membered ring CKA 2-methylene-1,3-dioxepane (MDO), with vinyl acetate (VAc) was investigated using the reversible addition-fragmentation chain transfer (RAFT), also known as MADIX (Macromolecular Design *via* Interchange of Xanthates) polymerization, in order to yield well-defined copolymers of poly(MDO-*co*-VAc) with controlled molecular weights and narrow dispersities. The copolymer composition was also found to be easily changed by varying the amount of MDO in the reaction mixture to produce poly(MDO-*co*-VAc) samples with tunable degradability. This methodology was also applied to other less activated monomers including *N*-vinylpyrrolidone (NVP), *N*-vinylpiperidone (VPip) and vinyl chloroacetate (VClAc). While the controlled nature of these polymerizations was successfully confirmed by the retention of the RAFT end-group functionality on the polymer chains, as observed by ^{1}H NMR spectroscopy and SEC analysis, some limitations were also encountered. Indeed, a loss of control was occurring when the copolymerizations were carried out for longer reaction times and for aiming for higher monomer conversions, hence showing the unsuitability of the process to be used for full monomer conversions. Despite the limitations, this work represents the first example of the copolymerization of MDO using the RAFT/MADIX polymerization technique aimed at preparing well-defined copolymers based on CKA monomers with controlled molecular weights, which have so far mainly been investigated *via* conventional free radical polymerization.

The successful preparation of degradable copolymers with pendent functional groups able to be further modified *via* post-polymerization modification techniques was also achieved by

the copolymerization of MDO and vinyl bromobutanoate (VBr), a bromine functionalized vinyl acetate derived monomer. Such type of monomer was easily synthesized by the palladium catalyzed vinyl exchange reaction between vinyl acetate and bromobutyric acid and led to a functional monomer able to be homo- and copolymerized with MDO also using the RAFT/MADIX polymerization technique. The degradability of these copolymers was additionally found to be easily tunable by varying the MDO content within the polymer backbone. Degradation was confirmed by hydrolysis experiments in a basic environment, revealing that a lower rate of degradation was observed for a lower amount of MDO within the polymer backbone, whereas a faster rate of degradation was noted when a higher amount of MDO was incorporated in the copolymers. More interestingly, the post-polymerization modification of the copolymer, poly(MDO-*co*-VBr), was found to be simply achieved *via* the use of azidation and 1,3-dipolar cycloaddition reactions to incorporate further functionalities and properties within the copolymers, as demonstrated by the formation of PEG-grafted degradable copolymers based on poly(MDO-*co*-Vinyl esters). While the controlled nature of the process was also reported for this system, a loss of control was again observed when higher incorporation of MDO was attempted. Investigation of the copolymerizations of MDO and VAc, as well as the homopolymerization of MDO, using the RAFT/MADIX polymerization technique revealed that while a good retention of the RAFT end-group was occurring during the early stage of the polymerization, a competitive side-reaction also emerged as a consequence of the fragmentation of the Z-group of the chain transfer agent (CTA) leading to the formation of carbonodithioate functionalities terminating the growth of the polymer chains. While this fragmentation was confirmed by ^{13}C NMR spectroscopic analysis, the use of a different chain transfer agent, *p*-methoxyphenyl xanthate (CTA 4), was found, to a certain degree, to enable the formation of copolymers with a higher targeted amount of MDO and higher monomer conversions while still maintaining a good control over the molecular weights and forming polymers with narrow dispersities.

The optimized methodology for the preparation of well-defined copolymers *via* the RAFT/MADIX copolymerization of MDO with vinyl monomers was further expanded to a novel class of hydrophilic monomers: ethylene glycol methyl ether vinyl acetate (MeOVAc), di(ethylene glycol) methyl ether vinyl acetate (MeO_2VAc) and tri(ethylene glycol) methyl ether vinyl acetate (MeO_3VAc). While these monomers were simply synthesized using the palladium catalyzed vinyl exchange reaction between VAc and the corresponding carboxylic acid, they represent a notably interesting new class of monomers, which exhibit hydrophilic properties similar to the commercially available di(ethylene glycol) acrylate based monomers which have been dominating the biomedical applications of polymeric materials alongside other PEG-based polymers. The polymerization of these monomers with MDO enables the formation of poly(MDO-*co*-MeO_nVAc) copolymers demonstrating both degradable and hydrophilic properties. Interestingly, while the copolymers were found to be soluble in aqueous medium, they were also found to present thermoresponsive properties. Indeed, while most copolymers were found to show good solubility at low temperatures, a phase separation was observed (evidenced by the occurrence of a cloud point) as the temperature of the polymer solution was increased. Furthermore, the cloud points were found to be easily tunable by varying the copolymer composition of the final materials as well as the length of the oligo ethylene glycol side chain of the monomers, MeOVAc, MeO_2VAc and MeO_3VAc to target degradable materials with thermoresponsive properties close to body temperature.

Furthermore, the copolymerization of VAc and VBr with MDO using a poly(NVP) macro-CTA has also been reported to successfully form amphiphilic block copolymers of poly(NVP)-*b*-poly(MDO-*co*-VAc), which were found to self-assemble in water to form nanoparticles. While the degradability of the nanoparticles could potentially be changed by varying the final incorporation of MDO within the hydrophobic part of the block copolymer, the size of the nanoparticles could also be easily varied by modifying the length of each

hydrophilic or hydrophobic segment as confirmed by Dynamic Light Scattering (DLS), Static Light Scattering (SLS) and Transmission Electron Microscopy (TEM) analysis. Such an approach confirmed that the formation of self-assembled degradable polymers *via* a single polymerization technique is now viable, in comparison to the two step process of using ring opening-polymerization in conjunction with RAFT or ATRP which is currently used in the field of polymeric amphiphilic degradable nanoparticles.

In summary, the thesis has developed a methodology for the preparation of well-defined copolymers with targetable functionalities and degradability by the copolymerization of CKAs and vinyl monomers using the RAFT/MADIX process. This approach using CKA monomers and the formation of novel vinyl acetate derived monomers can greatly expand the range of accessible degradable and functional polymers currently available. Initial investigations in to the use of this methodology to prepare degradable nanoparticles has been reported and hence revealed the great potential in using such methodology to produce polymeric materials for biomedical applications such as drug delivery or tissue engineering scaffolds.

7.2 Future work

Whilst an established procedure to synthesize degradable copolymers of CKAs and vinyl monomers has been established in this thesis, there are many more opportunities for further exploration. Indeed, while the use of the palladium catalyzed vinyl exchange reaction has been reported in this thesis for the synthesis of two new types of monomers, the application of such a synthetic procedure could enable the preparation of a wide range of other vinyl acetate derived monomers. These could be copolymerized with MDO and would enable the formation of a large array of novel degradable copolymers with a wide range of properties. For example, further investigation into the copolymerization of MDO with vinyl monomers containing fluorine functional groups and subsequent self-assembly, could potentially enable

the preparation of degradable nanoparticles to be used as contrast agents for magnetic resonance imaging (MRI). Furthermore, the incorporation of a third co-monomer within the system could also, depending on the incorporated functionalities (*e.g.* thiol, alkyne, azide), enable the formation of cross-linked or hydrogel materials with degradable sections which could encapsulate and release drugs or small molecules for biomedical applications. Another extension of this thesis could be focused on the copolymerization of MDO with MeOVAc, MeO_2VAc or MeO_3VAc with a macro-CTA in order to prepare amphiphilic block copolymers that could self-assemble to produce nanoparticles bearing thermoresponsive properties. Additionally, the use of another hydrophilic block copolymer could also be investigated to produce an amphiphilic polymer having dual thermoresponsive properties depending on the temperature and medium in which it is studied. Such approaches could also be further extended to produce different types of self-assembled structures, such as cylinders or vesicles presenting degradable and stimuli responsive properties.